StructuralComponents 5.0

Super element based tool for early design collaboration applied to mid-rise buildings

by

Babette L. Hohrath

10 April 2018

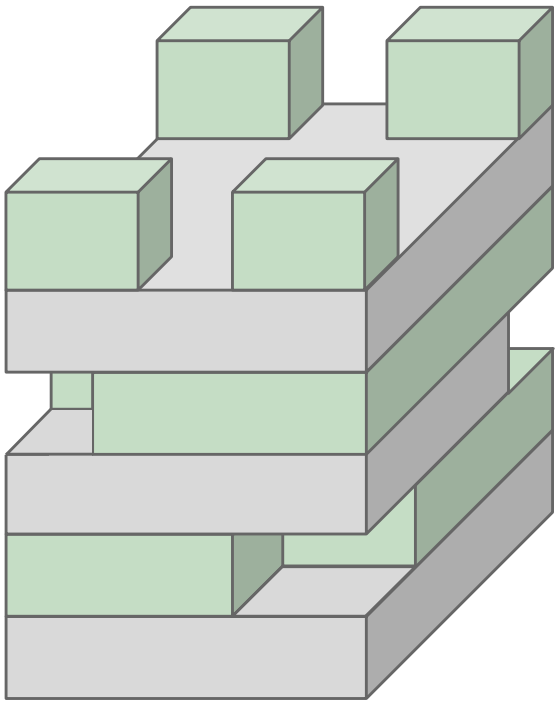

StructuralComponents 5.0
Super element based tool for early design collaboration applied to mid-rise buildings

by

Babette L. Hohrath

Student number: 4514319

in partial fulfilment of the requirements for the degree of

Master of Science

in Structural Engineering

at the Delft University of Technology and

in cooperation with White Lioness technologies,

to be defended publicly on the 17th of April 2018.

Supervisor:	Prof. dr. ir. J. G Rots	TU Delft
Thesis committee:	Dr. ir. M. Turrin	TU Delft
	Dr. ir. P. C. J. Hoogenboom	TU Delft
	Dr. ir. J. L. Coenders	White Lioness technologies
	ir. A. Rolvink	White Lioness technologies
	Prof. dr. ir. R. Steenbergen	TNO and UGent

TU Delft Delft University of Technology

Preface

This report is the documented result of the Master's thesis project of Babette Hohrath, the fifth development in a series of the StructuralComponents graduation projects. This research discusses the development of a flexible conceptual design tool providing real-time behaviour analysis and feasibility results for the collaboration between architects and structural engineers.

The graduation committee members were:

Prof. dr. ir. J.G. Rots (Chairman)

e-mail: J.G.Rots@tudelft.nl
affiliation: Delft University of Technology
Faculty of Civil Engineering and Geosciences

Ir. A. Rolvink (Daily Supervisor)

e-mail: ankerolvink@whilte-lioness.com
affiliation: Founder and CEO of White Lioness technologies

Dr. Ir. J. Coenders (Daily Supervisor)

e-mail: jeroencoenders@white-lioness.com
affiliation: Founder and CEO of White Lioness technologies

Dr. Ir. M. Turrin

e-mail: M.Turrin@tudelft.nl
affiliation: Delft University of Technology
Faculty of Architecture

Dr. Ir. P. Hoogenboom

e-mail: P.Hoogenboom@tudelft.nl
affiliation: Delft University of Technology
Faculty of Civil Engineering and Geosciences

Dr. Ir. R. Steenbergen

e-mail: raphael.steenbergen@tno.nl
Raphael.Steenbergen@UGent.be
affiliation: TNO, Delft
University of Gent
Faculty of Engineering and Architecture

Acknowledgements

The many people that provided helpful input, whether they were directly involved or not, are sincerely thanked!

First of all I would like to sincerely thank my graduation committee, which consisted of J.G. Rots, dr. ir. J. Coenders, ir. A. Rolvink, dr. ir. M. Turrin, dr. ir. P. C. J. Hoogenboom and Prof. dr. ir. R. Steenbergen, for their valued guidance and comments. Special thanks go to my daily supervisors Jeroen Coenders and Anke Rolvink, who not only introduced me to the field of computational design tools, but also allowed me to complete the vast majority of my work at White Lioness technologies.

I thank all the people working at White Lioness technologies for supporting me, especially Arie Bovenberg and Dion Jansen who helped me set up the toolbox and advised me throughout the development phase.

Also, many thanks goes to Frank Huijben from ABT and Sander Flach from Klunder Architecten for taking the time to talk to me about the Energeikwartier used for the case study. Their information was very valuable to show a practical application of the research.

Finally, I especially thank Dion Jansen for taking the time to discuss my thesis and for reviewing parts of my report. I also thank my friends and family for their motivation throughout this project.

Summary

Building design is composed of multiple phases during which various disciplines work together to complete a project (Coenders, 2011). However, currently technology mostly provides architects with modelling tools that focus on geometric creativity and overlook structural performance, while structural engineers use analysis software that requires the final shape and details unknown in the conceptual design phase (Mueller and Ochsendorf, 2013). These tools focus on the individual disciplines, instead of supporting collaboration throughout the design process. Some methods and tools have been developed for the early design stage, however, they are often limited to 2D structures, to specific structure types, lack structural checks or are actually mainly applicable in later stages.

The paradox between the lack of information and the availability design freedom throughout the design process, illustrated by the well known MacLeamy curve (2010), is a hindrance to collaboration. Architect's design freedom gets more limited throughout the project, while structural engineers can only analyse the structure in detail once all the parameters are fixed, at which point it's very costly to make changes. Therefore, the ability to make smart and informed design choices early on in the design process has the potential to reduce project costs and save time. Due to the lack of tools that support the collaboration required between the architects and structural engineers during the conceptual design phase, this paper investigates one possible solution.

The objective of this paper is:

Research and develop a collaborative tool prototype of StructuralComponents to rapidly validate the structural and geometric feasibility of architectural designs of concrete mid-rise buildings in the conceptual design phase.

The purpose of the feasibility tool itself is to improve and speed up the collaboration process between the structural engineer and the architect, by enabling the structural engineer to model and analyse possible load bearing structures equivalent to the various alternative architectural designs considered during an initial brainstorm session.

In order to achieve this general goal, a few more specific goals were determined:

1. Implement a modelling process that is suited for the flexibility requirements of the early design phase.
2. Determine the structural and architectural feasibility of conceptual designs by only considering the main load bearing structure.
3. Enable result visualisation that is understandable by the structural engineer and architect, enabling them to collaborate and improve the design.

The geometric freedom requirement was addressed in three points. First, a few building blocks, see Figure 1, with relevant topologies were implemented to test the functionality of the tool. Their geometry is parametrically adaptable and the structural analysis is calculated accordingly. These can be combined quickly to support the geometric creativity involved in the architectural design process.

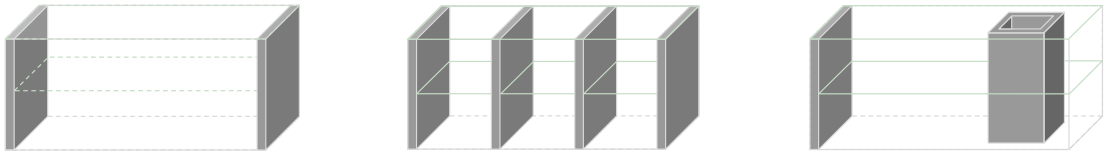

(a) two parallel walls *(b) four parallel walls* *(c) one wall and one core*

Figure 1: Fully implemented building blocks

Second, the parametric modelling capabilities allow the users to quickly consider various dimensions and, in combination with the feasibility checks, test the dimension limits of a feasible conceptual design. Third, the building blocks can be stacked to compose more complex structures with various types of topologies.

For the analysis of the mid-rise buildings, a Super Element Method (SEM) (Qu, 2004) is implemented to decompose a building into substructures. This method benefits the users, since they are able to quickly construct an entire building given a few "pre-constructed" building blocks (super elements). Instead of using the finite element model for the analysis, a differential equation method was used due to two main advantages. First, this method provides quick insight into the force flow of the structure, a key point of interest for the structural engineer during the conceptual design phase (Steenbergen, 2007). Secondly, the differential equations can be derived symbolically, enabling near real-time parametric modelling.

Example feasibility checks for both the structural and architectural requirements were implemented. The architect examines the aesthetics, functionality, movement flow, amount of sunlight as well as other factors for the building, so an example check relating to the sunlight entering the building was used. Structural requirements usually include stability, stiffness and strength, for which equations describing the global behaviour of a building were implemented. It is important to note that some architectural requirements cannot be quantified and that the tool does not provide structural guidance, requiring the architect and structural engineer to collaborate during the meeting to find solutions.

To satisfy the result visualisation goal of the feasibility tool, the near real-time deflection, rotation, moment and shear force results are displayed along the height and the dead and live normal forces at the bottom, see Figure 2a. The feasibility checks are visualised by the colour of the structural element, see Figure 2b. These outputs help both the structural engineer and architect understand the structure.

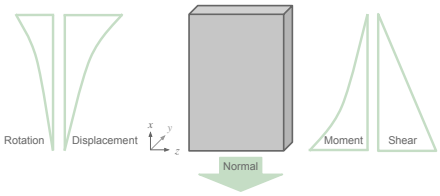

(a) Structural behaviour

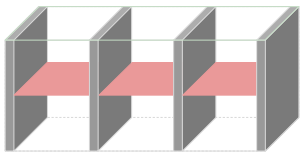

(b) Feasibility check results

Figure 2: Structural behaviour and feasibility results

The super elements are stored in an external Python library and are accessed through the GhPython component. The Rhino-Grasshopper interface allows the users to parametrically alter the dimensions of the substructures and visualise the structure as well as results in real-time.

The proposed building block concept provides a flexible and quick modelling method, compared to traditional software. Plus, the implemented symbolic differential equation analysis method successfully enables near real-time behaviour and feasibility analysis of 3D parametric structures given little information. The combination of these features are expected to encourage the collaboration between the architect and structural engineer during the early design phase. In conclusion, the super element method based tool prototype is appropriate for the early design phase and with further development, especially addressing the lack of horizontal connections, it is also a useable option in practice.

Contents

1 Introduction

Building design is composed of multiple phases during which various disciplines are meant to work together to complete a project as described by Coenders (2011). The structural engineer is mostly involved in the conceptual, preliminary, final and tender design phase, while the architect already starts a bit earlier to come up with a design. Technological advances are becoming more relevant for the disciplines involved in each of the design phases. Architects are taking advantage of recent developments in computational design systems for their design concepts (Coenders, 2011), while structural engineers are now able to provide extremely accurate results for complete structures using finite element programs (Steenbergen, 2007). However, currently technology mostly provides architects with modelling tools that focus on geometry, but overlook the structural performance, and leaves engineers with tools used for structural analysis that require a final geometrical shape (Mueller and Ochsendorf, 2013). Therefore, the link between the two disciplines regarding technology still needs improvement.

1.1 Motivation

A common issue during the conceptual design phase is the paradox between the lack of information and the available design freedom during the early design stage as Coenders (2011) illustrates in Figure 1.1. At the start of a project the most design freedom exists, but also the least information is known, hence, many decisions have to be made by the various stakeholders that determine in which direction the project continues. Good decisions have the potential to save time and money in the long run, while poor decisions can cause severe problems that are difficult, expensive or even impossible to solve in later stages. Collaboration and thoughtful design is critical in making good decisions in this early design stage.

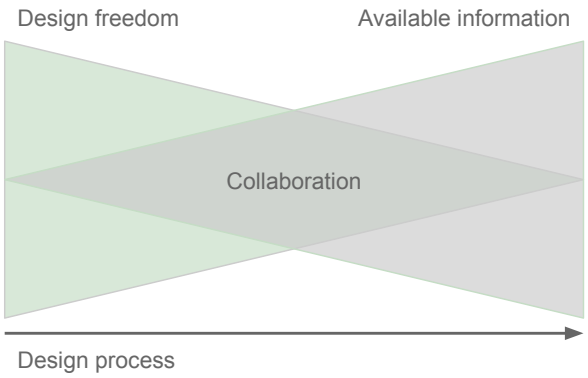

Figure 1.1: Conceptual design paradox adopted from (Coenders, 2011) based on the MacLeamy curve introduced in 2004.

However, as mentioned, not many tools exist to support this communication, where the collaboration between the architect and the structural engineer plays a key role. The gap between architectural and structural responsibilities needs to be filled in order to address current and future design demands. Coenders (2011) highlights higher financial and environmental pressures on projects as well as an increasing number of stakeholders, which require more efficient designs. Less time is available for elaborate studies while higher quality results are required to meet safety levels. Additionally, the number of socially acceptable design errors have decreased as well as the time to fix them in the case that they do occur. Using computational design to improve the efficiency of the early design stage would address these demands by not only speeding up the design process, but also significantly improving the design quality.

In order to investigate the mentioned software gap further and determine required tool features, current design tools were researched. This research focuses on structural modelling and analysis tools and methods that are commercially used or are still in the research phase. In order to determine what types of tools are already available and if they satisfy designer's demands, not only tools from the building industry are investigated but also those from the aerospace and automotive industries.

1.2 Building Industry

1.2.1 Building Design Procedure

The design of a building is neither the first nor the last step of a project. Coenders (2011) summarises the building life cycle, including the initiation, design, engineering and construction phase. During the initiation phase a client decides on a project and creates a business case to ensure it is financially appealing. Then the design process starts with the conceptual design phase. The project requirements are determined and the architect works on a design concept before other engineers join with their specific knowledge. Among those engineers is the structural engineer who's responsibility is the load bearing structure. During the conceptual design phase he or she focuses on predicting the behaviour of the overall system. Only later, in the preliminary and final design stage does the structural engineer start to analyse on an element-level. During the tender phase contractor services are secured and then the construction may begin. However, the design and engineering phases do not necessarily end before the tender phase, in fact they may continue into the construction phase (Coenders, 2011).

Two key factors that early design stage tools should address are:

1. **Little known information vs. design freedom**
   Architects have the most design freedom in the early design phase, but that also means that very little information about the design is fixed, which requires assumptions to be made for an initial analysis. Therefore, civil engineering design tools "must operate in an environment with uncertainty, ambiguity, and approximation" in the conceptual design phase (Ching, 2014).
2. **Rapid prototyping**
   Due to the large design freedom, limited time and financial pressure in the conceptual phase, the design idea must be narrowed down rapidly. Therefore, it is important for the conceptual design tool to quickly create multiple design alternatives and provide quick and insightful analyses to help during the decision making process (Rolvink, 2010).

1.3 Tools in the Building Industry

This section discusses a selection of current software in the architecture, engineering and construction (AEC) industry. It focuses on commercial software used by and available to architects and structural engineers when designing buildings. The goal is to assess if the tools are adequate for collaboration practices in the early design phase. Structural behaviour considerations are usually not included in this conceptual design phase, however, earlier integration of structural knowledge could improve the decision making process of the final design (Lindemann et al., 2010).

1.3.1 Commercial Drawing Tools

Based on the general architectural requirements set earlier, architects are mostly focused on the building concept, the space outside of and within the building as well as the transitions. These are all factors that influence the geometry, but don't necessarily consider the structural performance. A common tool for architects to create a design concept is pen and pencil. This is an iterative process, where sketches are continuously edited (Lindemann et al., 2010). Computer aided designs are usually introduced later, once the design has been narrows down.

In order to integrate structural analysis earlier, the structural system has to be modelled digitally. Therefore, commercially available drawing software is investigated to determine if it can be used to quickly model the structural system of a conceptual design.

SketchUp
SketchUp Pro (Trimble Inc., 2018a) is a sketching tool that uses a direct modelling method. Geometry can be directly manipulated by pushing or pulling corners and faces of an object. It can create 3D models, share walkthrough animations with realistic lighting and import files from other 3D modelling programs (Trimble Inc., 2017). The geometric freedom enabled by the direct modelling method can be very useful to designers and architects in the early design phase. However, this modelling method is time consuming and therefore not optimal to quickly determine possible load bearing structures for an architectural conceptual design. Also, this tool does not offer any structural performance analysis nor technical documentation.

Other commercially available and used tools are Computer-Aided Drafting (CAD) tools. CAD is technology for automated design and technical documentation, which can replace manual drafting (Autodesk Inc., 2018). This software enables 3D modelling and recently also scripting capabilities to make even more impressive and complex forms (Mueller, 2014). Two examples (from many) of CAD software currently available and used by architectural offices are:

ArchiCAD
ArchiCAD (Graphisoft, 2018) is advertised as a BIM (Building Information model) software, which allows architects to create 3D geometry in a central model, provide design documentation and photo-realistic rendering among other features.

Revit
Revit (Autodesk Inc., 2018e) is also advertised as a BIM software which can be used to model and analyse structures as well as share and visualise designs to improve collaboration. Revit is available for many industries, including architectural and structural engineering fields. The architectural additions include Revit Live (Autodesk Inc., 2018d) and Revit Recap (Autodesk Inc., 2018c) and allow the user to not only create 3D geometry, but also import point cloud data and render models.

However, CAD systems still have severe problems with creating rapid computable designs, which makes them unfit for the early design process. CAD systems are also unable to automatically update relating information after the designer implements a change. Instead, the changes in affected areas have to be implemented manually by the designer. For example, after changing the size of a room, the size of the adjacent rooms also has to change, or if an exterior wall becomes an interior wall (Flemming and Woodbury, 1995).

A newer modelling software that addresses the rigidity of CAD software to design changes is parametric and associative design (PAD) software. PAD tools "regards objects, such as structural elements of buildings, as a series of user-defined changeable parameters and derives other objects through a set of user-defined changeable associations" (Rolvink et al., 2014). This allows the user to easily change the parameters, such as dimensions, and the program automatically updates that object as well as attached objects following the associated logic. PAD tools are an effective way to generate alternative designs and adapt them in close to real time, which is why they provide an opportunity to improve existing structural design approaches. An example is Rhino-Grasshopper (Davidson, 2017).

Grasshopper
Grasshopper (Davidson, 2017) is a parametric graphical algorithm editor used to create geometry, which does not required programming or scripting knowledge. Grasshopper contains a VB.net and C# component, which allow custom functionality to be added (Davidson, 2018). A GhPython (Piacentino, 2018) plugin, the Python (Python Software Foundation, 2018) interpreter component for Grasshopper, provides scripting capabilities to users without having to be a programmer.

Dynamo
Another PAD tool example is Dynamo (Autodesk Inc., 2018b), which is advertised as an open source graphical programming and BIM compatible software tool. Through logic routines users can create, adapt and shift through geometry options (Autodesk Inc., 2018a). It can be extended through user-created packages, Python scripting or by directly importing dll's (Autodesk Inc., 2018a).

When creating parametric geometry, there is often a trade off between the efficiency and the flexibility of the model. It is important to realise that as the number of parameters increase, the work required also increases (Ledermann et al., 2005). Another disadvantage of PAD tools is that while it is easy to change the parameters of the objects, it is difficult to change the design logic towards the end of the design phase without having to re-model parts or the whole design. It is also difficult to generate different structural scenarios that include imperfections (Rolvink et al., 2014).

1.3.2 Commercial Analysis Tools

Structural engineers are mainly concerned with the performance of the load bearing structure. Depending on the complexity of the structure hand or excel calculations may suffice, however, for more complex structures various advanced tools are available. A standard analysis method used by structural analysis software is the finite element method (FEM). The finite element method is a "numerical method of solving partial differential equations", which is particularly useful for solving complex geometries (Wells, 2011).

Some examples of finite element analysis tools are:

Revit
As already mentioned, Revit software is not only available for architectural purposes but also available for structural engineers. It can be used to draw the structural geometry, convert it into an analytical model to perform the structural finite element analysis (FEA) and provide structural checks from various building codes. It also provides other capabilities such as modelling the concrete reinforcement and documentation for concrete and steel details. While it seems very convenient that Revit is available for both architects and structural engineers, users have to create a separate structural model for the architectural model in order to analyse its structural performance. Creating separate models can be an easy source of mistakes and differences in design, so some tools exist that can detect mismatches such as the Solibri Model Checker (Solibri Inc., 2018). However, creating separate architectural and structural models still seems redundant and very inefficient especially in the early design phase when many changes are made. Despite this inefficiency most software tools exist for purely the structural model and are used during the entire design phase. Additional examples of similar programs are DIANA FEA 9.5 (2017), SAP2000 (Computers and Structures, 2018), SOFiSTiK (2017), SCIA (Nemetschek Group, 2018), Tekla (Trimble Inc., 2018b), Digital Project (Gehry Technologies, 2017) and Bentley Systems Inc. (2018).

It is also possible to model a structure in one program and then analyse the final geometry in another software. This is especially useful when working with the parametric modelling software such as Grasshopper or Dynamo, which on their own have no analysis functionalities.

Geometry Gym
Geometry Gym (Mirtschin, 2017) is a plug-in for Rhino and Grasshopper that allows the import and export to Revit, Digital Project, Bentley and other analysis tools. This data transferring process is very useful for the detailed structural analysis of a final design, but it is very time consuming during the early design phase when geometric changes are constantly made.

Instead of separating the the modelling and the structural analysis process, real-time analysis could improve especially the early design phase. It would help the structural engineer understand the structure better, speed up the initial analysis procedure and potentially improve the decision making process during this phase. Two example tools are discussed below.

CSI Model Alive
SAP2000 (Computers and Structures, 2018) and ETABS (Computers & Structures Inc., 2018) are both tools from Computers & Structures Inc. (CSI). SAP2000 focuses on structural analysis and design, while ETABS has a broader focus including drafting. ETABS also uses "building components" to allow users to discretise models into different substructures. However, both have the "model alive" feature, allows a user to make geometric, property or loading changes and the structural results respond instantly. While this feature is useful in the early design phase, it can only be used on small to medium sized structures, limiting its usability (Computers and Structures, 2016).

Karamba
Another software that provides real-time analysis is Karamba (2017). Karamba is a parametric structural engineering plug-in for Rhinoceros that provides structural analysis results for spatial trusses, shells and frames. In short, the user can make a parametric model in Grasshopper, define member types, define loading and plug those into an analysis component. The displacement, stress and internal force results can then be viewed in real-time as dimensions or loadings change. Viewing structural results in real-time is very beneficial in the early design phase, because it allows the structural engineer to immediately see the behaviour changes when dimensions or loading conditions change. Again, this understanding can influence the decision making process in the early design phase and possibly lead to improved structural systems. Therefore, Karamba is a viable product to evaluate one or multiple chosen structural designs. However, since the modelling process is still based on Rhino and Grasshopper, it would take too long to create a design during a very early stage meeting between an architect and structural engineer.

A large number of commercial structural analysis tools are currently available for structural engineers. However, many structural analysis tools require an already defined geometry to analyse (Mueller and Ochsendorf, 2013), which is not usually the case in the conceptual design phase. Also, all of the discussed analysis tools use the finite element method. FEA software can be used during later design stages to calculate the final and detailed structural model (Steenbergen, 2007), however, in the early design phase it has some disadvantages. Each of the FEM steps require knowledge of geometric modelling, mechanics and the FEM, which can be difficult for non-engineers such as architects to follow or understand (Lindemann et al., 2010). Also, the FEA software can provide little understanding of the structural behaviour and its relationship to parameters (Steenbergen, 2007). Plus, while fast computers are available that can use FEM software to analyse structural models (Steenbergen, 2007), it is also worth to investigate other methods that may not be so computationally heavy.

1.3.3 Researched Analysis Tools

This section discusses other early design stage tools and methods that have been researched but are not commercially available yet. Most of these come from educational or academic backgrounds.

Graphic Static Tools
Graphic statics is a graphical method, as opposed to numerical method, of calculating internal forces in axially-loaded structures such a trusses, arches and cables. The method fundamentals were established in the 1800s and was widely used until the 1970s, when numerical methods became more popular due to the increase in computer power. However, recently graphic statics has received more interest again due to its simplicity and power. Researchers have used it to enable manipulation of structures with real time internal force results (Mueller, 2014).

Never the less, Graphic Static tools are limited, because they are only suitable for simple structures, generally 2D and statically determinate structures. Also, most of these tools require pre-set examples and are therefore not flexible enough to be implemented on different structures presented by the user (Mueller, 2014). Another disadvantage is that the design process is largely manual (Rolvink et al., 2014). Two examples are Active Statics (Greenwold and Allen, 2003) and eQUILIBRIUM (2012).

ForcePad
Forcepad (Lindemann et al., 2010) is a finite-element application that uses an image-editing method instead of the classical geometrical modelling technique to create finite-element models. One of its main foreseen applications was to be used in undergraduate mechanics courses taught at architecture and industrial design faculties. Instead of a geometric model an image is used for the finite-element model. White colour represents zero stiffness and black colour represents maximum stiffness and the stiffness of each element is calculated by averaging the pixel colours. The loads and boundary conditions are placed directly on the image and a rectangular grid is placed over the image when it's analysed. In the analysis feature Forcepad also supports real-time stress and displacement updates when loads are moved or rotated, allowing users to almost immediately see the results of different load cases. In addition to the real-time results feature, a topology optimisation module has also been added, which returns an optimal structure for the given sketch and load case (Lindemann et al., 2010).

A 3-dimensional version is also underway, however, the problem with a 3D version is that the image-editing metaphor doesn't work very well anymore and a new method has to be determined that enables a quick iterative design process (Lindemann et al., 2010).

ARCADE
Arcade is a program intended to enable a new way of teaching structural analysis with software. The interaction model is derived from computer games, which means the analysis and interpretation steps are combined. This allows the user to make changes to the model and see the effects in real-time. Arcade uses a computing method that is mainly used in computer games to allow visually realistic modelling, which is often called physics engine or particle system. This method allows for non-linear and large-displacement calculations (Martini, 2006). One current limitation is that

the program is limited to 2-dimensional analysis, however, Martini explains that a 3-dimensional version can be made based on the same computational method. The other limitation is that because the analysis runs on real time, it is computationally demanding and therefore the program is restricted to small scale and simple problems such as models with less than 100 nodes. Since the program is intentioned for educational purposes this complexity limitation is not a problem, however, if it were to be applied in practice this would be a significant issue. Another limitation is that the program does not include a standard section library nor code checks. Code checks are not necessary to understand the structural behaviour, however, standard sections would be useful (Martini, 2006).

Super Element Method
The super element method is a type of sub-structuring method, which originating in the aerospace industry as discussed in Section 1.4.3. Usually super elements are composed through a nodal condensation process, however, in Steenbergen's paper they represent a structure with the same topology along its height and it is formulated by a set of simultaneous differential equations with closed-form displacement function solutions. It's advantage over the finite element method is that it saves calculation time and provides a deeper understanding of the structural behaviour of buildings, especially for irregularly shaped ones (Steenbergen, 2007). This method was also applied to StructuralComponents (Rolvink et al., 2009), abstract pre-programmed blocks of differential equations, which can be used to construct models.

These academic tools and methods show that there are alternatives to the commercial analysis methods and tools. One severe limitation to the educational tools is that they are limited to simple structural systems, which would be a problem for commercial use. However, the mentioned super element method which uses differential equations to analyse structures could be an alternative analysis method in the early design phase.

Based on the software discussed in these sections, it seems that Mueller's observations are still accurate now. Especially for the very early design phase of buildings there still seems to be a gap between architectural and structural software. Advancing drawing software allows architects to visualise rough design ideas, detailed models, provide drawing documentation and final rendered images. However, structural analysis software is mostly available for later stages. Structural analysis tools can produce very accurate and detailed structural analysis results, but are not suited for the flexibility of the conceptual design phase and the complexity of real-life designs. To determine if tools that could address this gap, tools in the aerospace and automotive industry were also researched.

1.4 Aerospace Industry

Another industry that produces relatively large and customisable structures is the aerospace industry. Some tools and methods have already been adopted by civil engineers from the aerospace industry in the past, so their design phase and current tools are also researched to investigate their applicability to civil engineering.

1.4.1 Influential design topics

According to Howe (2000) the design code topics that are particularly influential in the conceptual design phase are:

- **Performance requirements** such as the definition of take-off and landing field lengths, residual climb capability after engine failure and performance if a landing approach is abandoned.
- **Flight requirements** such as static and dynamic stability, control characteristics and effectiveness as well as manoeuvre capability during critical flight phases. These characteristics influence the size and geometry of the secondary lifting surfaces and flight controls of other parameters.
- **Structural design** can broadly be described by stiffness and strength. The stiffness requirements prevent the airframe from distorting, while the strength requirements mainly consider combinations

of the normal (perpendicular to the flight path) manoeuvre factor (n) and speed (V) to calculate the structural loads.

The building industry has requirements that can be related to these. For example a performance requirement for a building could be heat loss or gain, instead of flight requirements there are usage requirements by the occupants of the building and structural stiffness and strength requirements. However, the architectural's and municipality's aesthetic requirements don't seem to have a counterpart in the aerospace industry.

1.4.2 Design procedure

Traditionally the aircraft design process is split into a conceptual design, preliminary design and a detailed design phase (Torenbeek, 1982), similar to the building industry. The first stage of the analysis involves determining the wing loading based on the previously determined fuselage dimensions and wing geometry along with the lift and drag representations. Next, an expression for the varying wind load with respect to thrust/power loading is found for each performance requirement. The combination of wind load and thrust/power loading that gives the maximum acceptable wind loading and/or lowest thrust/power loading should be selected. During the second stage the chosen load combination is used to calculate the corresponding mass. The load combination resulting in the lowest mass should be chosen. From the mass the wing size can be determined, producing the first layout configuration. At this point it may be necessary to compare alternative overall aircraft designs. Once a design is chosen more detailed and accurate calculations have to be completed, which will be used to re-evaluate the aircraft performance. Since this is an iterative process, it may be necessary to repeat the whole procedure until mass convergence is achieved.

As opposed to civil engineering, in aerospace engineering the structural configuration is already known during the analysis. For aerospace designers the main topic of interest is the structural synthesis, meaning how everything works together to get the most efficient design subject to the applied loads and temperature environment. Hence, the main goal is not the structural analysis of a given structure, but the generation of an optimal design (Przemieniecki, 1968).

1.4.3 Tools in the Aerospace Industry

Parametric and associative tools

In order to accommodate the various disciplines and provide flexible geometry to allow all sorts of imaginable configurations, parametric-associative geometry models are often used. The parametric software is able to quickly compare alternative aircraft design configurations during the conceptual design phase of aircraft design (Moerland, 2011). However, the most difficult aspect of the conceptual design phase is configuring the rules and defining the values that should be parameterised in a model (Vandenbrande et al., 2006).

As mentioned, complex CAD design for an entire aircraft cannot be done as one part. Associative models enable linkage between different geometric objects, so if one object is changed or moved, the other connected objects are automatically adapted (Ledermann et al., 2005). One example software is CATIA V5 (Dassault Systemes, 2017), which is a modern CAE system that uses consistent object oriented architecture and allows parameterising geometry, associating components and building hierarchical assemblies (Ledermann et al., 2005).

Analysis Tools

Also the Aerospace industry uses FEA programs for structural analysis.

Example software is CATIA V5 (Dassault Systemes, 2017), ANSYS Inc (2018b) and Nastran (Hexagon, 2018). However, often the number of structural elements needed to be analysed with matrix methods often exceeds the computer capacity of aerospace programs, which is why structural partitioning was applied. This method is used to divide an entire structure into a series of substructures, preferably in terms of physical specifications (Przemieniecki, 1968). An example is shown in Figure 1.2.

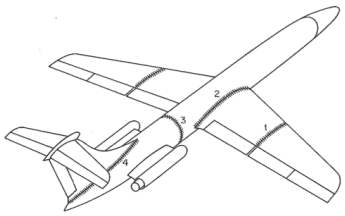

Figure 1.2: Typical substructuring of a conventional airplane (Przemieniecki, 1968)

A computational fluid dynamics (CFD) simulations must also be performed on aircrafts. Example programs used for these simulations are Fluent (ANSYS Inc, 2018a), Star-CMM+ (Siemens, 2018), in-house code or other software (Ledermann et al., 2005). This analysis is usually not required for buildings, so it will was not researched further.

Optimisation Tools

In aerospace structural design the minimisation of weight is a priority. Therefore, optimisation tools are widely used for aircraft design, especially multi-disciplinary optimisation (MDO). MDO is defined by (Sobieszczanski-Sobieski and Haftka, 1997) as "a methodology for the design of systems in which strong interactions between disciplines motivated designers to simultaneously manipulate variables in several disciplines". It is about enhancing the collaboration between various teams, also called concurrent engineering (CE), and integrating various engineering disciplines, bringing more information about the life-cycle into the design earlier.

1.4.4 Compared to the Building Industry

Adopting technology, such as parametric modelling and the super element method, from the aerospace industry was beneficial for the AEC industry. However, today their tools have migrated too much to optimisation to benefit the early design stage in the AEC industry. Not enough information is known during the conceptual design phase, plus the aesthetic requirements cannot be quantified to be optimised. Therefore, no aerospace tools or methods, that weren't already implemented in the civil engineering field, were considered as a feasibility tool for this project.

1.5 Automotive Industry

Based on reports from various automotive design and production firms, the conceptual design phase seems very similar among automotive companies. Their conceptual design phase has been described as a very artistic and emotional process (MercedesBenz, 2017) seeking aesthetics and harmony (Car Body Design, 2012).

1.5.1 Automotive Conceptual Design Process and Tools

The conceptual design phase usually starts with either hand or 2D computer-aided graphics software (Nissan Global, 2017). Full-scale tape drawings are also made for additional visualisation (Car Body Design, 2012). At this stage a first selection of the most promising designs are chosen (Nissan Global, 2017). Digital modellers use the 2D sketches to create more realistic 3D models including all the fine curve details and further determine the proportions (Nissan Global, 2017). For the 3D model the wheelbase, luggage compartment volume, engine sizes, safety regulations along with other factors are included in the silhouette design (Car Body Design, 2012). In the automotive industry a digital model is usually made using class A surfaces, which are "aesthetic/free surfaces that are visible to us (interior/exterior) ... and abide to the physical meaning of a product" (CATIA Tutor, 2017). Available Class-A software is offered by Autodesk Alias Detailed Stability InformationAutodeskAlias and ICEM Surf Detailed Stability InformationDassaultICEM as well as others. Based on the 3D models, a 1:4 ratio large clay model of the

car design is made. The special clay softens when heated and hardens when cooled, allowing the clay modellers to scrape and form the clay as required. Before the final design is determined a full-scale clay model is made of the exterior as well as the interior to present a more tangible experience (MercedesBenz, 2017). After the design teams developed the 1:1 scale models, another larger design competitions is held to decide on the final design concept (BMW, 2012). At BMW the conceptual design phase takes about 1 year (BMW, 2012) and is completed about 3 years before production begins (Car Body Design, 2012). Once the final design is chosen, the detailing and fine-tuning begins with the use of CAD software (Car Body Design, 2012).

1.5.2 Compared to the Building Industry

As opposed to the AEC industry, where the visual and load bearing structures are usually the same, the aesthetic and structural design processes in the automotive industry are separate since the outer shell is usually not load bearing. Hence, the automotive design and structural disciplines can work more independently with discipline specific tools, so the automotive tools were not considered further.

1.6 Evaluation of current tools

Despite not only researching conceptual design tools in the building industry, but also in the aerospace and automotive industry, a lack of tools that could address the gap between architectural and structural software was found. Aerospace conceptual design tools focus more on optimisation software, but for optimisation tools the goal parameters have to be well defined very early, which they are not in the AEC industry. For the automotive industry the structural performance and the aesthetics are separated, meaning they do not require a tool that links those two aspects as much as in the AEC industry.

Within the AEC industry advanced drawing tools are available, which could be used to model the structural system of an architectural design. Grasshopper would allow parametric modelling and custom scripting capabilities. Commercial structural analysis tools still have limitations during the conceptual design phase, but the super element method using differential equations could provide an alternative analysis method. This method could be implemented via the GhPython component into Grasshopper and extend the StructuralComponents developments. The combination of these two could also simplify the user interface and reduce the number of steps required in the analysis process.

2

Objective

After researching various types of design tools in the AEC industry and confirming the software gap between architectural and structural engineering tools, the objective, research questions, scope and methodology of this project were defined in this chapter.

2.1 Main Objective

As a key part of the early design phase, the architect and structural engineer have an opportunity to significantly improve the efficiency of the early design phase. However, the industry specific design tools limit their collaboration possibilities, costing the project more time and money. A new computational design tool which includes early design requirements from both the architectural and structural engineering disciplines could address these restrictions. Therefore, the following objective was formulated.

Research and develop a collaborative tool prototype of StructuralComponents to rapidly validate the structural and geometric feasibility of architectural designs of concrete mid-rise buildings in the conceptual design phase.

2.2 Research Question

The main objective is broken down into research questions guiding the research throughout this thesis.

1) What design tools are currently used in the early design phase of the architecture, engineering and construction (AEC) industry and in other similar areas?

This question examines whether the previously discussed software gap in the AEC industry still exists at the time of this project. For these tools it is important to highlight both their limitations and the positive features. This research point also proposes investigating other industries with a similar design process to determine if those fields have solutions that could also be applied in the AEC industry.

2) What modelling and analysis capabilities does the StructuralComponents prototype require?

The architectural and structural requirements for early design stage modelling should be researched. The modelling process must be suited for the early design phase, where little information is known, many design alternatives are considered and the design of a building should be decided as quickly as possible. These factors are especially important for the building composition method and geometric complexity of the resulting design.

3) Does a differential equation method suit the analysis process of the early design phase?

This question mainly explores whether the differential equation method meets the accuracy, speed and transparency requirements of an early phase analysis method. These requirements should be compared with the traditional finite element method (FEM).

4) What framework is necessary for the development of such an early design stage prototype?

It must be determined which existing software can be used for the modelling and visualisation process and how the proposed analysis method can be incorporated with it. Plus, since the prototype is not a complete tool, it should be expandable and the analysis method implemented independently to allow easy further development.

2.3 Scope

In order to keep this paper within the scope of a Master's thesis, some restrictions were set. The overall goal of this thesis is to present a proof of concept and not a fully developed tool, due to the time constraints. A few scope limitations are defined below based on key concepts used throughout this research. Additionally, many possible features are discussed for the feasibility tool, however, not all of them will be implemented into the prototype. The ones that are implemented serve as examples to show the possibilities, so if the tool were to be fully developed it would not necessarily be limited to these features. The prototype is developed to work for very simple mid-rise building structures and will therefore also only be tested with a simple structure.

Medium-rise building: a structure with height and slenderness restrictions that can be composed of a configuration of various topology types and functionalities.

Collaboration: the process between the architect and structural engineer in evaluating the feasibility of a conceptual building design and generating design solutions during a 1 hour meeting.

Feasibility: Satisfying the requirements set by the architect and structural engineer during the early design phase.

2.4 Methodology

This section describes the steps taken towards achieving the objective and answering the research questions. Overall there are 4 phases; research, system design, validation and discussion. While developing this thesis topic is an iterative process, the phases are listed here in a series of steps for clarity.

1. **Research mid-rise building design**
    - Software: Look into tools currently used in the architecture, engineering and construction (AEC) industry as well as methods and tools being researched. Other industries with a similar design process, such as the aerospace and automotive industries, should also be considered. Evaluate the available features and determine limitations of the investigated methods and tools regarding the individual disciplines but also their collaboration.
    - Conceptual design: Research the architectural and structural requirements applied to mid-rise buildings in the conceptual design phase. Investigate the required information and the feasibility requirements for both disciplines.
    - Structural mechanics: Research the main load bearing structure of concrete mid-rise buildings and the possibility of using the super element method for the structural analysis.
2. **System design**
    - Software: Decide on the prototype system architecture. Determine which existing software should be used for modelling and visualisation aspects and how it communicates with the element library and analysis method.
    - Conceptual design: Decide which mid-rise structural elements are necessary to show the possibilities of the prototype. Also, determine how to formulate and visualise the quantitative architectural and structural feasibility requirements. Then implement them into the prototype in a flexible way, allowing easy adjustments and extensions.
    - Structural mechanics: First, learn the super element method by calculating the structural behaviour for each required mid-rise element by hand or with available technology. Next, implement the method into the prototype and output the desired information.

3. **Validation**

   - Structural mechanics: Validate the derived governing differential equations and symbolic displacement equations with Steenbergen's dissertation (2007). The final numeric results should be validated with a finite element analysis (FEA) program. Compare the behaviour, while keeping in mind that the SEM only needs to give an indication of the exact behaviour.
   - Implementation: Test the implementation of the SEM with the previously validated calculations.
   - Prototype: Test the geometric freedom of the proposed modelling method and test the fully developed prototype with a simple structural model. Demonstrate the use process and evaluate the implemented features.

4. **Discussion**

   - Evaluation: Compare results to the stated objectives and corresponding research questions. Determine to what extent the implemented features address the structural and architectural flexibility criteria.
   - Conclusion: Critically examine the methodology and the quantitative as well as qualitative results of the StructuralComponents 5 concept. Discuss the possible impact of the results in current practice.
   - Future research: Offer opportunities of improvement and possibilities to expand the applicability/scope of this research.

3

Proposed Early Design Tool

This section will first give background information about the StructuralComponents papers, which all discuss the conceptual design phase. Afterwards, the specifics of conceptual design tools for medium-rise buildings developed throughout this thesis will be introduced.

3.1 StructuralComponents Background

This project, as already implied by the name, is the fifth addition part of a series of research papers discussing StructuralComponents in the conceptual design of buildings, which are summarised in this section, including NetworkedDesign (Coenders, 2011).

3.1.1 NetworkedDesign

Coenders (2011) discusses conceptual links in the structural engineering and design domain with the computational technology domain in order to improve the adoption of advanced computational technology in structural design. It aims to explore the advantages while preserving the key qualities that make up the design process. Coenders identifies multiple current issues with the structural design process where technology can provide the necessary support. Currently there is higher financial and environmental pressure on projects and their stakeholders, which requires more efficient structural designs. More efficient designs mean that less time can be spent on elaborate studies while the same or usually even higher quality results are demanded. Additionally, socially acceptable design errors have decreased as well as the time to fix them in the case that they do occur. Coenders argues that technology can improve insight and address the mentioned problems. Computational design can handle more detailed information, more flexible design, control and prevent mistakes, improve design manufacturing capabilities, use materials and energy more efficiently and connect more information throughout every project phase. However, there are also other challenges in the building industry that also affect computation. For example, there are many stakeholders and actors with different interests that have to communicate and manage the information. Also, the life cycle of a building is much longer than the usability of the data. Then, there are many unquantifiable measures that have to be incorporated into the design, as well as the problem of rapidly changing information. Coenders also emphasises the contrast between the lack of information and the available design freedom during the early design stage. In order to address these issues, Coenders introduced 'Networked Design', which is described as "a next generation infrastructure for computational structural design and engineering". It aims to provide the concept for the infrastructure for design tools and design frameworks. The system design concepts include object-oriented programming, modularity, replication, plugability, bi-directionality and multi-directionality (Coenders, 2011).

3.1.2 StructuralComponents 1

The first StructuralComponents (Breider, 2008) project is a response to the Structural Design Tools (SDT) approach, introduced by Coenders and Wagemans in 2005, and emphasises the quick generation and simple evaluation of designs. Breider's thesis enables structural engineers to design and analyse two-dimensional tall buildings. It allows the user to model a tall building structure using cores, columns and outriggers in a versatile and flexible way. This tool is based on GenerativeComponent (Aish, 2005) plug-ins and visualises the results in a user friendly dashboard (Breider, 2008).

3.1.3 StructuralComponents 2

Rolvink's (2010) objective was to develop an independent framework based on parametric and associative design (PAD) approach as well as research new design methods for the early design stage of tall buildings, which were then implemented into a toolbox. The toolbox consists of two components, the independent framework and the user-interface representation layer. After also evaluating various modelling methods, various structural components were developed, such as core, outrigger, column, frame and shear wall elements as well as their typologies. These components were then implemented and evaluated in 4 different example high-rise structures using the Finite Element Method. As a result, the implemented design knowledge in combination with the toolbox output provides the structural engineer sufficient insight to see the influence of changes on key design aspects during the conceptual design stage (Rolvink, 2010).

3.1.4 StructuralComponents 3

This project (van de Weerd, 2013) focused on emphasising and expanding the synthesis phase using the abstraction system. It also focused on developing a finite element analysis for tall buildings where the super element method is not suited and to separate the functionality of the prototype along a client-server divide. Van de Weerd discusses how the nature of design in an iterative process, where each iteration is composed on a synthesis, analysis and inference phase. The synthesis phase is in charge of generating alternatives, while the analysis phase measures the performance of that design and the inference phase states the key aspects of the design. He concludes that a higher emphasis on the synthesis phase can indicate the effect of certain parameter changes and therefore help find better or worse solutions as well as measure the risk and flexibility of later stages. Implementing finite element analysis provides additional versatility to objects, however, it also comes at the cost of ease of modelling. Thirdly, re-implementing the prototype along a client-server divide, essentially removing external software dependencies, will provide full data structure openness and more flexibility (van de Weerd, 2013).

3.1.5 StructuralComponents 4

Bovenberg's (2015) focuses on supporting the creative design exploration and composition of design justification. It extends the previous focus from high-rise buildings to other typologies as well as to a more complete design story approach. Various conceptual components are discussed to aid the early design process.

- 'Blank slate' components (follow designer's needs)
- Hierarchical component breakdown (breakdown of structure into substructures)
- Reflective design reasoning (justification behind a design)
- Analysis models as automated reasoning (adaptation of parameter changes)
- Alternative values (represent alternatives in parallel)
- Component variants (support complex alternatives)
- Allow alternative representations of the same model

The above mentioned components were implemented and validated in a multi-story prototype. The validation shows that the conceptual components sufficiently address the design requirements for the early design phase and serves as a proof of concept for future development (Bovenberg, 2015).

3.2 Tool Purpose

StructuralComponents 1 (Breider, 2008) and StructuralComponents 2 (Rolvink, 2010) already discuss a conceptual design tool for high-rise buildings. StructuralComponents 4 (Bovenberg, 2015) starts the transition by defining conceptual components for other building topologies such as multi-story buildings, which this project will focus on. It intends to bridge the gap between architectural and structural engineering software during the conceptual design phase by researching and developing a tool prototype that improves the collaboration between architects and structural engineers.

As discussed in Section 1.3, there are many CAD tools available which allow architects to rapidly model increasingly complex conceptual designs. Analysis software, however, is lagging behind since they use the finite element method, which requires too much information to provide efficient analysis in the conceptual design phase. This also prevents modelling and analysis tools to work well together, making the collaboration process between architects and structural engineers more difficult and time consuming. Currently, they bounce design ideas and solutions back and forth. The architect emails a single or a few design ideas before a meeting, so the structural engineer has some time to come up with solutions. During the meeting they discuss those pre-determined designs and solutions and must repeat the same process every time changes are made or a new design idea is generated. These constant meetings and design changes can be time consuming and expensive for a construction project, providing motivation to improve this process (S. Pasterkamp, personal communication, August 30, 2017).

Usually many members, such as the client or mechanical engineer etc., are also involved in the conceptual design process, but this tool prototype focuses on the collaboration between the architect and structural engineer. Based on this the following definition for collaboration is used.

Collaboration, for this project, refers to the process between the architect and structural engineer in evaluating the feasibility of a conceptual building design and generating design solutions during a brainstorm session.

The purpose of this tool prototype is to integrate the two disciplines together and speed up the collaboration process between the structural engineer and architect through a tool that enables the structural engineer to model and analyse possible load bearing structures within the meeting time. The tool should give real-time feedback to both the structural engineer and the architect about its feasibility, which they can use to improve or generate a new design during the brainstorm session. Allowing architects and structural engineers to suggest changes or generate new designs together and evaluate them during the same meeting could save the project time and money.

In order to achieve this purpose, the following goals have been set for this tool:

Tool Goals:

1. Implement a modelling process that is suited for the flexibility requirements of the early design phase.
2. Determine the structural and architectural feasibility of conceptual designs by only considering the main load bearing structure.
3. Enable result visualisation that is understandable by the structural engineer and architect, enabling them to collaborate and improve the design.

3.3 Limited Scope

Ideally this tool would be available for every building type, however, for this prototype the structural size and type are limited to mid-rise concrete shear wall and core buildings. These are discussed in the next section, followed by other assumptions made during this project.

3.3.1 Mid-rise Building

For this proof of concept concrete mid-rise buildings were chosen as the design objects, however, there are no strict classifications for the "tallness" of buildings to distinguish their properties and requirements. The definitions or guide lines that do exist have changed over the years partly due to technological advances enabling the construction of even taller buildings (Eisele and Kloft, 2003). A few example definitions can be found in Appendix A.1, while the definition for this prototype is discussed below.

This tool prototype is intended for modelling and analysing the structural performance of a medium-rise building in collaboration with architects. However, the tool itself only models and calculates the load bearing structure and does not include the surroundings, the users are responsible for that. Therefore, focusing the definition of a medium-rise building for this tool prototype on the structural aspects is justified. Especially in medium-rise buildings many different configurations are possible and considered due to structural and architectural reasons in the early design phase. Therefore, the general definition of a medium-rise building for this tool prototype is formulated as follows:

A medium-rise building is a structure that can be composed of a configuration of various topology types and functionalities.

However, this definition gives no geometric limitations regarding size or analysis complexity. According to the Eurocode, dynamic analysis is not required until a building exceeds 100m or the slenderness ratio is greater than 1:4 (NEN-EN 1991-1-4, 2005). Dynamic analysis capabilities are not included in this prototype version, so an additional definition of a medium-rise building for this report is given:

A medium-rise building is geometrically limited to an above ground level structure that is up to 100m tall and does not exceed a slenderness ratio of 1:4.

It is important to note that performing dynamic analysis with this method is possible and could be incorporated in the future, which could expand the scope for the tool to also high-rise buildings with height greater than 100m.

3.3.2 Structural System

Buildings can have many different structural systems, however, as the height increases not all systems remain suitable. Both rigid frame and core-wall systems for example are not recommended for buildings above 100m as described in the TU Delft Reader for Structural calculations of High Rise Structures (Ham and Terwel, 2017). Since this tool is intended for mid-rise buildings which do not exceed 100m, these systems suffice. Rigid frame systems are not very effective in transferring horizontal loads to the foundation because the columns and beams experience bending (Hoenderkamp, 2002). Also, they are often not used for buildings higher than 5-10 storeys in the Netherlands for economic reasons. Core systems, as well as wall systems, are much more suitable for taking lateral loads and can be built up to 100-120m tall (Ham and Terwel, 2017). Therefore, this tool will focus on concrete shear wall and core systems for medium-rise structures, which are illustrated in the Figure below.

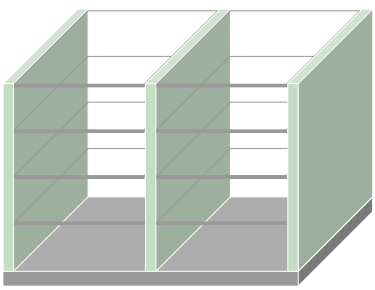

(a) Shear wall system

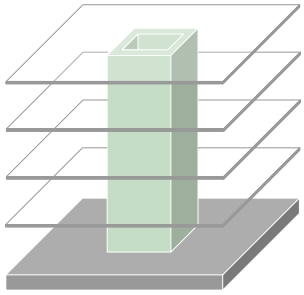

(b) Shear core system

Shear wall system

Shear walls, as shown in Figure 3.1a can be applied to almost every type of building structure. They are usually positioned to limit their impact on the functional use of the building, such as around stairwells, elevator shafts, installation shafts or as end walls. That way there is a very small likelihood they will have to be moved throughout the life cycle of the building. Structurally they are significant, because the in-plane stiffness of the walls contributes to the lateral stiffness of a building (TU Delft, 2017). Concrete has low tensile strength and excessive reinforcement is undesirable, therefore concrete shear walls are usually placed in a location where they take large vertical forces to counteract the tensile stresses due to the lateral load (Dijkstra, 2008).

There are two main types of shear wall structures: non-twisting structures and twisting structures (Dijkstra, 2008). In non-twisting structures the resultant lateral force intersects the torsion centre of the structure, for example for a building with the axis of symmetry along the resultant force. For twisting structures the resultant lateral force is applied eccentric to the torsion centre. These structures require at least three shear walls, whose axis may not intersect all in one point.

Core system

When shear walls enclose a stairwell, elevator shaft or another opening they form a box-shaped section, resulting in a core system. The cross-sectional moment of inertia of a core is much larger compared to a single wall, it contributes to the lateral stiffness in more than one direction and provides the torsional stiffness. The core dimensions must increase with the height of the building, possibly exceeding the staircase perimeter (TU Delft, 2017). However, the core width is usually not larger than 15m to achieve satisfactory gross-nett ratio (Ham and Terwel, 2017). Also, core systems do not have to be closed, such

as in Figure 3.1b. They can also be I-shaped as in the case of some residential buildings where the walls separating homes are connected with a cross wall over the height of the building.

3.3.3 Assumptions

Since this is only a proof of concept, various assumptions were made throughout the requirement sections. These are collected to give an overview of the applicability of the tool prototype.

Early Design Phase

- Instead of looking for exact dimensions, the main goal is to determine the main structural features.
- This design collaboration takes place in the early design phase where no specific dimensions are known, only the building location and function. Initial ideas for the general shape, rough floor areas and elevations may be available, but are free to change.
- The current early design process consists of a time consuming design and solution 'ping-pong' between the architectural and structural engineering offices.
- The collaboration meetings takes place only between the architect and the structural engineer. No doubt other parties are also involved in the design phase such as the client, mechanical engineers, the municipality etc., however, this tool focuses only on the interaction between the architect and the structural engineer.

Structural

- The structural engineer has in-depth structural knowledge and previous structural design experience. It is assumed that an experienced structural engineer is in a leadership position where he/she discussed initial design options and solutions directly with the architect.
- He/She has knowledge about constructible dimensions of elements.
- He/She structural engineer has very limited architectural knowledge.
- The structural engineering firm uses a parametric environment for 3D modelling, such as Rhino-Grasshopper. Therefore, the structural engineer is assumed to have experience with parametric tools and in this case specifically with Grasshopper.
- The global analysis checks of the main load bearing structure give insight into the structural behaviour of the complete detailed building.

Architectural

- The architect has in-depth architectural knowledge and experience. Again, it is assumed the architect is in a leadership position where he/she discussed initial design options and solutions directly with the structural engineer.
- The architect has limited structural knowledge.
- The architectural firm uses a parametric environment for 3D modelling, such as Rhino-Grasshopper. Therefore, the architect is assumed to have experience with parametric tools and in this case specifically with Grasshopper.

3.4 Tool Requirements

In order to improve the collaboration between structural engineers and architects during the early design phase, the requirements for each collaboration phase and for each party have to be determined. These are outlined below and discussed in more detail in the following sections.

- **Modelling**
  In order to foster the collaboration between the structural engineer and the architect, this tool should be developed on a platform that both architects and structural engineers are familiar with and understand.

- **Feasibility Analysis**
  To address collaboration it should also include feasibility requirements from both disciplines. This would guide involved parties to consider and check the feasibility requirements from each other. However, not all of the later discussed checks were implemented, once a few checks are implemented it is clear that further checks can also be implemented.
- **Result Visualisation**
  To aid collaboration while interpreting results and suggesting changes, both the structural engineer and architect must understand the results. The structural engineer should interpret the structural behaviour of the building, and both must understand the feasibility check results to suggest improvements or alternatives.

In order to improve this process and fulfil the goals mentioned in Section 3.2, the modelling, analysis and result interpretation requirements are determined.

3.4.1 Modelling Requirements

This conceptual design tool is intended to be mostly used by the structural engineer to model a possible load bearing structure of the architectural design, however, requirements from both the architect and the structural engineer must be included to enable their collaboration.

Usability

Even though this conceptual design tool is intended to be mostly used by the structural engineer, both should be able to use it in case the architect suggests changes during the meeting. Therefore, also a person with no technical background in structural mechanics should be able to understand and use this tool, which leads to the following requirements:

- use building blocks instead of individual structural elements (wall, beam, floor slab etc.)
- provide understandable and simple connection between building blocks

Real-time modelling

The load bearing structure should be modelled during the brainstorm session with time to study the analysis and examine design alternatives. This leads to the following desired features:

- arrange (stack) whole building blocks of one typology to configure the load bearing structure of an entire building, instead of tediously placing individual structural elements
- implement tool with a program that provides real-time modelling where these building blocks can be incorporated, such as Rhino-Grasshopper

Geometric flexible modelling

Architectural models may be quite complex and design alternatives may require small to dramatic design changes, requiring the modelling process and model to be geometrically flexible. Therefor the following modelling adjustments should be possible.

- parametric changes: dimension or location changes of structural elements
- topology changes: relocate, change or add/remove structural elements
  (see Section 3.5.1 about building blocks)

In the context of this project, geometric flexibility will be defined as follows:

Geometric flexibility corresponds to both: changing the entire structural element types used and adjusting the dimensions and location of each structural element.

3.4.2 Feasibility Analysis Requirements

Not only the structural engineer has analysis requirements, also the architect is interested in dimensions and locations of the model.

Specific Architectural Requirements

For the purpose of this tool it is assumed that the architect not only considers his/her specific requirement, but also others such as the building regulations determined by the government or municipality. Therefore, architectural and other requirements that have to do with the aesthetic design and experience inside the building are included in this section. Structural checks will not be included in this section, even if architects may use some rules of thumb in their conceptual design.

The main architectural feasibility requirements incorporated in the conceptual design of a medium-rise building will focus on:

- **Aesthetics**
  Architects have aesthetic and 'building experience' requirements that relate to the idea behind the model, which can often not be quantified. Therefore, the architect must be present to voice those requirements during the meeting.
- **Functionality**
  In order to accommodate the expected functions of a building, the indoor spatial organisation is determined and floor areas are calculated. The spatial organisation considers the adjacency of indoor spaces, distances between indoor spaces and indoor spaces connected to the outdoor spaces etc., while floor areas indicate the available space for specific functions, which also relates to revenue estimates for the client. Providing the adequate functionality could be checked via floor areas, distances, a simulation and practical experience.
- **Vertical movement**
  Vertical transportation facilities are usually incorporated inside a structural core, so adjustments made to the elevators or stairs also affect the structural mechanics of the whole structure (Timmer, 2011). The horizontal movement is also important from an architectural perspective, however it will not be considered in the conceptual design tool since floor separation walls are mostly non-structural and therefore do not have to be designed in the early design stage. Fire safety standards constraining the horizontal and vertical movement, can be incorporated via the distance and time it takes to get to a fire escape.
- **Daylight**
  The daylight entering a building affects the experience inside, but is also regulated with limits such as the window opening size, the depth of a room and the environment. Determining adequate daylight can therefore be quantified by a dimensions and/or based on practical experience.
- **Other**
  There are other requirements set by the architect or municipality such as the ceiling height or a maximum time to reach a fire escape, which could also be quantified.

The dimension requirements can be implemented with unit feasibility tests, where the tool determines if a value is within a certain range and outputs a warning message and/or changes the colour of the affected element. These are clear signs to the architect, which can be understood with or without a background in structural mechanics.

Specific Structural Requirements

Taranath (2016) emphasises that "the key to successful application of structural design ideas at the schematic stages of architectural design rests in being able to look at the big picture first without getting bogged down by the details". Therefore, the structure should be simplified to only include the most essential load bearing structure during the conceptual design phase.

The structural checks should indicate the structural feasibility of the mid-rise building. Structural feasibility indicates whether or not a structure can be built and used safely by evaluating dimensions, material costs, construction time and construction costs. However, for the purpose of this report, structural feasibility was limited to the global ultimate and serviceability limit state checks, which are illustrated in Figure 3.2. The analysis of individual local members is not included, because the purpose is not to complete a final detailed analysis, but an initial feasibility analysis of the design concept.

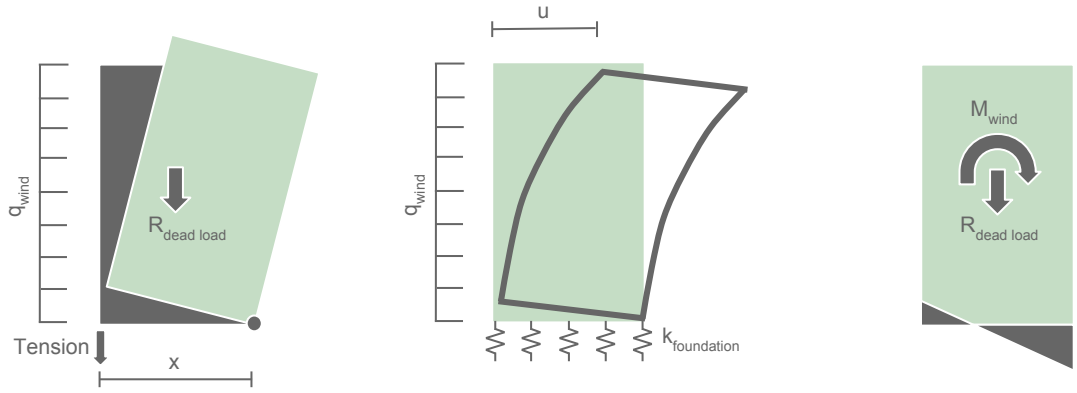

(a) Stability *(b) Stiffness* *(c) Strength*

Figure 3.2: Structural feasibility checks

Stability refers to limiting the tensile stresses in concrete corresponding to the moment caused by wind and eccentricity, see Equation 3.5 and 3.1. The building stiffness limits its lateral deflection, which is a serviceability requirement (SLS), due to wind and/or earthquake loads (earthquake loads are not included). See Equations 3.3 if the foundation is assumed to be rigid and Equation 3.4 if the stiffness of the foundation was calculated. The strength requirement demands a certain compressive strength of the building material, see Equation 3.6. The following equations were adopted from the TU Delft course readers for Highrise Buildings (Ham and Terwel, 2017), Building Structures 2 (TU Delft, 2017) and Eurocode 1992 (British Standards (BSI), 2004).

See below for the equations for the global structural checks:

- **Stability**

$$ULS: \quad \frac{\gamma_Q * c_d * M_{w+e}}{x} < \gamma_{G,inf} * R_d \tag{3.1}$$

- **Stiffness**
  inter-storey drift:

$$SLS: \quad \frac{c_d * q_w * h_{storey}^4}{8 * E_{eff} I} < \frac{h_{storey}}{300} \tag{3.2}$$

  assumed fixed foundation:

$$SLS: \quad \frac{c_d * q_w * h^4}{8 * E_{eff} I} < \frac{h}{750} \tag{3.3}$$

  including foundation stiffness (k):

$$SLS: \quad \frac{c_d * q_w * h^4}{8 * E_{eff} I} + \frac{c_d * 2 * M * h}{k_{found} * x^2} < \frac{h}{500} \tag{3.4}$$

- **Strength**

$$ULS: \quad +\frac{\gamma_Q * M_w}{W} - \frac{\gamma_{G,inf} * N_{dead}}{A} < 0 \tag{3.5}$$

$$ULS: \quad -\frac{\gamma_Q * M_w}{W} - \frac{\gamma_{G,inf} * N_{dead}}{A} < f_{cd} \tag{3.6}$$

Checks for torsional resistance should also be considered, however, this project will only focus on the listed checks. For these it is important to note that the global structural checks only apply to the main load bearing structure, so they only provide exact checks for the main estimated structure and not for a detailed building model.

The displacement, force and stress analysis results from the main load bearing structure are assumed to indicate the order of magnitude of the detailed model results. Therefore, if the structural checks for the main structure are met, then the design concept is considered feasible and the detailed structure should also be possible to build safely.

Structural feasibility is defined as satisfying the presented global structural checks in the conceptual design phase, assuming the calculated behaviour results indicate the order of magnitude of the detailed design behaviour.

Note: In order for the structural feasibility definition to hold, a comparison between a load bearing structure and the detailed design of a building should be completed to show whether these equations really give enough insight into the final design behaviour.

3.4.3 Feasibility Results

The structural engineer and the architect must be able to understand their respective feasibility results and checks, and be able to use them to adapt the design accordingly during the meeting.

Real-time results

The feasibility results should be calculated in real-time in order to see the effects of changes immediately, which leads to the following requirements.

- be able to discuss changes/solutions during the brainstorm session
- use symbolic algebra with differential equations to allow for quick calculations

Visual results

The results should be clear to also people without structural mechanics knowledge, in order to promote collaboration by discussing the results. The following points are expected to help do this.

- visualise internal forces and displacements along the height
- feasibility checks show up as warning messages and/or change colour of affected element

3.5 Modelling Architecture

As a result of the modelling requirements from Section 3.4.1, whole buildings will be composed by arranging 'building blocks' together. Each building block represents one type of floor plan, which is referred to as 'topology'. This section will discuss the possible building blocks available, how they can be arranged on a global level to represent an entire building, and how they connect to each other.

3.5.1 Building blocks

The architectural geometric freedom requirement is addressed in two main points. First, different topologies are available for the user via many types of building blocks. Second, the individual elements in each block can be parametrically adapted, allowing flexible topologies.

For the scope of this project a number of geometric building blocks will be presented here, but not all of them will provide analysis feedback. The analysis will only be done for 3 of them to provide a proof of concept and show that more of them could be calculated in the future. The analysis and other limitations of the calculated building blocks will be discussed in Section 3.6.

Fully implemented geometric and analysis building blocks

Three types of topologies are fully implemented, meaning their geometry is parametrically adaptable and the structural analysis is calculated accordingly.

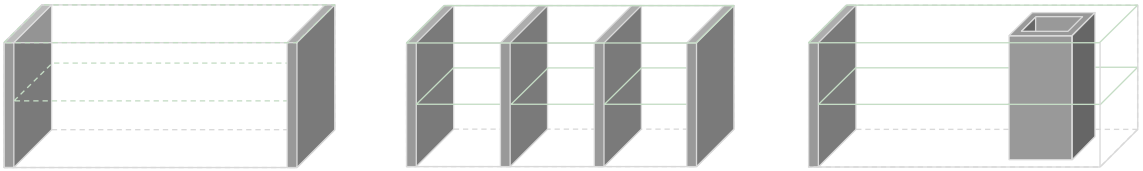

(a) two parallel walls without floor stiffness *(b) four parallel walls with floor stiffness* *(c) one wall and one core with floor stiffness*

Figure 3.3: Building block with parametric topology

Potential geometric and analysis building blocks

These building blocks are only available geometrically, so the geometry can be parametrically adjusted. Analysis capabilities could be implemented using the already determined general method, but is not necessary to do for this project, since the method has already been implemented in three other cases.

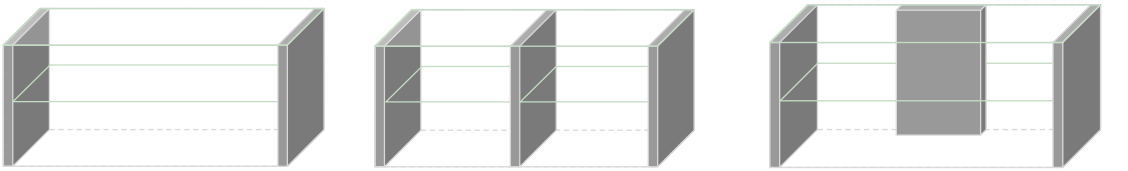

(a) two parallel *(b) three parallel* *(c) two parallel and one perpendicular*

Figure 3.4: Building blocks with various wall arrangements including floor stiffness

(a) 1 core *(b) 2 cores*

Figure 3.5: Building blocks with multiple cores including floor stiffness

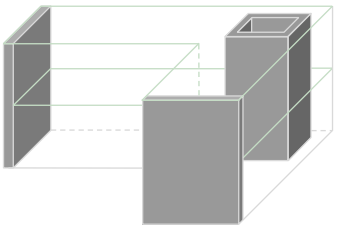

Figure 3.6: Building block with both cores and walls

Geometric building blocks requiring further research into the floor stiffness

These building blocks are also only available geometrically, so they can be parametrically adjusted, but not analysed. Further research outside of this project must be done regarding the stiffness of cantilevering floors or floors with openings.

(a) floor cantilever *(b) floor with opening*

Figure 3.7: Building blocks with cantilevering floor or openings in floor

Parametric topologies

The dimensions and location of the individual elements in each building block can be adjusted through parametric modelling. However, if the number or type of an individual element should be changed a different building block has to be chosen. Grasshopper and Dynamo for example are parametric modelling programs, which allow users to 'program' a model by connecting components in a visual interface. Parametric design will be discussed further in relation to the building blocks in the following section.

Figure 3.8 illustrate how the individual elements within an example building block can be changed.

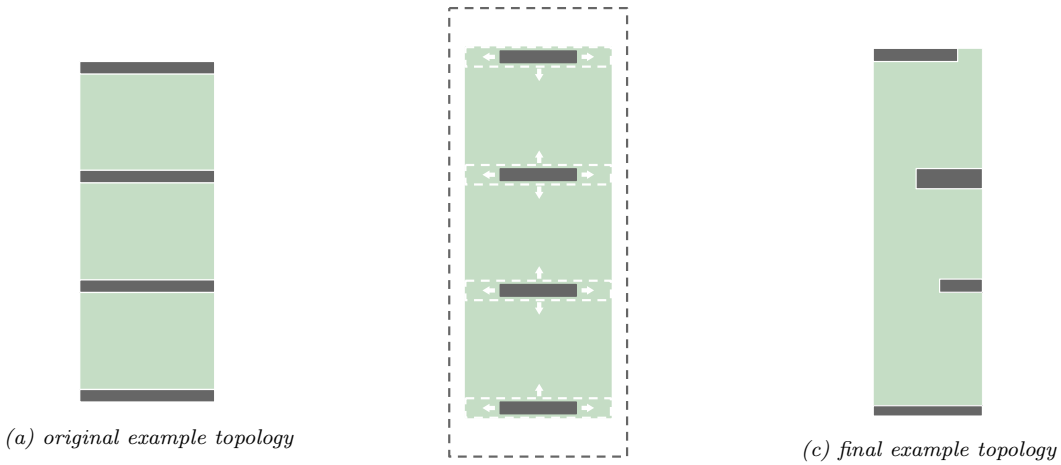

(a) original example topology *(b) optional geometric changes* *(c) final example topology*

Figure 3.8: Building block with parametric topology

3.5.2 Global arrangement of building blocks

The selection of geometric building blocks can then be placed vertically and horizontally relative to each other, shown in Figure 3.9, resulting in the complete design. The analysis of a structure is possible if the building blocks are connected vertically, if they are connected horizontally then they will be considered as separate entities. This limitation will be discussed further in the analysis Section 3.6.

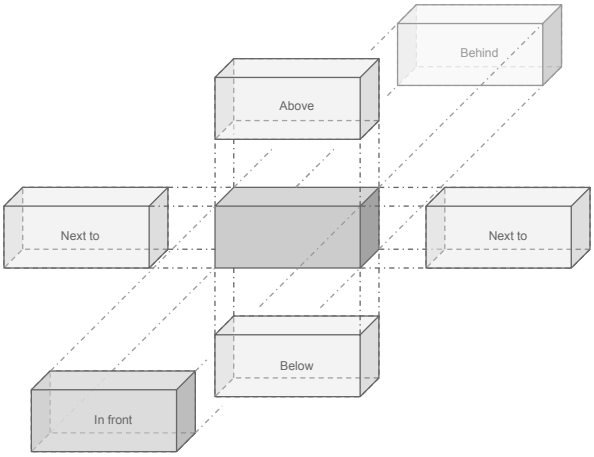

Figure 3.9: Global arrangement diagram of the building blocks

The exterior of a building often expresses an architectural idea, requiring geometric freedom of, in this case the building blocks. Some examples are displayed in Figure 3.10. The final building configurations are not limited to these specific examples, they are only shown to illustrate how the building blocks connect. Plus, they are not guaranteed to be structurally or architecturally feasible.

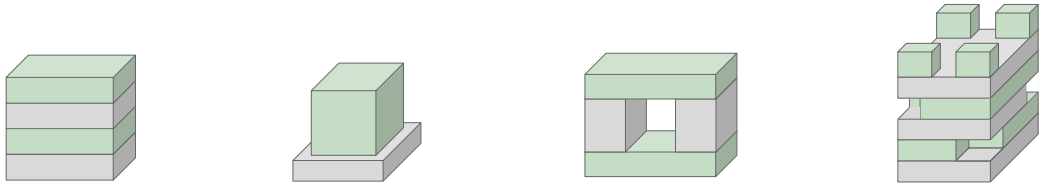

(a) very simple *(b) simple* *(c) medium* *(d) complex*

Figure 3.10: Building block arrangement complexity

This type of modelling lends itself to the "stacking" architectural technique, but is not limited to it. However, free-form structures with very irregular shapes or curved facades are difficult to represent with these blocks, for example the bottom part of the structure in Figure 3.11. Since the curved part is not supported, either a simplified representation could be used or a building block for each floor is required, which would be very tedious to model.

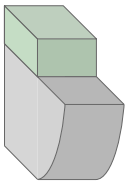

Figure 3.11: A structural design that would be very inconvenient to model with this tool

3.5.3 Local connections of building blocks

The global geometric arrangement of the building blocks have been discussed, so now their physical connection is discussed. A few connection options are discussed, before settling on the second one.

1. Connect individual blocks to previously defined points and determine the connection by common nodes.
    - Connect via two points that represent the entire 'space' of the building block
    - Connect individual stability elements to points on grid
2. Connect an individual block directly to another one and so forth.
    - Connect via two points that represent the entire 'space' of the building block
    - Connect individual stability elements to stability elements in another building block

Using previously defined points could be helpful to model a specific architectural model, or directly use the architectural model. This method would allow the load bearing structure to match very well with the architectural model and even adjust along with dimensional changes made to the architectural model. In the conceptual design stage, however, it is unlikely that only one design will be considered and that only small changes will be made. This would be more likely later in the design process. In the early design stage often many designs are considered. It is important to be able to make not only small dimension changes, but also design changes on a larger scale such as changing the topology or overall shape. This would be easier to do if the building blocks were directly connected together, plus the user could see more clearly how the building blocks connect structurally. Therefore, the second method is implemented.

Within this method there are two further options. One way is to connect building blocks via two points representing the entire block area, see Figure 3.13. However, this method does not indicate where the stability elements can be located. If one block is above another, then the stability elements in the top block must have stability elements underneath, they cannot float.

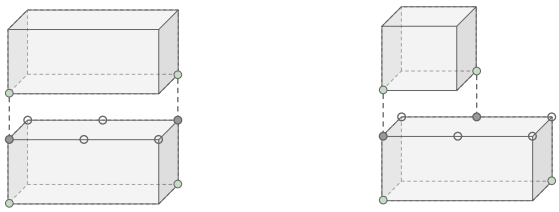

Figure 3.12: Building blocks connected with 2 points

The other method addresses this point by requiring the top end points from the stability elements in the bottom building block as input for the bottom end points of the stability elements in the top building block. To make the connection simpler, the wall end points form a line, representing the connection curve. Since the connection line is made up of two points, it also transfers the motion limit to a connected stability element.

Figure 3.13: Building blocks connected with stability element lines

An even better way to connect them would be with a rectangle, then also the thickness of the lower stability element can be included as a limitation.

3.6 Feasibility Analysis

As already mentioned, the feasibility analysis implementation is limited to a proof of concept, rather than a full implementation. Three of the building blocks include individual feasibility analysis and two of those three can be combined to form a larger structure with feasibility analysis. The feasibility analysis results in visual internal forces and displacements as well as the structural and architectural checks.

3.6.1 Individual analysis

The three building blocks with analysis capabilities are shown in Figure 3.14. The analysis method is described in detail in Chapter 4.

The first building block, see 3.14a is the simplest, and only requires two symmetric walls to be calculated. The walls will be represented as two Euler-Bernoulli beams that can resist in-plane lateral forces and calculated using differential equations. The second (also symmetric) building block, see 3.14b, contains four walls instead of two, and includes the floor stiffness. The third building block, see Figure 3.14c, with analysis includes a core, meaning it has a torsional stiffness and can resist lateral forces from both directions. Walls and cores are included in these building blocks, because they are very common structural elements in mid-rise buildings as discussed in Section 3.3.2.

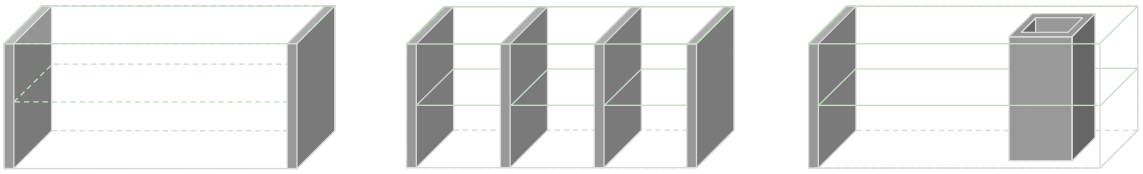

(a) two parallel walls without floor stiffness

(b) four parallel walls with floor stiffness

(c) one wall and one core with floor stiffness

Figure 3.14: Building block with parametric topology

Floor stiffness significance
In practice many firms assume the floor stiffness to be infinitely stiff during the conceptual design phase (P. Hoogenboom, June 09, 2017, Personal Communication), however, Steenbergen (2007) shows in his dissertation that the floor stiffness causes different internal force and displacement results along the height when building parts with different topologies are placed on top of each other. Therefore, the floor stiffness will be included in the calculations.

3.6.2 Combined analysis

Combined analysis will be supported for the building block with 2 and 4 walls. These can be combined with each other to compose a building with multiple topologies, different dimensions and loading. However, not only a topology change requires a different building block, also a change in the loading conditions, see Figure 3.15b. For example if the functionality of the building changes from commercial to residential, the floor area loads change and therefore require a different building block. The same happens when the wind load changes along the height.

(a) Different topology or dimensions

(b) Different loading

Figure 3.15: Geometry changes and load changes require different building blocks

The supported combinations are shown in Figure 3.16.

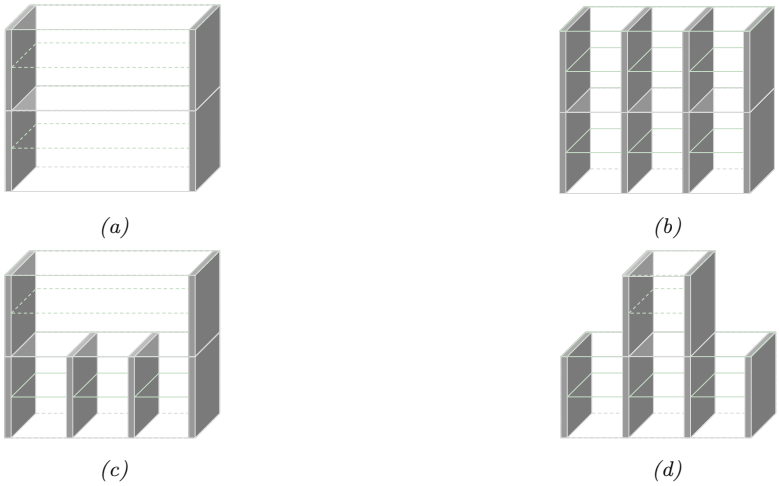

(a) *(b)* *(c)* *(d)*

Figure 3.16: Building block combinations

3.7 Feasibility Results

The feasibility checks should be understood by both the structural engineer and the architect, while the structural behaviour results are aimed at the structural engineer.

3.7.1 Internal forces and displacements

The structural behaviour will be conveyed through the internal forces (moment and shear), normal forces and the displacements and rotations. The normal forces will be displayed at the bottom nodes, while the internal shear and moment forces, as well as the displacement and rotation results, will be visualised along the height of the total structure.

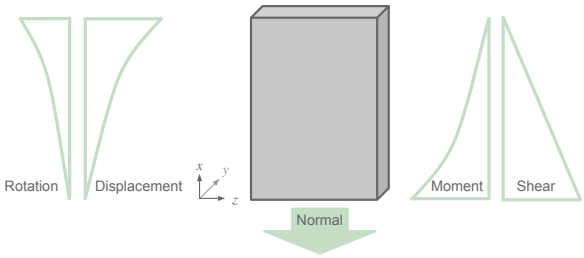

Figure 3.17: Structural behaviour of stability element(s)

The feasibility checks can be visualised by the colour of the structural element as shown in Figure 3.18. For example if the depth to the window exceeds the limit, the floor turns from grey to red and when the stiffness check is not satisfied for a wall, only that wall will turn red.

(a) Failure of a stability element check *(b) Failure of floor check*

Figure 3.18: Visualisation of feasibility checks

3.8 Use process

From a user's perspective the framework was designed to be very simple. Figure 3.19 illustrates how the features described in this Chapter work together in terms of the user. The user starts off with a "starting info" component in Grasshopper, to which he/she can attach a "building block" component with a specific structural topology. Additional building blocks can be connected vertically to the previously ones to compose a whole building. All of the building blocks must then be connected to the "analysis" component in order to calculate the feasibility results and visualise them via the "result viewer" component.

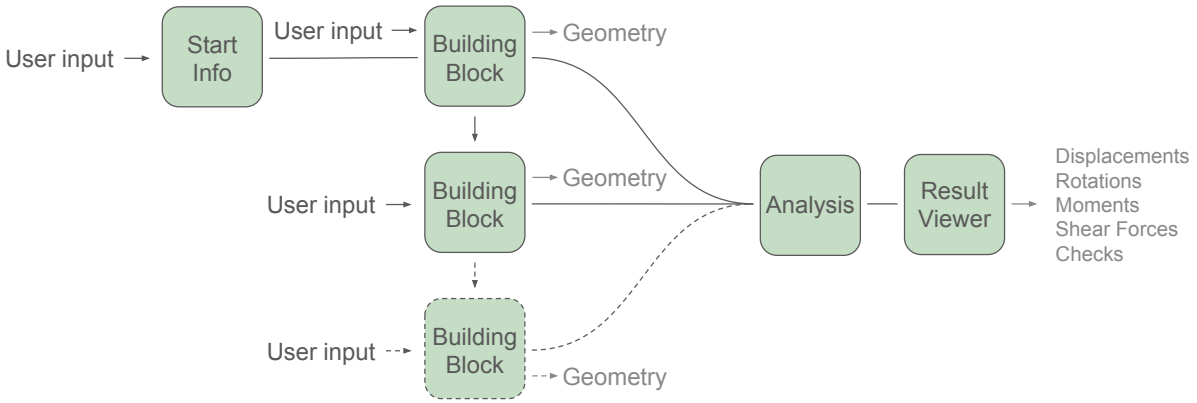

Figure 3.19: Overview of tool architecture

Intended Users
The main user to configure the building blocks is intended to be the structural engineer, since he/she is tasked with finding a feasible load bearing structure based on architectural input. However, the architect should also be able to use the tool to make desired changes when necessary, rather than explaining them. After evaluating the visualised results and checks, additional changes can be made by the structural engineer and the architect. Whole new structures can also be made for alternative designs. For examples see Chapter 6.

Tool usage
The individual tool usage steps are described here. Building design is an iterative process, so adjustments can be made at every step including changing the design idea in the first step.

1. The architect present one or multiple conceptual designs.
2. The structural engineer chooses a structural system and construction method that support not only the physical design, but is also in-line with the architectural concept.
3. Next, the building is divided into building blocks representing the main load bearing structure that matches the topology and loading of the chosen structural system.
4. The various building blocks are connected via the stability elements.
5. Estimated loading is applied based on the location and function of the building.
6. Determine the design feasibility by evaluating the structural and architectural checks.
7. Based on the visualised reaction forces, deflection and internal forces the structural engineer and architect can learn and understand more about the structural behaviour.
8. Changes can be made by adapting dimensions and locations parametrically and/or by adding/ removing/ switching building blocks until the structure as a whole is structurally and architecturally feasible.

3.8.1 Feature and Use Check List

Figure 3.20 shows a table comparing the tool requirements during the conceptual design phase with the provided features. The shaded in boxes underneath "component library" are a lighter shade of grey, because only a few building blocks will be implemented in this tool prototype. More building block components would allow much more flexibility and freedom and be necessary to properly use this tool, however, they are not necessary for a proof of concept. There is a separate "discussion" column to include the collaboration occurring during the meeting but outside of the tool. The architect for example has to determine if the structure meets the aesthetic requirements, since these cannot be quantified into the feasibility checks. The structural engineer is in charge of designing the load bearing structures based on architectural drawings, the tool does not automatically create structures from architectural input. Also, structural design changes that relate to the structural behaviour or architectural input are determined by the structural engineer and not the tool. This way also the unquantifiable requirements can be included in the final design.

Requirements vs. Features			Tool Features								Meeting
			Rhino - Grasshopper		Building blocks		Feedback			Analysis	
			3D model	Parametric	Component library	Dimensions & location	Dimension Checks	Internal Forces & displacements	Stress Checks	Symbolic differential equations	Discussion
Conceptual Phase Requirements	Architectural	Geometric freedom	■	■	■	■					
		Aesthetics									■
		Vertical movement	■	■	■	■					
		Daylight & other				■	■				
		Feasibility feedback	■				■			■	
	Structural	Stability							■		
		Stiffness (inter-storey)							■		
		Stiffness (fixed foundation)							■		
		Stiffness (estimated foundation)							■		
		Behaviour transparency	■	■				■		■	
		Feasibility feedback							■	■	
		Guidance									■
	Collaboration	Quick modelling		■	■	■				■	
		Support unknown information								■	
		Real-time results								■	
		Visual results	■				■	■	■		

Figure 3.20: Requirements vs. Features Comparison

4

Super Element Method

In order to analyse mid-rise buildings, a not so traditional structural analysis method is proposed. It is a type of super element method which discretises an entire structure based on topology. This process intends to simplify the analysis process by dividing the entire structure into topology types (part of building with the same cross section), instead of into every member (column, beam, wall etc.).

4.1 Traditional Super Element Method

According to Qu (2004) a super element is "a group of finite elements in which part of the degrees of freedom are condensed out for computational and modelling purposes". Super elements have to physically form a structural component on their own and mathematically have to be rank-sufficient. The super element method has 3 main steps, which are illustrated in Figure 4.1. First, the complete structure is decomposed into substructures in such a way that as many possible components have the same shape. The second step is to construct a super element from the substructures. In this step, usually, a full finite element model is developed for the substructure, which is then condensated to remove part or all of the internal degrees of freedom. Next, create the super element by assembling the reduced models. The third step assembles the super elements to formulate the reduced global model of the complete structure. The size of the final global model should be much smaller than the full finite element model, especially if repetitive substructures were used.

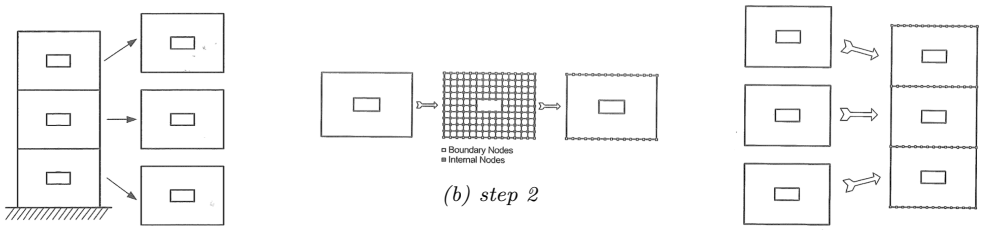

(a) step 1 *(b) step 2* *(c) step 3*

Figure 4.1: Steps involved in the traditional super element method

Within the second step many different condensation methods can be used. For static super elements the static condensation or Guyan method is used. However, there is also the exact and dynamic condensation approach, which produce exact and dynamic super elements respectively. However, for this thesis only static super elements will be used, therefore the other more accurate but also complex super elements will not be discussed further. The super element method provides advantages over the normal finite element method, because it contains more information but requires smaller storage space and is valid for a comparative complex component, which finite elements are not. One disadvantage for traditional static super elements is that they are not beneficial for modelling simple structures, because the results are usually the same as if a course finite element mesh was used. It is also important to know that only the lowest natural frequencies are close to the exact value.

The decomposition of a large and complex structure into substructures may continue hierarchically, in the sense that the super elements are made up of other smaller super elements. This leads to the use of multilevel super elements. The implementation of this technique into a general FEM program called Super Element Structural Analysis Modules (SESAM) was introduced in 1974 and later a database to program multilevel super elements was introduced in 1983 by Jacobsen called ICES (Qu, 2004).

4.2 Super Element Method using Differential Equations

For the analysis of mid-rise buildings a slightly different super element method is used. It still involves decomposing a structure into substructures, such as walls, cores and floors, and combining these to construct super elements, see Figure 4.2. However, instead of using a condensed finite element model for the substructure, a differential method will be used. As stated by Steenbergen and Blaauwendraad (2007), the use of a differential super element method "is intended as a powerful tool for the structural designer in the preliminary design stage, when the main interest is gathering insight into the force flow in the structure for different preliminary designs". This method allows quick analysis of only the structurally important elements and gives insight into their behaviour, enabling the designers to make necessary changes early on during the design process. Finite element method (FEM) programs are available for detailed structural analysis during later design stages. The computing time necessary for FEM software is not a problem with modern computer power. They are able to quickly analyse a particular building, but

not give real-time results for a conceptual parametric building model (Steenbergen and Blaauwendraad, 2007).

For now only the static analysis of the mid-rise buildings will be explored, however, the dynamic equations can also be derived using the differential super element method in cases where the dynamic behaviour of a structure is important.

This approach was first applied by Dusseldorp (2000) on slender structures and Steenbergen (2007), who expanded its applicability to stocky and slender structures. Some of the super elements derived by Steenbergen (2007) will be used in this project, since the overall method presented remains the same. These super elements are universally valid and can be applied to other building plans as long as the stiffness matrix is derived accordingly.

4.2.1 Super elements

Three types of super elements will be discussed in this section. All of three were also used by Steenbergen (2007) and are illustrated in Figure 4.2.

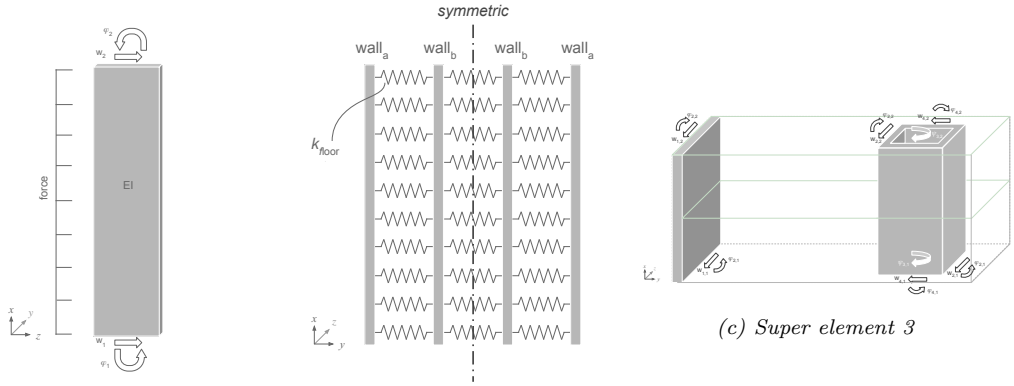

(a) Super element 1

(b) Super element 2

(c) Super element 3

Figure 4.2: Derived Superelements

Super element 1, see Figure 4.2a, is composed of a single wall with the possibility of applying an in-plane distributed wind load. This element is the simplest one and will be used to demonstrate how the differential super element method works. Super element 2 is slightly more complicated as it is composed of four parallel walls and includes a representation for floor systems between walls, shown as springs in Figure 4.2b. The floor system transfers the wind load from the facade to the stability elements. It is also possible to assume a stiff floor system in the conceptual design phase, because the force transfer doesn't have to be exact in this phase. However, Steenbergen (2007) found that the floor stiffness plays a particularly important role at the vertical connection of building floors with different topologies. Since the floor plan often changes in mid-rise buildings, the floor stiffness is not assumed to be infinitely stiff and instead calculated with the super element method. The third super element, see Figure 4.2c, is composed of one core and one shear wall, enabling resistance to an applied wind load in the z and y direction. This element was implemented, because cores occur quite frequently in mid-rise buildings. Plus, due to the core it can resist wind load from two directions and resist torsional loading.

In general, only the flexural stiffness (EI) of the stability elements in the main direction are considered. The in-plane deformation of the floors is included and represented by an elastic connection between the stability elements as shown in Figure 4.2b. Floors usually transfer forces in-plane (membrane action) or out-of-plane (bending action). However, in this paper only the membrane action is considered due to the construction method used in Western Europe (Steenbergen, 2007).

4.2.2 General procedure

The equation that describes the general procedure for the super element is well known:

$$f = Kd \tag{4.1}$$

where d is the vector containing the n degrees of freedom, K is the stiffness matrix and f is the force vector. In order to use this equation to analyse the super elements, the stiffness matrix and force vector have to be determined as well.

The general procedure followed for each super element is summarised in the following steps and described in more detail below:

0. **Choose sign convention**
   The chosen sign conventions for the internal and external forces have to be used consistently throughout the derivation.
1. **Determine the floor stiffness matrix**
   If the floors transfer forces between super elements, the floor stiffness for that arrangement has to be determined. When only one stability wall or two stability walls (with symmetric loading) are present in the super element, the floor stiffness does not contribute to the overall lateral load resistance.
2. **Derive the differential equations**
   The behaviour of each cross-sectional topology is represented by a governing differential equation, which is derived from the kinematic, equilibrium and constitutive equations, based on a previously designated sign convention.
3. **Calculate the stiffness matrix**
   During the third step the stiffness matrix is calculated from the displacement, rotation, moment and shear equations.
4. **Map the force transfer**
   The fourth step involves mapping the transfer of the externally applied forces to the sub-elements.
5. **Derive the nodal equivalent forces**
   For externally applied forces that are not located at the end nodes, the nodal equivalent forces are determined.
6. **Assemble and partition f = Kd to solve for unknowns**
   Here, the displacement vector, stiffness matrix and force vector are assembled and partitioned in order to solve for the unknown displacements and internal nodal forces.
7. **Calculate the structural behaviour equations**
   During the last step the integration constants are solved for using the known boundary conditions. Once all the integration constants are determined, they can be plugged back into the deflection, rotation, internal moment and internal shear equations to illustrate the structural behaviour of the building.

The detailed derivation procedure can be found in Appendix B.1

4.3 Super element Derivations

Each super element is derived separately in this section. Parts that are derived in full detail by Steenbergen (Steenbergen, 2007) will not be shown in full detail here, see his dissertation for more detail.

All of the derivations use the same sign convention discussed first. The super element derivations follow.

4.3.1 Sign Convention

The super elements are derived according to two sign conventions. Figure 4.3 shows the sign convention used for section forces (internal forces), while Figure 4.4 illustrates the sign convention for element forces (external forces).

Figure 4.3: Sign convention for the Euler-Bernoulli stiffness matrix validation

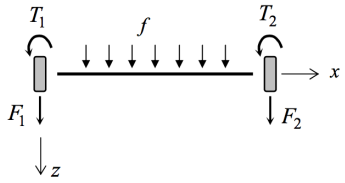

Figure 4.4: Steenbergen's sign convention for the super element 1 (Bernoulli beam) stiffness matrix derivation (Steenbergen, 2007)

4.3.2 Super element 1 derivation

The derivation for super element 1 is not in Steenbergen's (2007), because it yields a well known stiffness matrix and nodal force vector. Therefore, it will be derived in full here to illustrate and validate the procedure.

The first super element is composed of a single wall, shown in Figure 4.5, and is represented by the differential equation for an Euler Bernoulli beam. It can be combined with itself or other super elements, however, it does not support integrated floor systems, although a floor system could be added. Therefore it also skips the floor stiffness calculation step and starts with the differential equations.

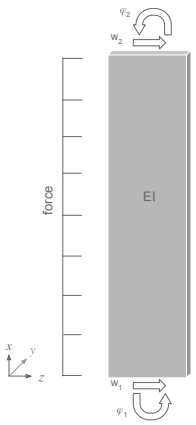

Figure 4.5: Super element 1

Differential equation

Since each end of the Euler Bernoulli beam contains one displacement (w) and one rotation (θ) degree of freedom, the d and f vector look as follows:

$$d = \begin{bmatrix} w_1 & \theta_1 & w_2 & \theta_2 \end{bmatrix}^T$$
$$f = \begin{bmatrix} F1 & T1 & F2 & T2 \end{bmatrix}^T$$

As already mentioned, an Euler Bernoulli beam is used to calculate the structural behaviour of a single wall. Although the differential equation for an Euler Bernoulli beam is well known, it will be derived to illustrate the procedure used also for the other super elements. First the kinematic equations are determined based on the previously designated sign convention and the following variables.

displacement	$= w$
rotation	$= \theta$
slope	$= \rho$
curvature	$= \kappa$
strain	$= \epsilon$

$$\theta = -\frac{dw}{dx} \tag{4.2}$$
$$\kappa = \frac{1}{\rho} \tag{4.3}$$
$$\epsilon = \frac{z}{\rho} = z\kappa \tag{4.4}$$

Next, the vertical and moment (M) equilibrium of an infinitely small beam piece with width dx is used to derive the equilibrium equations, where q is the distributive load, V is the shear force and M the moment.

$$-q = \frac{dV}{dx} \tag{4.5}$$
$$V = \frac{dM}{dx} \tag{4.6}$$

The constitutive equation is derived with the help of the kinematic relationships to result in:

$$M = EI\kappa = EI\frac{d\theta}{dx} = -EI\frac{d^2w}{dx^2} \tag{4.7}$$

Combining Equation 4.6 and Equation 4.7 with Equation 4.5 results in the governing differential equation for an Euler Bernoulli beam and for super element 1:

$$\frac{d^2}{dx^2}\left(EI\frac{d^2w}{dx^2}\right) = q \tag{4.8}$$

Stiffness matrix

Since the stiffness matrix of an Euler Bernoulli beam is well known, this derivation example serves as a verification of the procedure.

The homogeneous solution of Equation 4.8 is:

$$EI\frac{d^4w}{dx^4} = 0$$

Integrating both sides gives the displacement (w) equation including integration constants (C_i), from which the rotation, moment and shear equations can be determined.

$$w(x) = \frac{1}{EI}\left(\frac{1}{6}C_1x^3 + \frac{1}{2}C_2x^2 + C_3x + C_4\right) \tag{4.9}$$

$$\theta(x) = -\frac{dw}{dx} = \frac{1}{EI}\left(-\frac{1}{2}C_1x^2 - C_2x + C_3\right) \tag{4.10}$$

$$M(x) = EI\frac{d\theta}{dx} = -C1x - C2 \tag{4.11}$$

$$V(x) = \frac{dM}{dx} = -C1 \tag{4.12}$$

The derived differential equations for the displacement and rotation are then evaluated at the corresponding nodal position, and input into Equation B.1.

$$\begin{bmatrix} 0 & 0 & 0 & \frac{1}{EI} \\ 0 & 0 & -\frac{1}{EI} & \\ \frac{\ell^3}{6EI} & \frac{\ell^2}{2EI} & \frac{\ell}{EI} & \frac{1}{EI} \\ -\frac{\ell^2}{2EI} & -\frac{\ell}{EI} & -\frac{1}{EI} & 0 \end{bmatrix} \begin{bmatrix} C_1 \\ C_2 \\ C_3 \\ C_4 \end{bmatrix} = \begin{bmatrix} w_1\,(x=0) \\ \theta_1\,(x=0) \\ w_2\,(x=\ell) \\ \theta_2\,(x=\ell) \end{bmatrix}$$

This can be rearranged to $C = H^{-1}d$.

$$\begin{bmatrix} C_1 \\ C_2 \\ C_3 \\ C_4 \end{bmatrix} = \begin{bmatrix} \frac{12EI}{\ell^3} & -\frac{6EI}{\ell^2} & -\frac{12EI}{\ell^3} & -\frac{6EI}{\ell^2} \\ -\frac{6EI}{\ell^2} & \frac{4EI}{\ell} & \frac{6EI}{\ell^2} & \frac{2EI}{\ell} \\ 0 & -EI & 0 & 0 \\ EI & 0 & 0 & 0 \end{bmatrix} \begin{bmatrix} w_1 \\ \theta_1 \\ w_2 \\ \theta_2 \end{bmatrix}$$

Next the section force equations are arranged into Equation B.3 (f = GC).

$$\begin{bmatrix} V_1\,(x=0) \\ M_1\,(x=0) \\ V_2\,(x=\ell) \\ M_2\,(x=\ell) \end{bmatrix} = \begin{bmatrix} 1 & 0 & 0 & 0 \\ 0 & 1 & 0 & 0 \\ -1 & 0 & 0 & 0 \\ -\ell & -1 & 0 & 0 \end{bmatrix} \begin{bmatrix} C_1 \\ C_2 \\ C_3 \\ C_4 \end{bmatrix}$$

Now C is substituted by $H^{-1}d$ from Equation B.2 resulting in Equation B.4. From this it follows that $K = GH^{-1}$, which is evaluated below to give the stiffness matrix for an Euler-Bernoulli beam given the sign convention in Figure 4.4:

$$K = EI \begin{bmatrix} \frac{12}{\ell^3} & -\frac{6}{\ell^2} & -\frac{12}{\ell^3} & -\frac{6}{\ell^2} \\ -\frac{6}{\ell^2} & \frac{4}{\ell} & \frac{6}{\ell^2} & \frac{2}{\ell} \\ -\frac{12}{\ell^3} & \frac{6}{\ell^2} & \frac{12}{\ell^3} & \frac{6}{\ell^2} \\ -\frac{6}{\ell^2} & \frac{2}{\ell} & \frac{6}{\ell^2} & \frac{4}{\ell} \end{bmatrix}$$

The result matches the well known Euler-Bernoulli beam stiffness matrix, validating the procedure.

Force transfer

Super element 1 only takes symmetric loading, since it does not have torsional stiffness, making it easy to calculate the force on each all.

Nodal equivalent forces

Now the described procedure will be applied to super element 1.

One particular solution for the differential Equation 4.8 is:

$$w_{part}(x) = \frac{fx^4}{24EI}$$

The particular solution is then used to determine the element forces at the nodes via the constitutive equations and according to the sign conventions presented in Figure 4.3 and Figure 4.4.

$$v_1^{(1)} = \begin{bmatrix} F_1 \\ T_1 \\ F_2 \\ T_2 \end{bmatrix} = \begin{bmatrix} -V_1 \\ -M_1 \\ V_2 \\ M_2 \end{bmatrix} = \begin{bmatrix} 0 \\ 0 \\ -f\ell \\ -\frac{1}{2}f\ell^2 \end{bmatrix}$$

For the second part, the displacement vector due to the particular solution is calculated.

$$u_{part,1} = \begin{bmatrix} w_1 \\ \theta_1 \\ w_2 \\ \theta_2 \end{bmatrix} = \begin{bmatrix} 0 \\ 0 \\ +\frac{f\ell^4}{24EI} \\ -\frac{f\ell^3}{6EI} \end{bmatrix}$$

The negative of which is used to determine $v_1^{(2)}$, as well as the stiffness matrix calculated earlier.

$$v_1^{(2)} = K_1(-u_{part,1}) = \begin{bmatrix} \frac{12EI}{\ell^3} & -\frac{6EI}{\ell^2} & -\frac{12EI}{\ell^3} & -\frac{6EI}{\ell^2} \\ -\frac{6EI}{\ell^2} & \frac{4EI}{\ell} & \frac{6EI}{\ell^2} & \frac{2EI}{\ell} \\ -\frac{12EI}{\ell^3} & \frac{6EI}{\ell^2} & \frac{12EI}{\ell^3} & \frac{6EI}{\ell^2} \\ -\frac{6EI}{\ell^2} & \frac{2EI}{\ell} & \frac{6EI}{\ell^2} & \frac{4EI}{\ell} \end{bmatrix} \begin{bmatrix} 0 \\ 0 \\ -\frac{f\ell^4}{24EI} \\ +\frac{f\ell^3}{6EI} \end{bmatrix} = \begin{bmatrix} -\frac{1}{2}f\ell \\ \frac{1}{12}f\ell^2 \\ \frac{1}{2}f\ell \\ \frac{5}{12}f\ell^2 \end{bmatrix}$$

Adding the two force vectors $v_1^{(1)}$ and $v_1^{(2)}$ results in the required force matrix.

$$v_1 = -\left(\begin{bmatrix} 0 \\ 0 \\ -f\ell \\ -\frac{1}{2}f\ell^2 \end{bmatrix} + \begin{bmatrix} -\frac{1}{2}f\ell \\ \frac{1}{12}f\ell^2 \\ \frac{1}{2}f\ell \\ \frac{5}{12}f\ell^2 \end{bmatrix} \right) = \begin{bmatrix} \frac{1}{2}f\ell \\ -\frac{1}{12}f\ell^2 \\ \frac{1}{2}f\ell \\ \frac{1}{12}f\ell^2 \end{bmatrix}$$

This results in the well known Euler-Bernoulli force vector, validating the derivation process.

Assemble and partition

The assembled f = Kd equation for super element 1 is shown below:

$$\begin{bmatrix} \frac{1}{2}f\ell \\ \frac{1}{12}f\ell^2 \\ F1 \\ T1 \end{bmatrix} = EI \begin{bmatrix} \frac{12}{\ell^3} & \frac{6}{\ell^2} & -\frac{12}{\ell^3} & \frac{6}{\ell^2} \\ \frac{6}{\ell^2} & \frac{4}{\ell} & -\frac{6}{\ell^2} & \frac{2}{\ell} \\ -\frac{12}{\ell^3} & -\frac{6}{\ell^2} & \frac{12}{\ell^3} & -\frac{6}{\ell^2} \\ \frac{6}{\ell^2} & \frac{2}{\ell} & -\frac{6}{\ell^2} & \frac{4}{\ell} \end{bmatrix} \begin{bmatrix} w_2 \\ \theta_2 \\ 0 \\ 0 \end{bmatrix}$$

Next, Equation B.10 is used to solve for the the unknown w_2 and θ_2 with Gaussian Elimination.

$$\begin{bmatrix} \frac{1}{2}f\ell \\ \frac{1}{12}f\ell^2 \end{bmatrix} = EI \begin{bmatrix} \frac{12}{\ell^3} & \frac{6}{\ell^2} \\ \frac{6}{\ell^2} & \frac{4}{\ell} \end{bmatrix} \begin{bmatrix} w_2 \\ \theta_2 \end{bmatrix} + EI \begin{bmatrix} -\frac{12}{\ell^3} & \frac{6}{\ell^2} \\ -\frac{6}{\ell^2} & \frac{2}{\ell} \end{bmatrix} \begin{bmatrix} 0 \\ 0 \end{bmatrix}$$

Resulting in

$$\boxed{\begin{bmatrix} w_2 \\ \theta_2 \end{bmatrix} = \frac{1}{EI} \begin{bmatrix} \frac{f\ell^4}{8} \\ -\frac{f\ell^3}{6} \end{bmatrix}}$$

This result is plugged into Equation B.11 and solved.

$$\begin{bmatrix} F_1 \\ T_1 \end{bmatrix} = \frac{EI}{EI} \begin{bmatrix} -\frac{12}{\ell^3} & -\frac{6}{\ell^2} \\ \frac{6}{\ell^2} & \frac{2}{\ell} \end{bmatrix} \begin{bmatrix} \frac{f\ell^4}{8} \\ -\frac{f\ell^3}{6} \end{bmatrix} + EI \begin{bmatrix} \frac{12}{\ell^3} & -\frac{6}{\ell^2} \\ -\frac{6}{\ell^2} & \frac{4}{\ell} \end{bmatrix} \begin{bmatrix} 0 \\ 0 \end{bmatrix} = \begin{bmatrix} -\frac{1}{2}f\ell \\ \frac{5}{12}f\ell^2 \end{bmatrix}$$

From Equation B.12, the reactions follow,

$$\begin{bmatrix} \frac{1}{2}f\ell \\ -\frac{1}{12}f\ell^2 \\ \frac{1}{2}f\ell \\ \frac{1}{12}f\ell^2 \end{bmatrix} + \begin{bmatrix} R_{w_1} \\ R_{\theta_1} \\ 0 \\ 0 \end{bmatrix} = \begin{bmatrix} -\frac{1}{2}f\ell \\ \frac{5}{12}f\ell^2 \\ \frac{1}{2}f\ell \\ -\frac{1}{12}f\ell^2 \end{bmatrix}$$

Resulting in the reaction forces:

$$\boxed{\begin{bmatrix} R_{w_1} \\ R_{\theta_1} \end{bmatrix} = \begin{bmatrix} -fl \\ \frac{1}{2}fl^2 \end{bmatrix} \quad and \quad \begin{bmatrix} V_1 \\ M_1 \end{bmatrix} = \begin{bmatrix} f\ell \\ -\frac{1}{2}f\ell^2 \end{bmatrix}}$$

Structural behaviour equations

For super element 1 the integration constants C_1, C_2, C_3 and C_4 are unknown. Following the procedure from Step 7, the following set of equations are derived:

$$\begin{bmatrix} w(0) = 0 \\ \theta(0) = 0 \\ M(\ell) = -\frac{1}{2}f\ell^2 \\ V(\ell) = -f\ell \end{bmatrix} = \begin{bmatrix} 0 & 0 & 0 & \frac{1}{EI} \\ 0 & 0 & -\frac{1}{EI} & 0 \\ -\ell & -1 & 0 & 0 \\ -1 & 0 & 0 & 0 \end{bmatrix} \begin{bmatrix} C_1 \\ C_2 \\ C_3 \\ C_4 \end{bmatrix} - \begin{bmatrix} w_{part}(0) = f\ell \\ \theta_{part}(0) = -\frac{1}{2}f\ell^2 \\ M_{part}(\ell) = 0 \\ V_{part}(\ell) = 0 \end{bmatrix}$$

The integration constants can then be calculated

$$\begin{bmatrix} C_1 = f\ell \\ C_2 = -\frac{1}{2}f\ell^2 \\ C_3 = 0 \\ C_4 = 0 \end{bmatrix}$$

and plugged into the symbolic deflection, rotation, internal moment and internal shear equations.

$$w(x) = \frac{1}{6}\frac{f\ell}{EI}x^3 - \frac{1}{4}\frac{f\ell^2}{EI}x^2$$
$$\theta(x) = -\frac{1}{2}\frac{f\ell}{EI}x^2 + \frac{1}{2}\frac{f\ell^2}{EI}x$$
$$M(x) = -f\ell x$$
$$V(x) = -f\ell$$

4.3.3 Super element 2 derivation

Super element 2 is composed of four parallel shear walls with a floor system represented by springs, illustrated in Figure 4.6. It is symmetric, so it can also be split into two symmetric parts to simplify the analysis process. The two outer walls are type $wall_a$ and the inner walls are type $wall_b$. The general procedure as well as the sign convention, see Figures 4.3 and 4.4, to derive this super element remains the same as for super element 1. However, super element 2 has twice as many degrees of freedom and the floor stiffness contributes to the lateral force distribution. Therefore, each symmetric part is modelled as two Euler Bernoulli beams with a linear shear floor stiffness between them, where the floor stiffness is calculated including the supports from all four walls.

The derivation for super element 2 can be found in Steenbergen (2007), but is also summarised in Appendix B.2. Some parts were re-derived in order to present a complete derivation procedure for parts that were not necessary for super element 1, such as the floor stiffness and force transfer. The resulting displacement equations are shown in Equation 4.13 and 4.14.

$$\begin{aligned} w_a = {} & C1 + C2x + C3x^2 + C4x^3 \\ & + C5\frac{e^{-\gamma x}cos(\gamma x)}{\beta_a} + C6\frac{e^{-\gamma x}sin(\gamma x)}{\beta_a} + C7\frac{e^{\gamma x}cos(\gamma x)}{\beta_a} + C8\frac{e^{\gamma x}sin(\gamma x)}{\beta_a} \end{aligned} \tag{4.13}$$

$$\begin{aligned} w_b = {} & C1 + C2x + C3x^2 + C4x^3 \\ & + C5\frac{e^{-\gamma x}cos(\gamma x)}{\beta_b} + C6\frac{e^{-\gamma x}sin(\gamma x)}{\beta_b} + C7\frac{e^{\gamma x}cos(\gamma x)}{\beta_b} + C8\frac{e^{\gamma x}sin(\gamma x)}{\beta_b} \end{aligned} \tag{4.14}$$

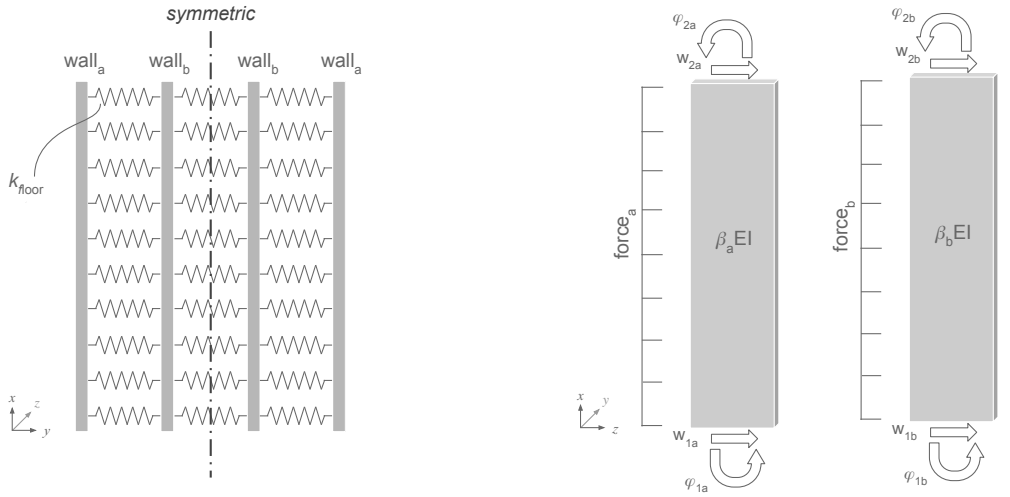

(a) Super element 2 arrangement

(b) Super element 2 wall degrees of freedom

Figure 4.6: Super element 2

4.3.4 Super element 3 derivation

Super element 3 is composed of one core and one wall with a floor system. It is not symmetric, so it cannot be simplified like the other two super elements already described, however the general derivation process remains the same. In addition to Euler Bernoulli beams representing the stability elements and the floor system, this third derived and implemented super element introduces torsional loading and torsional resistance of the core. Hence, it can resist loading from the y and z directions, which the other two elements cannot. The fourteen degrees of freedom are illustrated in Figure 4.7.

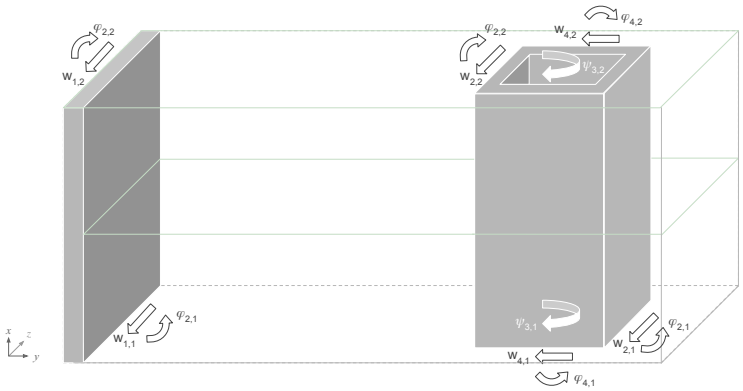

Figure 4.7: Superelement 3 degrees of freedom

Also the derivations for super element 3 can be found in Steenbergen (2007), and is summarised in Appendix B.3. The resulting displacement equations are shown below.

When the determinant is less than 0:

$$w_1 = S_1\left(\frac{x}{height}\right)^3 + S_2\left(\frac{x}{height}\right)^2 + S_3\frac{x}{height} + S_4\frac{x}{height} + S_5 + S_6 + \frac{1}{p_1}e^{-\alpha x}(S_{11}cos\beta x + S_{12}sin\beta x + \frac{1}{p_1}e^{\alpha(x-height)}(S_{13}cos\beta x + S_{14}sin\beta x) \tag{4.15}$$

$$w_2 = S_1\left(\frac{x}{height}\right)^3 + S_2\left(\frac{x}{height}\right)^2 + S_3\frac{x}{height} + S_4p_1\frac{x}{height} + S5 + S6p_1 + e^{-\alpha x}(S_{11}cos\beta x + S_{12}sin\beta x + e^{\alpha(x-height)}(S_{13}cos\beta x + S_{14}sin\beta x) \tag{4.16}$$

$$\begin{aligned}\psi_3 = {} & S_4p_2\frac{x}{height} + S_6p_2 \\ & + S_{11}p_3e^{-\alpha x}\big((\alpha^2-\beta^2)cos\beta x + 2\alpha\beta sin\beta x\big) \\ & + S_{12}p_3e^{-\alpha x}\big((\alpha^2-\beta^2)sin\beta x - 2\alpha\beta cos\beta x\big) \\ & + S_{13}p_3e^{\alpha(x-height)}\big((\alpha^2-\beta^2)cos\beta x - 2\alpha\beta sin\beta x\big) \\ & + S_{14}p_3e^{\alpha(x-height)}\big((\alpha^2-\beta^2)sin\beta x + 2\alpha\beta cos\beta x\big)\end{aligned} \tag{4.17}$$

When the determinant greater than 0:

$$w_1 = S_1\left(\frac{x}{height}\right)^3 + S_2\left(\frac{x}{height}\right)^2 + S_3\frac{x}{height} + S_4\frac{x}{height} + S_5 + S_6 + S_{11}\frac{1}{p_1}e^{-\gamma_1 x} + S_{12}\frac{1}{p_1}e^{\gamma_1(x-height)} + S_{13}\frac{1}{p_1}e^{-\gamma_2 x} + S_{14}\frac{1}{p_1}e^{\gamma_2(x-height)} \tag{4.18}$$

$$w_2 = S_1\left(\frac{x}{height}\right)^3 + S_2\left(\frac{x}{height}\right)^2 + S_3\frac{x}{height} + S_4p_1\frac{x}{height} + S_5 + S_6p_1 + S_{11}e^{-\gamma_1 x} + S_{12}e^{\gamma_1(x-height)} + S_{13}e^{-\gamma_2 x} + S_{14}e^{\gamma_2(x-height)} \tag{4.19}$$

$$\begin{aligned}\psi_3 = {} & S_4p_2\frac{x}{height} + S_6p_2 \\ & + S_{11}p_3\gamma_1^2e^{-\gamma_1 x} + S_{12}p_3\gamma_1^2e^{\gamma_1(x-height)} \\ & + S_{13}p_3\gamma_2^2e^{-\gamma_2 x} + S_{14}p_3\gamma_2^2e^{\gamma_2(x-height)}\end{aligned} \tag{4.20}$$

For all cases:

$$w_4 = S_7\left(\frac{x}{height}\right)^3 + S_8\left(\frac{x}{height}\right)^2 + S_9\frac{x}{height} + S_{10} \tag{4.21}$$

4.3.5 Super Element Combination

Appendix B.4 presents the method used to perform the analysis calculations on a combination of multiple super elements to form a new super-structure.

Physically the super elements are connected by the user in the visual user interface, in this case Grasshopper. In order for the connection to be realised in the code, checks on the node locations are completed to determine the position of each super element and which super element is below. Based on the location of the walls of each super element, the connection type is determined.

4.4 Super Element Validations

After the differential equations for each super element are derived, they are validated by comparing the results to a model calculated using the Finite Element Method (FEM). The FEM models was made with MatrixFrame (Matrix Software, 2018) as either a 2D wall or 3D frame depending on the super element. In order to compare the structural behaviour of the Super Element Method (SEM) using differential equations with the FEM results, the deflection, rotation and internal shear and moment are plotted along the height of each stability element.

4.4.1 Super Element 1 Validation

A wind load of $1kN/m^2$ is applied on one facade and the two walls are spaced 8m apart. Therefore, the wind load on each wall is:

$$f = 1\frac{kN}{m^2} * \frac{8m}{2} = 4\frac{kN}{m}$$

The other super element input parameters are outlined in Figure 4.8.

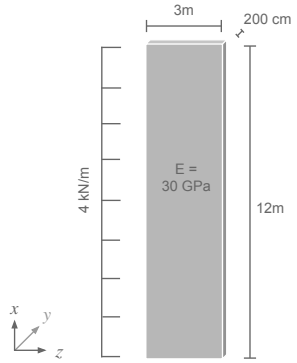

Figure 4.8: Input parameters for the validation of super element 1

A single wall was modelled using both methods. In MatrixFrame the wall was modelled as a "2D wall" (Matrix Software, 2018), the complete MatrixFrame model report can be found in Appendix C.1. The equations resulting from the super element method are shown below:

$$\begin{aligned} w_a &= -5.9\overline{259} * 10^{-7} * x^3 + 0.10\overline{6} * e^{-4} * x^2 + 1.234567901 * 10^{-8} * x^4 \\ \theta_a &= 0.1\overline{7} * e^{-5} * x^2 - 0.21\overline{3} * e^{-4} * x - 4.938271605 * 10^{-8} * x^3 \\ M_a &= 48x - 288 - 2x^2 \\ V_a &= 48 - 4x \end{aligned}$$

The deflection, rotation, internal moment and internal shear results are graphed together for comparison in the Figure 4.9. "FEM" stands for Finite Element Method and "SEM" for Super Element Method.

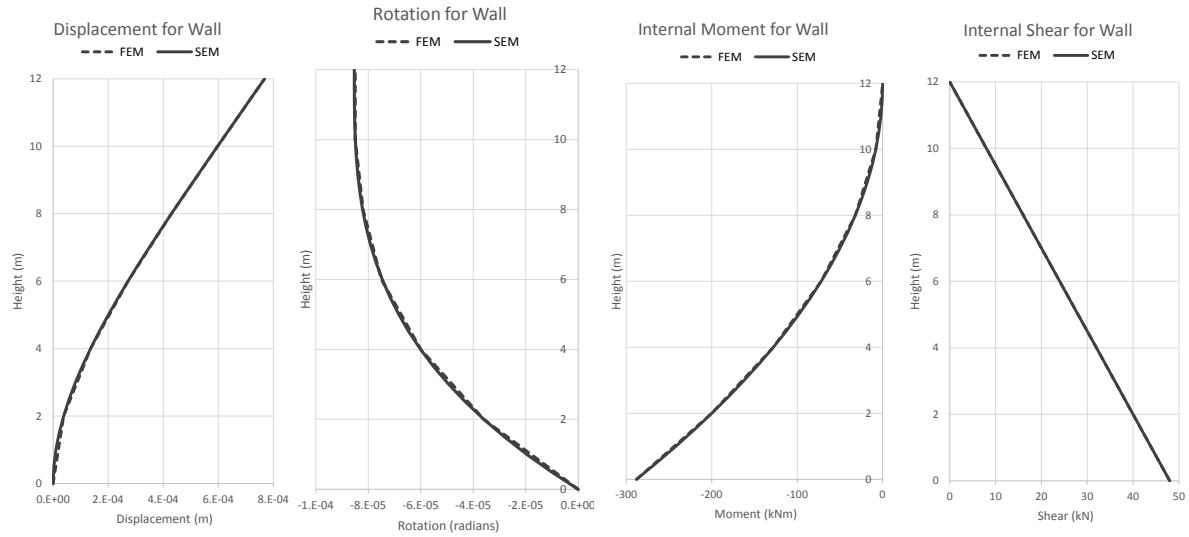

Figure 4.9: Super element 1 validation

As shown in the graphs, the FEM and SEM results are the same for super element 1.

4.4.2 Super Element 2 Validation: Equal Wall Dimensions

This comparison checks the validity of the differential equation method used for the super elements compared to finite element method calculations.
The same wind load of $1kN/m^2$ is applied on one facade of super element 2. Using the force transfer results from Figure B.6, the wind line load on each wall follow as:

$$f_a = 1\frac{kN}{m^2} * \frac{2}{5} * 8 = 3.2\frac{kN}{m}$$

$$f_b = 1\frac{kN}{m^2} * \frac{11}{10} * 8 = 8.8\frac{kN}{m}$$

For this check all the walls have equal dimensions which are shown in Figure 4.10.

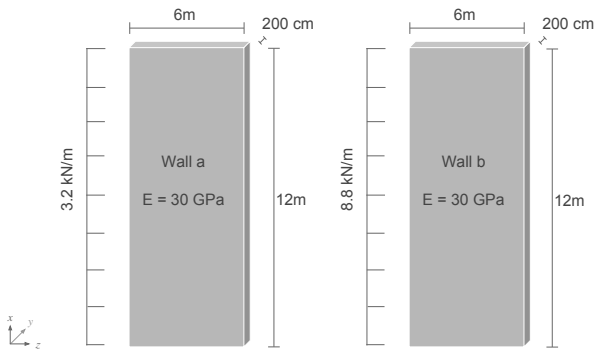

Figure 4.10: Input parameters for the validation of super element 2

The floor spans across all four wall, which are spaced 8m apart as shown in Figure 4.11.

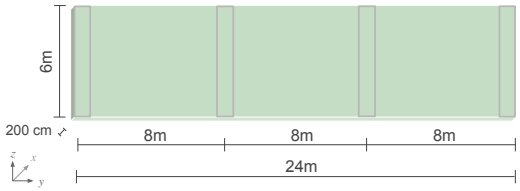

Figure 4.11: Input parameters for the floor of super element 2

In MatrixFrame the super element is modelled as a "3D frame" (Matrix Software, 2018), the complete MatrixFrame model report can be found in Appendix C.2.1. The equations resulting from the super element method are shown below:

$$
\begin{aligned}
w_a &= -0.5530854902e-5+0.1\overline{9}*e^{-5}*x^2-1.\overline{1}*10^{-7}*x^3\\
&+0.5361311954*e^{-5}*\exp(-0.1850207789*x)*\cos(0.1850207789*x)\\
&+0.5269672112*e^{-5}*\exp(-0.1850207789*x)*\sin(0.1850207789*x)\\
&+1.695429485*10^{-7}*\exp(0.1850207789*x)*\cos(0.1850207789*x)\\
&-7.790310568*10^{-8}*\exp(0.1850207789*x)*\sin(0.1850207789*x)\\
&+2.3\overline{148}*10^{-9}*x^4\\
\theta_a &= -0.3\overline{9}*e^{-5}*x+3.\overline{3}*10^{-7}*x^2\\
&+1.69552750*10^{-8}*\exp(-0.1850207789*x)*\cos(0.1850207789*x)\\
&+0.1966952952*e^{-5}*\exp(-0.1850207789*x)*\sin(0.1850207789*x)\\
&-1.695527510*10^{-8}*\exp(0.1850207789*x)*\cos(0.1850207789*x)\\
&+4.578266168*10^{-8}*\exp(0.1850207789*x)*\sin(0.1850207789*x)\\
&-9.259259264*10^{-9}*x^3\\
M_a &= -431.\overline{9}+72*x-39.64293850*\exp(-0.1850207789*x)*\sin(0.1850207789*x)\\
&+38.96532961*\exp(-0.1850207789*x)*\cos(0.1850207789*x)\\
&+1.253644768*\exp(0.1850207789*x)*sin(0.1850207789*x)\\
&+0.5760358759*\exp(0.1850207789*x)*\cos(0.1850207789*x)-3*x^2\\
V_a &= 72+0.1253717244*\exp(-0.1850207789*x)*\sin(0.1850207789*x)\\
&-14.54416300*\exp(-0.1850207789*x)*\cos(0.1850207789*x)\\
&+0.1253717249*\exp(0.1850207789*x)*\sin(0.1850207789*x)\\
&+0.3385289379*\exp(0.1850207789*x)*\cos(0.1850207789*x)-6*x\\
w_b &= 0.5530854908*e^{-5}+0.1\overline{9}*e^{-5}*x^2-1.111111112*10^{-7}*x^3\\
&-0.5361311954e-5*\exp(-0.1850207789*x)*\cos(0.1850207789*x)\\
&-0.5269672112e-5*\exp(-0.1850207789*x)*\sin(0.1850207789*x)\\
&-1.695429485*10^(-7)*\exp(0.1850207789*x)*\cos(0.1850207789*x)\\
&+7.790310568*10^(-8)*\exp(0.1850207789*x)*\sin(0.1850207789*x)\\
&+2.314814816*10^(-9)*x^4\\
\theta_b &= -0.3\overline{9}*e^{-5}*x+3.\overline{3}*10^{-7}*x^2\\
&-1.69552750*10^{-8}*\exp(-0.1850207789*x)*\cos(0.1850207789*x)\\
&-0.1966952952*e^{-5}*\exp(-0.1850207789*x)*\sin(0.1850207789*x)\\
&+1.695527510*10^{-8}*\exp(0.1850207789*x)*\cos(0.1850207789*x)\\
&-4.578266168*10^{-8}*\exp(0.1850207789*x)*\sin(0.1850207789*x)\\
&-9.259259264*10^{-9}*x^3\\
M_b &= -431.\overline{9}+72*x+39.64293850*\exp(-0.1850207789*x)*\sin(0.1850207789*x)\\
&-38.96532961*\exp(-0.1850207789*x)*\cos(0.1850207789*x)\\
&-1.253644768*\exp(0.1850207789*x)*\sin(0.1850207789*x)\\
&-0.5760358759*\exp(0.1850207789*x)*\cos(0.1850207789*x)-3*x^2\\
V_b &= 72-0.1253717244*\exp(-0.1850207789*x)*\sin(0.1850207789*x)\\
&+14.54416300*\exp(-0.1850207789*x)*\cos(0.1850207789*x)\\
&-0.1253717249*\exp(0.1850207789*x)*\sin(0.1850207789*x)\\
&-0.3385289379*\exp(0.1850207789*x)*\cos(0.1850207789*x)-6*x
\end{aligned}
$$

Figure 4.12 shows the result comparison for the outside wall (wall a) and Figure 4.13 for the inside wall (wall b).

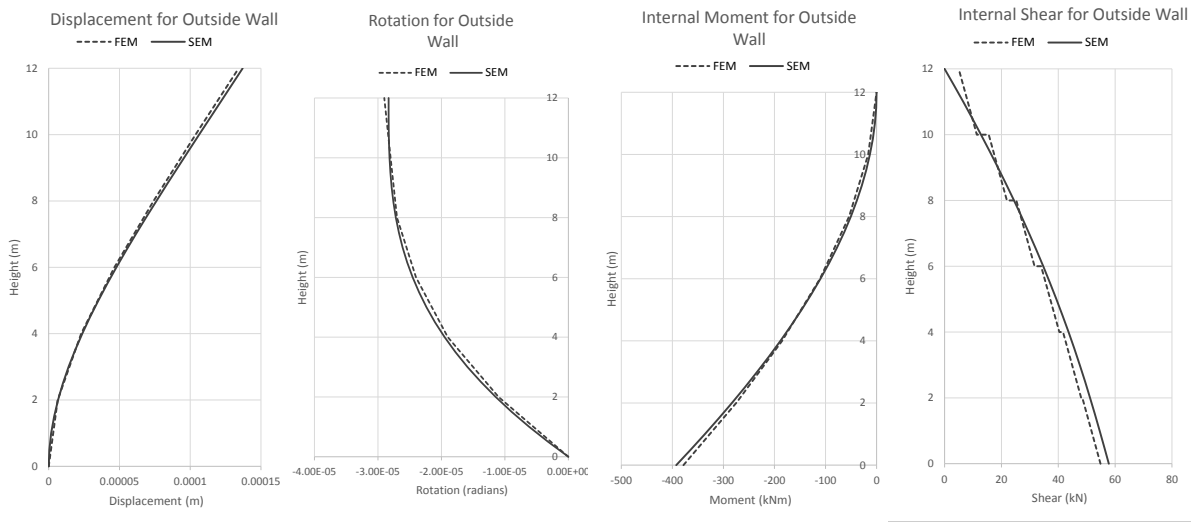

Figure 4.12: Super element 2 validation for wall A

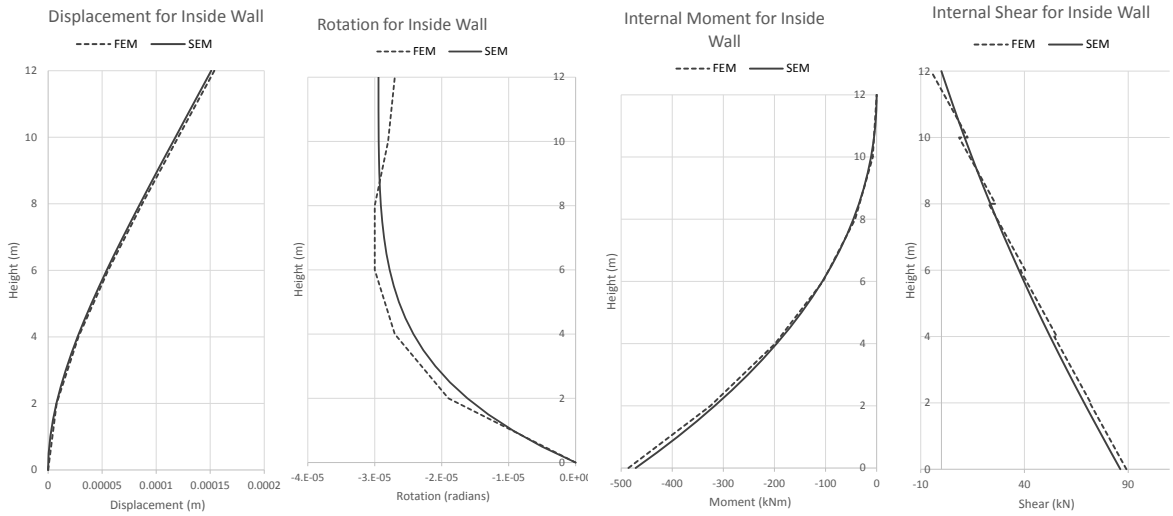

Figure 4.13: Super element 2 validation for wall B

As can be seen from the graphs, the results are very close for super element 2. The finite element internal shear forces change in steps, because the lateral wind force is only transferred at every floor (which are 2m apart) instead of transferred continuously using the super element method. Additionally, the rotation graph is not the same, because there is a rounding error. MatrixFrame, used for the FEM validation, only rounds to six decimal points for the rotation and since the walls are quite wide the rotation along the height of the walls is quite small.

4.4.3 Super Element 2 Validation: Different Wall Dimensions

This comparison checks the accuracy of super element 2 when the inner and outer walls have different dimensions. The same parameters, except the wall width, are chosen as for the super element validation where all the walls have the same dimensions.

As a recap, the parameters are summerized in Figure 4.14.

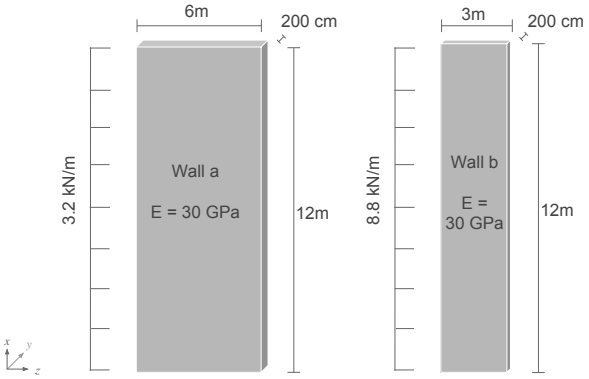

Figure 4.14: Input parameters for the validation of super element 2 for walls with different dimensions

For this validation it is important to note that the current equations of the floor stiffness and force transfer derivations do not support the case where the walls do not have the same stiffness. In the implemented equations it is assumed that all the walls have the same dimensions. Therefore, some differences are expected in the results for this validation. To make the results a bit more accurate, the floor width is set at the average wall width, 4.5m, even though the floor is actually 6m wide as shown by the dashed lines in Figure 4.15. This is a temporary solution intended only to be used for the tool proof of concept. For the actual development of this tool the proper adjustments should be made to the floor stiffness and the force transfer derivations. Possible solutions for these adjustments are possible and discussed later.

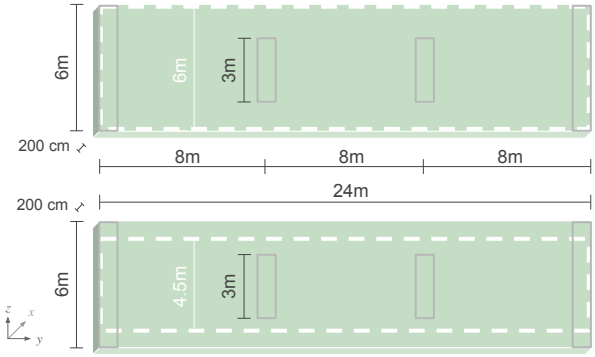

Figure 4.15: Change in floor area for super element 2

In MatrixFrame the super element is modelled as a "3D frame", the complete MatrixFrame model report can be found in Appendix C.2.2.

Figure 4.16 shows the results for the outside wall (wall a) and Figure 4.17 for the inside wall (wall b).

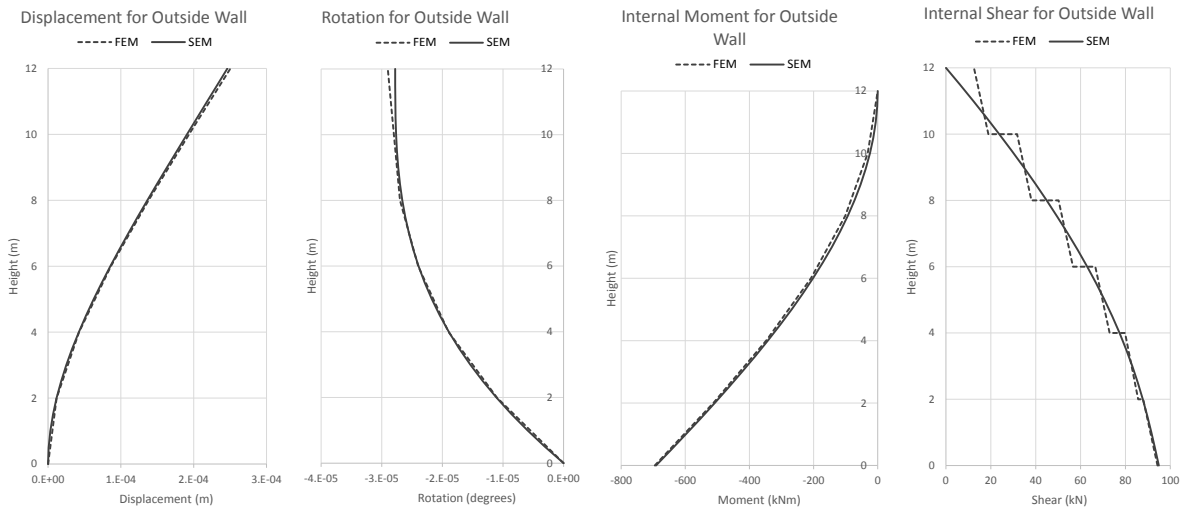

Figure 4.16: Super element 2 validation for wall A

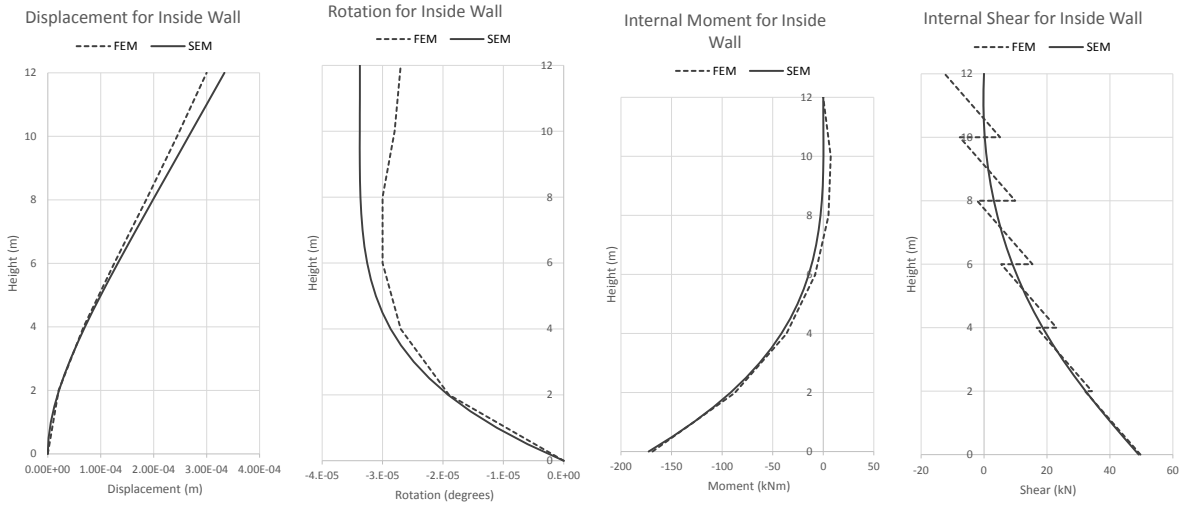

Figure 4.17: Super element 2 validation for wall B

The graphs show that setting the floor width to the average of the wall widths does present quite similar results. Again, the rounding error for the rotation and stepped shear force can be observed. The results in general are more accurate for the outside wall (wall a) compared to the inside wall (wall b). This is because the wall stiffness between the two inside walls is over estimated with the 4.5m wide floor. Plus, the currently implemented force distribution doesn't consider the stiffness of the wall. Therefore, the applied wind load on the inner walls is larger than it should be and causes larger deformation and rotation as shown in Figure 4.17.

To solve these issues the force transfer derivation and floor stiffness equation has to be adjusted. This could be done by represented the walls as springs with their corresponding stiffness (EI_a and EI_b) as shown in Figure 4.18.

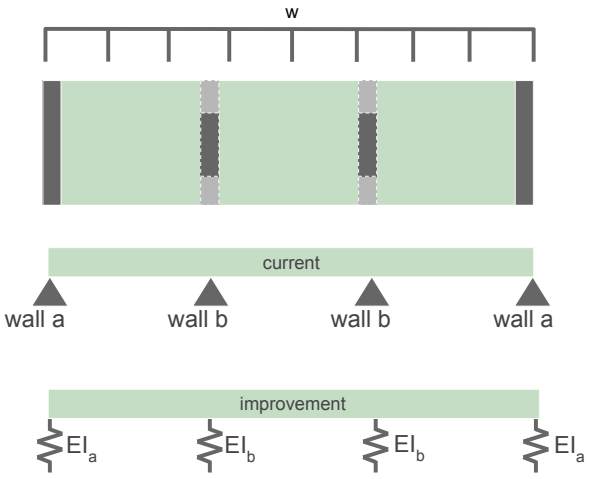

Figure 4.18: Wall Support Representation

Representing the walls as springs rather than pinned supports would enable the wind force distribution to consider the stiffness of the walls, leading to lower wind loads on the less stiff walls. This would also cause the floor stiffness to be lower between walls with smaller cross sections and less stiffness.

The way the walls are represented in the calculations is important, because a walls dimensions has a significant impact on its stiffness, since in this case the width is cubed. The wall's flexural stiffness is equal to its modulus of elasticity * moment of inertia. For example the outer walls may be twice as wide as the inner walls, but they be 8 times as stiff as the inner walls, shown in the following equations.

$$EI_a = E * I = E * \frac{1}{12} * n^3 * t$$

$$EI_b = E * I = E * \frac{1}{12} * \left(\frac{n}{2}\right)^3 * t$$

4.4.4 Super Element Combination A Validation

Combination A is composed of super element 1 placed on top of super element 2, lining up on the outside walls (walls a) as shown in Figure 4.19.

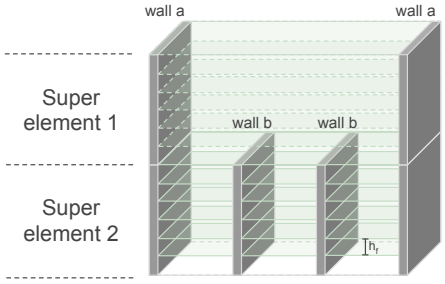

Figure 4.19: Structure composed of super element 1 and 2 (adopted from (Steenbergen, 2007))

The same wind load of $1kN/m^2$ is applied on one facade. Super element 2 walls are again spaced 8m apart, while two super element 1 walls are spaced at 3*8m = 24m apart. The wind transfer remains the same as for the individual cases and are summarised below:

$$f_1 = 1\frac{kN}{m^2} * \frac{24m}{2} = 12\frac{kN}{m}$$

$$f_{2a} = 1\frac{kN}{m^2} * \frac{2}{5} * 8 = 3.2\frac{kN}{m}$$

$$f_{2b} = 1\frac{kN}{m^2} * \frac{11}{10} * 8 = 8.8\frac{kN}{m}$$

The other super element input parameters are the same as for the individual cases, except that all walls are 6m wide and the floors. The summarised shear wall parameters are shown in Figure 4.20a and the floor parameter are shown in Figure 4.20b.

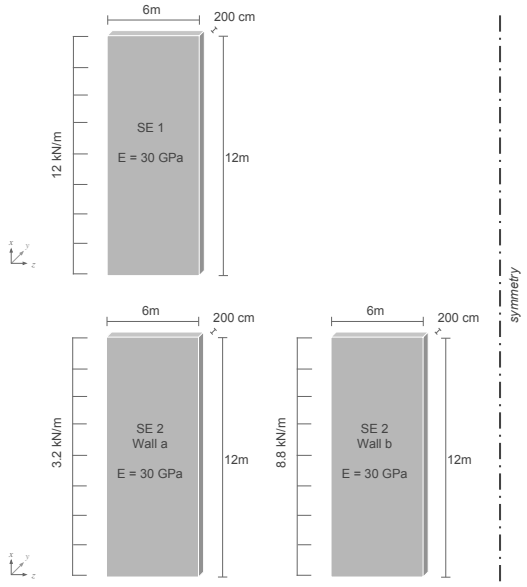

(a) Wall inputs

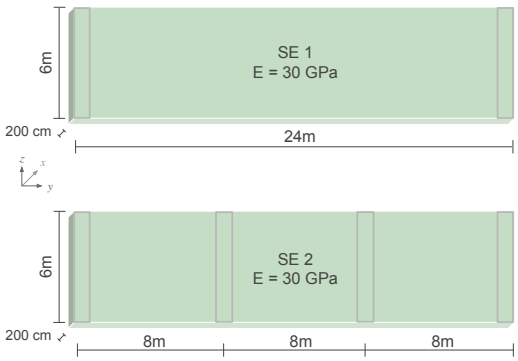

(b) Floor system inputs

Figure 4.20: Combination A validation inputs

In MatrixFrame the combined case is modelled as a "3D frame", the complete MatrixFrame model report can be found in Appendix C.3.1.

Figure 4.21 shows the results for the outside wall (wall a) and Figure 4.22 for the inside wall (wall b).

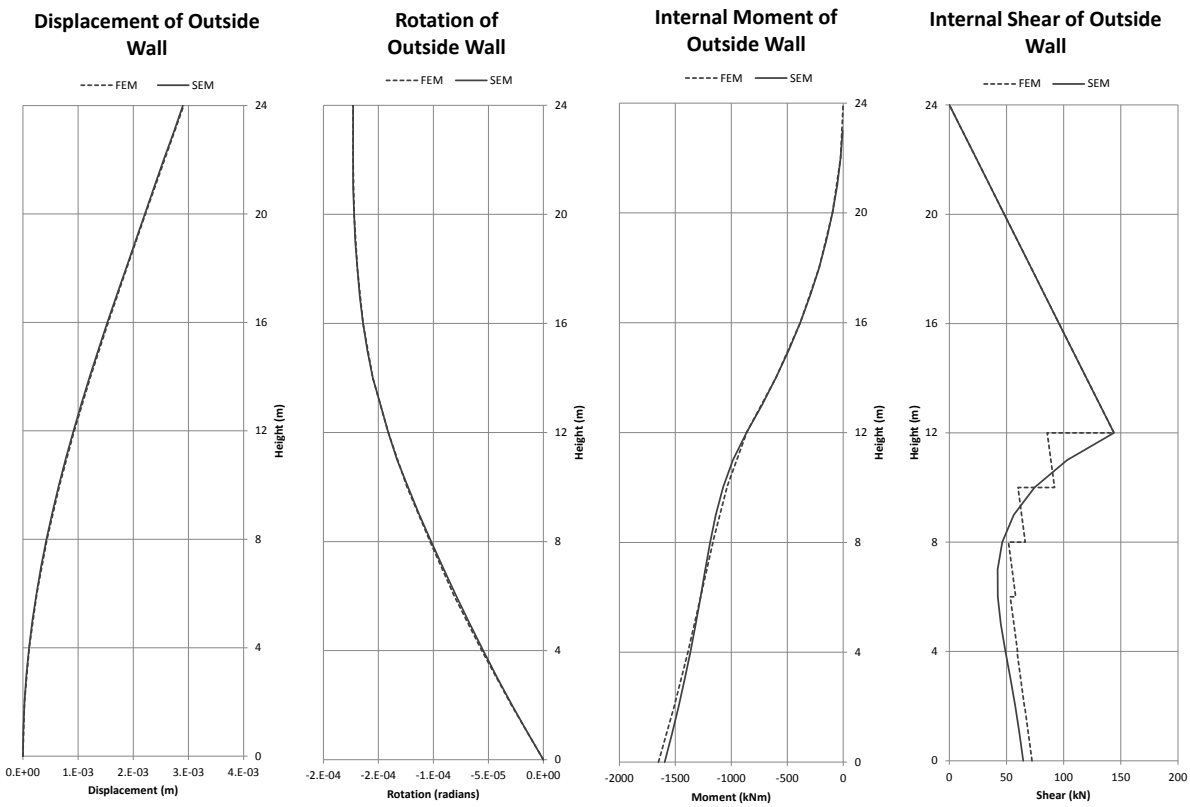

Figure 4.21: Combination A: Validation of outside walls

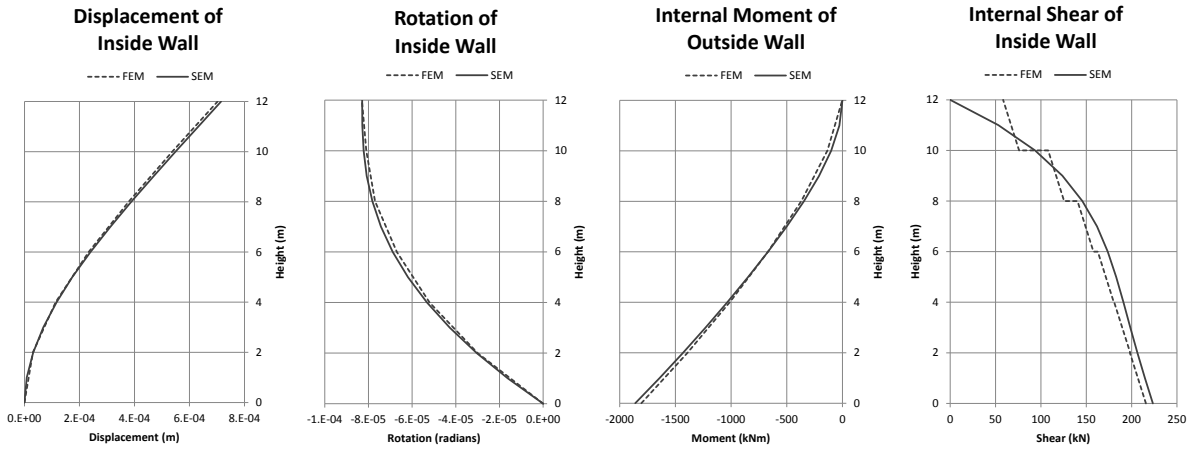

Figure 4.22: Combination A: Validation of inside walls

As shown in the graphs, the results are also very close for the combination case A of super element 1 and 2. The same phenomenas about the shear and rotation can be observed here. The finite element internal shear forces change in steps, because the lateral wind force is only transferred at every floor (which are 2 m apart) instead of transferred continuously using the super element method. Again there is a rounding error in the rotation due to MatrixFrame, however, it is not as visible here since the rotations are larger.

4.4.5 Super Element Combination B Validation

Combination B is composed of super element 1 placed on top of super element 2, lining up on the inside walls (walls b) as shown in Figure 4.23.

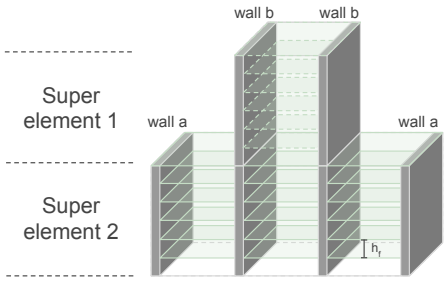

Figure 4.23: Structure composed of super element 1 and 2 (adopted from (Steenbergen, 2007))

The same wind load of $1kN/m^2$ is applied on one facade. Super element 2 walls are again spaced 8m apart, while two super element 1 walls are spaced at 3*8m = 24m apart. The wind transfer remains the same as for the individual cases and are summarised below:

$$f_1 = 1\frac{kN}{m^2} * \frac{8m}{2} = 4\frac{kN}{m}$$

$$f_{2a} = 1\frac{kN}{m^2} * \frac{2}{5} * 8 = 3.2\frac{kN}{m}$$

$$f_{2b} = 1\frac{kN}{m^2} * \frac{11}{10} * 8 = 8.8\frac{kN}{m}$$

Just like for the validation of combination A, the other super element input parameters are the same as for the individual cases, except that all walls are 6m wide and the floors. The summarised shear wall parameters are shown in Figure 4.24a and the floor parameter are shown in Figure 4.24b.

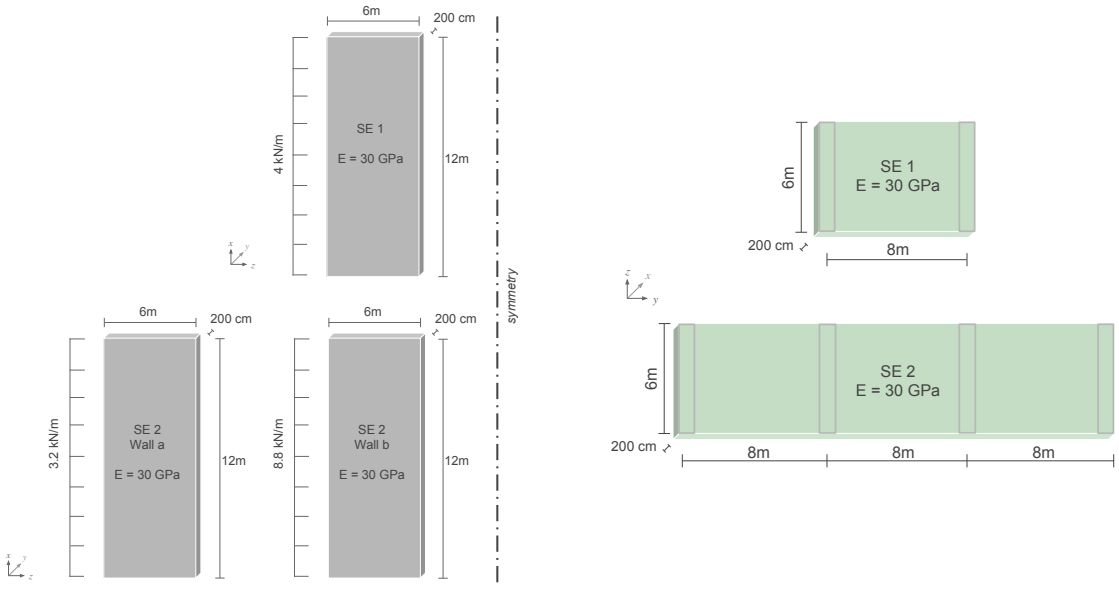

(a) Wall inputs *(b) Floor system inputs*

Figure 4.24: Combination B validation inputs

Also for this validation the MatrixFrame model is a "3D frame" (Matrix Software, 2018), the complete MatrixFrame model report can be found in Appendix C.3.2.

Figure 4.25 shows the results for the outside wall (wall a) and Figure 4.26 for the inside wall (wall b).

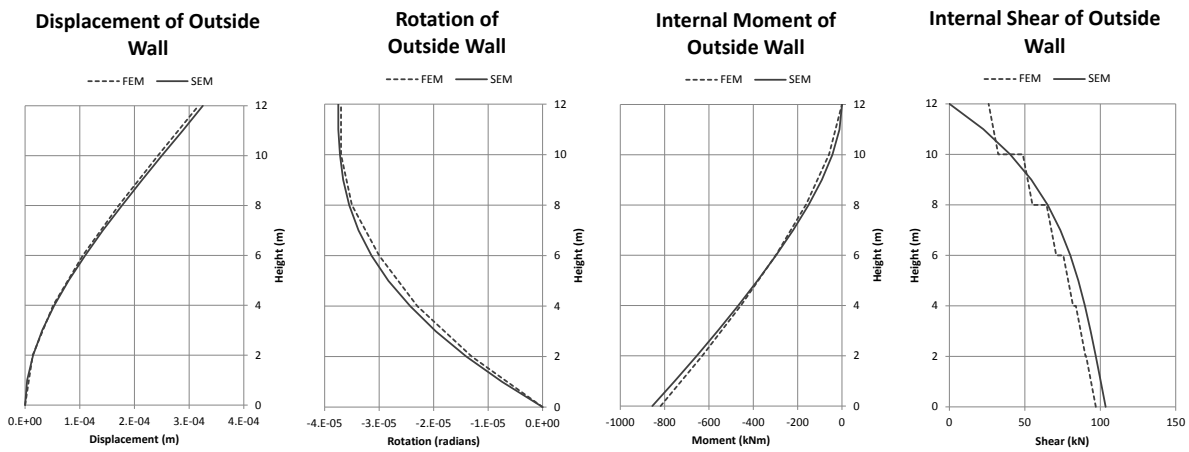

Figure 4.25: Combination B: Validation of outside walls

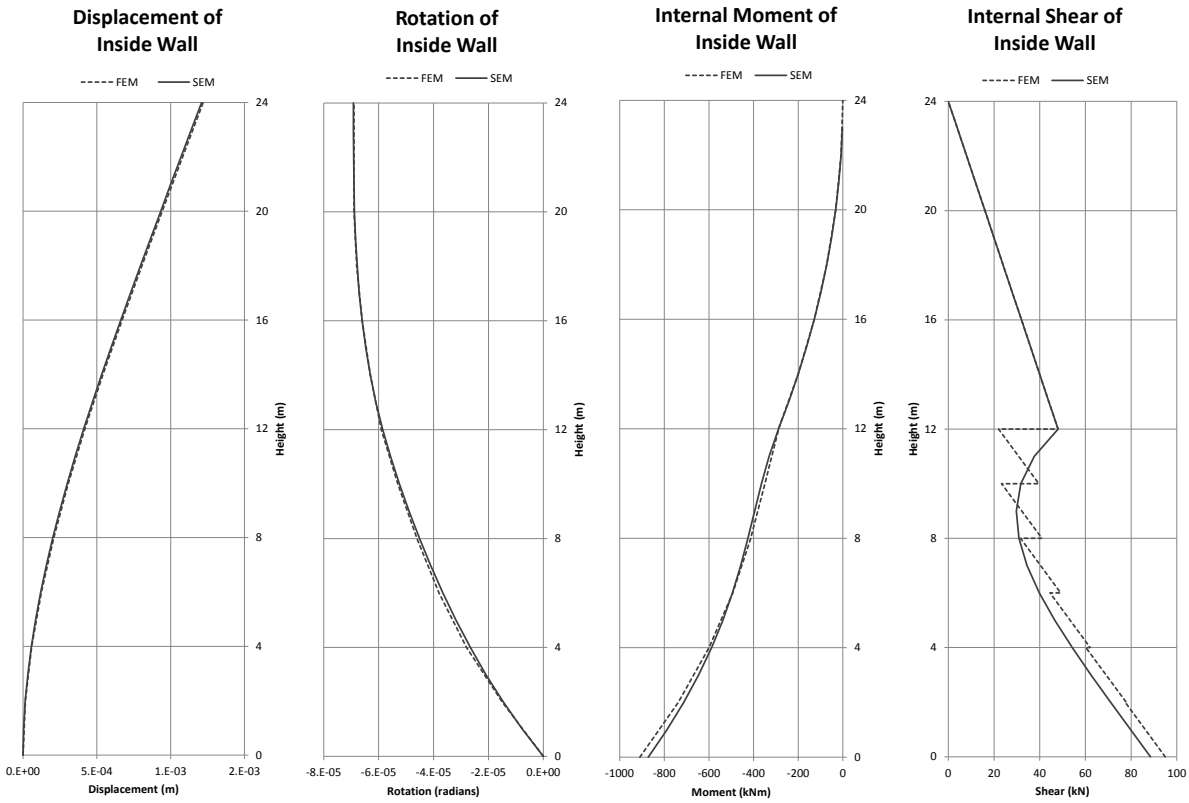

Figure 4.26: Combination B: Validation of inside walls

Also the comparison for this combination is very close. The same phenomenas about the shear and rotation can be observed here. Again, the finite element internal shear forces change in steps, because the lateral wind force is only transferred at every floor (which are 2m apart) instead of transferred continuously using the super element method. Again there is a rounding error in the rotation due to MatrixFrame, however, it is not as visible here since the rotations are larger.

4.4.6 Super Element 3 Validation

In order to validate the third super element, composed of one core, one wall and a floor system, the dimensions of the super element were chosen to result in a negative and a positive determinant.

Determinant is less than zero

The stability element and floor dimensions resulting in a negative determinant are illustrated in Figure 4.27.

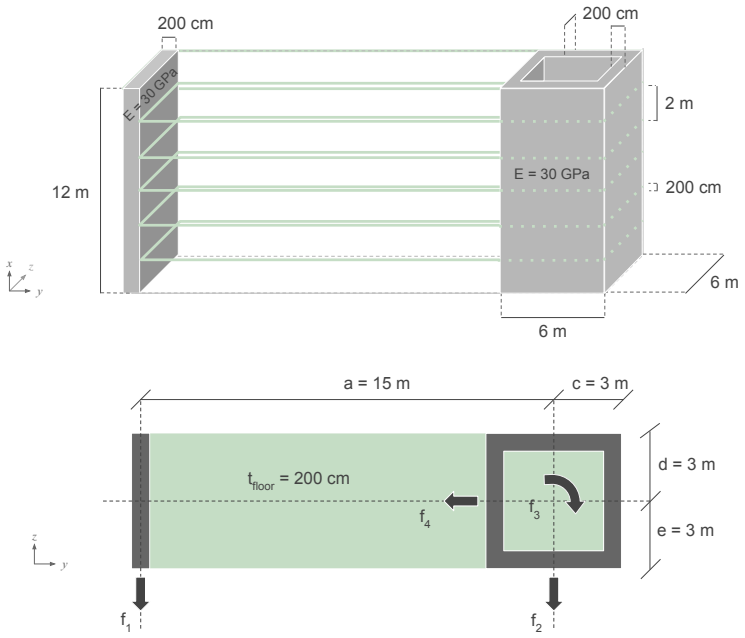

Figure 4.27: Validation parameter inputs resulting in $D < 0$

A wind load of $1\,kN/m^2$ was applied on both sides of the super element, resulting in the following wind line loads on the stability elements:

$$f_1 = 5.625\,kN/m$$
$$f_2 = 12.375\,kN/m$$
$$f_3 = -23.625\,kNm/m$$
$$f_4 = 6.0\,kN/m$$

In MatrixFrame the super element is modelled as a "3D frame" (Matrix Software, 2018). The line loads are applied along the height of the stability elements. The only exception is that MatrixFrame does not have an option to apply a torsional line load along the height, so point loads are placed at every meter along the height instead. This causes the MatrixFrame torsion results to change in steps at every meter, instead of a continuous line. The compete MatrixFrame model report can be found in Appendix C.4.1.

The deflection, rotation, internal moment, internal shear internal torsion results are graphed together for comparison, see

Figure 4.28 shows the result comparison for the wall, and Figures 4.29 - 4.31 for the core.

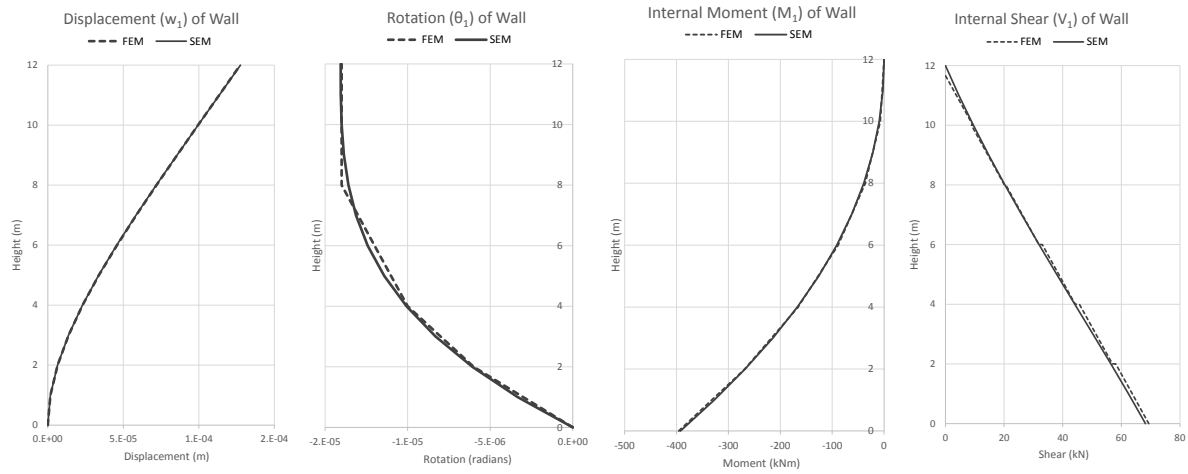

Figure 4.28: Super element 3 validation for degree of freedom 2 (wall)

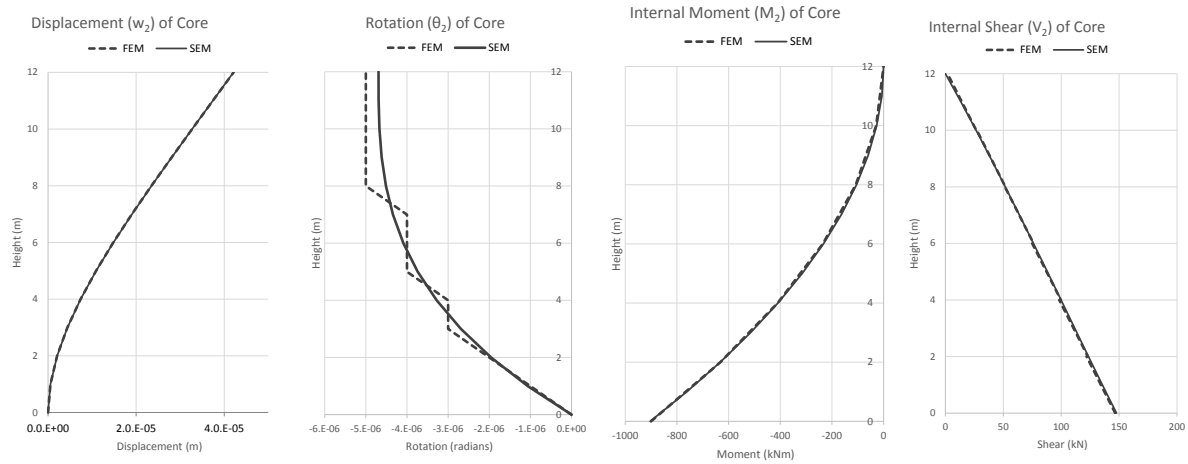

Figure 4.29: Super element 3 validation for degree of freedom 2 (wall and core)

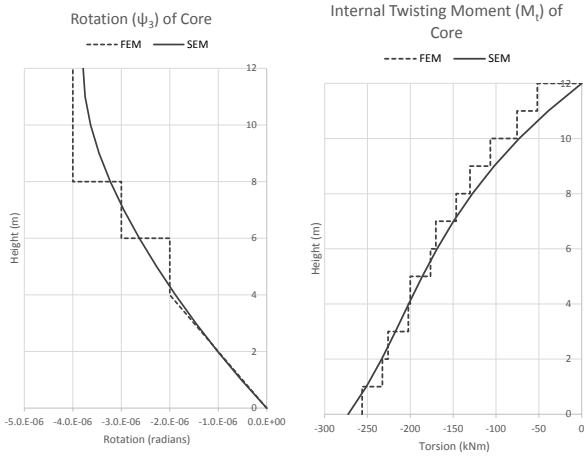

Figure 4.30: Super element 3 validation for degree of freedom 3 (core)

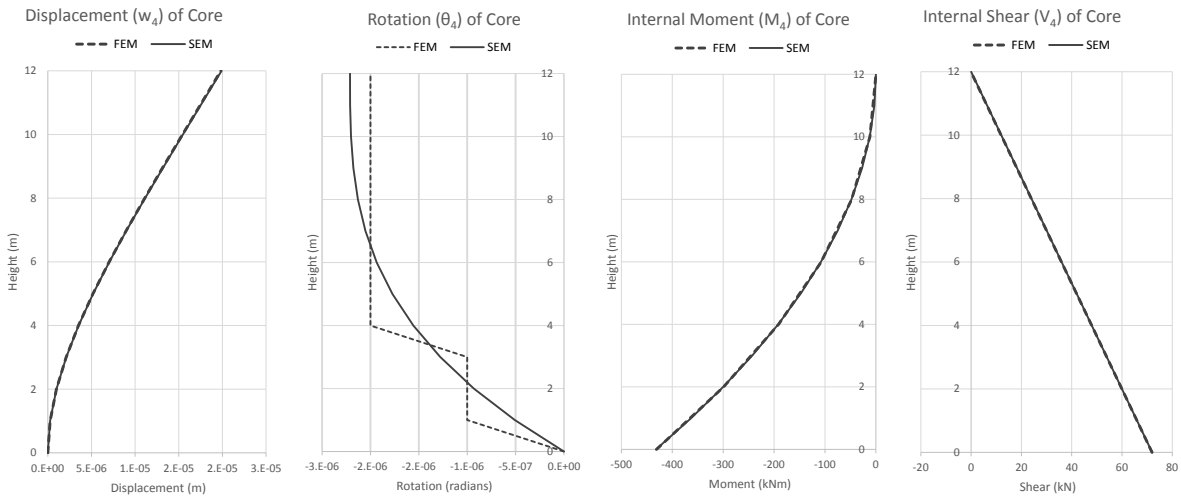

Figure 4.31: Super element 3 validation for degree of freedom 4 (core)

The MatrixFrame FE results (continuous lines) and the results from the differential method (dashed lines) from the graphs match up very well for super element 3 when the determinant is less than zero. However, a few observed differences should be explained. The internal torsion forces from MatrixFrame increase in steps at every meter, because the torsional loading had to be applied as a series of point loads instead of a distributed load along the height, as explained earlier. In this case the difference in results is explained by the difference in loading, showing no major difference in the behaviour of the structure. However, every two meters the step increase is smaller than the applied -23.625 kNm point loads. In MatrixFrame the walls also have torsional stiffness, unlike in the method using differential equations where walls are assumed to have no torsional stiffness. Although the wall's torsional stiffness is very small, some of the torsional load is transferred from the core through the floors (spaced 2 m apart) to the wall, reducing the internal torsional forces in the core. Since the actual torsional wall stiffness is very small, also the difference in results is quite small, so the results are still considered to be accurate and the assumption as valid. Similar to the previous validations, the finite element internal shear forces for degree of freedom one and two change in steps, because the wind force is transferred at every floor instead of transferred continuously using the super element method. Also, there is a rounding error in the rotation due to MatrixFrame. In conclusion, these graphs illustrate that the super element method applied in the tool gives very accurate results compared to a finite element model with the same dimensions and almost identical loading. Confirming the accuracy of the introduced analysis method using differential equations when also torsional loading and resistance is introduced.

Determinant is greater than zero

The stability element and floor dimensions resulting in a positive determinant are illustrated in Figure 4.32.

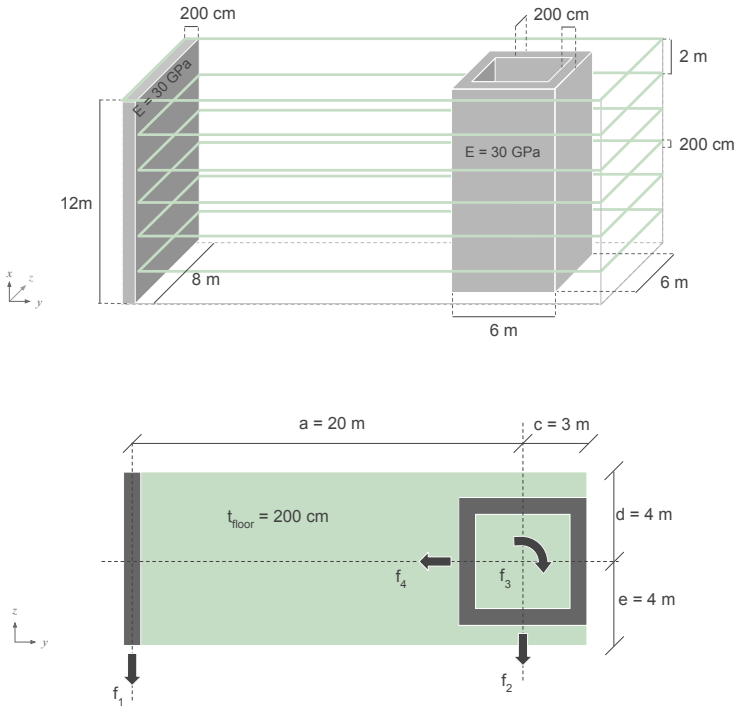

Figure 4.32: Validation parameter inputs resulting in $D < 0$

A wind load of $1\,kN/m^2$ was applied on both sides of the super element, resulting in the following wind line loads on the stability elements:

$$f_1 = 7.5\,kN/m$$
$$f_2 = 15.5\,kN/m$$
$$f_3 = -45.5\,kNm/m$$
$$f_4 = 8.0\,kN/m$$

In MatrixFrame the super element is modelled as a "3D frame" (Matrix Software, 2018). The line loads are applied along the height of the stability elements. Again, the only exception is that MatrixFrame does not have an option to apply a torsional line load along the height, so point loads are placed at every meter along the height instead. This causes the MatrixFrame torsion results to change in steps at every meter, instead of a continuous line. The compete MatrixFrame model report can be found in Appendix C.4.2.

Figure 4.33 shows the result comparison for the wall, and Figures 4.34 - 4.36 for the core.

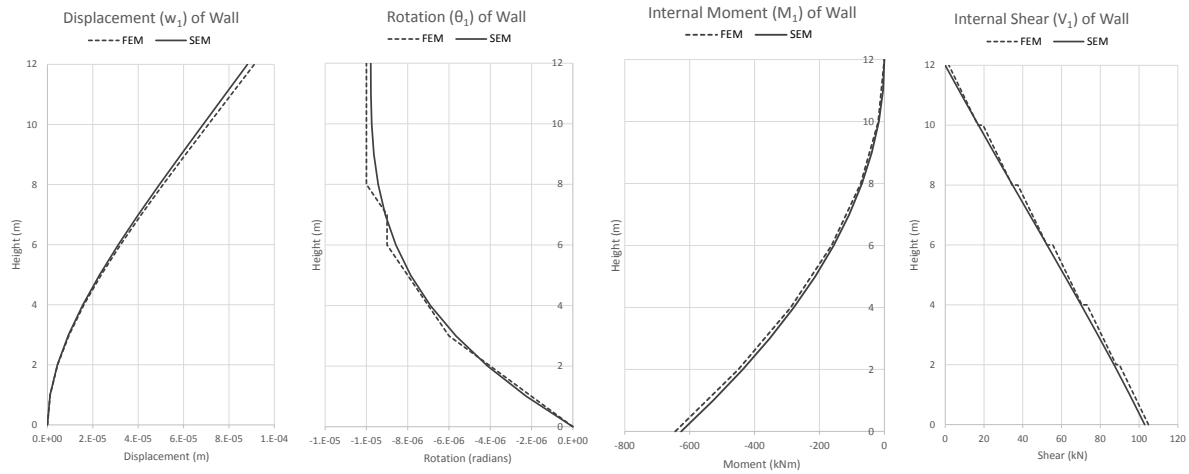

Figure 4.33: Super element 3 validation for degree of freedom 2 (wall)

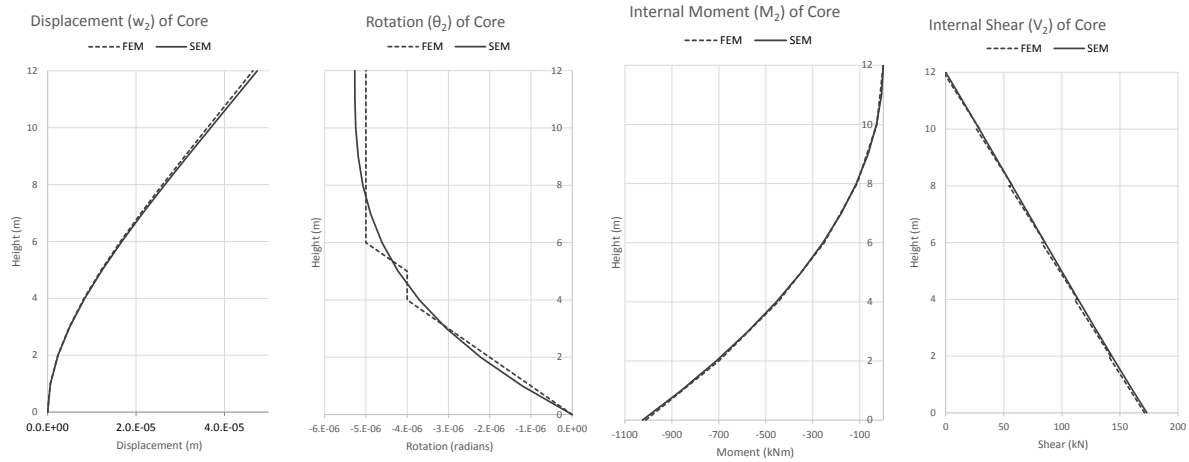

Figure 4.34: Super element 3 validation for degree of freedom 2 (wall and core)

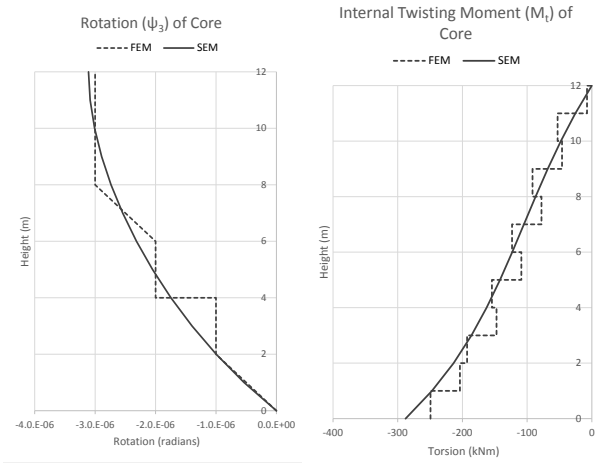

Figure 4.35: Super element 3 validation for degree of freedom 3 (core)

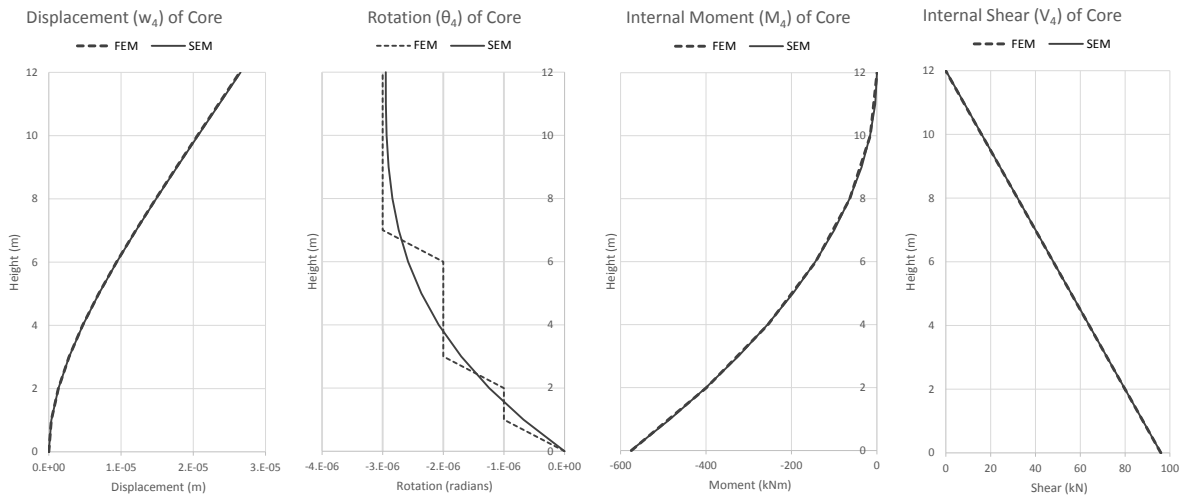

Figure 4.36: Super element 3 validation for degree of freedom 4 (core)

The MatrixFrame FE results (continuous lines) and the results from the differential method (dashed lines) from the graphs match up very well for Super element 3 when the determinant is less than zero. However, a few observed differences should be explained. Also when the determinant is larger than zero, the torsion results from MatrixFrame increase in steps at every meter, because the torsional loading had to be applied as a series of point loads instead of a distributed load along the height, as explained earlier. In this case the difference in results is explained by the difference in loading, showing no major difference in the behaviour of the structure. However, every two meters the internal torsional forces decrease slightly. In MatrixFrame the walls also have torsional stiffness, unlike in the method using differential equations where walls are assumed to have no torsional stiffness. Although the wall's torsional stiffness is very small, some of the torsional load is transferred from the core through the floors (spaced 2 m apart) to the wall, reducing the internal torsional forces in the core. Since the actual torsional wall stiffness is very small, also the difference in results is quite small, so the results are still considered to be accurate and the assumption as valid. Similar to the previous validations, the finite element internal shear forces for degree of freedom one and two change in steps, because the wind force is transferred at every floor instead of transferred continuously using the super element method. Also, there is a rounding error in the rotation due to MatrixFrame. In conclusion, these graphs illustrate that the super element method applied in the tool gives very accurate results compared to a finite element model with the same dimensions and almost identical loading. Confirming the accuracy of the introduced analysis method using differential equations when also torsional loading and resistance is introduced.

5

System Architecture

This chapter discusses the main parts of the software system behind the feasibility tool. It focuses on the system organisation, the data flow, implementation and validation and concludes with the final interface of the tool prototype.

5.1 Conceptual System

In Chapter 3 the concept behind the tool was explained. It discussed the features of the super elements, how to connect them and how to visualise the results and feedback. This section discusses the concept of the software system behind the tool concept. The system design is composed of various components, which work together to result in the proposed feasibility tool. The various components and the data flow through these components are discussed in the following subsections.

5.1.1 System components

The main components involved in the software system are the 3D viewer, the parametric modelling interface and the super element library.

1) Super element library

The super element library, written in Python (Python Software Foundation, 2018), contains the fully implemented super elements and completes the structural analysis. A Python plug-in for Grasshopper, GhPython (Piacentino, 2018), was used as a sandbox environment for simple Python scripting. It provided a dynamic interface between the inputs from Grasshopper to the library as well as the outputs from the library back to Grasshopper. Therefore a GhPython component was included in every building block component and analysis component to tie the super element logic from the Python library into Grasshopper. Each super element from the library corresponds to one fully implemented Grasshopper building block type. An instance of a super element is created when the parameters of a building block are defined by a user. When connected to the analysis component, see Figure 5.1, the super element instance is analysed.

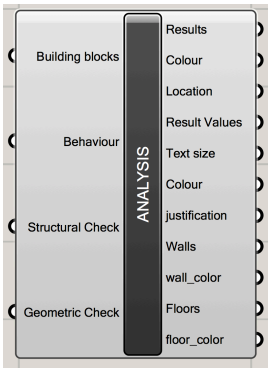

Figure 5.1: Grasshopper analysis component

2) Parametric modelling

Parametric modelling was set as a tool feature requirement to allow quick considerations of various dimensions, loading values, location changes and various structural concepts. Therefore, Grasshopper, a parametric and associative design (PAD) plug-in for Rhinoceros (McNeel, 2018), was chosen as the modelling interface. Grasshopper was already discussed in Section 1.3.

Via Grasshopper's parametric modelling interface custom building block components were created for three different building topology types. For the first (bottom) building block a start component is required. Some example start components and building block components are shown in Figure 5.2 and Figure 5.3 respectively. The start components can be used for any building block that requires their outputs, which are also shown in Figure 5.2. The components with an asterix (*) were not fully implemented for this prototype, they are only geometric structures and cannot be analysed. These structural building blocks can be combined vertically to model larger custom structures. Conceptual examples were shown in Figure 3.10.

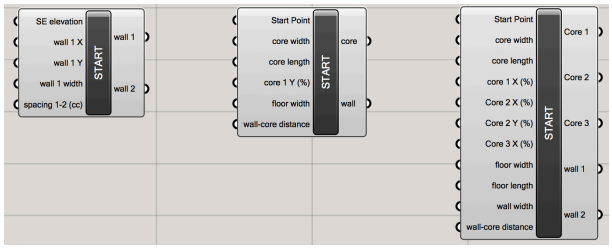

Figure 5.2: Grasshopper start components

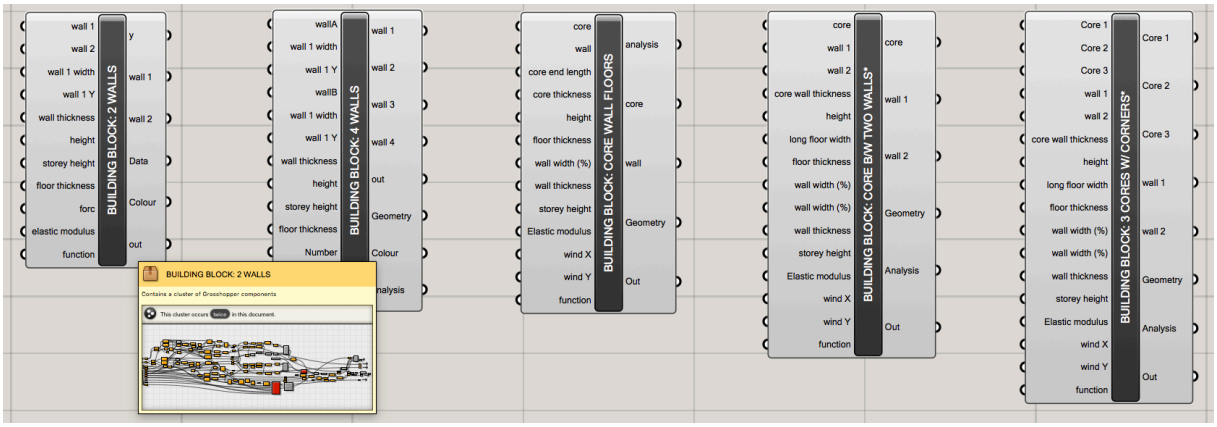

Figure 5.3: Grasshopper building block components

3) 3D viewer

Rhinoceros is used for the 3D viewer for this tool prototype. It is 3D modelling software systems that allow parametric modelling (via Grasshopper) due to its native scripting interface. It visualises the tool output (geometry, analysis result values, behaviour surfaces and feasibility checks) for the user.

5.1.2 Data flow

The data flow through these system components is illustrated in Figure 5.4.

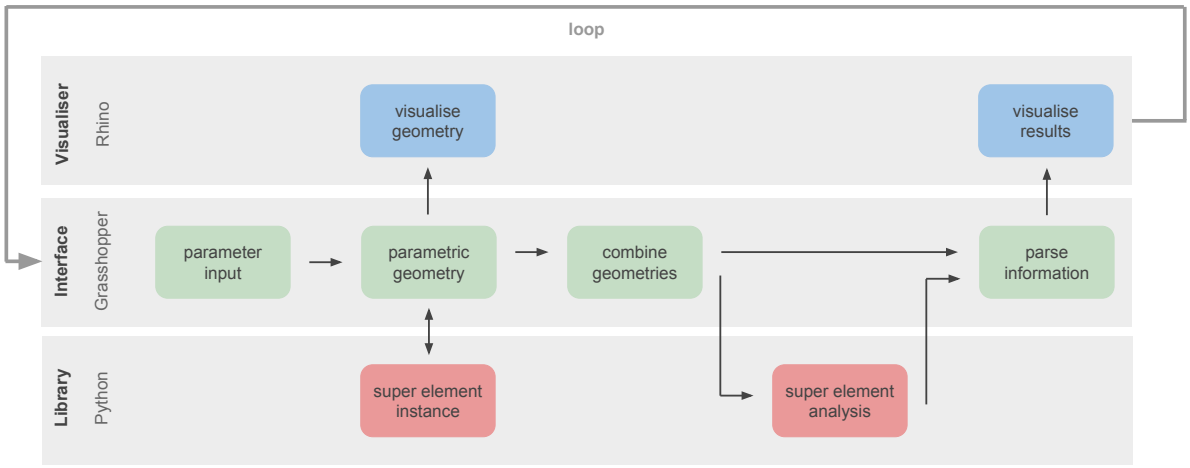

Figure 5.4: General system framework

The system starts with the user defining input parameters for a building block in Grasshopper, which creates parametric geometry that is visualised with Rhinoceros. When a building block is defined, a super element instance is created in the Python library. Multiple super elements can be defined and combined

with each other. For analysis their building block components have to be connected to the analysis component. The information from the super element instances is combined, analysed and the results output back to the Grasshopper python component. The Grasshopper component parses the analysis information along with the geometry and Rhino visualises the results for each building block. The data flows through the system every time an input parameter is changed, building blocks are connected differently or additional building blocks are added to the whole structure.

The separation of the Python code allows it to be used independently from Rhinoceros and Grasshopper, developed further and tested independently.

5.2 Python library

The Python library contains the super elements that correlate to the Grasshopper building blocks and contain the analysis script of the Grasshopper analysis component. In this section the API (Application programming interface), the code layout, implementation and validation are discussed.

5.2.1 API

Since mainly two different programs were used for this tool, it was necessary to provide an API for them to communicate.

An **API** "is a software intermediary that allows two applications to talk to each other" (MuleSoft Inc., 2018).

Input parameters are passed from the GhPython component to the super element library and results are fed back to the GhPython component. This is done on two occasions. Once, when the user defines the dimensions, loading, material and position of a building block and the super element instance is created. Figure 5.5 is a pseudocode, simplified code, of this procedure. Corresponding to the building block type the super element model is imported and the variables are defined based on the user's input values. With this information the super element a super element instance is created specific to these inputs. Note that the instantiation of the super element is not the structural analysis. The super element library returns the instance to the GhPython component.

```
# CREATE A SUPERELEMENT
from superelement_library import models

superelement_1_input = models.TwoWallsInput(
    location=[x=0, y=0, z=0],
    height=6.0,
    **other_arguments
)
superelement_1 = models.SuperElementTwoWalls(superelement_1_input)
    # create superelement instance
    # prepares initial calculations
    # evaluates symbolic information with given input

print superelement_1
```

Figure 5.5: Pseudocode: create a super element

The second occasion is when the Grasshopper building blocks are connected to the analysis component. Figure 5.6 shows another pseudocode to show the communication for this part. In this case the super element instances are collected in a super element list. The calculations function is run over these instances and returns the results, which include the structural behaviour and check results, to the Grasshopper python component.

```
# ANALYSE SUPERELEMENTS
from superelement_library import analysis

# collect combined superelements in a list
superelements = [superelement_1, **other_superelements]
results = analysis.calculations(superelements)
print results

# where
results = [
    displacements,
    rotations,
    moments,
    shearforces,
    normalforces,
    feedback
]
```

Figure 5.6: Pseudocode: analyse super elements

5.2.2 Code layout

The external Python library was written with object oriented programming (OOP) principles.

The **object oriented programming** paradigm revolves around objects containing data and functionalities (Swaroop, C. H, 2014). A class creates a type of something, and the object is the instance of that class. For example if one would create a class called 'car', then a 'Jeep' would be an instance of that class. Plus, variables and functions can be assigned to a class or an object. For example, the class 'car' should have a function 'drive', meaning every instance of the car class, including the Jeep, has a drive function. Some functions or variables can also be specific to an instance. For example the 'Jeep' object or instance has the function 'four wheel drive', which other instances of the car class may not.

For the prototype every super element, which corresponds to one type of topology, represents a class. These super element classes all contain attributes and functions specific to them. For example the 'SuperElementTwoWalls' class always has 4 total degrees of freedom, while the 'SuperElementFourWalls' class always has 8 degrees of freedom. However, both classes also inherit from the overarching 'SuperElement' class. Any attributes or functions defined for the overarching 'SuperElement' class also apply to the classes underneath it. Figure 5.7 shows the hierarchy principle of the classes.

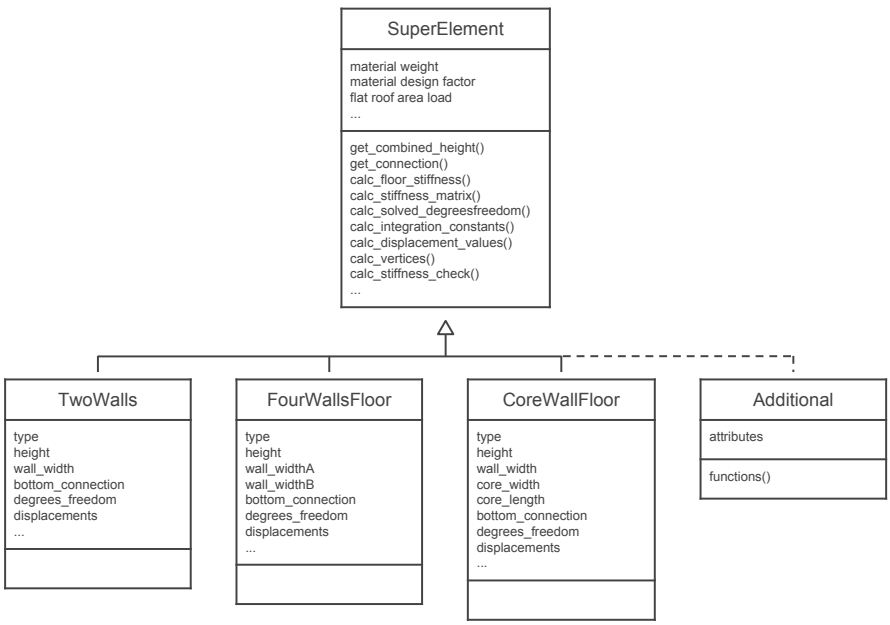

Figure 5.7: Class UML diagram

The OOP style was chosen, because it provided a clear organisation of the elements involved, allows easy

implementation of additional elements and is a DRY (Don't Repeat Yourself) (Ferreira and Casasín, 2014) coding style. However, since only a prototype was developed and to save time, not all of the functions are defined for the SuperElement class. Many are still defined for each sub-class, meaning the prototype super element library is not as DRY as it could be.

5.2.3 Implementation

The implementation of the external Python library is quite simple with the GhPython component. Through the path to the external Python library the required files are imported into a Grasshopper python component. In the case for creating the super elements, the input values from the user are connected to the inputs of the python script, loaded into the function and the result is sent to an output of the component. A similar process is done for the analysis component, just instead of input values various super element instances are connected to the analysis component and sent through the analysis function. The GhPython component within the building block with two walls and the script is shown in Figure 5.8.

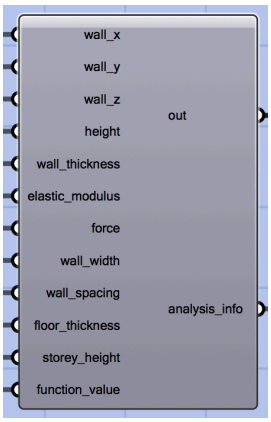

(a) GhPython component

```
from superelements import models

given = models.TwoWallsInput(
    location = [wall_x,wall_y,wall_z],
    height=height,
    wall_width=wall_width,
    wall_thickness=wall_thickness,
    wall_spacing=wall_spacing,
    floor_thickness=floor_thickness,
    storey_height=storey_height,
    force=force,
    elastic_modulus=elastic_modulus,
    function_value = function_value
)

analysis_info =
models.SuperElementTwoWalls(given)

print analysis_info
```

(b) GhPython script

Figure 5.8: Example GhPython component and script

During the analysis process numerical and symbolic algebra is used to calculate the structural behaviour of the super elements. Python has a Numpy (NumPy developers, 2017) and Sympy (SymPy Development Team, 2016) library, which perform these tasks. However, these libraries are very difficult to import into Grasshopper for Windows and it's not possible to import them into mac version, because it is based on IronPython (Community, 2007). This is a limitation to using Grasshopper as the modelling interface, but it was possible to work around it. Better plug-ins are being developed for Grasshopper to support such external libraries (AbdelRahman, 2017).

5.3 System validation

In order to make sure the analysis calculations remain correct throughout the development process, a series of tests were completed, which are summarised in Figure 5.9.

First hand calculations were done to derive the differential and displacement equations for each super element. These were checked with Steenbergen (2007).

The hand derived symbolic behaviour equations for the super element with two walls and four walls with the floor stiffness were input into Maple. With Maple the required symbolic matrices and vectors were calculated. The final displacement, rotations, moments and shear forces along the height of the stability elements were also calculated so that they could be checked with the finite element program MatrixFrame. The same procedure was done for the super element with one core, one wall and the floor stiffness, except using Mathematica instead of Maple. Mathematica could solve the symbolic algebra much quicker, partly because it did not automatically render the resulting symbolic matrices for the user to see.

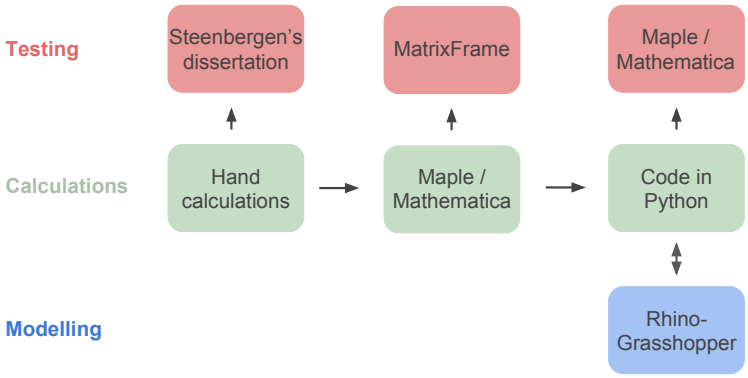

Figure 5.9: Development process

Only once the results matched and the differences could be logically explained was the procedure rewritten into a python script. Within the external python library the script was also tested. Individual (stand-alone) functions were verified with Unit Tests (UT) and the whole process starting with the super element inputs and ending with the behaviour results was testing with End To End (E2E) tests. The E2E tests were verified by comparing the final behaviour results from the Python code and the Maple or Mathematica results after choosing the same input values. Once also these calculations were validated with almost 200 tests, the python code was integrated into the Grasshopper building blocks and analysis component.

5.4 Tool Prototype

Combining the conceptual features discussed in Chapter 3 and the implementation of the tool from this Chapter, the final tool is presented briefly in this section. The theory behind the components and the super element library were already discussed, so the purpose of this section is only to show the outcome of this prototype from the user's perspective.

5.4.1 Rhino-Grasshopper building blocks

The resulting fully implemented building blocks visualised in Rhino-Grasshopper are shown in Figure 5.10.

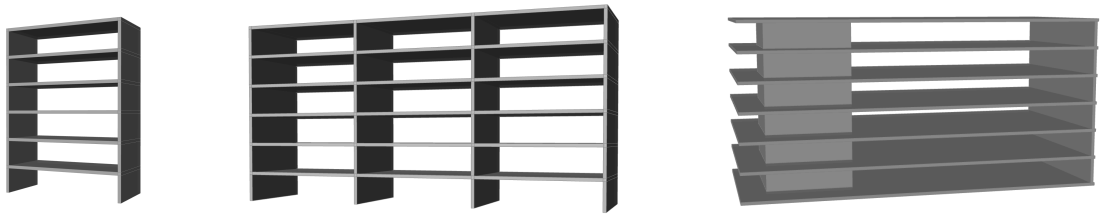

(a) Two walls *(b) Four walls* *(c) One core and one wall*

Figure 5.10: Grasshopper building blocks

5.4.2 Modelling

The use process diagram explained in section 3.8 is implemented in Grasshopper with Python as shown in Figure 5.11. As already explained, the input parameters can be set by the user and the Grasshopper building blocks can be combined with wires between the stability element inputs and outputs.

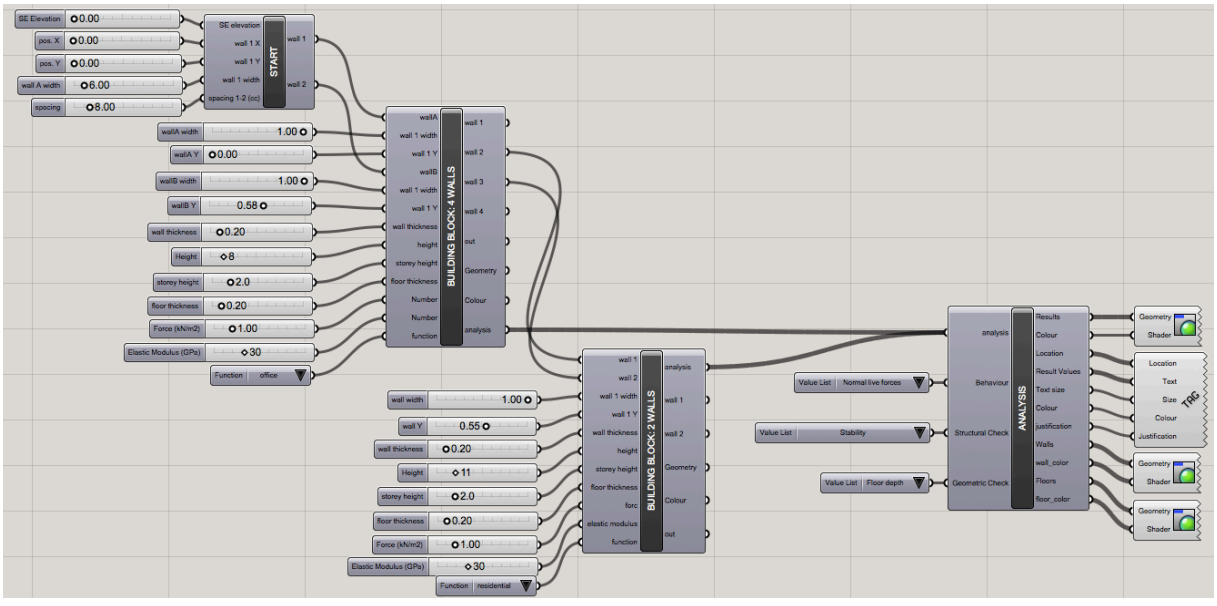

Figure 5.11: Grasshopper modelling process

5.4.3 Behaviour

In order to determine the structure's feasibility, they have to be connected to the analysis component. The results for each structural behaviour result, see Figure 5.12 and 5.13, and feasibility check can be displayed by choosing from a list input.

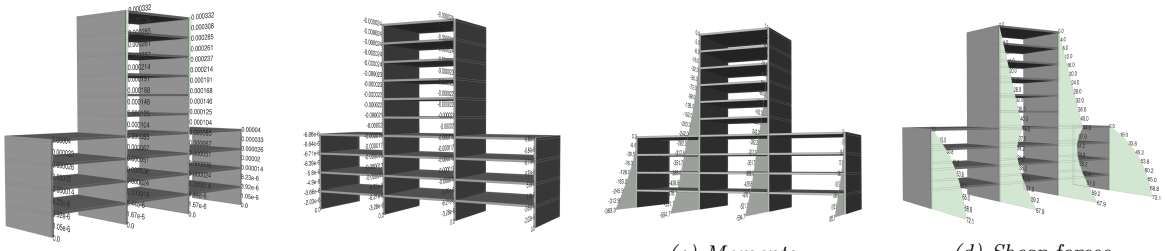

(a) Displacements *(b) Rotations* *(c) Moments* *(d) Shear forces*

Figure 5.12: Visualised behaviour along stability elements

(a) Normal dead reactions *(b) Normal live reactions*

Figure 5.13: Visualised vertical load reactions

5.4.4 Feasibility

Depending if the check was satisfied or not, the colour of the corresponding structural element turns grey or red respectively, as shown in Figure 5.14.

(a) Failed stability check for the top building block *(b) Failed floor depth check for bottom building block*

Figure 5.14: Visualised feasibility checks

6
Case Study

A case study, about the Energiekwartier in Den Haag, Netherlands, (ABT, 2018) is introduced to show how the tool should be used during the conceptual design process and how its structural predictions perform compared to detailed calculation results. First, the case study will be explained in more detail and then the three main aspects that the tool is used for during the conceptual design phase; modelling, determine feasibility and predict structural behaviour.

6.1 Energiekwartier

The Energiekwartier is a collection of concrete residential buildings currently under construction in Den Haag, Netherlands. The architects involved in this project are Architecten (Klunder Architecten, 2018) in Rotterdam and ABT (ABT, 2018) provided the structural calculations. The individual buildings are labelled in Figure 6.1.

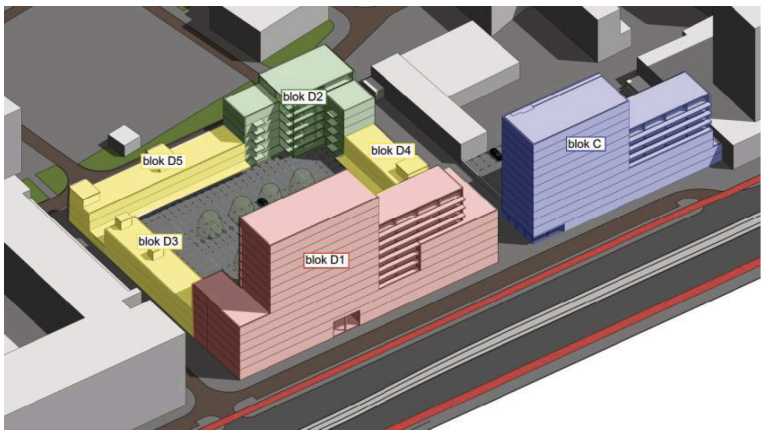

Figure 6.1: Energiekwartier Buildings provided by ABT

Since block D1 is geometrically the most complex, its design will be used to test the geometric flexibility of the modelling method implemented in the feasibility tool. Blocks D3, D4 and D5 were constructed with 8 to 10 parallel concrete in-situ walls, prefab floor slabs and an in-situ top layer connecting the floor slabs. The in-situ top layer has no structural function regarding the floor bending, but does ensure the in-plane action of the floors, which transfers the wind load from the facade to the stability walls (Steenbergen, 2007). The structural system and construction technique is similar to the fully implemented building blocks with parallel walls, so blocks D3, D4 and D5 were used for the structural calculations and the feasibility analysis.

6.2 Conceptual Project Information

During the conceptual design phase less information about the design is know compared to the final design phase.

In the early stages the architect can still take advantage of the design freedom, illustrated by the MacLeamy curve in Figure 1.1, while structural engineers have to make assumptions in order to predict the structural behaviour.

In reality all the information for the Enegiekwartier is known, since it is currently being constructed. However, in order to compare the conceptual results with those from the detailed design phase, some information is assumed to be unknown (or forgotten) for the conceptual calculations using the tool prototype. Below the assumed knowledge for the Energiekwartier in the conceptual design phase is summarised.

The below information is usually fixed for a project.

- Location: Den Haag, Netherlands
  Knowing the location enables the structural engineer to estimate environmental factors such as wind loading and soil conditions.
- Neighbourhood: residential
  The type of neighbourhood is important for the architect, because in this case the new building should match the residential environment.

- Plot area: (assumed) 85 m by 25 m
  The maximum plot area sets the limits for the size and dimensions of the new design.
- Function: residential with the possibility of office spaces on the ground floor
  The function of a building strongly affects the architectural space inside and the location and type of stability elements, which in turn also influences the construction method.

Depending on the level of detail in the architectural model, the structural engineer may adopt the structural members indicated in the architectural sketch or create a new load bearing structure. Either way, the following information must be decided on during the meeting to complete a feasibility analysis.

- Rough dimensions
  In order to analyse a structure in the conceptual design phase the rough dimensions of the load bearing structure, such as the floor system and stability elements, must be known.
- Materials
  Also initial materials for the load bearing structure and facade must be chosen to complete the analysis.
- Construction Method
  The construction method may change the force flow and materials required.

These parameters are not fixed, in fact they should be easily changeable to explore alternative options. The purpose is to narrow down the selection of design ideas to a few that can be explored further in more detail after the conceptual design phase.

It is important to note that the discussed 'known' information during the conceptual design phase is all estimated, it most likely does not include the exact final dimensions and loading. Therefore, the results from the feasibility study are expected to be slightly different from the detailed analysis results. In order to give enough insight into the structural behaviour the results should be in the same order of magnitude.

6.3 Geometric Flexibility

This section will go through the modelling aspect of a brainstorm session with the architect and structural engineer in the conceptual design phase with the feasibility tool. The geometric flexibility of a modelling tool is very important for the architect's creative design ideas. A goal of this case study is to model possible load bearing structures for alternative architectural designs with the building block method. Block D1 from the Energiekwartier project was used as an example to test the geometric freedom and modelling speed of the tool's modelling method. One simple architectural design and the more complex final design are considered.

6.3.1 Simple Design

Prior to the meeting with a structural engineer, the architects not only consider the 'good' designs, but also designs that are not recommended to highlight important aspects. For example in the case study, block D1 was also visualised as a very simple box shape, see Figure 6.2. The design would be very easy for the structural engineer to calculate and the contractor to build, but it did not pass the architectural nor the municipality's aesthetic requirements. This boxy and quite tall design did not suit the residential area it was located in and was therefore not chosen. However, for the purpose of this case study this design will be considered further and go through the whole conceptual design phase using the feasibility tool.

In the first step during the meeting, the architect presents a conceptual design, see Figure 6.2. The design may range from a rough shape or space to a detailed model including a facade, windows, lighting and other aspects to sell the design to the client or municipality. Regardless, the aim of the meeting is to model and analyse the feasibility of the main load bearing structure.

The architectural shape, in this case, is very simple, so many structural systems could be considered for the interior. In this second step the architect should collaborate with the structural engineer to choose a

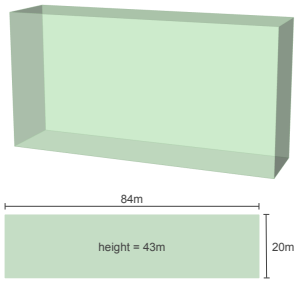

Figure 6.2: Simple Conceptual Box Design

system and construction method. Even, or especially, when the architectural shape is more complex the feasibility tool would allow the architect and structural engineer to quickly explore various systems and rough member dimensions. For the box shape one possible structural system is composed of 3 cores and multiple parallel walls, see Figure 6.3a. This system could be simplified further to only include the most important structural members, such as the 3 cores, see Figure 6.3b. Since forces flow to the stiffer and stronger elements, the shear walls between the cores are not as significant and can be neglected in this conceptual design. Once the main structural system has been chosen, the structural engineer divides the design into sections with the same floor plan.

(a) Structural system

(b) Simplified structural system

Figure 6.3: Box design floor plan

This design was composed very quickly with the feasibility tool in the third step. Only a start component and one building block, see Figure 6.4, was required to model it. The two components are connected by the location of the stability elements and the dimensions were set by sliders.

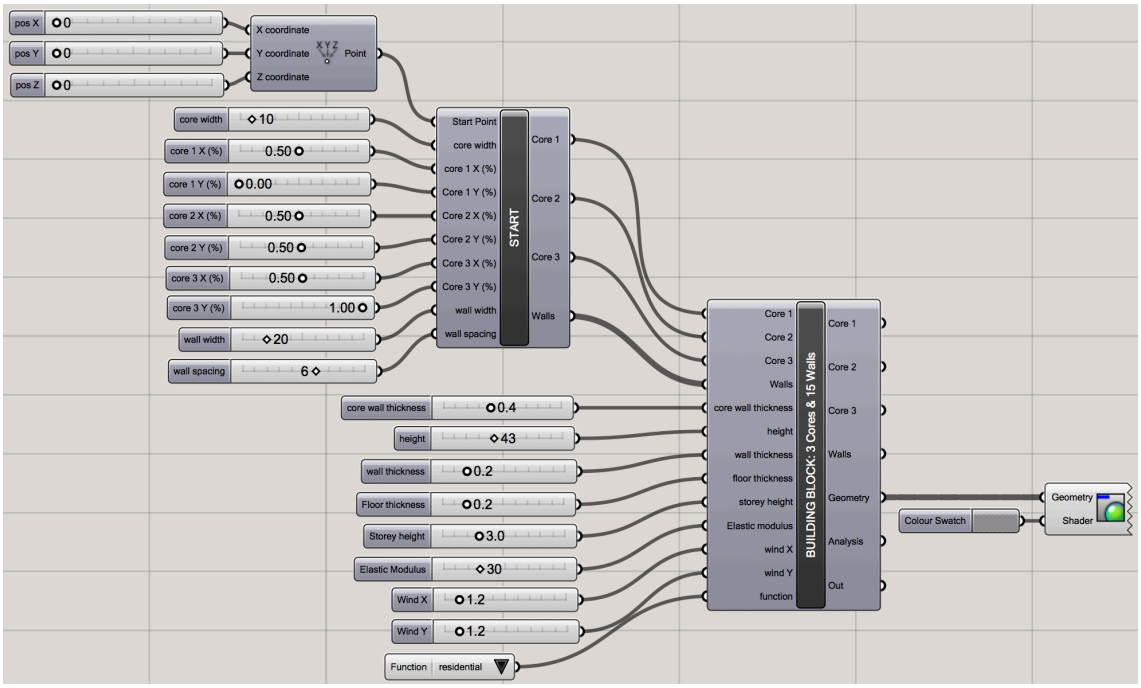

Figure 6.4: Grasshopper components for the simple design

The dimensions and locations of members can be changed parametrically until the architectural and structural requirements are met. This is an iterative process, so additional changes can be made to improve the design or reduce the cost of materials. Other structural designs can also be considered by creating a new model.

6.3.2 Complex (actual) Design

The more complex actual design of block D1, see Figure 6.5a, is used to demonstrate the modelling speed and geometric flexibility of a building with various topologies. The initial given information is the same, and the design dimensions are illustrated in Figure 6.5b.

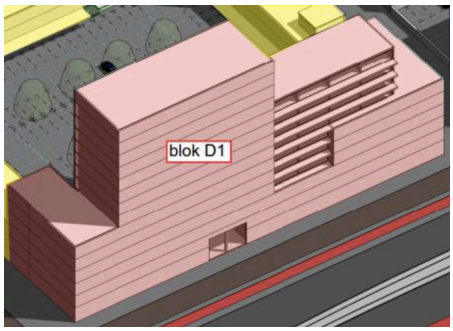

(a) Design

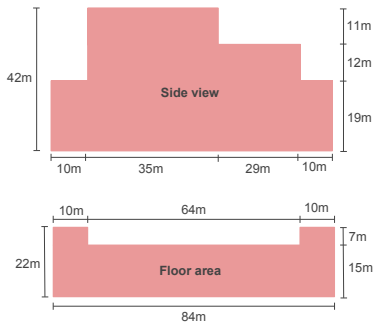

(b) Dimensions

Figure 6.5: Energiekwartier Block D1

Given the architect's floor plan, the structural engineer identifies the main structural elements throughout the building and again divides the building into floor plan types. For block D1 the general floor plans are illustrated in Figure 6.6. In the bottom floor plan the cores provide most of the resistance along with the two walls on either end of the corners, so the walls between the cores are neglected. Only one core is

present in the middle floor plan and the remaining walls are represented by the two walls on either side of the core. The top floor plan only includes one core with a single wall.

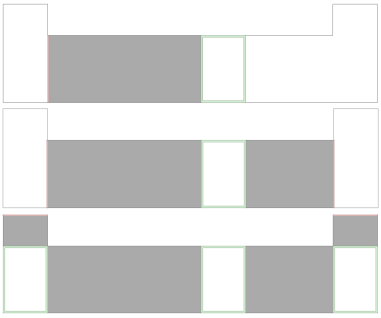

Figure 6.6: Block D1 general floor plans

Once the general floor plans were identified, building blocks from the component library with a matching topology and loading were used to model the design. For this building the client wanted the ground floor to be for commercial stores, while the rest is commerical. Therefore, the ground level was modelled with a separate building block even though the floors above had the same topology. See Figure 6.7 for the 3D configuration.

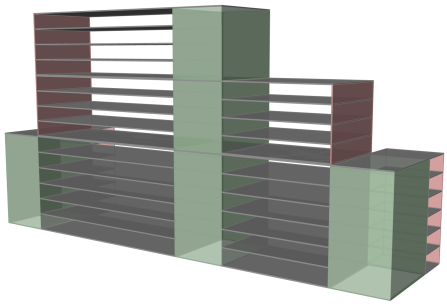

Figure 6.7: Simplified block D1 model

In total 4 building blocks with 3 different topology types were combined in Grasshopper, see Figure 6.8, by connecting shear core walls and single walls. When single walls are connected with core walls, a small separate component is required which indicates on which of the four core walls the single wall should be placed. It important to note that the physically and mathematically model of such a connection is not the same, but this difference is discussed later. With this modelling method many geometric, material and load parameters can be adjusted parametrically and whole components can be switched out to examine alternative designs.

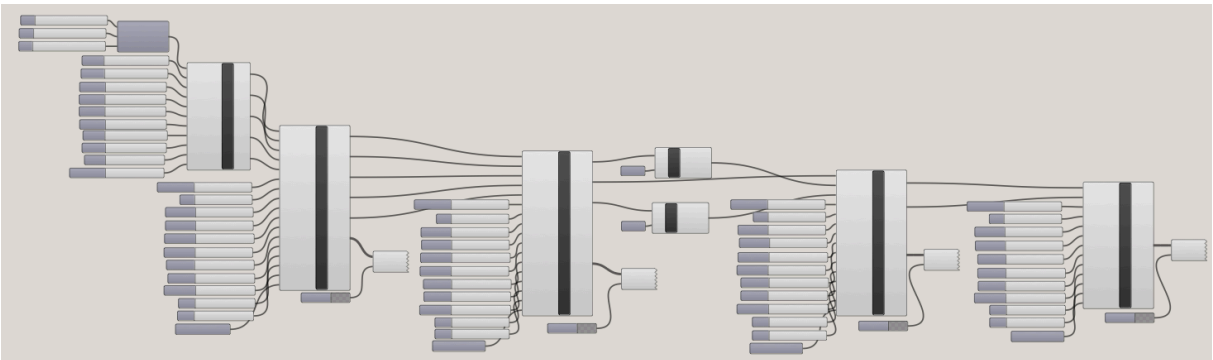

Figure 6.8: Block D1 GH components

Since the used building blocks had simple topologies, it would be reasonable to assume that they would be available in an extensive component library. Focusing on the main structural members in the conceptual

design phase reduces the requirement for many different and detailed building blocks in the component library, making the proposed modelling and analysis method more viable.

As highlighted in this case study, the physical connection between a core and a single wall is different from the mathematical connection. Usually, when designing a building, the physical walls are connected to other walls, so that they can transfer forces down to the foundation. However, with the super element method all stability elements can only be connected via their bottom and top node. For example, in order to place one super element on top of another, the bottom node of a wall is connected to the top node of another wall. For wall connections the physical and mathematical models match. However, since cores are considered as a single stability element and not four separate walls, it also only has a single top and bottom node. Therefore, if a wall is attached to the top of a core, the physical and mathematical connections do not match, as shown in Figure 6.9. In the physical model the wall is connected directly to one of four core walls and in the mathematical model it is connected to the centre of the top of the core.

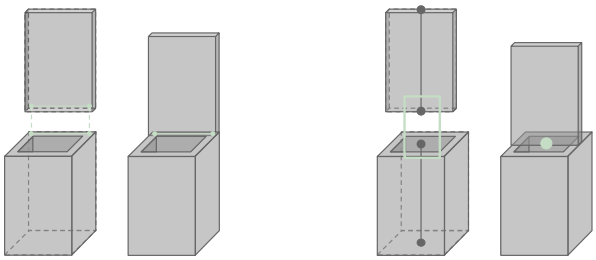

(a) Physical connection *(b) Mathematical connection*

Figure 6.9: Physical vs. mathematical connection

6.4 Structural Analysis

Block D3 from the case study, see Figure 6.10, is used to demonstrate the tool use process regarding the feasibility and structural behaviour and to compare the estimated structural results from the early design phase with the actual behaviour resulting from ABT's (2018) detailed model. Block D3 is used instead of block D1, because its geometry is simpler and can be represented with the fully developed building blocks from this project. The project information from Section 6.2 still applies.

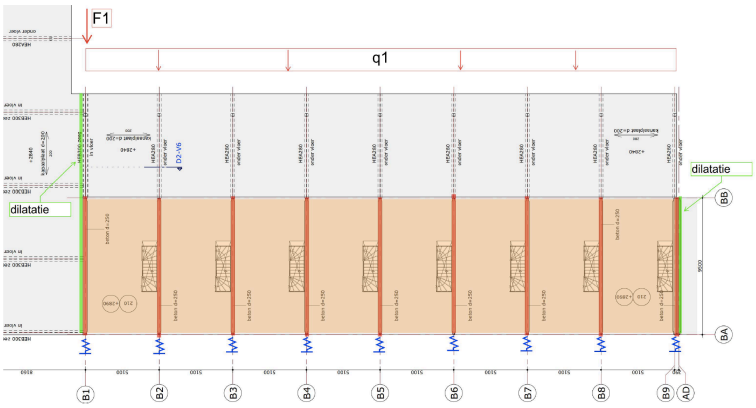

Figure 6.10: Stability walls (ABT)

6.4.1 Block D3 Information

In order to model and analyse block D3, the known information in the conceptual and detailed design phase are summarised in the following two sections.

Block D3 Conceptual Information

The main dimensions used are summarised in Figure 6.11. Building block D3 was modelled to have 250mm thick in-situ walls, 200mm thick prefabricated floor slabs, 10.0m wide walls spaced 5m apart and designed to have up to 4 residential floors. The prefab floors were assumed to be made of C30/37 and the in-situ walls of C25/30.

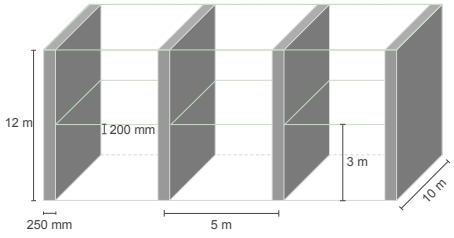

Figure 6.11: Four-walled building block dimensions representing block D3

Additional material and loading information is summarised below. These are either estimated based on the location of the building or well-known Euro code values.

Density of concrete	(γ_c):	$25\,kN/m^3$
Density of masonry	(γ_m):	$20\,kN/m^3$
Wind load	(q_{wind}):	$1.00\,kN/m^2$
Residential floor load	(q_{res}):	$1.75\,kN/m^2$
Roof load	(q_{roof}):	$1.00\,kN/m^2$
Foundation rotational stiffness	(c):	$2000\,MNm/rad$

Detailed Stability Information

For the detailed stability calculations done by ABT, more accurate information is available compared to the conceptual design phase. Building block D3 was constructed from in-situ 250mm thick walls and 210mm thick prefabricated floor slabs with an in-situ top layer with 70mm thickness. Block D3 has nine 9.50m wide walls with a spacing of 5.10m and was designed to have up to 4 residential floors. The prefab floors were made of C30/37 and the in-situ walls of C25/30.

The location of the building is in a wind area of level II with wind pressure 0.92 kN/m^2. To consider the negative wind pressure the wind factor is calculated.

$$(0.8 + 0.5) * 0.85 = 1.105$$

Resulting in a total facade wind pressure of $1.0166kN'm^2$, which is slightly higher than the initially estimated wind load.

$$1.105 * 0.92 = 1.0166\,kN/m^2$$

The foundation was taken into account by calculating its rotational stiffness, $2030MNm/rad$, and spring stiffness, $55000kN/m$, which are slightly higher than estimated. Imperfections were not taken into account in the conceptual analysis, but are included in the detailed analysis. The second-order effects were neglected in both due to the large number of parallel stability walls.

6.4.2 Feasibility Analysis

The feasibility analysis helps the structural engineer and the architect determine if a conceptual design meets the requirements from both discipline. Several checks have to be satisfied for a design to considered feasible.

Feasibility checks

The available checks in the tool prototype for the structural engineer are shown in grey in Figure 6.12 and the architectural checks in green. The user can select which structural and architectural check should be visualised by the tool. When all checks are satisfied the structure remains grey, but if a check fails, the affected part of the building (wall or floors) turns red. This is illustrated later for the case study.

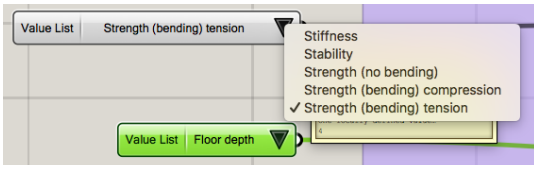

Figure 6.12: Feasibility checks offered by the tool, visualised in Rhino-Grasshopper

Supplementing the visualised checks, members from both disciplines must also provide verbal input. However, since only the final visual design and paper calculations were available for this project, the meeting input cannot be considered. Since the Energiekwartier is being constructed in Den Haag, it is assumed that the specifications from the structural analysis deem the building safe and feasible according to the European and Dutch national building codes. Therefore, the feasibility tool should show that all the checks pass based on the dimensions, materials and loading of this case study.

Block D3 feasibility prediction

When the building is modelled in the feasibility tool, the whole structure remains grey, see Figure 6.13a and nothing turns red, meaning the building passes all the feasibility checks. Hence, the feasibility tool would have accepted this building design as feasible if it had been used in the conceptual design phase, matching up with the feasibility of the final design currently being built in Den Haag.

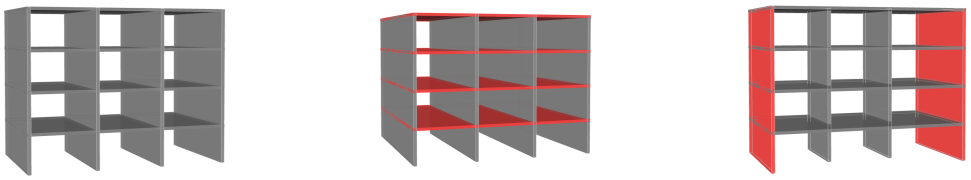

(a) Feasible *(b) Floor depth check fail* *(c) Strength check fail*

Figure 6.13: Case study feasibility outputs

6.4.3 Behaviour Analysis

This case study considers two main types of structural calculations; a stability analysis for the governing middle wall and a strength analysis for the inner and outer walls. Other calculations may have been required to construct this building, however, only these are compared because they have the greatest affect on the building's structural feasibility. Also, since not all of the detailed information is known in the conceptual design phase, the results are not expected to be the same. Reliable results from the conceptual analysis are expected to indicate the order of magnitude of the results from the detailed analysis. The project information from Section 6.2 and estimated dimension and loading from Section 6.4.1 apply to the conceptual calculations, while the actual dimensions and loading apply to the ABT calculations.

During the design process the structural engineer can make structural recommendations based on practical experience or on the visualised behaviour results. The tool visualises the deflection, rotation, shear forces and moments along the height of the building, even if it is composed of various building blocks. The normal forces are shown at the bottom of the structure, where it would meet the foundation.

Conceptual Stability Calculations

Both the conceptual and detailed stability calculations were completed for the middle wall of block D3, because it had the governing (least desirable) conditions. The ULS load combination, $Q_{ULS} = 1.5{*}Q_{wind}$, was applied to determine the foundation moment and shear forces while the SLS combination, $Q_{SLS} = 1.0 * Q_{wind}$, was applied to determine the top deflection of the stability wall. The raw results the tool provides do not include any factors to keep the tool transparent, but the user can manually include a factor with the wind load input when necessary.

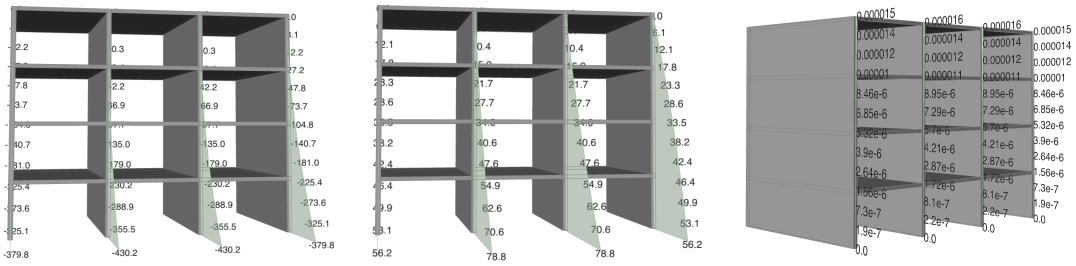

*(a) Moments (1.5*Qk)* *(b) Shear forces (1.5*Qk)* *(c) Deflections (1.0*Qk)*

Figure 6.14: Tool stability results

One significant difference to the ABT calculations is that the tool does not include the foundation stiffness in the behaviour results. In order to compare the total deflection values, a separate calculation to include the effect of the foundation's rotational stiffness (c) is incorporated. Equation 6.1 (Dicke, 1991) is used to calculate the total deflection, where the deflection due to the foundation stiffness is calculated with Equation 6.2. The foundation stiffness could be included in the tool solver in the future to make the moment and shear results more accurate.

$$w_{total} = w_{bending} + w_{foundation} \tag{6.1}$$

where

$$w_{foundation} = \frac{q_{wind} * height^3}{2 * c} \tag{6.2}$$

resulting in

$$w_{total} = 0.015mm + 2.376mm = 2.391\,mm$$

Detailed Stability Calculations

The stability calculation method used in the ABT calculations differs slightly from the differential method used in the tool. First the wind force is distribution from the facade to the floors with simple hand calculation. That load is applied to the floors and analysed in TechnoSoft Inc. (2018) to determine the point loads on the walls. A separate Technosoft model is made for the walls with the floor point loads to calculate the resulting moments, shear forces and the top deflection, see Figure 6.15. The same load combinations were used in the detailed stability calculations as in the conceptual calculations.

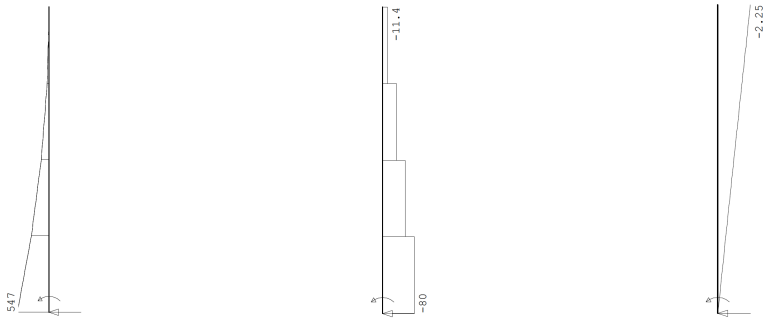

(a) Moments (ABT) *(b) Shear forces (ABT)* *(c) Deflections (ABT)*

Figure 6.15: Case study stability results

Stability Calculation Comparison

Including the conceptual foundation stiffness calculation, the tool's results, seen in Figure 6.16, indicate the order of magnitude correctly, validating the tool's reliability for the stability calculations of block D3. 6.16.

Stability Calculation Comparison			
	Case study	Tool	Error (%)
Foundation moment (kNm)	547	430.2	-21.35%
Foundation shear forces (kN)	80	78.8	-1.50%
Foundation deflection (mm)	2.25	2.39	6.22%

Figure 6.16: Stability Calculation Comparison

The comparison for this building shows that the feasibility tool can give significant insight into the structural behaviour due to lateral loading of a conceptual building design. However, as expected the results are not the same and have about a 20 % error. One main reason is that the exact dimensions, applied wind loading and foundation stiffness were used in the detailed analysis, while estimate values were used for the conceptual model. Plus, the case study calculations were done for a building with 9 parallel walls, while for the calculation using the feasibility tool a building block with only 4 walls was used. This affects the wind force transfer from the floors to the walls along the height of the building, causing different loads applied to the stability elements. Also, the case study used a different approach to transfer the wind load from the floors to the walls. The individual floor analysis resulted in a reaction load where they meet each wall (hence the stepped shear diagram). The feasibility tool, as already discussed, uses a distributed floor stiffness (continuous shear diagram).

Conceptual Strength Calculations

The conceptual strength calculations only take into account the dead and live load mentioned in Section 6.4.1. Additional normal loading is determined later in the design process and included in the detailed analysis, but is still unknown in the early design phase. Example loadings are plant, floor and roof tiles dead load as well as moveable wall live loading. Hence, the results are not expected to be exactly the same as in the detailed phase, but should indicate the order of magnitude.

For efficiency, the strength calculations were only done for the inside and outside wall. The normal dead loads calculated by the feasibility tool only include the dead weight of the main structural elements visualised in the model, see Figure 6.17. The live loads include the floor area load corresponding to the functionality of the space (residential vs. office space). The total normal forces are calculated in the same way as in the case study. The inner walls carry the floor loads of the full floor width and the outer walls carry the floor loads of only half the floor width. The tool's normal force results are summarised in Figure 6.17.

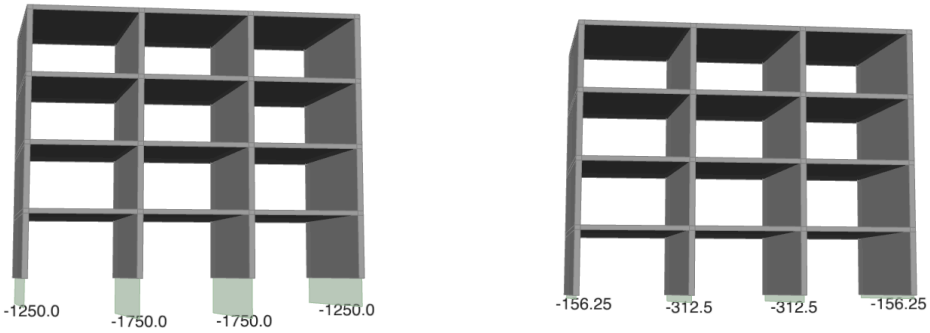

(a) Dead normal forces

(b) Live normal forces

Figure 6.17: Tool normal forces

Some important loads are missing in the tool; the ground level floor dead and live loads and facade loads. These can be easily implemented given the calculations below:

Dead floor load:

$$\gamma_{concrete} * volume \tag{6.3}$$

For the inside wall:

$$25kN/m^3 * 0.200m * 5.0m * 10.0m = 250.0\,kN$$

For the outside wall:

$$25kN/m^3 * 0.200m * 2.50m * 10.0m = 125\,kN$$

Live floor load:

$$q_{function} * area \tag{6.4}$$

For the inside wall:

$$1.75kN/m^2 * 5.0m * 10.0m = 87.5\,kN$$

For the outside wall:

$$1.75kN/m^2 * 2.50m * 10.0m = 43.75\,kN$$

The facade is made of masonry, approximate density 20 kN/m^3, and is approximately 0.100m thick.

Facade load:

$$\gamma_{masonry} * volume \tag{6.5}$$

For the inside wall:

$$20kN/m^3 * 0.100m * 3.0m * (5.00m * 2) = 60.0\,kN$$

For the outside wall:

$$20kN/m^3 * 0.100m * 3.0m * ((2 * 2.50m) + 10.00m) = 90.0\,kN$$

Including these values, the inner wall and foundation below have to hold 2060 kN of dead load and 400 kN of live load. The outer wall and below foundation must hold 1465 kN dead load and 200 kN live load.

Detailed Strength Calculations

For the detailed strength calculations, all the dead and variable (live) vertical loads are known and collected in a spreadsheet. Block D3 also includes balconies on the first floor (at the ground level) for the residents to park their car, however, to simplify the structure these were neglected.

The detailed strength calculations were only done for the wall between block D3 and block D1 (wall 1 or tussenwand), which was also applied to the inner walls, and for the outer wall on the other side (wall 2 or wand B1), see Figure 6.18.

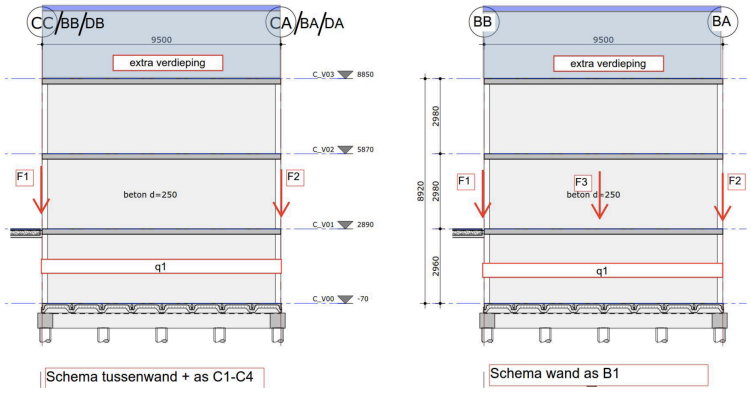

Figure 6.18: Strength walls (from ABT)

The summation of all the distributed loads resulted in a dead and a live line load on the foundation at the location of wall 1, represented by q_1 in Figure 6.18. Also, vertical point loads from the facade were applied to the foundation at each end of the wall, labelled as F1 and F2 in Figure 6.18. Excluding the balconies and foundation, the total normal dead load resulted in 2551 kN and the total normal live load resulted in 342 kN.

Again the summation of all the distributed loads resulted in a dead and a live line load on the foundation at the location of wall 2, see Figure 6.18. Also, for this wall, vertical point loads from the facade were applied, see F1, F2 and F3 in Figure 6.18. However F3 is a balcony loading, so it was included in this comparison. The total normal dead load resulted in 1875.5 kN and the total normal live load resulted in 171 kN.

The normal force results from the case study are summarised in Figure 6.19.

(a) Dead normal forces *(b) Live normal forces*

Figure 6.19: Case study normal forces

Strength Calculation Comparison

The case study normal forces from wall 1, which were applied to all the inner walls of block D3, and wall 2 will be compared to the inner and outer wall results calculated by the feasibility tool respectively. The

summarised total normal loads are shown in Figure 6.20.

Strength Calculation Comparison						
		Case study	Tool	Error (%)	Case study (no psi)	Error (%)
Inner walls	Normal dead loads (kN)	2551	2060.0	-19.25%	-	-
	Normal live loads (kN)	342	400.0	16.96%	494	-19.03%
Outer walls	Normal dead loads (kN)	1875.5	1465.0	-21.89%	-	-
	Normal live loads (kN)	171	200.0	16.96%	247	-19.03%

Figure 6.20: Normal load comparison

The predicted strength results from the conceptual calculations indicate the order of magnitude correctly, validating the tool's reliability for the strength calculations of block D3. However, again as expected the results are not the same and have about a 25 % error. The dead loads calculated with the tool represent about 80 % of the dead load from the case study, because ABT's final calculations considered other more detailed loads such as insulation, roof tiles, plants on the roof, cast in situ top layer (placed over the prefab concrete floor), installations, ceilings and floor tiles. To compensate for this difference an additional dead load factor, that represents the estimated additional load, should be introduced by the experienced structural engineer. The live loads also partially differ, because in the case study the live load of the ground floor and one other floor were multiplied by a factor, $\psi_0(psi) = 0.4$, which was not done in the feasibility tool. The tool intentionally provides all behaviour outputs without factors to remain transparent and allow the user to manually combine these values in various combinations during the meeting. Excluding the ψ_0 factor, the feasibility results are also about 80 % of the case study results. This is because ABT considered an additional variable load for moveable partition walls, which is too detailed for the early design phase. Again, to compensate for the lack of detailed loading in the feasibility tool during the early design phase a live load factor should be introduced by the experienced structural engineer. In future research, outside of this project, new building blocks that include balconies can be developed and, as already mentioned, foundation estimation capabilities should be added.

7 Discussion

This section will address the research objective, research questions and discuss the limitatations.

7.1 Reflection of the objectives

The main objective of this project was:

Research and develop a collaborative tool prototype of StructuralComponents to rapidly validate the structural and geometric feasibility of architectural designs of concrete mid-rise buildings in the conceptual design phase.

This objective was split into sub-objectives:

1) Research design tools that are currently used in the early design phase of the architecture, engineering and construction (AEC) industry and in other similar areas.
This objective was achieved by first researching the design procedure and design tools in the AEC industry, which concluded that indeed the software gap between architectural and structural tools is still present today. The aerospace and automotive industries were also investigated, but have slightly different design procedures and goals, so the focus remained on methods and design tools used in and researched for the AEC industry. The features and limitations of the methods and tools were evaluated and addressed regarding the requirements for a conceptual design tool.

2) Determine the modelling and analysis capabilities that the StructuralComponents prototype requires.
This objective was achieved by researching architectural and structural requirements for the early design phase and applying those in conjunction with existing software features and solutions for limitations. The resulting flexibility, complexity and speed requirements were geared towards determining the feasibility of mid-rise building types composed of shear walls and cores. Examples of adopted modelling features included near real-time and parametric modelling, while a feature not used in practice is modelling with pre-determined building blocks and connecting them at the nodes of the stability elements. Adopted analysis features included calculating and visualising the structural behaviour in real-time and a new feature was automating global feasibility checks and visualising the outcome by changing the colour of the affected stability elements in near real-time.

3) Investigate whether a differential equation method suits the analysis process of the early design phase.
Due to limitations of the finite element analysis method in the early design phase, the super element method, which uses differential equations to represent structural elements, was investigated. This objective was achieved by researching other projects where it had been applied and determining that it provides more transparency and can lead to improved understanding of an early stage design. Also the accuracy of the super element method was compared to existing finite element method before it was implemented into the prototype.

4) Determine what type of framework is necessary for the development of such an early design stage prototype.
Since the developed tool is a prototype and not a fully developed tool, the framework required additional flexibility. Therefore, this objective was achieved by creating the Python super element library independent from the Grasshopper user interface and allowing easy extensions and changes to the super element library.

The combination of the modelling and analysis method, flexible framework, both structural and architectural checks and near real-time result visualisation this prototype is expected to promote the collaboration between structural engineers and architects and allow rapid validation of architectural designs in the conceptual design phase of mid-rise buildings.

7.2 Limitations

This section discusses the limitations of the researched and developed prototype within the scope of this thesis and beyond.

Project scope

- The initial research into conceptual tools in various industries only considers the building, aerospace and the automotive industry. Other industries, such as product design, with similar design procedures were not considered, possibly neglecting design tools that could improve the collaboration in the AEC industry.
- The building type explored is limited to concrete mid-rise buildings, according to the definition given in Section 3.3.1, composed of shear walls and cores. This narrow focus is justified for the scope of this project, but severely limits its practical use.
- The scope of developing a prototype also limits the number of implemented features. Among those are architectural checks regarding the floor area and space within a building. While these could easily be implemented, only the floor depth check was included as an example. Also, not all structural checks were included, for example torsional checks. Only a few example equations were fully implemented.
- Three different types of super elements were fully implemented, which is clearly not enough to model many mid-rise buildings and limits the versatility of this prototype. However, each super element added an important feature to model mid-rise buildings, demonstrating possible features of additional super elements.
- Due to the earlier defined building type, only static analysis was implemented with the super element method. If the building type is expanded to for example high-rise buildings, additional analysis capabilities must be implemented.

Low-fidelity methods

During the conceptual design phase the point of interest is the approximate behaviour and feasibility of a design, so low fidelity techniques are commonly used in the conceptual design phase.

- In order to simplify and speed up the modelling and analysis process, only the main structural elements are modelled with the developed prototype. For example if a floor plan contains numerous shear walls and cores, then the cores are assumed to be the main structural elements. While low fidelity representations are applied in the conceptual phase, this proposed modelling method was not validated in practice, so the structural results should be compared.
- The global structural equations in Section 3.4.2 used to check the overall feasibility of a building come from an academic background and weren't validated in practice. It would be beneficial to compare those equations with checks used by structural firms.

The super element method

- The super element method results were only validated for few dimension and loading cases with a finite element analysis program. Edge cases weren't investigated for this prototype, but should be studied for proper validation.
- In order to speed up the calculation process, symbolic equations, matrices and vectors were calculated with Maple and Mathematica and then stored in the Python super element library. However, the more degrees of freedom a super element has, the more complex the symbolic information becomes. Already for the third super element (core and wall) Maple and Mathematica struggles to calculate symbolic stiffness matrix and were unable to render and display it. Instead, the symbolic H and G matrices were stored and the stiffness matrix was calculated from them numerically once the input values were given. Therefore, current symbolic algebra software may also limiting the complexity of the super elements.
- A super element represents a structural system with a constant topology along the height. When a different topology is introduced along the height of a design, a new super element must be chosen and placed above the previous super element. During the design process not only the topology along the height of a design may change, but also the topology within an already modelled storey.

The way to deal with changing topology within a storey is to replace the whole super element with another one that contains the exact required topology. The inability to connect super elements horizontally extends the amount of required super elements dramatically and reduces the modelling flexibility, a major requirement for a conceptual design tool.

- Also, the vertical connection reveals limitations, because the physical and mathematical connection differ between a core and a wall, highlighted in Section 6.3.2. Connecting the 3D stability element geometry, for example placing a single wall on top of one of the four walls in a core, represents the physical connection. However, mathematically each stability element, walls and cores, can only be connected via a top and bottom node. Therefore, when connected super elements are analysed, the bottom centre-point of a stability element is connected to the top centre-point of another element. The difference in results is assumed to be very small, but the connection between a core and a wall requires further investigation.
- The floor system that transfers load from the facade and floors to the stability elements is represented by an Euler-Bernoulli beam. The calculation for the floor stiffness was simplified by assuming the supporting stability elements can be represented by pin or fixed supports. This simplification neglects the stiffness of the stability elements and therefore the stiffness of the floor supports. Since the tool is developed for the very early design stage where the goal is only to determine an indication of the structural behaviour, the assumption may be justified, but the extend of the result differences should be evaluated.
- The super element method used for this prototype applies to a specific construction method, where the stability elements are cast-in-situ and an in-situ cover layer is poured over the pre-fab floors. This method is commonly used in the Netherlands and other countries, but limits its use to a certain type of structure and construction method.

Prototype system design

- The super element library was scripted in Python, and implemented with the GhPython component, limiting its capabilities and extensions to the Python language. While this may not be a problem, it may be worth exploring other languages that may provide more flexibility.
- External libraries such as Numpy and Sympy cannot be imported with the GhPython component. Since Numpy couldn't be used, numerical and matrix algebra functions had to be scripted for the super element analysis method. Plus, instead of using Sympy, symbolic matrices and vectors from Maple and Mathematica had to be stored in string format for each super element. Numpy and Sympy could speed up the calculation process and save time when extending the element library.

Conceptual design tools

- Several architectural requirements were mentioned in Section 3.4.2, however, some aspects are difficult to implement in software. Especially aesthetic aspects are difficult to quantify and they easily change from project to project. Therefore, the architect and structural engineer must also discuss the requirements with each other, purely the tool is not enough.
- A tool is not enough to improve the collaboration on its own, the people involved must have confidence in the tool to take advantage of the technology (Coenders, 2011).

8 Conclusions

This section draws the conclusions regarding the main- and sub-objectives of the developed collaborative feasibility tool.

The main objective was:

Research and develop a collaborative tool prototype of StructuralComponents to rapidly validate the structural and geometric feasibility of architectural designs of concrete mid-rise buildings in the conceptual design phase.

In order to achieve this main objective the super element method was used to discretise a building into pieces of the same topology, which were then represented by differential equations. The topology models can then be combined vertically to compose unique building design alternatives. It was found that a super element method based tool provides the necessary abstraction to rapidly generate building designs and supplements the required behaviour insight and feasibility checks. The tool prototype resulted in a middle ground between the architectural and structural models, bringing the two disciplines closer together. However, the implemented differential equations do not allow for horizontal connections, requiring the development of a large building block library. Hence, such a super element method based tool is suitable for the early design phase and with further development, including addressing the lack of horizontal connections, it is also a viable option to be used in practice.

The conclusions regarding the sub-objectives are discussed below.

1) Research design tools that are currently used in the early design phase of the architecture, engineering and construction (AEC) industry and in other similar areas.
By first researching the early design phase it was found that two main key characteristics of the early design phase are the lack of known information but presence of design freedom, as illustrated by the MacLeamy curve shown in Figure 1.1, and the need for rapid design prototyping. These characteristics highlight the need for multiple disciplines to be able to work together in order to determine the direction of the project as quickly as possible. After researching currently available design tools, it was concluded that a software gap between architectural and structural conceptual design tools is still present. The available tools are too discipline specific and do not support the collaboration necessary in the early design phase.

Conceptual tools in the aerospace and automotive industry were also researched, but due to differences in known information and discipline relationships their technology was not adopted in the research and development of this project.

2) Determine and implement modelling and analysis capabilities that the StructuralComponents prototype requires.
The modelling and analysis capabilities were determined based on researched architectural, structural and collaboration requirements. The research was based on literature, own experience and communication with people such as Sander Flach from Klunder Architekten, Mr. Pasterkamp from TU Delft with also practical experience as a structural engineer and Dr. Huijben from ABT.

Among the structural engineer's requirements is real-time structural behaviour analysis, which allows them to understand the force flow and make better informed decisions during the conceptual design process. Another tool requirement is to determining the structural feasibility. This was achieved by using global stiffness, stability and strength checks, which accurately predicted the feasibility of block D3 from the Energiekwartier case study.

Architectural requirements implemented in the tool include the geometric freedom of changing dimensions and locations of structural elements, but also the topology type and arrangement. The geometric freedom and modelling speed were demonstrated in the case study, where block D1 of the Energiekwartier, see Figure 6.5a, was successfully modelled with four building blocks in only a few minutes. Similar to the structural requirement, also the feasibility from an architectural perspective is necessary. Quantitative requirements are possible to implement, which was demonstrated with the maximum floor depth check. Additionally, the transparency of the tool is important. Many current engineering tools are only usable by people with a technical background, making it difficult for architects to understand and ultimately use the software. Therefore, an abstract building composition method was implemented and the force flow is visualised in near real-time along the stability elements.

The ability to rapidly generate building designs is a collaboration requirement, because it is important for both disciplines due to the time pressure in the conceptual design phase. This modelling approach was realised with the building block modelling method, where each building block represents a building topology type. Another collaboration requirement are multi-disciplinary checks; design feasibility checks

from multiple involved disciplines, which force the users to consider not only the requirements from their own area, but also others. This prototype focused on the interaction between the architect and structural engineer, therefore, quantifiable check examples from these disciplines were implemented.

3) Investigate whether a differential equation method suits the analysis process of the early design phase.
Based on the requirements for early stage and structural design, the analysis method used must indicate the order of magnitude of the final results, provide near real-time results and support a modular modelling method. For this project the proposed super element method using differential equations is compared in these areas with the traditionally used finite element analysis method.

The differential equation method was found to accurately calculate the structural behaviour of a concrete building, which was validated by comparing results with MatrixFrame, a FEM program. In order to determine if the tool can predict the order of magnitude of the final detailed structure's behaviour, given only estimated parameters known in the conceptual design phase, it was tested on block D3 from the Energiekwartier. The case study concluded that the differential method with estimated input parameters indeed predicted the order of magnitude of the detailed results provided by ABT, validating the necessary accuracy during the conceptual design phase for that building.

Not only the analysis speed, but also the modelling speed is important for collaboration during the early design phase. Since the super element method requires fewer details, it can model and analyse concrete mid-rise structures faster (in near real-time) compared to traditional FEM software.

The super element method, by design, provides a modular system for rapid prototyping. The differential equations, representing a topology type, can be connected vertically to compose a whole building. However, connecting differential equations horizontally is not possible, but this can be solved by choosing the topology component that represents the whole floor topology accurately.

Given these advantages and considering that the disadvantages can be overcome with further development, it was concluded that the super element method addresses the defined early design stage and structural requirements and is more suitable for the analysis of concrete mid-rise buildings than FEM software in the early design phase.

4) Determine what type of framework is necessary for the development of such an early design stage prototype.
The tool framework, see Figure 8.1, must support the previously determined early design stage, architectural, structural and collaboration requirements.

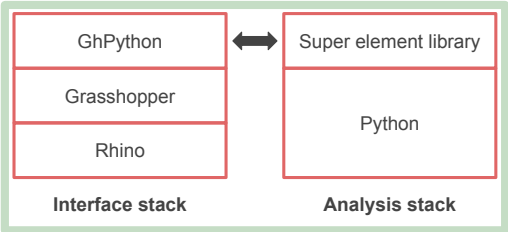

Figure 8.1: Tool framework

The parametric modelling and near real-time visualisation through Rhino-Grasshopper supports the required early design prototyping and architectural geometric freedom. The Python super element library contains the structural topology types and the solver that calculates the required structural behaviour and multi-disciplinary feasibility checks. Since the developed tool is only a prototype, the super element library was organised into a class system to enable easy addition of super elements with different topologies. The GhPython component communicates the Grasshopper inputs from the user to the super element library and the calculated results from the library back to Grasshopper in near real-time. The framework was split into two stacks; the interface and the analysis stack, to be able to use the developed Python super element library also with other existing modelling software.

The implemented framework meets the previously defined requirements and provides flexibility for further development, concluding that the proposed modular setup is suitable for such an early design stage prototype.

9 Recommendations

This section discusses the recommendations for the developed collaborative feasibility tool.

The research areas and developed prototype provided an initial investigation of such a conceptual design tool, concluding that it is a viable option and should be investigated further. Some recommendations for further research and development are discussed below:

Extend super element library
An extensive super element library must be available to model the load bearing structure of an architectural model. The tool should provide super elements that address typical geometry in simple residential and office buildings, but also the geometric freedom of more complex and high-profile building. Different combinations and number of stability elements must be included, but also super elements with columns, cantilevering floors, openings and other architectural and structural features. Therefore, other geometric features should researched as well as the method of implementation.

- Cantilevers, for example, occur routinely in residential buildings to support balconies, but they can also be one of the most fascinating feature of a building, for example in the Hyatt (2018) buildings in Düsseldorf, Germany. While cantilevering floors can already be represented by the differential equation method, some additional research into the implementation is required.
- Atriums are also an extra ordinary building feature, which can be found especially in large-scale buildings such as hotels, shopping malls and office buildings (Hung, 2001). Simply put, atriums are openings in the floor slabs and openings in a floor system affect the floor stiffness and the force transfer to the stability elements. Instead of representing floors as a beam with a constant thickness, like is done in the current prototype, it should be investigated if the floor cross-section could reflect the size of the opening in the floor.
- Super elements using the same derivation method as the three available ones for the prototype, for example super elements with multiple parallel shear walls and cores, can be directly implemented into the external Python super element library. Also more complex super elements can be easily added to the library, but additional research for the derivation is required first.

Custom super element creator
Since horizontal connections are not possible with the proposed super element method, an alternative method to quickly change the topology should be researched. For example, custom super elements specified by the user could be developed.

In the current prototype the symbolic matrices, vectors and equations needed for each super element are calculated separately by hand, with Maple and Mathematica and simply stored as Python strings. However, it should be investigated if the Sympy library can be used to internalise those symbolic calculations, allowing a user to create a new custom super element. Each stability element and the floor is still represented by the differential equation of an Euler Bernoulli beam. First, the hand calculations should be calculated with Sympy, since this part was not automised. Next the symbolic algebra from Maple and Mathematica should be tested and automated in Sympy. Operations required to solve for the governing symbolic differential equations and the final symbolic behaviour equations, h-matrix, g-matrix, nodal equivalent force vector and upart vector include solving linear systems and solving differential equations, which Sympy is able to do.

If the symbolic algebra can be completed with Sympy, then custom super elements could indeed be used in the modelling process. The custom super element could be visualised from above. The floor shape specified first and then stability element types dragged and dropped to the initial desired locations. Their locations and dimensions can still be adjusted later on in the design process, only the number and type of stability elements cannot be changed.

Additional feasibility checks
The implemented structural and architectural feasibility checks served as examples to demonstrate the implementation method and result visualisation. In practice more checks are required, demanding more research into high-level checks during the conceptual design phase. Automating these numerical checks in the tool, rather than expecting the engineer or architect to calculate them on paper during a brainstorm session, is expected to save a lot of time and are very easy to add due to the library layout.

Structural analysis options
Especially during the case study it became apparent that the implemented analysis is not enough for a conceptual design tool.

- The foundation stiffness can be critical in countries with poor soil conditions. Dicke (1991) explains

a simplified method of accounting for the foundation stiffness, which was already applied (by hand) in the Energiekwartier case study in Section 6.4.3.

- Calculating imperfections should also be researched and included in the analysis.
- For high wind loads and tall buildings dynamic analysis can show a better insight into the behaviour of a structure. Dynamic analysis with the super element method has already been done by Steenbergen (2007). In the dynamic case with stochastic wind loading it was determined that the super element method could not only be used in the conceptual or preliminary design phase, but also in the final design phase, because FEM software was and may still not be able to include stochastic wind loading.

Note that not all analyse methods are required for every design, only if they are expected to have a significant effect on the results.

Other Disciplines
This project was part of a larger framework, which aims to include other disciplines, such as finance, sustainability, building services etc., into the toolbox. These disciplines also influence the decision process in the conceptual design phase and should be researched.

Result viewer
The structural behaviour and feasibility checks are visualised directly on the model to help the architect and structural engineer understand the structure. For the initial real-time results this is expected to be a good option, which also many other tools use, such as Karamba. However, this view limits the results to only the selected deformation, internal forces and check. A result viewer should also be implemented that gives the user an overview and highlights the critical results.

Building type
For the larger framework the scope should also be expanded to other building types, building materials and construction methods.

- Other building types could include high-rise or underground buildings. High-rises can easily be modelled with differential equations and as already mentioned the required dynamic analysis method is also possible. Fully or partially underground buildings could also be modelled with the super element method, if the soil stiffness is represented by linear springs along the height of the building.
- Additional material types could include steel or timber. However, these will require extensive research, since also the stability element types and construction method will change.
- The super element method used for this prototype corresponds to a specific construction method for concrete buildings, commonly used in the Netherlands and other countries. To expand the applicability of this tool, it should be expanded to other construction methods used for building made of concrete and other materials.

Testing
More case studies should be done to test the tool's usability and to compare the conceptual design results with the detailed results from the final design stage. As more super elements and features are introduced, this tool should be tested with increasingly complex structures.

Bibliography

ABT (2018). *ABT* [website]. https://www.abt.eu/. Last Accessed 11/01/2018.

Autodesk Inc. (2018). *What is CAD softwware?* Retrieved from https://www.autodesk.com/solutions/cad-software. Last Accessed on 21/02/2018.

BMW (2012). *The new BMW 1 series: designer interview.* Retrieved from https://www.youtube.com/watch?v=4UYWSHhLwic. Last Accessed 10/08/2017.

Bovenberg, A. (2015). *StructuralComponents 4: Conceptual building models with structural design justification* (master's thesis). Technical University of Delft. Retrieved from http://repository.tudelft.nl/islandora/object/uuid%3A3729f412-028e-4a77-b4bf-8c60181b2278?collection=research.

Breider, J. (2008). *StructuralComponents – development of parametric associative design tools for the structural design of high-rise buildings* (master's thesis). Technical University of Delft.

British Standards (BSI) (2004). Eurocode 2: design of concrete structures. Retrieved from https://connect.nen.nl/Account/LogOn?ReturnUrl=%2f. Last Accessed 28/05/2017.

Brook McIlroy Planning & Urban Design/Pace Architects (2010). Avenues & mid-rise buildings study. Retrieved from http://www1.toronto.ca/City%20Of%20Toronto/City%20Planning/Urban%20Design/Mid-rise/midrise-FinalReport2.pdf. Last Accessed 26/05/2017.

Car Body Design (2012). *The design process at the BMW Group.* Retrieved from http://www.carbodydesign.com/2012/03/the-design-process-at-the-bmw-group/. Last Accessed 27/07/2017.

CATIA Tutor (2017). *Class A Surfacing.* Retrieved from https://catiatutor.com/class-a-surfacing/. Last Accessed 27/07/2017.

Ching, F. D. K. (2014). *Building Structures Illustrated.* John Wiley & Sons Inc.

Coenders, J. (2011). *NetworkedDesign: next generation infrastructure for computational design* (dissertation). Technical University of Delft. Retrieved from http://repository.tudelft.nl/islandora/object/uuid%3Abf930678-d676-4c4f-85c1-c7188b6718f7?collection=research.

CTBUH (2017). Ctbuh height criteria. Retrieved from http://www.ctbuh.org/TallBuildings/HeightStatistics/Criteria/tabid/446/language/en-US/Default.aspx. Last Accessed 21/07/2017.

Davidson, S. (2018). *Scripting and Code Tutorials.* Retrieved from http://www.grasshopper3d.com/page/scripting-and-code-tutorials. Last Accessed on 21/02/2018.

Dicke, D. (1991). *Stability of Designers.* Delftse Publishing Company: Delft, The Netherlands (in Dutch).

Dijkstra, A. J. (2008). *High-rise: exploring the ultimate limits* (master's thesis). Technical University of Delft. Retrieved from https://repository.tudelft.nl/islandora/object/uuid%3A50e95ac8-47a6-4f0f-b844-95b8686923c0?collection=education. Last Accessed 27/05/2017.

Eisele, J. and Kloft, E. (2003). *High-rise manual: typology and design, construction, and technology.* Birkhäuser-Publishers for Architecture, Basel, Boston.

Ferreira, G. and Casasín, J. (2014). *Programming principles* [website]. Retrieved from https://www.python.org/. Last Accessed on 21/02/2018.

Feuerversicherungen, V. K. (2015). *Brandschutzrichtlinie.* Berne.

Flemming, U. and Woodbury, R. (1995). Software Environment to Support Early Phases in Building Design (SEED): Overview. *Journal of Architectural Engineering*, 1(4):147–152.

Ham, P. and Terwel, K. (April 2017). *Structural calculations of High Rise Structures*. TU Delft.

Hoenderkamp, J. (2002). Critical loads of lateral load resisting structures for tall buildings. *Struct. Design Tall Build*, 11:221–232.

Howe, D. (2000). *Aircraft conceptual design synthesis*. Professional Engineering Publishing, London, England.

Hung, W. Y. (2001). A review on architectural aspects of atrium buildings. *Architectural SCience Review*, 44(3).

Hyatt Corp. (2018). *Hyatt* [website]. Retrieved from https://www.hyatt.com/. Last Accessed 24/02/2018.

Klunder Architecten (2018). *Klunder Architecten* [website]. http://www.klunderarchitecten.nl/. Last Accessed 11/01/2018.

Ledermann, C., Hanske, C., Wenzel, J., Ermanni, P., and Kelm, R. (2005). Associative parametric cae methods in the aircraft pre-design. *Aerospace Science and Technology*, 9:641–651.

Lindemann, J., Sandberg, G., and Damkilde, L. (2010). Finite-element software for conceptual design. *Egnineering and Computational Mechanics*, 163 Issue EMI:15–22.

MacLeamy, P. (2010). *The future of the building industry (3/5): The Effort Curve* [video file]. Retrieved from https://www.youtube.com/watch?v=9bUlBYc_Gl4. Last Accessed 04/04/2017.

MercedesBenz (2017). *The design process at MercedesBenz*. Retrieved from https://www.mercedes-benz.co.in/content/india/mpc/mpc_india_website/enng/home_mpc/passengercars/home/world/design/design_process.html. Last Accessed 27/07/2017.

Moerland, E. (2011). *Development of an aeroelastic analysis tool for structural sizing of high-lift devices during preliminary design* (master's thesis). Technical University of Delft. Retrieved from http://repository.tudelft.nl/islandora/object/uuid%3Afeca38a2-e2f4-4249-9b73-5bcc4171ca9d?collection=education. Last Accessed 16/05/2017.

Mueller, C. (2014). *Computational exploration of the structural design space* (dissertation). MIT. Retrieved from http://hdl.handle.net/1721.1/91293. Last Accessed 16/05/2017.

Mueller, C. and Ochsendorf, J. (2013). Digital brainstorming: An interactive evolutionary framework for creativity, diversity, and performance in conceptual structural design. *Keynote Presentation at the 12th U.S. National Congress on Computational Mechanics*.

MuleSoft Inc. (2018). *What is an API?* Retrieved from https://www.rhino3d.com/. Last Accessed on 02/19/2018.

NEN-EN 1991-1-4 (2005). *Eurocode 1: Actions on structures*. Nederlands Normalisatie-instituut.

Nissan Global (2017). *The Car Design Process*. Retrieved from http://www.nissan-global.com/EN/DESIGN/DATSUN/PROCESS/. Last Accessed 27/07/2017.

NTA 4614-3 (2012). *Covenant high-rise buildings - Part 3: Structural safety*. Nederlands Normalisatie-instituut.

Przemieniecki, J. S. (1968). *Theory of matrix structural analysis*. McGraw Hill, New York.

Qu, Z. (2004). *Model order reduction techniques; with applications in finite element analysis*. Springer-Verlag, London, England.

Rolvink, A. (2010). *StructuralComponents 2: A parametric and associative toolbox for conceptual design of tall building structures* (master's thesis). Technical University of Delft.

Rolvink, A., Breider, J., and Coenders, J. (2009). Structuralcomponents - a parametric associative design toolbox for conceptual structrual design. *IASS International Symposium on Shell and Spatial Structures*, pages 1124–1135.

Rolvink, A., Mueller, C., and Coenders, J. (2014). State on the Art of Computational Tools for Conceptual Structural Design. *Shells, Membranes and Spatial Structures (IASS).*

Sobieszczanski-Sobieski, J. and Haftka, R. T. (1997). Multi-disciplinary aerospace design optimization: survey of recent developments. *In Structural Optimization*, 14(1):1–23.

Steenbergen, R. (2007). *Super elements in high-rise buildings under stochastic wind load* (dissertation). Technical University of Delft. Retrieved from http://repository.tudelft.nl/islandora/object/uuid%3Abc62e51b-5ed4-4101-968b-3d2be3dbca92?collection=research.

Steenbergen, R. D. and Blaauwendraad, J. (2007). Closed-form super element method for tall buildings of irregular geometry. *International Journal of Solids and Structures*, 44:5576–5597.

Swaroop, C. H (2014). *Object Oriented Programming* [website]. Retrieved from https://python.swaroopch.com/oop.html. Last Accessed on 02/19/2018.

Taranath, B. S. (2016). *Tall Building Design: Steel, Concrete, and Composite Systems.* CRC Press.

Timmer, S. G. C. (2011). *Tall timber buildings: feasibility study* (master's thesis). Technical University of Delft. Retrieved from https://repository.tudelft.nl/islandora/object/uuid%3A5da007ef-1021-46be-98ab-13284dba0505?collection=education. Last Accessed 27/05/2017.

Torenbeek, E. (1982). *Synthesis of subsonic airplane design.* Delft University Pres, Delft, Holland.

Trimble Inc. (2017). *SketchUp Help Center.* Retrieved from https://help.sketchup.com/en/content/sketchup-pro. Last Accessed on 21/02/2018.

TU Delft (2017). *Concrete Building Structures.* Technical University of Delft.

van de Weerd, B. M. (2013). *StructuralComponents: A client-server software architecture for FEM-based structural design exploration* (master's thesis). Technical University of Delft. Retrieved from http://repository.tudelft.nl/islandora/object/uuid%3A6d95dd31-e1a7-41c9-abc9-49a8fcb80926?collection=education.

Vandenbrande, J. H., Grandine, T. A., and Hogan, T. (2006). The search for the perfect body: shape control for multidisciplinary design optimization. *44th AIAA Aerospace Sciences Meeting and Exhibit*, 15. doi: 10.2514/6.2006-928.

Wells, G. N. (2011). The finite element method: An introduction version 0.2. University of Cambridge and Delft University of Technology.

Software References

AbdelRahman, M. (2017). *GH_CPython*. Retrieved from https://github.com/MahmoudAbdelRahman/GH_CPython. Last Accessed on 02/19/2018.

Aish, R. (2005). *Introduction to GenerativeComponents: A parametric and associative design system for architecture, building engineer and digital fabrication.* Bentley Systems Inc.

ANSYS Inc (2018a). *ANSYS Fluent*. Retrieved from https://www.ansys.com/Products/Fluids/ANSYS-Fluent. Last Accessed 21/02/2017.

ANSYS Inc (2018b). *ANSYS Structures*. Retrieved from https://www.ansys.com/products/structures. Last Accessed 21/02/2017.

Autodesk Inc. (2018a). *Discover Dynamo*. Retrieved from http://dynamobim.org/explore/#feat. Last Accessed 21/02/2018.

Autodesk Inc. (2018b). *Explore Dynamo* [website]. Retrieved from http://dynamobim.org/. Last Accessed 21/02/2018.

Autodesk Inc. (2018c). *Recap*. Retrieved from https://www.autodesk.com/products/recap/overview. Last Accessed on 21/02/2018.

Autodesk Inc. (2018d). *Revit Live*. Retrieved from https://www.autodesk.com/products/revit-live/overview. Last Accessed on 21/02/2018.

Autodesk Inc. (2018e). *Revit* [website]. Retrieved from https://www.autodesk.com/products/revit-family/overview. Last Accessed on 21/02/2018.

Bentley Systems Inc. (2018). *Bentley* [website]. Retrieved from https://www.bentley.com/en. Last Accessed on 21/02/2018.

Community, I. (2007). *IronPython* [website]. Retrieved from http://ironpython.net/. Last Accessed on 02/19/2018.

Computers and Structures (2016). *ETABS Integrated building design software user's guide*. Retrieved from http://docs.csiamerica.com/manuals/etabs/User's%20Guide.pdf. Last Accessed 16/05/2017.

Computers and Structures (2018). *SAP2000* [website]. Retrieved from https://www.csiamerica.com/products/sap200. Last Accessed 28/05/2017.

Computers & Structures Inc. (2018). *ETABS 2016 Overview* [website]. Retrieved from https://www.csiamerica.com/products/etabs. Last Accessed on 01/03/2018.

Dassault Systemes (2017). *CATIA* [website]. Retrieved from https://www.3ds.com/products-services/catia. Last Accessed 18/05/2017.

Davidson, S. (2017). *Grasshopper* [website]. Retrieved from http://www.grasshopper3d.com. Last Accessed on 05/04/2017.

DIANA FEA 9.5 (2017). *TNO DIANA BV* [website]. Retrieved from https://dianafea.com/content/DIANA. Last Accessed 28/04/2017.

eQUILIBRIUM (2012). In *BLOCK Research Group ETH Zurich* [website]. Retrieved from http://block.arch.ethz.ch/equilibrium/. Last Accessed 25/04/2017.

Gehry Technologies (2017). *Products: Digital Project* [website]. Retrieved from http://www.gehrytechnologies.com/en/products/. Last Accessed 26/05/2017.

Graphisoft (2018). *ARCHICAD* [website]. Retrieved from http://www.graphisoft.com/archicad/. Last Accessed on 21/02/2018.

Greenwold, S. and Allen, E. (2003). *Active Statics*. Retrieved from /urlhttp://acg.media.mit.edu/people/simong/statics/data. Last Accessed 25/04/2017.

Hexagon (2018). *MSC Nastran: Multidisciplinary Structural Analysis*. Retrieved from http://www.mscsoftware.com/product/msc-nastran. Last Accessed 21/02/2018.

Karamba (2017). *Karamba: parametric engineering* [website]. Retrieved from http://www.karamba3d.com/. Last Accessed 21/02/2018.

Lindemann, J., Sandberg, G., and Damkilde, L. (2010). Finite-element software for conceptual design. *Egnineering and Computational Mechanics*, 163 Issue EMI:15–22.

Martini, K. (2006). A New Kind of Software for Teaching Structural Behavior and Design. *Building Technolgoy Educator's Symposium*, pages 279–288.

Matrix Software (2018). *MatrixFrame* [website]. Retrieved from https://www.matrix-software.com/uk/structuralengineering/matrixframe/. Last Accessed 01/03/2018.

McNeel, R. (2018). *Rhinoceros* [website]. Retrieved from https://www.rhino3d.com/. Last Accessed on 02/19/2018.

Mirtschin, J. (2017). *Geometry Gym BIM*. Retrieved from http://www.grasshopper3d.com/group/geometrygym. Last Accessed 16/05/2017.

Nemetschek Group (2018). *SCIA* [website]. Retrieved from https://www.scia.net/en. Last Accessed on 21/02/2018.

NumPy developers (2017). *NumPy* [website]. Retrieved from http://www.numpy.org/. Last Accessed on 19/02/2018.

Piacentino, G. (2018). *GHPYTHON*. Retrieved from http://www.food4rhino.com/app/ghpython?page=4&ufh=. Last Accessed on 21/02/2018.

Python Software Foundation (2018). *Python* [website]. Retrieved from https://www.python.org/. Last Accessed on 02/19/2018.

Siemens (2018). *STAR-CCM+*. Retrieved from https://mdx.plm.automation.siemens.com/star-ccm-plus. Last Accessed 21/02/2017.

SOFiSTiK (2017). In *SOFiSTiK AG* [website]. Retrieved from http://www.sofistik.eu/sofistik/. Last Accessed 28/04/2017.

Solibri Inc. (2018). *Solibri* [website]. Retrieved from https://www.solibri.com/. Last Accessed on 21/02/2018.

SymPy Development Team (2016). *SymPy* [website]. Retrieved from http://www.sympy.org/. Last Accessed on 19/02/2018.

TechnoSoft Inc. (2018). *TechnoSoft adaptive modelling* [website]. Retrieved from http://www.technosoft.com/. Last Accessed 01/03/2018.

Trimble Inc. (2018a). *SketchUP Pro* [website]. Retrieved from https://www.sketchup.com/products/sketchup-pro. Last Accessed on 21/02/2018.

Trimble Inc. (2018b). *Tekla* [website]. Retrieved from https://www.tekla.com/. Last Accessed on 21/02/2018.

List of Figures

Appendices

A

Appendix A

A.1 Mid Rise Building Definitions

Some cities give guide lines for building proportions during the planning of a larger project. For example the City of Toronto in Canada is planning a large scale mid-rise redevelopment throughout the Avenues to accommodate an expected large increase in population. For this project the height of a mid-rise building is capped at the width of the street right-of-way, as shown in Figure A.1 or defined between 5 and 11 storeys (36m).

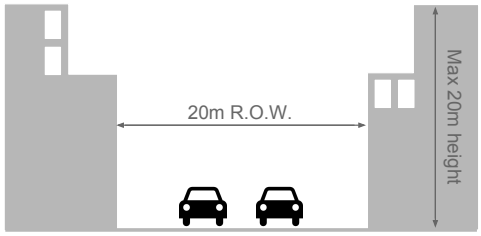

Figure A.1: Maximum mid-rise building height in the City of Toronto (Brook McIlroy Planning & Urban Design/Pace Architects, 2010)

However, this definition for a mid-rise building is too specific to use as a general rule. The street width of cities vary and it might leave a gap between the definition of a mid-rise and a high-rise building. Therefore, defining a medium-rise building based on current high-rise definitions is an alternative worth exploring.

In Germany high-rise buildings are defined by a minimum height of 30m based on fire protection requirements and medium-rise buildings with a height of up to 30m (Feuerversicherungen, 2015). The Dutch national standard for high-rise buildings, Nationaal Covenant Hoogbouw 2012, in contrast requires a height of 70m to be considered a high-rise, which is more than 2 times the German height definition. Hence, even the definition for high-rise buildings vary substantially.

The Council of Tall Buildings and Urban Habitats (CTBUH, 2017) defines the "tallness" of buildings according to multiple qualities rather than purely the height. They consider the "height relative to context", the "proportion" and the required "tall-building technologies".

1. Height relative to context, which defines the building tallness based on the surrounding built environment

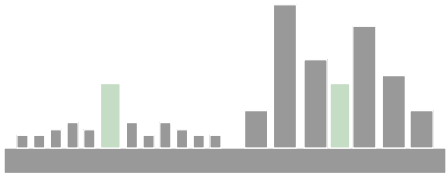

Figure A.2: Height of building with respect to surrounding built environment, adopted from (CTBUH, 2017)

2. Proportion describes the building's slenderness, so if its width is too large compared to the height it is not considered a tall building

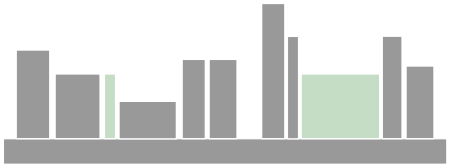

Figure A.3: Height of building with respect to slenderness, adopted from (CTBUH, 2017)

3. Tall-building technologies are advanced technologies required for "tall" buildings such as vertical transportation technologies and special lateral force-resisting and damping systems etc.

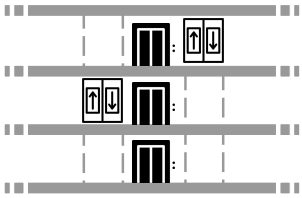

Figure A.4: Height of building with respect to required technology, adopted from (CTBUH, 2017)

Hence, when defining building "tallness", the height is not the only factor that needs to be considered. Also, when all the qualities are considered, the resulting definition is subjective and may not even apply to the same building over the course of its life time if the built environment around it changes.

B
Appendix

B.1 Detailed derivation procedure

Here is a detailed procedure for each step involved in deriving the super elements.

Pre Step) Determine sign convention The super elements are derived according to two sign conventions. The first one is used for section forces (internal forces) and the second sign convention is for the element forces (external forces).
For an example see Section 4.3.1.

Step 1) Determine the floor stiffness matrix
First the floor system is represented by a beam with bending and shear stiffness (Timoshenko beam) with supports corresponding to the lateral stiffness members of the super elements. Using the direct displacement method the floor stiffness matrix can be assembled.

Step 2) Derive the differential equation
Also the stability elements are represented by Shear beams, Euler-Bernoulli beams or Timoshenko beams. These are added to the floor stiffness matrix to represent the behaviour of the whole super element. From this system of equations the symbolic differential equations can be derived.

Step 3) Calculate the stiffness matrix
In order to determine the stiffness matrix (K), the displacement, rotation, moment and shear equations for the super element are derived. These are found by integrating the homogeneous solution of the governing differential equation. Integrating both sides gives the displacement, rotation, moment and shear equations.

From the displacement and rotation equations the following relation is determined, where C is a vector containing the unknown integration constants and d is a vector with the degrees of freedom at each node.

$$HC = d \tag{B.1}$$

Since H is a n by n matrix (based on the geometry of the super element) it can be inverted and brought to the other side.

$$C = H^{-1}d \tag{B.2}$$

Similar to Equation B.1 the equations for the section forces derived from the homogeneous solution are represented as follows:

$$f = GC \tag{B.3}$$

Here too the H matrix is inverted to bring it to the other side and the C vector is replaced with Equation B.2.

$$f = GH^{-1}d \tag{B.4}$$

Without knowing the integration constants it is now possible to determine the stiffness matrix.

$$K = GH^{-1} \tag{B.5}$$

Step 4) Map the force transfer
Externally applied forces, such as wind, influence the stability members differently depending on their geometric arrangement. Therefore, the applied load from the structure has to be translated to forces on the individual stability members. For this process the direct displacement method is applied again.

Step 5) Determine nodal equivalent forces
In order to apply a distributed load along the height of a super element, the nodal equivalent forces have to be determined. This procedure fully restrains the nodes of the super element and determines the reaction forces of the clamped element in a process illustrated in Figure B.1 and described next. The equivalent load vector is then equal to the negative clamped reaction forces.

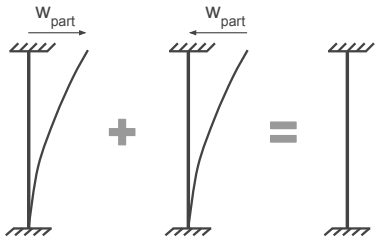

Figure B.1: Procedure to find clamped reaction forces

The required displacement, rotation, moment and shear equations are derived from the particular solution of the governing differential equation. The particular solution is integrated to give the displacement equation, from which the rotation, shear and moment equations can be determined.

This is the first part of the clamped reaction force vector are the reaction forces derived from the particular displacement. The shear and moment equations are evaluated at the nodes, resulting in the section forces. Based on the sign convention these are converted to the element forces and collected in $v^{(1)}$.

$$v^{(1)} = \begin{bmatrix} F_1 \\ T_1 \\ ... \\ F_i \\ T_i \end{bmatrix} = \begin{bmatrix} \pm\, V_1 \\ \pm\, M_1 \\ ... \\ \pm\, V_i \\ \pm\, M_i \end{bmatrix}$$

The second part of the clamped reaction force vector is composed of the forces required to zero the displacement again. First the particular displacement vector is calculated by evaluating the displacement and rotation equations at the nodes.

$$u_{part} = \begin{bmatrix} w_1 & \theta_1 & ... & w_i & \theta_i \end{bmatrix}^T \tag{B.6}$$

Next, the force vector ($v^{(2)}$) is calculated using $-u_{part}$.

$$v^{(2)} = K(-u_{part}) \tag{B.7}$$

The total reaction forces of the clamped super element is the summation of $v^{(1)}$ and $v^{(2)}$, which is equal to the negative nodal equivalent force vector (v).

$$v = -(v^{(1)} + v^{(2)}) \tag{B.8}$$

Step 6) Assemble and partition f = Kd
In the last step the displacement vector, force vector and stiffness matrix are assembled with the degrees of freedom matching with the forces.

The known equivalent forces are inserted into the force partition corresponding to the free nodes (f_f) and the known degrees of freedom (constraints) are inserted into the partition related to the prescribed nodes (a_p). The f = Kd equations are re-arranged so that the forces corresponding to the free nodes (subscript f) are collected together and the equations corresponding to the prescribed nodes (subscript p) are grouped as shown in Equation B.9:

$$\begin{bmatrix} f_f \\ f_p \end{bmatrix} = \begin{bmatrix} k_{ff} & k_{fp} \\ k_{pf} & k_{pp} \end{bmatrix} \begin{bmatrix} a_f \\ a_p \end{bmatrix} \tag{B.9}$$

In order to solve for the unknown nodal forces (f_p) and the unknown degrees of freedom (a_f), the partitioned Equation B.9 is split into the following two equations:

$$f_f = k_{ff} a_f + k_{fp} a_p \tag{B.10}$$
$$f_p = k_{pf} a_f + k_{pp} a_p \tag{B.11}$$

First, Equation B.10 is used to solve for the unknown degrees of freedom (a_f) using Gaussian Elimination. Once all the degrees of freedoms are known, the unknown forces (f_p) can be solved for with Equation B.11 using simple arithmetic.

Finally, in order to solve for the unknown reaction forces, the equivalent nodal force vector is subtracted from the f vector based on the relationship given in Equation B.12.

$$f_{equivalent} + f_{reaction} = f \tag{B.12}$$

Step 7) Parametric structural behaviour equations
The parametric equations for the deflection, rotation, internal moment and internal shear were already derived in Step 3 to determine the symbolic stiffness matrix. However, the integration constants are still unknown. In order to solve for them, the same number of boundary conditions as integration constants are required. These are collected in a d vector with the corresponding homogenous solutions in matrix H and particular solution (at the corresponding boundary condition) in vector P, resulting in the following equation:

$$\begin{bmatrix} d \end{bmatrix} = \begin{bmatrix} \quad H \quad \end{bmatrix} \begin{bmatrix} C \end{bmatrix} - \begin{bmatrix} P \end{bmatrix} \tag{B.13}$$

Then to solve for the integration constants the particular solution is added to the d matrix and the multiplied by the inverse of H (H^{-1}).

$$\begin{bmatrix} C \end{bmatrix} = \left(\begin{bmatrix} d \end{bmatrix} + \begin{bmatrix} P \end{bmatrix} \right) * \begin{bmatrix} \quad H^{-1} \quad \end{bmatrix} \tag{B.14}$$

B.2 Super element 2 derivation

Steps 1 and 2 are switched during the derivation procedure for super element 2, because its symmetry was used to simplify the derivation.

B.2.1 Differential equations

The kinematic and constitutive equations remain the same, however, the equilibrium changes since a linear stiffness between the walls is introduced. If only one beam on an elastic foundation is considered, the following equilibrium relation is determined:

$$\frac{dV}{dx} - k_{found}\, w = -q \tag{B.15}$$

Combining this equation with the kinematic and constitutive equations results in the differential equation for one beam on a soil:

$$EI\frac{d^4w}{dx^4} + k_{found}\ w = q \tag{B.16}$$

However, if two walls are connected through a linear shear stiffness, the differential equation for each wall are as follows:

$$EI\frac{d^4w_a}{dx^4} + k_{fl}\ w_a - k_{fl}\ w_b = q_a \tag{B.17}$$

$$EI\frac{d^4w_b}{dx^4} + k_{fl}\ w_b - k_{fl}\ w_a = q_b \tag{B.18}$$

B.2.2 Floor stiffness

Even though the general direct displacement method was already outlined in Step 6, the floor stiffness will be derivation in detail to show the application of the direct displacement method for floor systems. For this procedure symmetry between the two inner walls ($wall_b$) will be used. Node one will be at $wall_a$, node 2 is at $wall_b$ and node 3 is in the middle of the two inner walls, see Figure B.2 for reference.

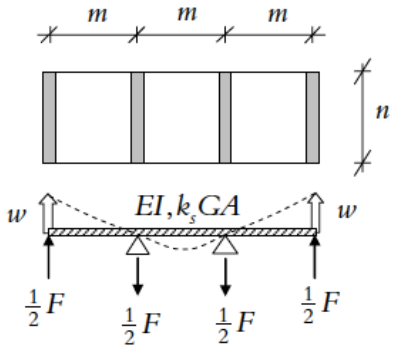

Figure B.2: Stiffness of one floor in super element 2 (Steenbergen, 2007)

The degrees of freedom vector and the applied force vector for the symmetric part, determined from equilibrium, are as follows:

$$d = \begin{bmatrix} w_1 = w \\ \theta_1 \\ w_2 = 0 \\ \theta_2 \\ w_3 \\ \theta_3 = 0 \end{bmatrix} \quad and \quad f = \begin{bmatrix} V_1 = \frac{1}{2}f \\ M_1 = 0 \\ V_2 = -\frac{1}{2}f \\ M_2 = 0 \\ V_3 = 0 \\ M_3 = \frac{1}{2}f\ell \end{bmatrix}$$

Since the floor is schematised as a beam with bending and shear, it can be represented as a Timoshenko beam, for which the stiffness matrix is well known and $\theta = \frac{12EI}{GAl^2}$. This stiffness matrix is evaluated for the first element reaching from node 1 to 2 and the second element reaching from node 2 to 3. These are combined following the direct stiffness method, where the stiffness at the common node is combined. However, this matrix is singular, so it cannot be inverted which is necessary to solve the system of equations. Hence, the rows where the forces = 0 and the columns where the displacements = 0 can be removed to result in the reduced non-singular matrix.

$$K = \frac{2EI}{\ell(1+\theta)} \begin{bmatrix} \frac{6}{\ell^2} & \frac{3}{\ell} & \frac{3}{\ell} & 0 \\ -\frac{6}{\ell^2} & -\frac{3}{\ell} & \frac{9}{\ell} & -\frac{48}{\ell^2} \\ 0 & 0 & (2-\theta) & -\frac{12}{\ell} \end{bmatrix}$$

From f = Kd it can be solved for d by inverting the K. Resulting in $d = K^{-1}f$. From this equation d results in

$$d = \begin{bmatrix} w = \frac{5}{12}\frac{f\ell^2}{EI} + \frac{f\ell}{2GA} \\ \theta_2 = -\frac{\ell^2 f}{2EI} \\ w_3 = -\frac{\ell^3 f}{16EI} \end{bmatrix}$$

Since we are interested in the floor stiffness related to the displacement at node 1 ($wall_a$),

$$w = \frac{5}{12}\frac{f\ell^3}{EI} + \frac{f\ell}{2GA}$$

Which results in

$$K_{floor} = \frac{f}{w} = \frac{12}{5}\frac{EI}{\ell^3} + \frac{1}{1 + \frac{6}{5}\frac{EI}{\ell^2 k_s GA}}$$

where $EI = Etn^3$ and $k_s GA = \frac{5}{6}nt$ for an isotropic cast-in-situ floor with constant thickness t.

k_{floor} is the stiffness of one floor. To find the distributed floor stiffness along the height of the element, the single floor stiffness must be divided by the storey height (h_f).

$$k_{floor} = \frac{K_{floor}}{h_f}$$

B.2.3 Stiffness matrix

The homogenous solution of the differential equation are presented below, where $\beta_a EI$ is the combined flexural stiffness of the outside walls and $\beta_b EI$ is the combined flexural stiffness of the inner walls.

$$\beta_a EI \frac{d^4 w_a}{dx^4} + k_{fl}\ w_a - k_{fl}\ w_b = 0 \tag{B.19}$$

$$\beta_b EI \frac{d^4 w_b}{dx^4} + k_{fl}\ w_b - k_{fl}\ w_a = 0 \tag{B.20}$$

Integrating these results in the displacement equation for $wall_a$ and $wall_b$.

$$\begin{aligned} w_a = {} & C1 + C2x + C3x^2 + C4x^3 \\ & + C5\frac{e^{-\gamma x}cos(\gamma x)}{\beta_a} + C6\frac{e^{-\gamma x}sin(\gamma x)}{\beta_a} + C7\frac{e^{\gamma x}cos(\gamma x)}{\beta_a} + C8\frac{e^{\gamma x}sin(\gamma x)}{\beta_a} \end{aligned} \tag{B.21}$$

$$\begin{aligned} w_b = {} & C1 + C2x + C3x^2 + C4x^3 \\ & + C5\frac{e^{-\gamma x}cos(\gamma x)}{\beta_b} + C6\frac{e^{-\gamma x}sin(\gamma x)}{\beta_b} + C7\frac{e^{\gamma x}cos(\gamma x)}{\beta_b} + C8\frac{e^{\gamma x}sin(\gamma x)}{\beta_b} \end{aligned} \tag{B.22}$$

$$\gamma = \sqrt[4]{\frac{k_{floor}}{4\beta_a\beta_b EI}} \tag{B.23}$$

From these the rotation, moment and shear equations can be derived and used to calculate the stiffness matrix following the detailed procedure from Step 3. For an example see the stiffness matrix derivation for super element 1, which is shown in detail. The resulting symbolic stiffness matrix would cover multiple pages, so it will not be shown.

B.2.4 Force transfer

Wind load on buildings is first transferred to the facade, then to the floor and finally to the stability elements, summarised in Figure B.3.

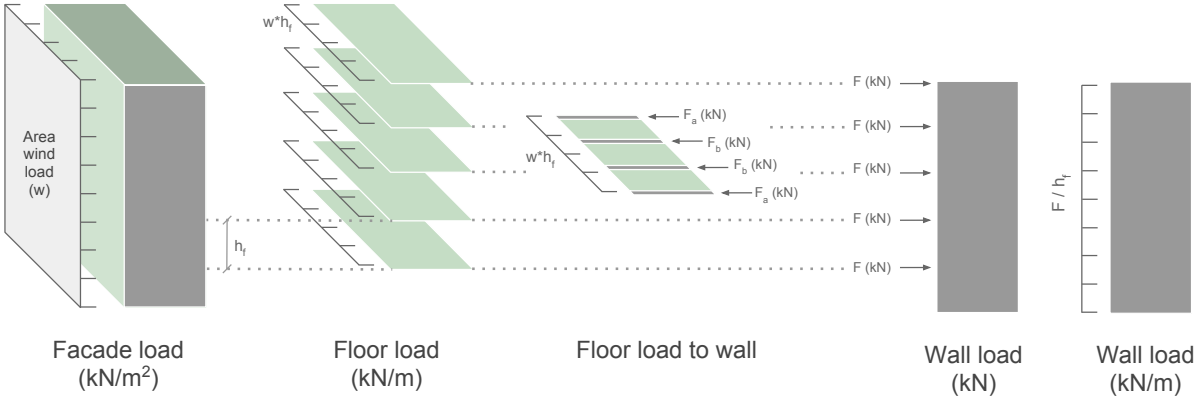

Figure B.3: Transfer of lateral forces from the facade, to the floor and finally to the stability elements

For the force transfer from the floor to the wall, the direct displacement method is applied again. The two middle supports are made redundant supports in order to solve the structurally indeterminate beam. First, the displacements at the two redundant support points is calculated based on the distributed wind load as shown in Figure B.4.

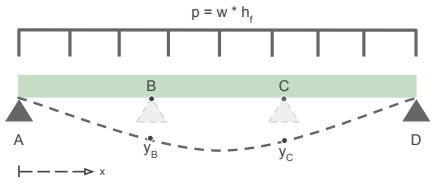

Figure B.4: Superelement 2 force transfer case 0

$$y = \frac{px}{24EI}(l^3 - 2lx^2 + x^3) \tag{B.24}$$

$$(y_B)_0 = (y_C)_0 = \frac{22m^4 * p}{24EI}$$

Next, a point load is applied at each of the redundant support locations in the opposite direction to the wind load as shown in Figure B.5. Due to symmetry the displacements are switched when the point load is applied at point B compared to point C.

(a) case 1 *(b) case 2*

Figure B.5: Superelement 2 force transfer case 1 and 2

$$y = \frac{R_B bx}{6lEI}(l^2 - x^2 + b^2) \tag{B.25}$$

$$(y_B)_1 = \frac{-8R_B m^3}{18EI}\, for\, case\, 1 \quad and \quad (y_B)_2 = \frac{-7R_C m^3}{18EI}\, for\, case\, 2$$

$$(y_C)_1 = \frac{-7R_B m^3}{18EI}\, for\, case\, 1 \quad and \quad (y_C)_2 = \frac{-8R_C m^3}{18EI}\, for\, case\, 2$$

Finally, the reaction forces can be calculated due to:
Symmetry:

$$R_B = R_C \quad and \quad R_A = R_D$$

Overall Equilibrium:

$$R_A + R_B + R_C + R_D = p * length$$

Zero Displacement:

$$(y_B)_0 + (y_B)_1 + (y_B)_2 = 0 \quad and \quad (y_C)_0 + (y_C)_1 + (y_C)_2 = 0$$

Resulting in the equivalent wind forces on each wall shown in Figure B.6.

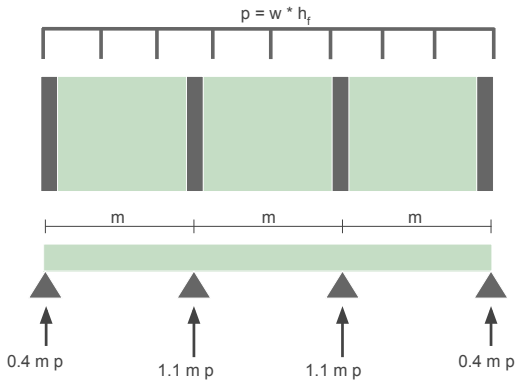

Figure B.6: Superelement 2 force transfer results

These series of point loads on the walls must be converted to a line load along the height of the wall. Since the floors are spaced at h_f, the wind force is divided by h_f, resulting in a distributed wind load with units $\frac{kN}{m}$.

$$f_a = 0.4\, m\, \frac{p}{h_f} = 0.4\, m\, w$$

$$f_b = 1.1\, m\, \frac{p}{h_f} = 1.1\, m\, w$$

B.2.5 Nodal equivalent forces

This part follows the same procedure outlined in Step 5. For an example see the derivation of super element 1 in Section 4.3.2.

B.2.6 Partitioning and assembly

This part follows the same procedure outlined in Step 6. For an example see the derivation of super element 1 in Section 4.3.2.

B.2.7 Structural behaviour equations

This part follows the same procedure outlined in Step 7. For an example see the derivation of super element 1 in Section 4.3.2.

The final symbolic equations describing the structural behaviour of super element 2 are also quite long due to the symbolic solution for the integration constants, so they will not be shown. However, the final equations can be seen in Sections 4.4.2, where they are solved for the specific parameters used for the validation.

B.3 Super element 3 derivation

This section outlines the derivation procedure for super element 3, which introduces torsional loading and resistance.

B.3.1 Kinematic, equilibrium and constitutive equations

The sign convention remains the same, so also the kinematic equations are the same as for super element 1 and 2.

$$\theta = -\frac{dw}{dx} \tag{B.26}$$

$$\kappa = \frac{1}{\rho} \tag{B.27}$$

$$\epsilon = \frac{z}{\rho} = z\kappa \tag{B.28}$$

A new force, torsion, is introduced in this super element, so the equilibrium and constitutive equations are summarised.

$$\begin{aligned} \theta &= -\frac{dw}{dx} \\ M &= EI\frac{d\theta}{dx} = -EI\frac{d^2w}{dx^2} \\ V &= \frac{dM}{dx} = -EI\frac{d^3w}{dx^3} \\ M_t &= GI_t\frac{d\psi}{dx} \end{aligned} \tag{B.29}$$

B.3.2 Floor stiffness matrix

The interaction between the floor system and the stability elements is more complex for this super element. The derivation of the differential equations is based on this interaction, so the derivation of the floor stiffness matrix is discussed first. Figure B.7 shows the degrees of freedom, nodal forces and the distance between the wall and core.

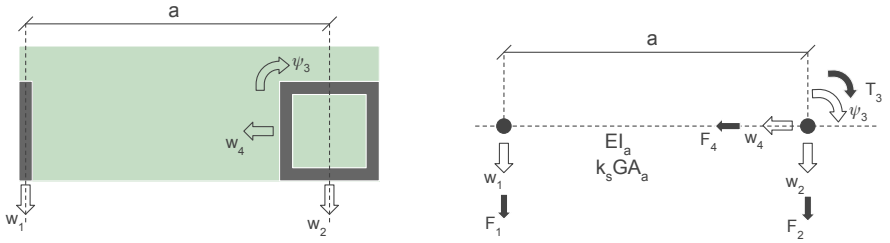

Figure B.7: Superelement 3 degrees of freedom

By relating each degree of freedom with each applied nodal force, the floor stiffness matrix is determined. To simplify the notation, stiffness $\tilde{A}$ is defined according to Figure B.8.

$$\tilde{A} = \frac{3EI_a}{a^3}\frac{1}{1+\frac{3EI}{a^2k_sGA_a}} \quad and \quad A = \frac{\tilde{A}}{storey\,height} \tag{B.30}$$

Each matrix cell is then defined in terms of $\tilde{A}$, resulting in the following floor stiffness matrix.

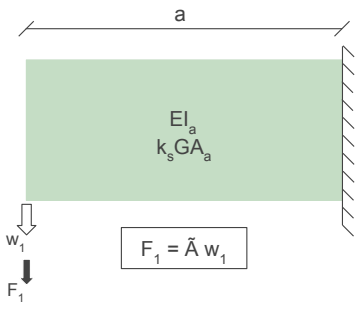

Figure B.8: Definition of $\tilde{A}$ for super element 3

$$\begin{bmatrix} \tilde{A} & -\tilde{A} & a\tilde{A} \\ -\tilde{A} & \tilde{A} & -a\tilde{A} \\ a\tilde{A} & -a\tilde{A} & a^2\tilde{A} \end{bmatrix} \begin{bmatrix} w_1 \\ w_2 \\ \psi_3 \end{bmatrix} = \begin{bmatrix} F_1 \\ F_2 \\ T_3 \end{bmatrix} \tag{B.31}$$

To get the floor stiffness matrix along the height of the super element the single floor stiffness ($\tilde{A}$) is replaced with the distributed floor stiffness (A) and the point forces F_1, F_2 and T_3 are replaced by the line loads f_1, f_2 and f_3 respectively.

$$\begin{bmatrix} A & -A & aA \\ -A & A & -aA \\ aA & -aA & a^2A \end{bmatrix} \begin{bmatrix} w_1 \\ w_2 \\ \psi_3 \end{bmatrix} = \begin{bmatrix} f_1 \\ f_2 \\ f_3 \end{bmatrix} \tag{B.32}$$

B.3.3 Differential equations

In order to determine the differential equations, the bending term ($EI_i w_i^{''''}$) is added to the diagonals (i) of the floor stiffness matrix that describe the bending of the walls. The torsion term ($-GI_3\psi^{''}$) is added to the diagonal of the third row in the floor stiffness matrix, corresponding to the torsional stiffness of the core. The final differential equations are:

$$\begin{aligned} Aw_1 + EI_1 w_1^{''''} \quad & -Aw_2 & & +aA\psi & &= f_1 \\ -Aw_1 & +Aw_2 + EI_2 w_2^{''''} & & -aA\psi & &= f_2 \\ aAw_1 & -aAw_2 & & +a^2A\psi - GI_3\psi^{''} & &= f_3 \\ & & & & EI_4 w_4^{''''} &= f_4 \end{aligned} \tag{B.33}$$

B.3.4 Stiffness matrix

In order to determine the stiffness matrix, the homogeneous solutions of the total displacement, rotation, moment and shear equations are required. This process was summarised in this report, but the detailed calculations can be found in Steenbergen's dissertation (2007).

$$\begin{aligned} Aw_1 + EI_1 w_1^{''''} \quad & -Aw_2 & & +aA\psi & &= 0 \\ -Aw_1 & +Aw_2 + EI_2 w_2^{''''} & & -aA\psi & &= 0 \\ aAw_1 & -aAw_2 & & +a^2A\psi - GI_3\psi^{''} & &= 0 \\ & & & & EI_4 w_4^{''''} &= 0 \end{aligned} \tag{B.34}$$

The fourth equation from Equations B.34 can be uncoupled and solved on its own. Next, by combining the first three equations, w_1 and Ψ_3 can be expressed in terms of w_2. Plugging these two equations back into the second equation results in the expression below, which is only in terms of w_2.

$$d_4 w_2^{''''} + d_2 w_2^{''} + d_0 w_2 = j(x) \tag{B.35}$$

where

$$j(x) = \frac{A}{EI_1}\left(\frac{1}{6}C_5 x^3 + \frac{1}{2}C_6 x^2 + C_7 x + C_8\right) - \frac{aA}{GI_3}(C_9 x + C_{10}) \tag{B.36}$$

and

$$d_4 = EI_2, \qquad d_2 = -\frac{a^2 AEI_2}{GI_3}, \qquad d_0 = A\left(\frac{EI_2}{EI_1} + 1\right) \tag{B.37}$$

To solve Equation B.35, the characteristic equation is determined by substituting $Ce^{\theta x}$ and replacing θ^2 with λ.

$$d_4\lambda^2 + d_2\lambda + d_0 = 0 \tag{B.38}$$

The determinant of this equation is:

$$D = (d_2)^2 - 4d_4 d_0) = \left(\frac{-a^2 AEI_2}{GI_3}\right)^2 - 4 * AEI_2\left(\frac{EI_2}{EI_1} + 1\right) \tag{B.39}$$

When the determinant is less than zero, the output is four complex solutions with opposite and complex conjugate roots.

$$\alpha = \frac{\sqrt{\sqrt{p^2 + q^2} + p}}{\sqrt{2}}, \qquad \beta = \frac{\sqrt{\sqrt{p^2 + q^2} - p}}{\sqrt{2}} \tag{B.40}$$

where,

$$p = -\frac{d_2}{2d_4}, \qquad q = \frac{\sqrt{|D|}}{2d_4} \tag{B.41}$$

When the determinant is larger than zero, there are two pairs of opposite roots.

$$\gamma_1 = \sqrt{p + q}, \qquad \gamma_2 = \sqrt{p - q} \tag{B.42}$$

where,

$$p = -\frac{d_2}{2d_4}, \qquad q = \frac{\sqrt{D}}{2d_4} \tag{B.43}$$

The case where the determinant is equal to zero was not implemented, because it is very rare. If it does occur the user will be asked to choose slightly different parameters.

Depending on the sign of the determinant, the homogeneous and the particular solution for Equation B.38 can now be determined. The summation of the homogeneous and particular part returns the total solution of the differential equation for w_2. Once the behaviour equation for w_2 was determined, the total solutions for the other two equations (w_1 and Ψ_3) can be derived, again for each case of the determinant.

Below are the final total symbolic equations for the displacements or rotation for each degree of freedom.

For $D < 0$:

$$\begin{aligned} w_1 = {} & S_1\left(\frac{x}{height}\right)^3 + S_2\left(\frac{x}{height}\right)^2 + S_3\frac{x}{height} + S_4\frac{x}{height} + S_5 + S_6 \\ & + \frac{1}{p_1}e^{-\alpha x}(S_{11}cos\beta x + S_{12}sin\beta x + \frac{1}{p_1}e^{\alpha(x-height)}(S_{13}cos\beta x + S_{14}sin\beta x) \end{aligned} \tag{B.44}$$

$$\begin{aligned} w_2 = {} & S_1\left(\frac{x}{height}\right)^3 + S_2\left(\frac{x}{height}\right)^2 + S_3\frac{x}{height} + S_4 p_1\frac{x}{height} + S5 + S6p_1 \\ & + e^{-\alpha x}(S_{11}cos\beta x + S_{12}sin\beta x + e^{\alpha(x-height)}(S_{13}cos\beta x + S_{14}sin\beta x) \end{aligned} \tag{B.45}$$

$$\begin{aligned}\psi_3 = {} & S_4 p_2 \frac{x}{height} + S_6 p_2 \\ & + S_{11} p_3 e^{-\alpha x}\big((\alpha^2-\beta^2)cos\beta x + 2\alpha\beta sin\beta x\big) \\ & + S_{12} p_3 e^{-\alpha x}\big((\alpha^2-\beta^2)sin\beta x - 2\alpha\beta cos\beta x\big) \\ & + S_{13} p_3 e^{\alpha(x-height)}\big((\alpha^2-\beta^2)cos\beta x - 2\alpha\beta sin\beta x\big) \\ & + S_{14} p_3 e^{\alpha(x-height)}\big((\alpha^2-\beta^2)sin\beta x + 2\alpha\beta cos\beta x\big)\end{aligned} \tag{B.46}$$

For $D > 0$:

$$\begin{aligned}w_1 = {} & S_1\left(\frac{x}{height}\right)^3 + S_2\left(\frac{x}{height}\right)^2 + S_3\frac{x}{height} + S_4\frac{x}{height} + S_5 + S_6 \\ & + S_{11}\frac{1}{p_1}e^{-\gamma_1 x} + S_{12}\frac{1}{p_1}e^{\gamma_1(x-height)} + S_{13}\frac{1}{p_1}e^{-\gamma_2 x} + S_{14}\frac{1}{p_1}e^{\gamma_2(x-height)}\end{aligned} \tag{B.47}$$

$$\begin{aligned}w_2 = {} & S_1\left(\frac{x}{height}\right)^3 + S_2\left(\frac{x}{height}\right)^2 + S_3\frac{x}{height} + S_4 p_1\frac{x}{height} + S_5 + S_6 p_1 \\ & + S_{11}e^{-\gamma_1 x} + S_{12}e^{\gamma_1(x-height)} + S_{13}e^{-\gamma_2 x} + S_{14}e^{\gamma_2(x-height)}\end{aligned} \tag{B.48}$$

$$\begin{aligned}\psi_3 = {} & S_4 p_2 \frac{x}{height} + S_6 p_2 \\ & + S_{11} p_3 \gamma_1^2 e^{-\gamma_1 x} + S_{12} p_3 \gamma_1^2 e^{\gamma_1(x-height)} \\ & + S_{13} p_3 \gamma_2^2 e^{-\gamma_2 x} + S_{14} p_3 \gamma_2^2 e^{\gamma_2(x-height)}\end{aligned} \tag{B.49}$$

For all cases:

$$w_4 = S_7\left(\frac{x}{height}\right)^3 + S_8\left(\frac{x}{height}\right)^2 + S_9\frac{x}{height} + S_{10} \tag{B.50}$$

where the S_i terms are the integration constants, which can be solved for with later defined boundary conditions and loading. p_1, p_2 and p_3 are defined as follows:

$$p_1 = -\frac{EI_1}{EI_2} \qquad p_2 = -\frac{EI_1 + EI_2}{aEI_2} \qquad p_3 = \frac{aEI_2}{GI_3} \tag{B.51}$$

The rotation, moment and shear equations are derivatives of the displacements following the equilibrium and constitutive equations shown previously.

The displacement and rotation equations are required for the h-matrix and the shear and moment equations for the g-matrix. These should be set up in the same way as described in Step 3 in Section B.1. The stiffness matrix can then be calculated by taking the matrix inverse and with matrix multiplication. The resulting symbolic stiffness matrix is too large to show, so only the equation used to derive it is shown.

$$K = GH^{-1} \tag{B.52}$$

B.3.5 Force transfer

To calculate the force transfer from the floors to the stability elements, the floor parts in the x and z direction are represented by beams, see Figure B.9. The core provides a fixed support, while the wall provides a pinned support in the direction of the strong axis of the wall. f_1, f_2, f_3 and f_4 are line loads on the stability elements.

Distributed area loads $wind_1$ and $wind_2$ are applied on two faces, resulting in two line loads on the floor edges. The same procedure as for the super element with four walls is applied, resulting in the following line loads along the height of the stability elements.

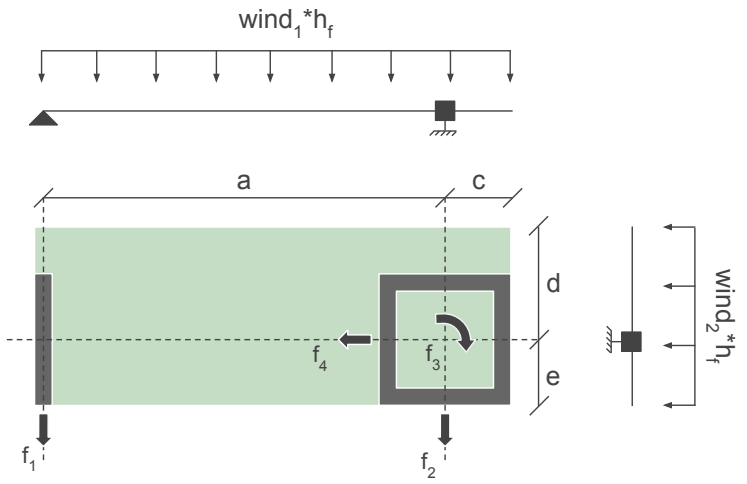

Figure B.9: Superelement 3 force transfer diagram

$$
\begin{aligned}
f_1 &= \frac{3}{8} wind_1 a \\
f_2 &= wind_1 \left(\frac{5}{8} a + c \right) \\
f_3 &= wind_2 \left(\frac{1}{2} e^2 - \frac{1}{2} d^2 \right) - wind_1 \left(\frac{1}{8} a^2 - \frac{1}{2} c^2 \right) \\
f_4 &= wind_2 (e + d)
\end{aligned}
\tag{B.53}
$$

B.3.6 Nodal equivalent forces

To calculate the nodal equivalent forces, the particular solutions to the differential equations, see below, are required.

$$
\begin{aligned}
Aw_1 + EI_1 w_1'''' \quad & -Aw_2 \quad && +aA\psi && = f_1 \\
-Aw_1 \quad & +Aw_2 + EI_2 w_2'''' && -aA\psi && = f_2 \\
aAw_1 \quad & -aAw_2 && +a^2 A\psi - GI_3 \psi'' && = f_3 \\
& && && EI_4 w_4'''' = f_4
\end{aligned}
\tag{B.54}
$$

During the derivation integration constants are not introduced, because the goal is to determine an arbitrary particular solution. Many particular solutions are possible, so a more convenient solution considering later calculations will be chosen.

Again, the fourth equation can be uncoupled and solved for on its own. Also the particular solution for w_1 and Ψ_3 can be written in terms of w_2. When they are plugged into the second equation from Equations B.54, the result is:

$$
d_4 w_2'''' + d_2 w_2'' + d_0 w_2 = j(x) \tag{B.55}
$$

where

$$
j(x) = \frac{A}{24 EI_1} (f_1 + f_2) x^4 - \frac{aA}{2GI_3} (af_2 + f_3) x^2 + f_2 \tag{B.56}
$$

and again,

$$
d_4 = EI_2, \qquad d_2 = -\frac{a^2 AEI_2}{GI_3}, \qquad d_0 = A \left(\frac{EI_2}{EI_1} + 1 \right) \tag{B.57}
$$

A general solution in the same format as Equation B.55, is substituted in order to find a particular solution for w_2.

$$w_{2,part} = r_2 x^4 + s_2 x^2 + t_2 \tag{B.58}$$

Based on this equation w_1 and Ψ_3 can also be solved for, resulting in the following possible particular solutions.

$$\begin{aligned} w_{1,part} &= r_1 x^4 + s_1 x^2 + t_1 \\ w_{2,part} &= r_2 x^4 + s_2 x^2 + t_2 \\ \psi_{3,part} &= s_3 x^2 + t_3 \\ w_{4,part} &= r_4 x^4 \end{aligned} \tag{B.59}$$

where,

$$r_1 = -\frac{EI_2}{EI_1} r_2 + \frac{1}{24EI_1}(f_1 + f_2), \qquad s_1 = -\frac{EI_2}{EI_1} s_2, \qquad t_1 = -\frac{EI_2}{EI_1} t_2 - \frac{f_2}{A}$$

$$r_2 = \frac{A}{d_0 24EI_1}(f_1 + f_2), \qquad s_2 = -\frac{aA}{d_0 2GI_3}(af_2 + f_3) - \frac{d_2 A}{d_0^2 2EI_1}(f_1 + f_2)$$

$$t_2 = -\frac{d_4 A}{d_0^2 EI_1}(f_1 + f_2) + \frac{d_2 aA}{d_0^2 GI_3}(af_2 + f_3) + \frac{d_2^2 A}{d_0^3 EI_1}(f_1 + f_2)$$

$$r_2 = -\frac{1}{2GI_3}(af_2 + f_3), \qquad s_3 = \frac{aEI_2}{GI_3}, \qquad t_3 = \frac{aEI_2}{GI_3} 2s_2$$

$$r_4 = \frac{f_4}{24EI_4}$$

The equivalent nodal vector is derived the same way as in the general instructions in Section B.1.

$$v_3 = \begin{bmatrix} F_{1,1} \\ T_{1,1} \\ F_{2,1} \\ T_{2,1} \\ T_{3,1} \\ F_{4,1} \\ T_{4,1} \\ F_{1,2} \\ T_{1,2} \\ F_{2,2} \\ T_{2,2} \\ T_{3,2} \\ F_{4,2} \\ T_{4,2} \end{bmatrix} = \begin{bmatrix} -V_{1,1} \\ -M_{1,1} \\ -V_{2,1} \\ -M_{2,1} \\ -M_{3,1} \\ -V_{4,1} \\ -M_{4,1} \\ V_{1,2} \\ M_{1,2} \\ V_{2,2} \\ M_{2,2} \\ M_{3,2} \\ V_{4,2} \\ M_{4,2} \end{bmatrix} = \begin{bmatrix} 0 \\ -EI_1 2s_1 \\ 0 \\ -EI_2 2s_2 \\ 0 \\ 0 \\ 0 \\ EI_1 24 r_1 height \\ EI_1(12 r_1 height^2 + 2s1) \\ EI_2 24 r_2 height \\ EI_2(12 r_2 height^2 + 2s_2 \\ -GI_3 2 s_3 height \\ EI_4 24 r_4 height \\ EI_4 12 r_4 height^2 \end{bmatrix} + \begin{bmatrix} K_3 \end{bmatrix} \begin{bmatrix} t_1 \\ 0 \\ t_2 \\ 0 \\ t_3 \\ 0 \\ 0 \\ r_1 height^4 + s_1 height^2 + t_1 \\ -4 r_1 height^3 - 2 s_1 height \\ r_2 height^4 + s_2 height^2 + t_2 \\ -4 r_2 height^3 - 2 s_2 height \\ s_3 height^2 + t_3 \\ r_4 height^4 \\ -4 r_4 height^3 \end{bmatrix} \tag{B.60}$$

B.3.7 Partitioning and assembly

This part follows the same procedure outlined in Step 6. For an example see the derivation of super element 1 in Section 4.3.2.

B.3.8 Structural behaviour equations

This part follows the same procedure outlined in Step 7. For an example see the derivation of super element 1 in Section 4.3.2. The final symbolic equations describing the structural behaviour of super element 2 are also quite long due to the symbolic solution for the integration constants, so they will not be shown.

B.4 Super Element Combination

The previous sections discussed the analysis mathematics of a single super element, which is also used for their combination. This section will present the method used to perform the analysis calculations on a combination of multiple super elements to form a new super-structure.

B.4.1 Simple Connection Procedure

The wall connection type then determines how the stiffness matrices (K) and equivalent nodal force vectors (f) are combined. Most of the connections are quite simple, since all of the lower wall nodes (prescribed) of the top super element coincide with all of the top wall nodes (free) of the lower super element. In this case the stiffness matrix (K^2) of the top super element is added to the stiffness matrix (K^1) of the lower super element where only the k^2_{ff} part of the top super element stiffness matrix overlaps with the k^1_{pp} part of the lower super element. This type of connection is always applied when super elements of the same type are placed on top of each other, but also in other connection types such as placing the super element with two walls on top of the two inner walls of the super element with four walls (connection B). The same procedure applies to the equivalent nodal force vector (f). The stiffness matrix and force vector combination is illustrated below, where 1 indicated the lower stiffness matrix and 2 the upper stiffness matrix:

$$k_{combined} = \begin{bmatrix} k^1_{ff} & k^1_{fp} & 0 \\ k^1_{pf} & k^1_{pp} + k^2_{ff} & k^2_{fp} \\ 0 & k^2_{pf} & k^2_{pp} \end{bmatrix} \qquad f_{combined} = \begin{bmatrix} f^1_f \\ f^1_p + f^2_f \\ f^2_p \end{bmatrix} \tag{B.61}$$

B.4.2 Detailed Connection Procedure

In order to analyse a structure composed of different types of super elements placed on top of each other, special attention on the connected degrees of freedom is placed. Only the values at shared nodes are added. This procedure is illustrated with the example of placing the super element with two walls on top of the two outside walls of the super element with four walls (connection A).

The four walled super element has eight nodes, one node at the end of each wall ($2 * 4 = 8$), and two degrees of freedom at each node. However, the total number of degrees of freedom is simplified from sixteen to eight due to the symmetry (see Section B.2). The two walled super element is also simplified due to symmetry (see Section 4.3.2) and therefore only has four degrees of freedom. Their individual stiffness matrix and equivalent nodal force vector look as follows:

$$k^1 = \begin{bmatrix} k_{11} & k_{12} & k_{13} & k_{14} & k_{15} & k_{16} & k_{17} & k_{18} \\ k_{21} & k_{22} & k_{23} & k_{24} & k_{25} & k_{26} & k_{27} & k_{28} \\ k_{31} & k_{32} & k_{33} & k_{34} & k_{35} & k_{36} & k_{37} & k_{38} \\ k_{41} & k_{42} & k_{43} & k_{44} & k_{45} & k_{46} & k_{47} & k_{48} \\ k_{51} & k_{52} & k_{53} & k_{54} & k_{55} & k_{56} & k_{57} & k_{58} \\ k_{61} & k_{62} & k_{63} & k_{64} & k_{65} & k_{66} & k_{67} & k_{68} \\ k_{71} & k_{72} & k_{73} & k_{74} & k_{75} & k_{76} & k_{77} & k_{78} \\ k_{81} & k_{82} & k_{83} & k_{84} & k_{85} & k_{86} & k_{87} & k_{88} \end{bmatrix} \qquad k^2 = \begin{bmatrix} k_{11} & k_{12} & k_{13} & k_{14} \\ k_{21} & k_{22} & k_{23} & k_{24} \\ k_{31} & k_{32} & k_{33} & k_{34} \\ k_{41} & k_{42} & k_{43} & k_{44} \end{bmatrix}$$

Since for this connection only degrees of freedom 5 and 6 coincide, only the values in row and column 5 and 6 are added together. The rest are placed in their corresponding degree of freedom location. Again, the same process is applied to the equivalent nodal force vector.

$$k_{comb} = \begin{bmatrix} k_{11}^1 & k_{12}^1 & k_{13}^1 & k_{14}^1 & k_{15}^1 & k_{16}^1 & k_{17}^1 & k_{18}^1 & 0 & 0 \\ k_{21}^1 & k_{22}^1 & k_{23}^1 & k_{24}^1 & k_{25}^1 & k_{26}^1 & k_{27}^1 & k_{28}^1 & 0 & 0 \\ k_{31}^1 & k_{32}^1 & k_{33}^1 & k_{34}^1 & k_{35}^1 & k_{36}^1 & k_{37}^1 & k_{38}^1 & 0 & 0 \\ k_{41}^1 & k_{42}^1 & k_{43}^1 & k_{44}^1 & k_{45}^1 & k_{46}^1 & k_{47}^1 & k_{48}^1 & 0 & 0 \\ k_{51}^1 & k_{52}^1 & k_{53}^1 & k_{54}^1 & k_{55}^1+k_{11}^2 & k_{56}^1+k_{12}^2 & 0 & 0 & k_{57}^2 & k_{58}^2 \\ k_{61}^1 & k_{62}^1 & k_{63}^1 & k_{64}^1 & k_{65}^1+k_{21}^2 & k_{66}^1+k_{22}^2 & 0 & 0 & k_{67}^2 & k_{68}^2 \\ k_{71}^1 & k_{72}^1 & k_{73}^1 & k_{74}^1 & k_{75}^1 & k_{76}^1 & k_{77}^1 & k_{78}^1 & 0 & 0 \\ k_{81}^1 & k_{82}^1 & k_{83}^1 & k_{84}^1 & k_{85}^1 & k_{86}^1 & k_{87}^1 & k_{88}^1 & 0 & 0 \\ 0 & 0 & 0 & 0 & k_{31}^2 & k_{32}^2 & 0 & 0 & k_{33}^2 & k_{34}^2 \\ 0 & 0 & 0 & 0 & k_{41}^2 & k_{42}^2 & 0 & 0 & k_{43}^2 & k_{44}^2 \end{bmatrix} \quad f_{comb} = \begin{bmatrix} f_1^1 \\ f_2^1 \\ f_3^1 \\ f_4^1 \\ f_5^1+f_1^2 \\ f_6^1+f_2^2 \\ f_7^1 \\ f_8^1 \\ f_3^2 \\ f_4^2 \end{bmatrix} \tag{B.62}$$

C

Appendix B

This Appendix contains the MatrixFrame reports used to validate the differential equation method with a finite element model.

C.1 Super Element 1 MatrixFrame Report

Here the MatrixFrame report for super element 1 is included

Super element 1 Validation			
Job Name	superelement1	Job Number	
Part Description		Structural Engineer	Babette Hohrath
Client		Units	m, kN, kNm
File	H:\Thesis\se1_valiation_14_09.mxe		

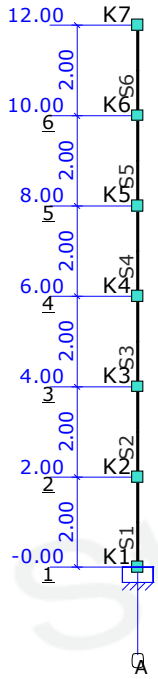

Pic. Geometrie 1: Raamwerk

Pic. Geometrie 2: Raamwerk

Sections

Section	Section Name	Area	Iy	Material	Angle
P1	R200x3000	6.0000e-01	4.5000e-01	C30/37	0
-	-	m2	m4	-	°

Section Shapes

Section	Tapered	hB	hE	tf	tw	tf2	B	b1	b2	Castellate	Height
P1	No	3.000000	3.000000	0.000000	0.000000	0.000000	0.200000	0.000000	0.000000	No	0.000000
-	-	m	m	m	m	m	m	m	m	-	m

Materials

Material Name	Density	Youngs mod.	Lin. Exp.
C30/37	25.000	3.0000e+07	10.0000e-06
-	kN/m3	kN/m2	C°m

Supports

Support	Node	X	Z	Yr	AngleYr
O1	K1	fixed	fixed	fixed	0
-	-	kN/m	kN/m	kNmrad	°

B.G.1: Wind load

Type	Value Begin	Value End	Dist. Begin	Dist. End	Direction	Member/Node
B.G.1: Wind load						
q	4,000	4,000	0,000000	2,000000(L)	X"	S1-S6
Sum of loads	**X:48,000 kN**	**Z: 0,000 kN**				
-	-	-	m	m	-	-

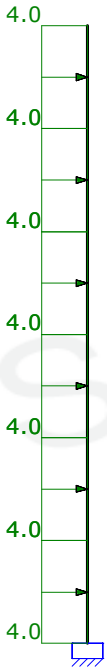

B.G.1: Wind load

Analysis Assumptions

Linear Elastic Analysis performed

Pic. B.G.1: Wind load Verplaatsingen

L.C. Nodal Displacements

Node	L.C.	X	Z	Ry
K1	B.G.1	0.0000000	0.0000000	-0.000e-03
K2		0.0000381	0.0000000	-0.036e-03
K3		0.0001359	0.0000000	-0.060e-03
K4		0.0002720	0.0000000	-0.075e-03
K5		0.0004298	0.0000000	-0.082e-03
K6		0.0005975	0.0000000	-0.085e-03
K7		0.0007680	0.0000000	-0.085e-03
-	**-**	**m**	**m**	**rad**

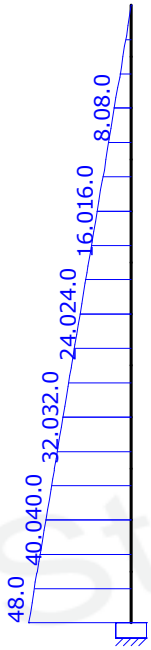

Pic. B.G.1: Wind load Dwarskracht (Vz)

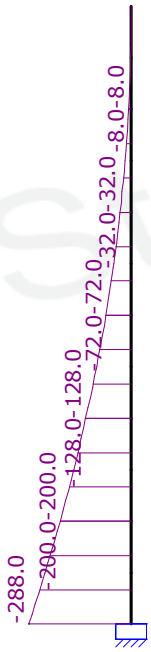

Pic. B.G.1: Wind load Momenten (My)

L.C. Member Forces

Member	L.C.	Mb	Mmax	xMmax	Me	x-M0	x-M0	TC	Nmax	Vb	Vmax	Ve
S1	B.G.1	-288.000			-200.000	0.000000	0.000000	-	0.000	48.000	48.000	40.000
S2	B.G.1	-200.000			-128.000	0.000000	0.000000	-	0.000	40.000	40.000	32.000
S3	B.G.1	-128.000			-72.000	0.000000	0.000000	-	0.000	32.000	32.000	24.000
S4	B.G.1	-72.000			-32.000	0.000000	0.000000	-	0.000	24.000	24.000	16.000
S5	B.G.1	-32.000			-8.000	0.000000	0.000000	-	0.000	16.000	16.000	8.000

Member	L.C.	Mb	Mmax	xMmax	Me	x-M0	x-M0	TC	Nmax	Vb	Vmax	Ve
S6	B.G.1	-8.000			0.000	0.000000	0.000000	-	0.000	8.000	8.000	0.000
-	**-**	**kNm**	**kNm**	**m**	**kNm**	**m**	**m**	**-**	**kN**	**kN**	**kN**	**kN**

C.2 Super Element 2 MatrixFrame Report

Here the MatrixFrame reports for super element 2 are included.

C.2.1 Super Element 2 with Equal Wall Dimensions

The report for super element two where all the walls are 6m wide.

Super Element 2 Validation		
Projectnaam	superelement2	Projectnummer	
Omschrijving		Constructeur	Babette Hohrath
Opdrachtgever		Eenheden	m, kN, kNm
Bestand	H:\Thesis\		

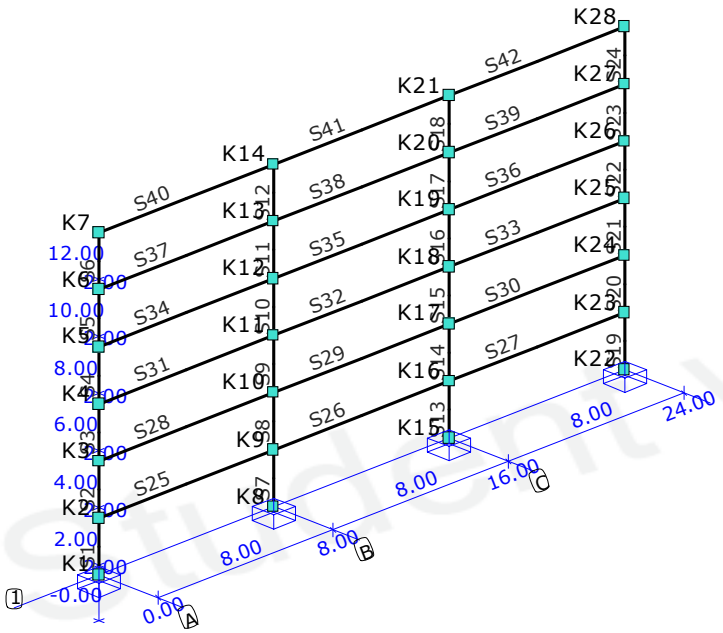

Afb. Geometrie 1: Raamwerk

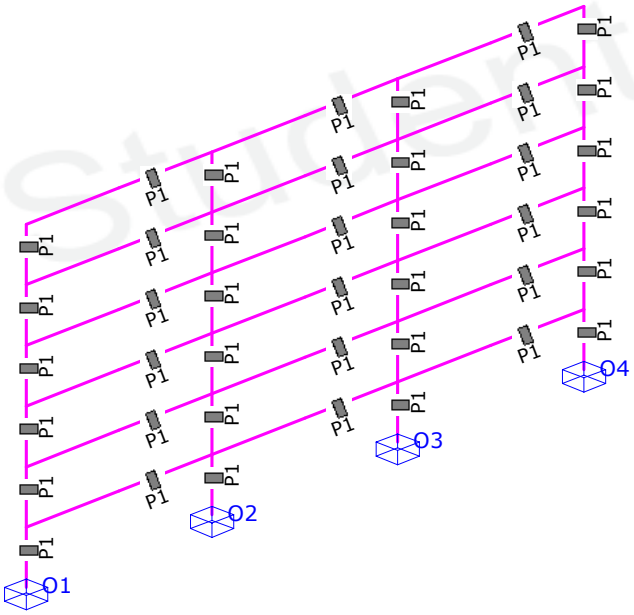

Afb. Geometrie 2: Raamwerk

Profielen

Profiel	Profielnaam	Oppervlakte	It	Iy	Iz	Materiaal	Hoek
P1	R6000x200	1.2000e+00	1.6000e-02	4.0000e-03	3.6000e+00	C30/37	0
-	-	m2	m4	m4	m4	-	°

Profielvormen

Profiel	Verlopende hoogte	hB	hE	tf	tw	tf2	B	bL	bR	Raatliggers	Mx
P1	Nee	0.200000	0.200000	0.000000	0.000000	0.000000	6.000000	0.000000	0.000000	Nee	0.000000
-	-	m	m	m	m	m	m	m	m	-	m

Materialen

Materiaalnaam	Poison	Dichtheid	E-Modulus	Uitzettingcoeff
C30/37	0.30	25.000	3.0000e+07	10.0000e-06
-	-	kN/m3	kN/m2	C°m

Opleggingen

Oplegging	Knopen	X	Y	Z	Xr	Yr	Zr	HoekXr	HoekYr	HoekZr
O1	K1	vast	vast	vast	vast	vast	vast	0	0	0
O2	K8	vast	vast	vast	vast	vast	vast	0	0	0
O3	K15	vast	vast	vast	vast	vast	vast	0	0	0
O4	K22	vast	vast	vast	vast	vast	vast	0	0	0
-	-	kN/m	kN/m	kN/m	kNmrad	kNmrad	kNmrad	°	°	°

B.G.1: Wind load

Type	Beginwaarde	Eindwaarde	Beginafstand	Eindafstand	Richting	Staaf of knoop
B.G.1: Wind load						
q	3,200	3,200	0,000000	2,000000(L)	Y"	S1-S6,S19-S24
q	8,800	8,800	0,000000	2,000000(L)	Y"	S7-S18
Som lasten	**X: 0,000 kN**		**Y: 288,000 kN**		**Z: 0,000 kN**	
-	-	-	m	m	-	-

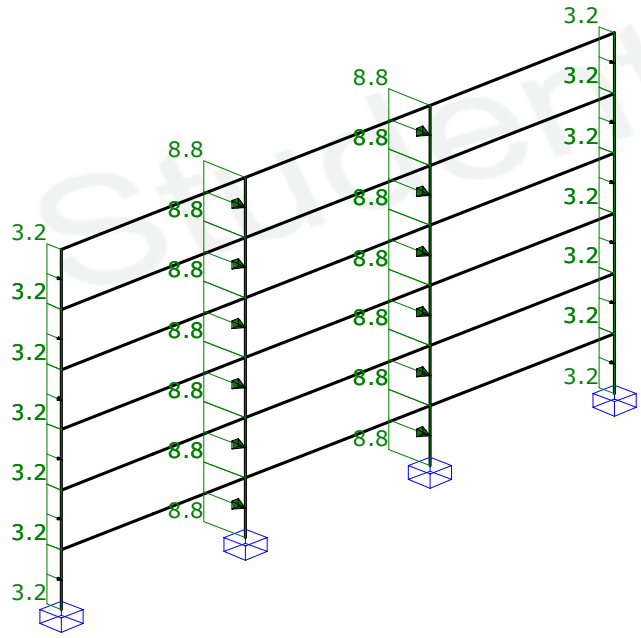

B.G.1: Wind load

Uitgangspunten van de analyse

Lineaire Elastische Analyse uitgevoerd

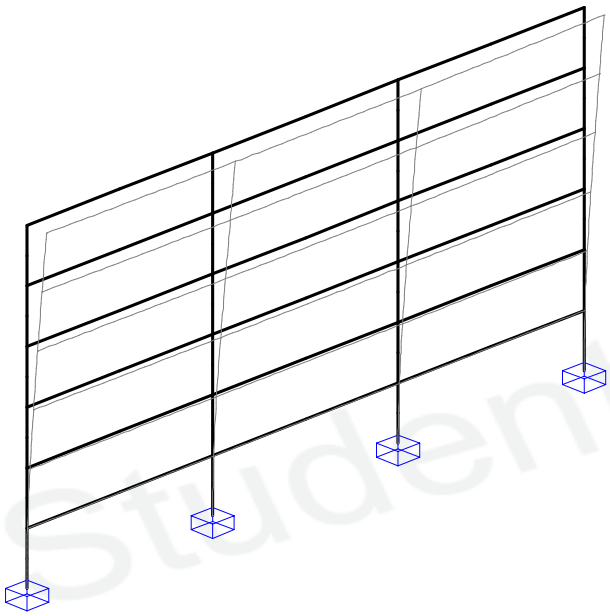

Afb. B.G.1: Wind load Verplaatsingen

L.C. Knoopverplaatsingen

Knoop	B.G.	X	Y	Z	Rx	Ry	Rz
K1	B.G.1	0.0000000	0.0000000	0.0000000	-0.000e-03	-0.000e-03	-0.000e-03
K2		0.0000000	0.0000063	0.0000000	-0.006e-03	-0.000e-03	-0.000e-03
K3		0.0000000	0.0000229	0.0000000	-0.010e-03	-0.000e-03	-0.001e-03
K4		0.0000000	0.0000464	0.0000000	-0.013e-03	-0.000e-03	-0.001e-03
K5		0.0000000	0.0000741	0.0000000	-0.014e-03	-0.000e-03	-0.002e-03
K6		0.0000000	0.0001038	0.0000000	-0.015e-03	-0.000e-03	-0.002e-03
K7		0.0000000	0.0001342	0.0000000	-0.015e-03	-0.000e-03	-0.003e-03
K8		0.0000000	0.0000000	0.0000000	-0.000e-03	-0.000e-03	-0.000e-03
K9		0.0000000	0.0000079	0.0000000	-0.007e-03	-0.000e-03	-0.000e-03
K10		0.0000000	0.0000280	0.0000000	-0.012e-03	-0.000e-03	-0.000e-03
K11		0.0000000	0.0000556	0.0000000	-0.015e-03	-0.000e-03	-0.001e-03
K12		0.0000000	0.0000871	0.0000000	-0.016e-03	-0.000e-03	-0.001e-03
K13		0.0000000	0.0001203	0.0000000	-0.017e-03	-0.000e-03	-0.001e-03
K14		0.0000000	0.0001538	0.0000000	-0.017e-03	-0.000e-03	-0.001e-03
K15		0.0000000	0.0000000	0.0000000	-0.000e-03	-0.000e-03	0.000e-03
K16		0.0000000	0.0000079	0.0000000	-0.007e-03	-0.000e-03	0.000e-03
K17		0.0000000	0.0000280	0.0000000	-0.012e-03	-0.000e-03	0.000e-03
K18		0.0000000	0.0000556	0.0000000	-0.015e-03	-0.000e-03	0.001e-03
K19		0.0000000	0.0000871	0.0000000	-0.016e-03	-0.000e-03	0.001e-03
K20		0.0000000	0.0001203	0.0000000	-0.017e-03	-0.000e-03	0.001e-03
K21		0.0000000	0.0001538	0.0000000	-0.017e-03	-0.000e-03	0.001e-03
K22		0.0000000	0.0000000	0.0000000	-0.000e-03	-0.000e-03	0.000e-03
K23		0.0000000	0.0000063	0.0000000	-0.006e-03	-0.000e-03	0.000e-03
K24		0.0000000	0.0000229	0.0000000	-0.010e-03	-0.000e-03	0.001e-03
K25		0.0000000	0.0000464	0.0000000	-0.013e-03	-0.000e-03	0.001e-03
K26		0.0000000	0.0000741	0.0000000	-0.014e-03	-0.000e-03	0.002e-03
K27		0.0000000	0.0001038	0.0000000	-0.015e-03	-0.000e-03	0.002e-03
K28		0.0000000	0.0001342	0.0000000	-0.015e-03	0.000e-03	0.003e-03
-	**-**	**m**	**m**	**m**	**rad**	**rad**	**rad**

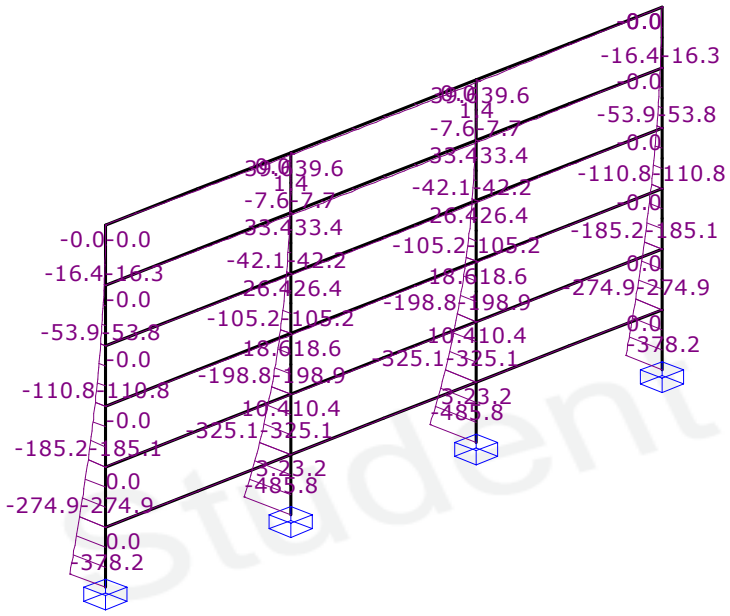

Afb. B.G.1: Wind load Momenten (Mz)

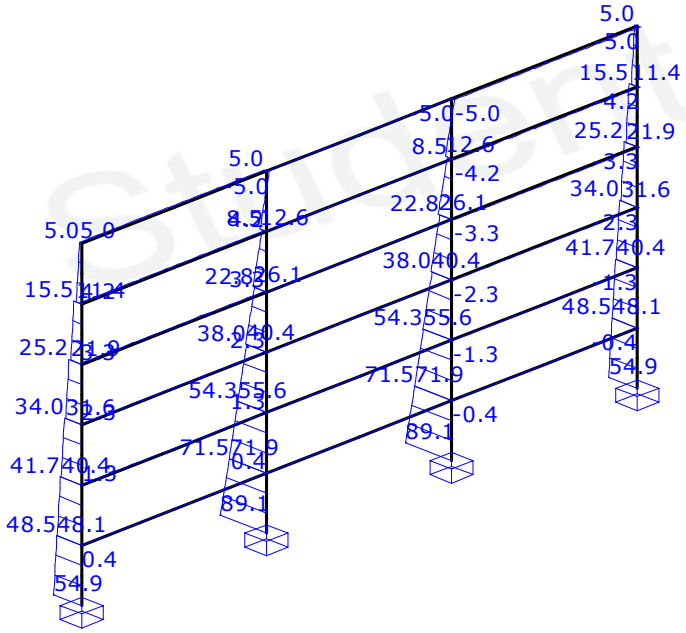

Afb. B.G.1: Wind load Dwarskracht (Vy)

L.C. Staafkrachten (My, Mz)

Staaf	B.G.	Waarde	Mb	Mmax	xMmax	Me	x-M0	x-M0
S1	B.G.1	My	0.000			0.000	0.000000	0.000000
		Mz	-378.239			-274.922	0.000000	0.000000
S2	B.G.1	My	0.000			0.000	0.000000	0.000000
		Mz	-274.889			-185.174	0.000000	0.000000
S3	B.G.1	My	0.000			0.000	0.000000	0.000000

Staaf	B.G.	Waarde	Mb	Mmax	xMmax	Me	x-M0	x-M0
		Mz	-185.128			-110.804	0.000000	0.000000
S4	B.G.1	My	0.000			0.000	0.000000	0.000000
		Mz	-110.757			-53.885	0.000000	0.000000
S5	B.G.1	My	0.000			0.000	0.000000	0.000000
		Mz	-53.843			-16.384	0.000000	0.000000
S6	B.G.1	My	0.000			0.000	0.000000	0.000000
		Mz	-16.347			-0.034	0.000000	0.000000
S7	B.G.1	My	0.000			0.000	0.000000	0.000000
		Mz	-485.761			-325.078	0.000000	0.000000
S8	B.G.1	My	0.000			0.000	0.000000	0.000000
		Mz	-325.111			-198.826	0.000000	0.000000
S9	B.G.1	My	0.000			0.000	0.000000	0.000000
		Mz	-198.872			-105.196	0.000000	0.000000
S10	B.G.1	My	0.000			0.000	0.000000	0.000000
		Mz	-105.243			-42.115	0.000000	0.000000
S11	B.G.1	My	0.000			0.000	0.000000	0.000000
		Mz	-42.157			-7.616	0.000000	0.000000
S12	B.G.1	My	0.000			0.000	0.000000	0.000000
		Mz	-7.653	1.430	1.436781	0.034	0.866672	0.000000
S13	B.G.1	My	0.000			0.000	0.000000	0.000000
		Mz	-485.761			-325.078	0.000000	0.000000
S14	B.G.1	My	0.000			0.000	0.000000	0.000000
		Mz	-325.111			-198.826	0.000000	0.000000
S15	B.G.1	My	0.000			0.000	0.000000	0.000000
		Mz	-198.872			-105.196	0.000000	0.000000
S16	B.G.1	My	0.000			0.000	0.000000	0.000000
		Mz	-105.243			-42.115	0.000000	0.000000
S17	B.G.1	My	0.000			0.000	0.000000	0.000000
		Mz	-42.157			-7.616	0.000000	0.000000
S18	B.G.1	My	0.000			0.000	0.000000	0.000000
		Mz	-7.653	1.430	1.436781	0.034	0.866672	0.000000
S19	B.G.1	My	0.000			0.000	0.000000	0.000000
		Mz	-378.239			-274.922	0.000000	0.000000
S20	B.G.1	My	0.000			0.000	0.000000	0.000000
		Mz	-274.889			-185.174	0.000000	0.000000
S21	B.G.1	My	0.000			0.000	0.000000	0.000000
		Mz	-185.128			-110.804	0.000000	0.000000
S22	B.G.1	My	0.000			0.000	0.000000	0.000000
		Mz	-110.757			-53.885	0.000000	0.000000
S23	B.G.1	My	0.000			0.000	0.000000	0.000000
		Mz	-53.843			-16.384	0.000000	0.000000
S24	B.G.1	My	0.000			0.000	0.000000	0.000000
		Mz	-16.347			-0.034	0.000000	0.000000
S25	B.G.1	My	0.000			0.000	0.000000	0.000000
		Mz	0.026			3.232	0.000000	0.000000
S26	B.G.1	My	0.000			0.000	0.000000	0.000000
		Mz	3.245			3.245	0.000000	0.000000
S27	B.G.1	My	0.000			0.000	0.000000	0.000000
		Mz	3.232			0.026	0.000000	0.000000
S28	B.G.1	My	0.000			0.000	0.000000	0.000000
		Mz	0.008			10.370	0.000000	0.000000
S29	B.G.1	My	0.000			0.000	0.000000	0.000000
		Mz	10.374			10.374	0.000000	0.000000
S30	B.G.1	My	0.000			0.000	0.000000	0.000000
		Mz	10.370			0.008	0.000000	0.000000
S31	B.G.1	My	0.000			0.000	0.000000	0.000000
		Mz	-0.003			18.607	0.001151	0.000000
S32	B.G.1	My	0.000			0.000	0.000000	0.000000
		Mz	18.606			18.606	0.000000	0.000000
S33	B.G.1	My	0.000			0.000	0.000000	0.000000
		Mz	18.607			-0.003	7.998849	0.000000
S34	B.G.1	My	0.000			0.000	0.000000	0.000000
		Mz	-0.006			26.447	0.001869	0.000000
S35	B.G.1	My	0.000			0.000	0.000000	0.000000

Staaf	B.G.	Waarde	Mb	Mmax	xMmax	Me	x-M0	x-M0
		Mz	26.444			26.444	0.000000	0.000000
S36	B.G.1	My	0.000			0.000	0.000000	0.000000
		Mz	26.447			-0.006	7.998131	0.000000
S37	B.G.1	My	0.000			0.000	0.000000	0.000000
		Mz	-0.005			33.380	0.001201	0.000000
S38	B.G.1	My	0.000			0.000	0.000000	0.000000
		Mz	33.377			33.377	0.000000	0.000000
S39	B.G.1	My	0.000			0.000	0.000000	0.000000
		Mz	33.380			-0.005	7.998798	0.000000
S40	B.G.1	My	0.000			0.000	0.000000	0.000000
		Mz	-0.042			39.608	0.008554	0.000000
S41	B.G.1	My	0.000			0.000	0.000000	0.000000
		Mz	39.587			39.587	0.000000	0.000000
S42	B.G.1	My	0.000			0.000	0.000000	0.000000
		Mz	39.608			-0.042	7.991446	0.000000
-	**-**	**-**	**kNm**	**kNm**	**m**	**kNm**	**m**	**m**

L.C. Staafkrachten (Nx, Vy, Vz, Mx)

Staaf	B.G.	T/D	Nmax	Waarde	Vb	Vmax	Ve	Mxb	Mxe
S1	B.G.1	-	0.000	Vz	0.000	0.000	0.000	-0.022	-0.022
				Vy	54.858	54.858	48.458		
S2	B.G.1	-	0.000	Vz	0.000	0.000	0.000	-0.049	-0.049
				Vy	48.058	48.058	41.658		
S3	B.G.1	-	0.000	Vz	0.000	0.000	0.000	-0.056	-0.056
				Vy	40.362	40.362	33.962		
S4	B.G.1	-	0.000	Vz	0.000	0.000	0.000	-0.054	-0.054
				Vy	31.636	31.636	25.236		
S5	B.G.1	-	0.000	Vz	0.000	0.000	0.000	-0.047	-0.047
				Vy	21.929	21.929	15.529		
S6	B.G.1	-	0.000	Vz	0.000	0.000	0.000	-0.042	-0.042
				Vy	11.356	11.356	4.956		
S7	B.G.1	-	0.000	Vz	0.000	0.000	0.000	-0.011	-0.011
				Vy	89.142	89.142	71.542		
S8	B.G.1	-	0.000	Vz	0.000	0.000	0.000	-0.024	-0.024
				Vy	71.942	71.942	54.342		
S9	B.G.1	-	0.000	Vz	0.000	0.000	0.000	-0.028	-0.028
				Vy	55.638	55.638	38.038		
S10	B.G.1	-	0.000	Vz	0.000	0.000	0.000	-0.027	-0.027
				Vy	40.364	40.364	22.764		
S11	B.G.1	-	0.000	Vz	0.000	0.000	0.000	-0.024	-0.024
				Vy	26.071	26.071	8.471		
S12	B.G.1	-	0.000	Vz	0.000	0.000	0.000	-0.021	-0.021
				Vy	12.644	12.644	-4.956		
S13	B.G.1	-	0.000	Vz	0.000	0.000	0.000	0.011	0.011
				Vy	89.142	89.142	71.542		
S14	B.G.1	-	0.000	Vz	0.000	0.000	0.000	0.024	0.024
				Vy	71.942	71.942	54.342		
S15	B.G.1	-	0.000	Vz	0.000	0.000	0.000	0.028	0.028
				Vy	55.638	55.638	38.038		
S16	B.G.1	-	0.000	Vz	0.000	0.000	0.000	0.027	0.027
				Vy	40.364	40.364	22.764		
S17	B.G.1	-	0.000	Vz	0.000	0.000	0.000	0.024	0.024
				Vy	26.071	26.071	8.471		
S18	B.G.1	-	0.000	Vz	0.000	0.000	0.000	0.021	0.021
				Vy	12.644	12.644	-4.956		
S19	B.G.1	-	0.000	Vz	0.000	0.000	0.000	0.022	0.022
				Vy	54.858	54.858	48.458		
S20	B.G.1	-	0.000	Vz	0.000	0.000	0.000	0.049	0.049
				Vy	48.058	48.058	41.658		
S21	B.G.1	-	0.000	Vz	0.000	0.000	0.000	0.056	0.056
				Vy	40.362	40.362	33.962		
S22	B.G.1	-	0.000	Vz	0.000	0.000	0.000	0.054	0.054
				Vy	31.636	31.636	25.236		
S23	B.G.1	-	0.000	Vz	0.000	0.000	0.000	0.047	0.047
				Vy	21.929	21.929	15.529		
S24	B.G.1	-	0.000	Vz	0.000	0.000	0.000	0.042	0.042

Staaf	B.G.	T/D	Nmax	Waarde	Vb	Vmax	Ve	Mxb	Mxe
				Vy	11.356	11.356	4.956		
S25	B.G.1	-	0.000	Vz	0.000	0.000	0.000	0.033	0.033
				Vy	0.401	0.401	0.401		
S26	B.G.1	-	0.000	Vz	0.000	0.000	0.000	0.000	0.000
				Vy	0.000	0.000	0.000		
S27	B.G.1	-	0.000	Vz	0.000	0.000	0.000	-0.033	-0.033
				Vy	-0.401	-0.401	-0.401		
S28	B.G.1	-	0.000	Vz	0.000	0.000	0.000	0.046	0.046
				Vy	1.295	1.295	1.295		
S29	B.G.1	-	0.000	Vz	0.000	0.000	0.000	0.000	0.000
				Vy	0.000	0.000	0.000		
S30	B.G.1	-	0.000	Vz	0.000	0.000	0.000	-0.046	-0.046
				Vy	-1.295	-1.295	-1.295		
S31	B.G.1	-	0.000	Vz	0.000	0.000	0.000	0.047	0.047
				Vy	2.326	2.326	2.326		
S32	B.G.1	-	0.000	Vz	0.000	0.000	0.000	0.000	0.000
				Vy	0.000	0.000	0.000		
S33	B.G.1	-	0.000	Vz	0.000	0.000	0.000	-0.047	-0.047
				Vy	-2.326	-2.326	-2.326		
S34	B.G.1	-	0.000	Vz	0.000	0.000	0.000	0.042	0.042
				Vy	3.307	3.307	3.307		
S35	B.G.1	-	0.000	Vz	0.000	0.000	0.000	0.000	0.000
				Vy	0.000	0.000	0.000		
S36	B.G.1	-	0.000	Vz	0.000	0.000	0.000	-0.042	-0.042
				Vy	-3.307	-3.307	-3.307		
S37	B.G.1	-	0.000	Vz	0.000	0.000	0.000	0.037	0.037
				Vy	4.173	4.173	4.173		
S38	B.G.1	-	0.000	Vz	0.000	0.000	0.000	0.000	0.000
				Vy	0.000	0.000	0.000		
S39	B.G.1	-	0.000	Vz	0.000	0.000	0.000	-0.037	-0.037
				Vy	-4.173	-4.173	-4.173		
S40	B.G.1	-	0.000	Vz	0.000	0.000	0.000	0.034	0.034
				Vy	4.956	4.956	4.956		
S41	B.G.1	-	0.000	Vz	0.000	0.000	0.000	0.000	0.000
				Vy	0.000	0.000	0.000		
S42	B.G.1	-	0.000	Vz	0.000	0.000	0.000	-0.034	-0.034
				Vy	-4.956	-4.956	-4.956		
-	-	-	kN	-	kN	kN	kN	kNm	kNm

C.2.2 Super Element 2 with Different Wall Dimensions

The MatrixFrame report where the outer walls are 6m wide and the inner walls are 3m wide will be included later.

C.3 Super Element Combination MatrixFrame Report

Here the MatrixFrame reports for combinations between super element 1 and 2.

C.3.1 Super Element Combination A

Here the MatrixFrame report for the combination (A) of super element 1 on top of super element 2. They are connected on the outer walls (walls a). INPUT CORRECT REPORT (SE 1 force = 12)

Super Element Combination A Validation		
Projectnaam	superelement combo A	Projectnummer	
Omschrijving		Constructeur	Babette Hohrath
Opdrachtgever		Eenheden	m, kN, kNm
Bestand	H:\Thesis\		

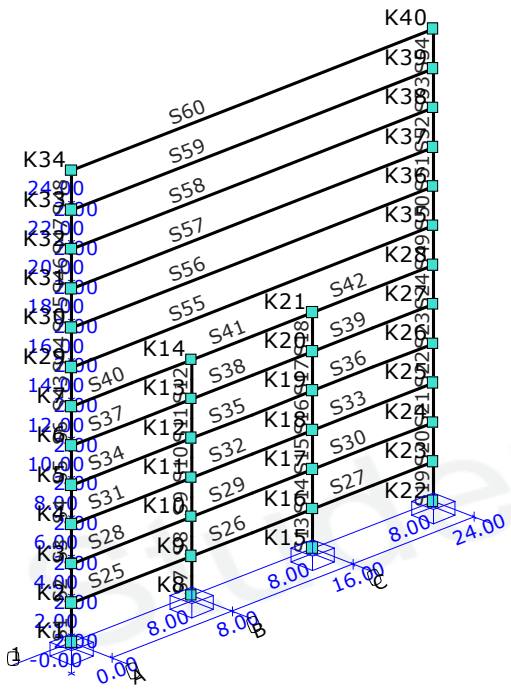

Afb. Geometrie 1: Raamwerk

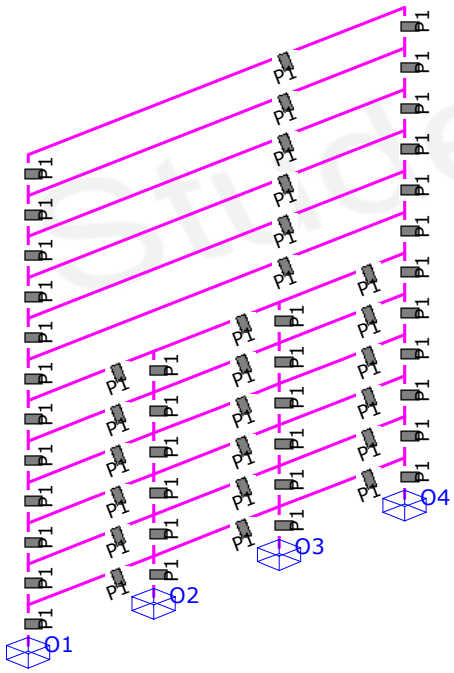

Afb. Geometrie 2: Raamwerk

Profielen

Profiel	Profielnaam	Oppervlakte	It	Iy	Iz	Materiaal	Hoek
P1	R6000x200	1.2000e+00	1.6000e-02	4.0000e-03	3.6000e+00	C30/37	0
-	-	m2	m4	m4	m4	-	°

Profielvormen

Profiel	Verlopende hoogte	hB	hE	tf	tw	tf2	B	bL	bR	Raatliggers	Mx
P1	Nee	0.200000	0.200000	0.000000	0.000000	0.000000	6.000000	0.000000	0.000000	Nee	0.000000
-	-	m	m	m	m	m	m	m	m	-	m

Materialen

Materiaalnaam	Poison	Dichtheid	E-Modulus	Uitzettingcoeff
C30/37	0.30	25.000	3.0000e+07	10.0000e-06
-	-	kN/m3	kN/m2	C°m

Opleggingen

Oplegging	Knopen	X	Y	Z	Xr	Yr	Zr	HoekXr	HoekYr	HoekZr
O1	K1	vast	vast	vast	vast	vast	vast	0	0	0
O2	K8	vast	vast	vast	vast	vast	vast	0	0	0
O3	K15	vast	vast	vast	vast	vast	vast	0	0	0
O4	K22	vast	vast	vast	vast	vast	vast	0	0	0
-	-	kN/m	kN/m	kN/m	kNmrad	kNmrad	kNmrad	°	°	°

Belastingsgevallen typen

Oplegg.	Staven	B.G.Type	Gunstig/Ong.	Element	Niveau	Veld	Psi0	Psi1	Psi2
B.G.1	Wind load	Windbelasting	-		N.v.t.	N.v.t.	0.60	0.20	0.00

B.G.1: Wind load

Type	Beginwaarde	Eindwaarde	Beginafstand	Eindafstand	Richting	Staaf of knoop
B.G.1: Wind load						
q	4,000	4,000	0,000000	2,000000(L)	Y"	S43-S54
q	3,200	3,200	0,000000	2,000000(L)	Y"	S1-S6,S19-S24
q	8,800	8,800	0,000000	2,000000(L)	Y"	S7-S18

Som lasten	X: 0,000	kN Y: 384,000	kN Z: 0,000	kN
-	-	-	m	m - -

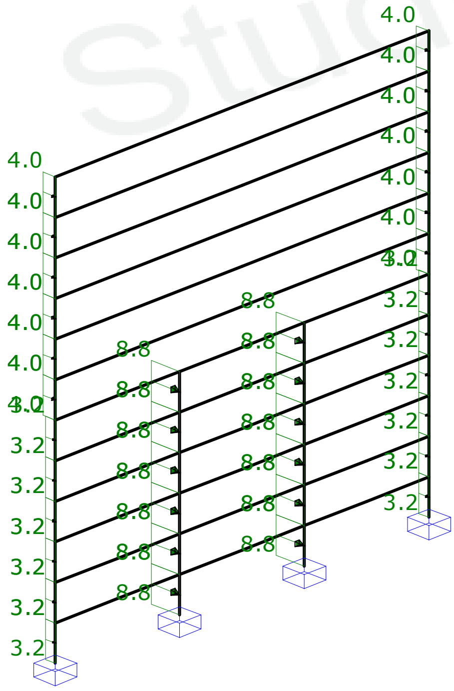

B.G.1: Wind load

Uitgangspunten van de analyse

Lineaire Elastische Analyse uitgevoerd

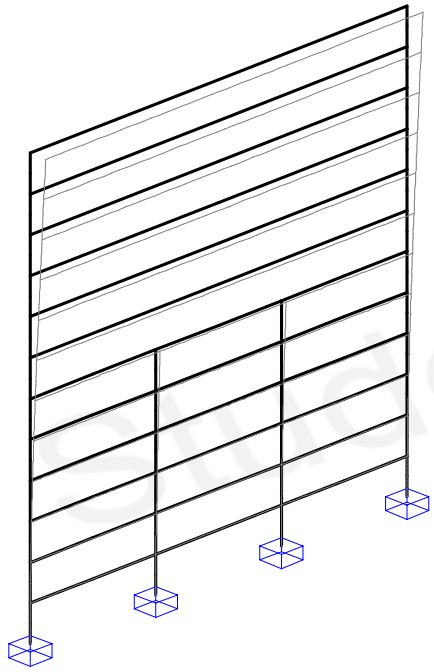

Afb. B.G.1: Wind load Verplaatsingen

L.C. Knoopverplaatsingen

Knoop	B.G.	X	Y	Z	Rx	Ry	Rz
K1	B.G.1	0.0000000	0.0000000	0.0000000	-0.000e-03	-0.000e-03	-0.000e-03
K2		0.0000000	0.0000141	0.0000000	-0.014e-03	-0.000e-03	-0.000e-03
K3		0.0000000	0.0000538	0.0000000	-0.026e-03	-0.000e-03	-0.000e-03
K4		0.0000000	0.0001151	0.0000000	-0.036e-03	-0.000e-03	0.000e-03
K5		0.0000000	0.0001950	0.0000000	-0.044e-03	-0.000e-03	0.002e-03
K6		0.0000000	0.0002907	0.0000000	-0.051e-03	-0.000e-03	0.005e-03
K7		0.0000000	0.0003995	0.0000000	-0.057e-03	-0.000e-03	0.009e-03
K8		0.0000000	0.0000000	0.0000000	-0.000e-03	-0.000e-03	-0.000e-03
K9		0.0000000	0.0000156	0.0000000	-0.015e-03	-0.000e-03	-0.000e-03
K10		0.0000000	0.0000565	0.0000000	-0.025e-03	-0.000e-03	-0.000e-03
K11		0.0000000	0.0001149	0.0000000	-0.032e-03	-0.000e-03	0.000e-03
K12		0.0000000	0.0001842	0.0000000	-0.036e-03	-0.000e-03	0.001e-03
K13		0.0000000	0.0002593	0.0000000	-0.038e-03	-0.000e-03	0.002e-03
K14		0.0000000	0.0003365	0.0000000	-0.039e-03	-0.000e-03	0.005e-03
K15		0.0000000	0.0000000	0.0000000	-0.000e-03	-0.000e-03	0.000e-03
K16		0.0000000	0.0000156	0.0000000	-0.015e-03	-0.000e-03	0.000e-03
K17		0.0000000	0.0000565	0.0000000	-0.025e-03	-0.000e-03	0.000e-03
K18		0.0000000	0.0001149	0.0000000	-0.032e-03	-0.000e-03	-0.000e-03
K19		0.0000000	0.0001842	0.0000000	-0.036e-03	-0.000e-03	-0.001e-03
K20		0.0000000	0.0002593	0.0000000	-0.038e-03	-0.000e-03	-0.002e-03
K21		0.0000000	0.0003365	0.0000000	-0.039e-03	-0.000e-03	-0.005e-03
K22		0.0000000	0.0000000	0.0000000	-0.000e-03	-0.000e-03	0.000e-03
K23		0.0000000	0.0000141	0.0000000	-0.014e-03	-0.000e-03	0.000e-03
K24		0.0000000	0.0000538	0.0000000	-0.026e-03	-0.000e-03	0.000e-03
K25		0.0000000	0.0001151	0.0000000	-0.036e-03	-0.000e-03	-0.000e-03
K26		0.0000000	0.0001950	0.0000000	-0.044e-03	-0.000e-03	-0.002e-03
K27		0.0000000	0.0002907	0.0000000	-0.051e-03	-0.000e-03	-0.005e-03
K28		0.0000000	0.0003995	0.0000000	-0.057e-03	-0.000e-03	-0.009e-03

Knoop	B.G.	X	Y	Z	Rx	Ry	Rz
K29	B.G.1	0.0000000	0.0005188	0.0000000	-0.062e-03	-0.000e-03	0.000e-03
K30		0.0000000	0.0006455	0.0000000	-0.065e-03	-0.000e-03	0.000e-03
K31		0.0000000	0.0007771	0.0000000	-0.067e-03	-0.000e-03	0.000e-03
K32		0.0000000	0.0009114	0.0000000	-0.068e-03	-0.000e-03	0.000e-03
K33		0.0000000	0.0010469	0.0000000	-0.068e-03	-0.000e-03	0.000e-03
K34		0.0000000	0.0011827	0.0000000	-0.068e-03	-0.000e-03	-0.000e-03
K35		0.0000000	0.0005188	0.0000000	-0.062e-03	-0.000e-03	-0.000e-03
K36		0.0000000	0.0006455	0.0000000	-0.065e-03	-0.000e-03	-0.000e-03
K37		0.0000000	0.0007771	0.0000000	-0.067e-03	-0.000e-03	-0.000e-03
K38		0.0000000	0.0009114	0.0000000	-0.068e-03	-0.000e-03	-0.000e-03
K39		0.0000000	0.0010469	0.0000000	-0.068e-03	-0.000e-03	-0.000e-03
K40		0.0000000	0.0011827	0.0000000	-0.068e-03	-0.000e-03	-0.000e-03
-	**-**	**m**	**m**	**m**	**rad**	**rad**	**rad**

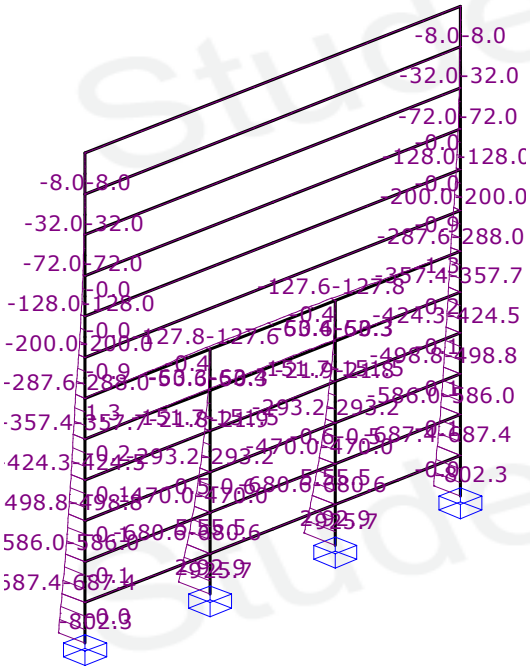

Afb. B.G.1: Wind load Momenten (Mz)

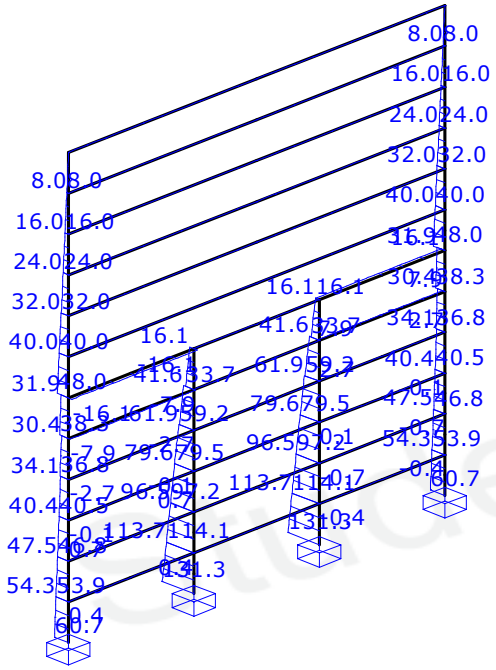

Afb. B.G.1: Wind load Dwarskracht (Vy)

L.C. Staafkrachten (My, Mz)

Staaf	B.G.	Waarde	Mb	Mmax	xMmax	Me	x-M0	x-M0
S1	B.G.1	My	0.000			0.000	0.000000	0.000000
		Mz	-802.313			-687.389	0.000000	0.000000
S2	B.G.1	My	0.000			0.000	0.000000	0.000000
		Mz	-687.365			-585.974	0.000000	0.000000
S3	B.G.1	My	0.000			0.000	0.000000	0.000000
		Mz	-585.977			-498.777	0.000000	0.000000
S4	B.G.1	My	0.000			0.000	0.000000	0.000000
		Mz	-498.849			-424.345	0.000000	0.000000
S5	B.G.1	My	0.000			0.000	0.000000	0.000000
		Mz	-424.521			-357.394	0.000000	0.000000
S6	B.G.1	My	0.000			0.000	0.000000	0.000000
		Mz	-357.695			-287.572	0.000000	0.000000
S7	B.G.1	My	0.000			0.000	0.000000	0.000000
		Mz	-925.687			-680.611	0.000000	0.000000
S8	B.G.1	My	0.000			0.000	0.000000	0.000000
		Mz	-680.635			-470.026	0.000000	0.000000
S9	B.G.1	My	0.000			0.000	0.000000	0.000000
		Mz	-470.023			-293.223	0.000000	0.000000
S10	B.G.1	My	0.000			0.000	0.000000	0.000000
		Mz	-293.151			-151.655	0.000000	0.000000
S11	B.G.1	My	0.000			0.000	0.000000	0.000000
		Mz	-151.479			-50.606	0.000000	0.000000
S12	B.G.1	My	0.000			0.000	0.000000	0.000000
		Mz	-50.305			-0.428	0.000000	0.000000
S13	B.G.1	My	0.000			0.000	0.000000	0.000000
		Mz	-925.687			-680.611	0.000000	0.000000
S14	B.G.1	My	0.000			0.000	0.000000	0.000000
		Mz	-680.635			-470.026	0.000000	0.000000
S15	B.G.1	My	0.000			0.000	0.000000	0.000000
		Mz	-470.023			-293.223	0.000000	0.000000
S16	B.G.1	My	0.000			0.000	0.000000	0.000000
		Mz	-293.151			-151.655	0.000000	0.000000
S17	B.G.1	My	0.000			0.000	0.000000	0.000000

Staaf	B.G.	Waarde	Mb	Mmax	xMmax	Me	x-M0	x-M0
		Mz	-151.479			-50.606	0.000000	0.000000
S18	B.G.1	My	0.000			0.000	0.000000	0.000000
		Mz	-50.305			-0.428	0.000000	0.000000
S19	B.G.1	My	0.000			0.000	0.000000	0.000000
		Mz	-802.313			-687.389	0.000000	0.000000
S20	B.G.1	My	0.000			0.000	0.000000	0.000000
		Mz	-687.365			-585.974	0.000000	0.000000
S21	B.G.1	My	0.000			0.000	0.000000	0.000000
		Mz	-585.977			-498.777	0.000000	0.000000
S22	B.G.1	My	0.000			0.000	0.000000	0.000000
		Mz	-498.849			-424.345	0.000000	0.000000
S23	B.G.1	My	0.000			0.000	0.000000	0.000000
		Mz	-424.521			-357.394	0.000000	0.000000
S24	B.G.1	My	0.000			0.000	0.000000	0.000000
		Mz	-357.695			-287.572	0.000000	0.000000
S25	B.G.1	My	0.000			0.000	0.000000	0.000000
		Mz	-0.003			2.931	0.007424	0.000000
S26	B.G.1	My	0.000			0.000	0.000000	0.000000
		Mz	2.930			2.930	0.000000	0.000000
S27	B.G.1	My	0.000			0.000	0.000000	0.000000
		Mz	2.931			-0.003	7.992576	0.000000
S28	B.G.1	My	0.000			0.000	0.000000	0.000000
		Mz	-0.059			5.504	0.084457	0.000000
S29	B.G.1	My	0.000			0.000	0.000000	0.000000
		Mz	5.474			5.474	0.000000	0.000000
S30	B.G.1	My	0.000			0.000	0.000000	0.000000
		Mz	5.504			-0.059	7.915542	0.000000
S31	B.G.1	My	0.000			0.000	0.000000	0.000000
		Mz	-0.104			-0.520	0.000000	0.000000
S32	B.G.1	My	0.000			0.000	0.000000	0.000000
		Mz	-0.572			-0.572	0.000000	0.000000
S33	B.G.1	My	0.000			0.000	0.000000	0.000000
		Mz	-0.520			-0.104	0.000000	0.000000
S34	B.G.1	My	0.000			0.000	0.000000	0.000000
		Mz	-0.138			-21.828	0.000000	0.000000
S35	B.G.1	My	0.000			0.000	0.000000	0.000000
		Mz	-21.897			-21.897	0.000000	0.000000
S36	B.G.1	My	0.000			0.000	0.000000	0.000000
		Mz	-21.828			-0.138	0.000000	0.000000
S37	B.G.1	My	0.000			0.000	0.000000	0.000000
		Mz	-0.151			-63.336	0.000000	0.000000
S38	B.G.1	My	0.000			0.000	0.000000	0.000000
		Mz	-63.413			-63.413	0.000000	0.000000
S39	B.G.1	My	0.000			0.000	0.000000	0.000000
		Mz	-63.336			-0.151	0.000000	0.000000
S40	B.G.1	My	0.000			0.000	0.000000	0.000000
		Mz	1.295			-127.815	0.080239	0.000000
S41	B.G.1	My	0.000			0.000	0.000000	0.000000
		Mz	-127.595			-127.595	0.000000	0.000000
S42	B.G.1	My	0.000			0.000	0.000000	0.000000
		Mz	-127.815			1.295	7.919761	0.000000
S43	B.G.1	My	0.000			0.000	0.000000	0.000000
		Mz	-288.000			-200.000	0.000000	0.000000
S44	B.G.1	My	0.000			0.000	0.000000	0.000000
		Mz	-200.000			-128.000	0.000000	0.000000
S45	B.G.1	My	0.000			0.000	0.000000	0.000000
		Mz	-128.000			-72.000	0.000000	0.000000
S46	B.G.1	My	0.000			0.000	0.000000	0.000000
		Mz	-72.000			-32.000	0.000000	0.000000
S47	B.G.1	My	0.000			0.000	0.000000	0.000000
		Mz	-32.000			-8.000	0.000000	0.000000
S48	B.G.1	My	0.000			0.000	0.000000	0.000000
		Mz	-8.000			0.000	0.000000	0.000000
S49	B.G.1	My	0.000			0.000	0.000000	0.000000

Staaf	B.G.	Waarde	Mb	Mmax	xMmax	Me	x-M0	x-M0
		Mz	-288.000			-200.000	0.000000	0.000000
S50	B.G.1	My	0.000			0.000	0.000000	0.000000
		Mz	-200.000			-128.000	0.000000	0.000000
S51	B.G.1	My	0.000			0.000	0.000000	0.000000
		Mz	-128.000			-72.000	0.000000	0.000000
S52	B.G.1	My	0.000			0.000	0.000000	0.000000
		Mz	-72.000			-32.000	0.000000	0.000000
S53	B.G.1	My	0.000			0.000	0.000000	0.000000
		Mz	-32.000			-8.000	0.000000	0.000000
S54	B.G.1	My	0.000			0.000	0.000000	0.000000
		Mz	-8.000			0.000	0.000000	0.000000
S55	B.G.1	My	0.000			0.000	0.000000	0.000000
		Mz	-0.851			-0.851	0.000000	0.000000
S56	B.G.1	My	0.000			0.000	0.000000	0.000000
		Mz	-0.009			-0.009	0.000000	0.000000
S57	B.G.1	My	0.000			0.000	0.000000	0.000000
		Mz	0.000			0.000	0.000000	0.000000
S58	B.G.1	My	0.000			0.000	0.000000	0.000000
		Mz	0.000			0.000	0.000000	0.000000
S59	B.G.1	My	0.000			0.000	0.000000	0.000000
		Mz	0.000			0.000	0.000000	0.000000
S60	B.G.1	My	0.000			0.000	0.000000	0.000000
		Mz	0.000			0.000	0.000000	0.000000
-	-	-	kNm	kNm	m	kNm	m	m

L.C. Staafkrachten (Nx, Vy, Vz, Mx)

Staaf	B.G.	T/D	Nmax	Waarde	Vb	Vmax	Ve	Mxb	Mxe
S1	B.G.1	-	0.000	Vz	0.000	0.000	0.000	-0.020	-0.020
				Vy	60.662	60.662	54.262		
S2	B.G.1	-	0.000	Vz	0.000	0.000	0.000	-0.017	-0.017
				Vy	53.895	53.895	47.495		
S3	B.G.1	-	0.000	Vz	0.000	0.000	0.000	0.041	0.041
				Vy	46.800	46.800	40.400		
S4	B.G.1	-	0.000	Vz	0.000	0.000	0.000	0.146	0.146
				Vy	40.452	40.452	34.052		
S5	B.G.1	-	0.000	Vz	0.000	0.000	0.000	0.284	0.284
				Vy	36.763	36.763	30.363		
S6	B.G.1	-	0.000	Vz	0.000	0.000	0.000	0.435	0.435
				Vy	38.261	38.261	31.861		
S7	B.G.1	-	0.000	Vz	0.000	0.000	0.000	-0.010	-0.010
				Vy	131.338	131.338	113.738		
S8	B.G.1	-	0.000	Vz	0.000	0.000	0.000	-0.009	-0.009
				Vy	114.105	114.105	96.505		
S9	B.G.1	-	0.000	Vz	0.000	0.000	0.000	0.021	0.021
				Vy	97.200	97.200	79.600		
S10	B.G.1	-	0.000	Vz	0.000	0.000	0.000	0.073	0.073
				Vy	79.548	79.548	61.948		
S11	B.G.1	-	0.000	Vz	0.000	0.000	0.000	0.142	0.142
				Vy	59.237	59.237	41.637		
S12	B.G.1	-	0.000	Vz	0.000	0.000	0.000	0.219	0.219
				Vy	33.739	33.739	16.139		
S13	B.G.1	-	0.000	Vz	0.000	0.000	0.000	0.010	0.010
				Vy	131.338	131.338	113.738		
S14	B.G.1	-	0.000	Vz	0.000	0.000	0.000	0.009	0.009
				Vy	114.105	114.105	96.505		
S15	B.G.1	-	0.000	Vz	0.000	0.000	0.000	-0.021	-0.021
				Vy	97.200	97.200	79.600		
S16	B.G.1	-	0.000	Vz	0.000	0.000	0.000	-0.073	-0.073
				Vy	79.548	79.548	61.948		
S17	B.G.1	-	0.000	Vz	0.000	0.000	0.000	-0.142	-0.142
				Vy	59.237	59.237	41.637		
S18	B.G.1	-	0.000	Vz	0.000	0.000	0.000	-0.219	-0.219
				Vy	33.739	33.739	16.139		
S19	B.G.1	-	0.000	Vz	0.000	0.000	0.000	0.020	0.020
				Vy	60.662	60.662	54.262		

Staaf	B.G.	T/D	Nmax	Waarde	Vb	Vmax	Ve	Mxb	Mxe
S20	B.G.1	-	0.000	Vz	0.000	0.000	0.000	0.017	0.017
				Vy	53.895	53.895	47.495		
S21	B.G.1	-	0.000	Vz	0.000	0.000	0.000	-0.041	-0.041
				Vy	46.800	46.800	40.400		
S22	B.G.1	-	0.000	Vz	0.000	0.000	0.000	-0.146	-0.146
				Vy	40.452	40.452	34.052		
S23	B.G.1	-	0.000	Vz	0.000	0.000	0.000	-0.284	-0.284
				Vy	36.763	36.763	30.363		
S24	B.G.1	-	0.000	Vz	0.000	0.000	0.000	-0.435	-0.435
				Vy	38.261	38.261	31.861		
S25	B.G.1	-	0.000	Vz	0.000	0.000	0.000	0.024	0.024
				Vy	0.367	0.367	0.367		
S26	B.G.1	-	0.000	Vz	0.000	0.000	0.000	0.000	0.000
				Vy	0.000	0.000	0.000		
S27	B.G.1	-	0.000	Vz	0.000	0.000	0.000	-0.024	-0.024
				Vy	-0.367	-0.367	-0.367		
S28	B.G.1	-	0.000	Vz	0.000	0.000	0.000	-0.003	-0.003
				Vy	0.695	0.695	0.695		
S29	B.G.1	-	0.000	Vz	0.000	0.000	0.000	0.000	0.000
				Vy	0.000	0.000	0.000		
S30	B.G.1	-	0.000	Vz	0.000	0.000	0.000	0.003	0.003
				Vy	-0.695	-0.695	-0.695		
S31	B.G.1	-	0.000	Vz	0.000	0.000	0.000	-0.072	-0.072
				Vy	-0.052	-0.052	-0.052		
S32	B.G.1	-	0.000	Vz	0.000	0.000	0.000	0.000	0.000
				Vy	0.000	0.000	0.000		
S33	B.G.1	-	0.000	Vz	0.000	0.000	0.000	0.072	0.072
				Vy	0.052	0.052	0.052		
S34	B.G.1	-	0.000	Vz	0.000	0.000	0.000	-0.175	-0.175
				Vy	-2.711	-2.711	-2.711		
S35	B.G.1	-	0.000	Vz	0.000	0.000	0.000	0.000	0.000
				Vy	0.000	0.000	0.000		
S36	B.G.1	-	0.000	Vz	0.000	0.000	0.000	0.175	0.175
				Vy	2.711	2.711	2.711		
S37	B.G.1	-	0.000	Vz	0.000	0.000	0.000	-0.300	-0.300
				Vy	-7.898	-7.898	-7.898		
S38	B.G.1	-	0.000	Vz	0.000	0.000	0.000	0.000	0.000
				Vy	0.000	0.000	0.000		
S39	B.G.1	-	0.000	Vz	0.000	0.000	0.000	0.300	0.300
				Vy	7.898	7.898	7.898		
S40	B.G.1	-	0.000	Vz	0.000	0.000	0.000	-0.428	-0.428
				Vy	-16.139	-16.139	-16.139		
S41	B.G.1	-	0.000	Vz	0.000	0.000	0.000	0.000	0.000
				Vy	0.000	0.000	0.000		
S42	B.G.1	-	0.000	Vz	0.000	0.000	0.000	0.428	0.428
				Vy	16.139	16.139	16.139		
S43	B.G.1	-	0.000	Vz	0.000	0.000	0.000	-0.860	-0.860
				Vy	48.000	48.000	40.000		
S44	B.G.1	-	0.000	Vz	0.000	0.000	0.000	-0.009	-0.009
				Vy	40.000	40.000	32.000		
S45	B.G.1	-	0.000	Vz	0.000	0.000	0.000	0.000	0.000
				Vy	32.000	32.000	24.000		
S46	B.G.1	-	0.000	Vz	0.000	0.000	0.000	0.000	0.000
				Vy	24.000	24.000	16.000		
S47	B.G.1	-	0.000	Vz	0.000	0.000	0.000	0.000	0.000
				Vy	16.000	16.000	8.000		
S48	B.G.1	-	0.000	Vz	0.000	0.000	0.000	0.000	0.000
				Vy	8.000	8.000	0.000		
S49	B.G.1	-	0.000	Vz	0.000	0.000	0.000	0.860	0.860
				Vy	48.000	48.000	40.000		
S50	B.G.1	-	0.000	Vz	0.000	0.000	0.000	0.009	0.009
				Vy	40.000	40.000	32.000		
S51	B.G.1	-	0.000	Vz	0.000	0.000	0.000	0.000	0.000
				Vy	32.000	32.000	24.000		
S52	B.G.1	-	0.000	Vz	0.000	0.000	0.000	0.000	0.000
				Vy	24.000	24.000	16.000		
S53	B.G.1	-	0.000	Vz	0.000	0.000	0.000	0.000	0.000

Staaf	B.G.	T/D	Nmax	Waarde	Vb	Vmax	Ve	Mxb	Mxe
				Vy	16.000	16.000	8.000		
S54	B.G.1	-	0.000	Vz	0.000	0.000	0.000	0.000	0.000
				Vy	8.000	8.000	0.000		
S55	B.G.1	-	0.000	Vz	0.000	0.000	0.000	0.000	0.000
				Vy	0.000	0.000	0.000		
S56	B.G.1	-	0.000	Vz	0.000	0.000	0.000	0.000	0.000
				Vy	0.000	0.000	0.000		
S57	B.G.1	-	0.000	Vz	0.000	0.000	0.000	0.000	0.000
				Vy	0.000	0.000	0.000		
S58	B.G.1	-	0.000	Vz	0.000	0.000	0.000	0.000	0.000
				Vy	0.000	0.000	0.000		
S59	B.G.1	-	0.000	Vz	0.000	0.000	0.000	0.000	0.000
				Vy	0.000	0.000	0.000		
S60	B.G.1	-	0.000	Vz	0.000	0.000	0.000	0.000	0.000
				Vy	0.000	0.000	0.000		
-	-	-	kN	-	kN	kN	kN	kNm	kNm

C.3.2 Super Element Combination B

Here the MatrixFrame report for the combination (B) of super element 1 on top of super element 2. They are connected on the inner walls (walls b).

Project name	core wall validation	Project number	
Part description		Structural engineer	
Client		Units	m, kN, kNm
File	D:\My Documents\Documents\Babette\Matrix Frame Models\validation_combB.mxe		

PIC. GEOMETRIE RAAMWERK

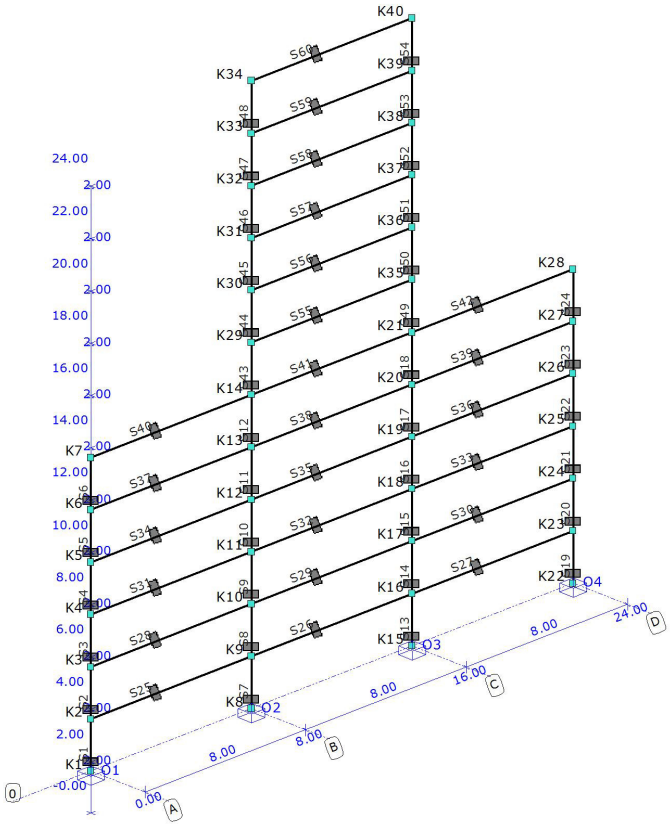

PIC. GEOMETRIE 1 STAVEN EN KNOPEN

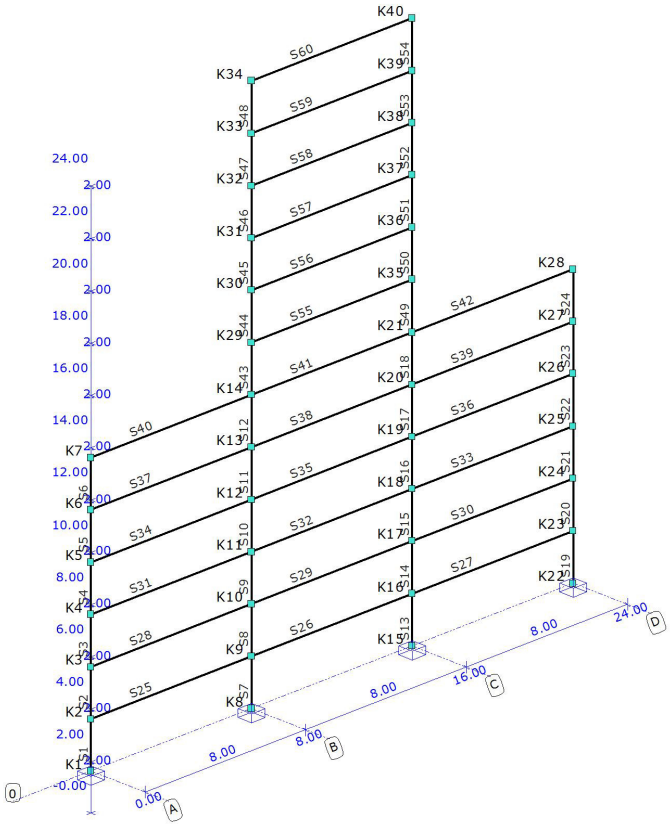

PIC. GEOMETRIE 2 STAVEN EN KNOPEN

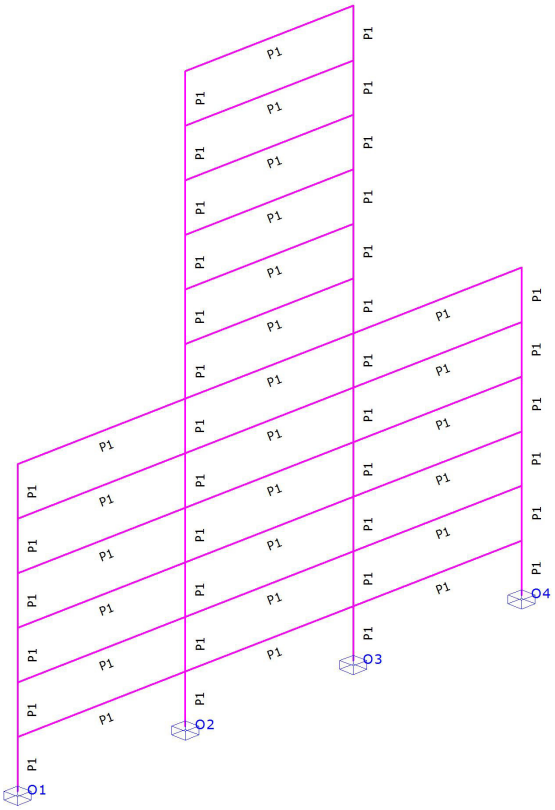

SECTIONS

Section	Section Name	Area	It	Iy	Iz	Material	Angle
P1	R6000x200	1.2000e+00	1.6000e-02	4.0000e-03	3.6000e+00	C30/37	0.0
-	-	m2	m4	m4	m4	-	°

SECTION SHAPES

Section	Tapered	hB	hE	tf	tw	tf2	B	b1	b2	Castellate	Height
P1	No	0.20000000	0.20000000	0.00000000	0.00000000	0.00000000	6.00000048	0.00000000	0.00000000	No	0.00000000
-	-	m	m	m	m	m	m	m	m	-	m

MATERIALS

Material Name	Poison	Density	Youngs mod.	Lin. Exp.
C30/37	0.30	25.000	3.0000e+07	10.0000e-06
-	-	kN/m3	kN/m2	C°m

SUPPORTS

Support	Nodes	X	Y	Z	Xr	Yr	Zr	AngleXr	AngleYr	AngleZr
O1	K1	fixed	fixed	fixed	fixed	fixed	fixed	0	0	0
O2	K8	fixed	fixed	fixed	fixed	fixed	fixed	0	0	0
O3	K15	fixed	fixed	fixed	fixed	fixed	fixed	0	0	0
O4	K22	fixed	fixed	fixed	fixed	fixed	fixed	0	0	0
-	-	kN/m	kN/m	kN/m	kNm/rad	kNm/rad	kNm/rad	°	°	°

PIC. LASTEN B.G.1 PERMANENT ACTIONS

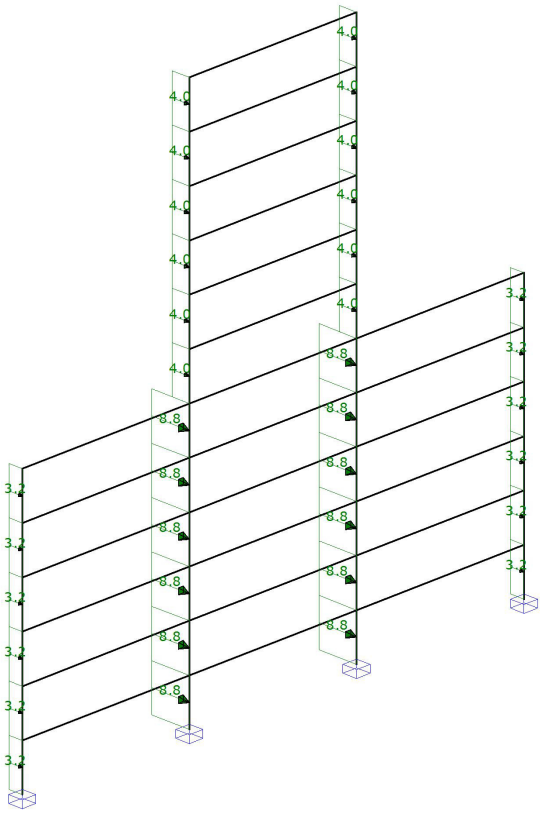

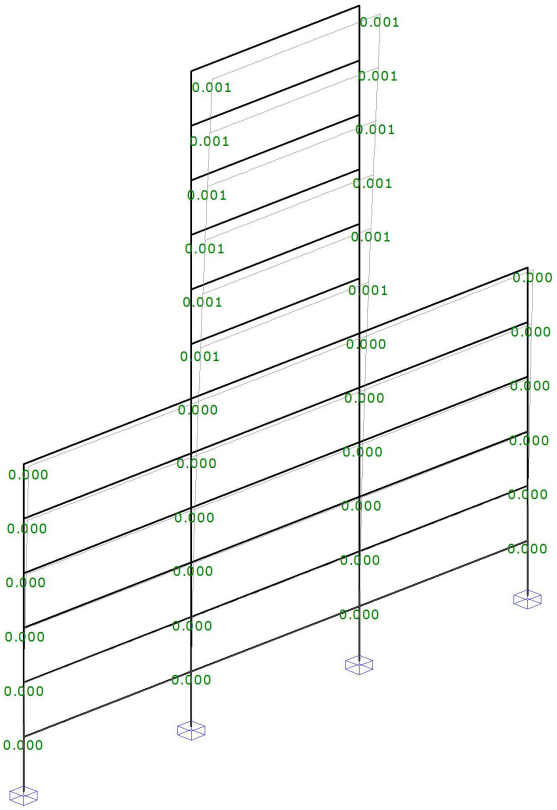

L.C. NODAL DISPLACEMENTS

Node	L.C.	X	Y	Z	Xr	Yr	Zr
K1	B.G.1	0.000000000	0.000000000	0.000000000	-0.000e-03	-0.000e-03	-0.000e-03
K2	B.G.1	0.000000000	0.000013971	0.000000000	-0.013e-03	-0.000e-03	-0.000e-03
K3	B.G.1	0.000000000	0.000051333	0.000000000	-0.023e-03	-0.000e-03	-0.001e-03
K4	B.G.1	0.000000000	0.000105655	0.000000000	-0.030e-03	-0.000e-03	-0.003e-03
K5	B.G.1	0.000000000	0.000171135	0.000000000	-0.035e-03	-0.000e-03	-0.006e-03
K6	B.G.1	0.000000000	0.000242813	0.000000000	-0.037e-03	-0.000e-03	-0.010e-03
K7	B.G.1	0.000000000	0.000316920	0.000000000	-0.037e-03	-0.000e-03	-0.015e-03
K8	B.G.1	0.000000000	0.000000000	0.000000000	-0.000e-03	-0.000e-03	-0.000e-03
K9	B.G.1	0.000000000	0.000015732	0.000000000	-0.015e-03	-0.000e-03	-0.000e-03
K10	B.G.1	0.000000000	0.000058889	0.000000000	-0.028e-03	-0.000e-03	-0.001e-03
K11	B.G.1	0.000000000	0.000124345	0.000000000	-0.038e-03	-0.000e-03	-0.001e-03
K12	B.G.1	0.000000000	0.000208125	0.000000000	-0.046e-03	-0.000e-03	-0.003e-03
K13	B.G.1	0.000000000	0.000307187	0.000000000	-0.053e-03	-0.000e-03	-0.005e-03
K14	B.G.1	0.000000000	0.000419080	0.000000000	-0.059e-03	-0.000e-03	-0.008e-03
K15	B.G.1	0.000000000	0.000000000	0.000000000	-0.000e-03	-0.000e-03	0.000e-03
K16	B.G.1	0.000000000	0.000015732	0.000000000	-0.015e-03	-0.000e-03	0.000e-03
K17	B.G.1	0.000000000	0.000058889	0.000000000	-0.028e-03	-0.000e-03	0.001e-03
K18	B.G.1	0.000000000	0.000124345	0.000000000	-0.038e-03	-0.000e-03	0.001e-03
K19	B.G.1	0.000000000	0.000208125	0.000000000	-0.046e-03	-0.000e-03	0.003e-03
K20	B.G.1	0.000000000	0.000307187	0.000000000	-0.053e-03	-0.000e-03	0.005e-03
K21	B.G.1	0.000000000	0.000419080	0.000000000	-0.059e-03	-0.000e-03	0.008e-03

Node	L.C.	X	Y	Z	Xr	Yr	Zr
K22	B.G.1	0.000000000	0.000000000	0.000000000	-0.000e-03	-0.000e-03	0.000e-03
K23	B.G.1	0.000000000	0.000013971	0.000000000	-0.013e-03	-0.000e-03	0.000e-03
K24	B.G.1	0.000000000	0.000051333	0.000000000	-0.023e-03	-0.000e-03	0.001e-03
K25	B.G.1	0.000000000	0.000105655	0.000000000	-0.030e-03	-0.000e-03	0.003e-03
K26	B.G.1	0.000000000	0.000171135	0.000000000	-0.035e-03	-0.000e-03	0.006e-03
K27	B.G.1	0.000000000	0.000242813	0.000000000	-0.037e-03	-0.000e-03	0.010e-03
K28	B.G.1	0.000000000	0.000316920	0.000000000	-0.037e-03	-0.000e-03	0.015e-03
K29	B.G.1	0.000000000	0.000541388	0.000000000	-0.063e-03	-0.000e-03	-0.000e-03
K30	B.G.1	0.000000000	0.000671152	0.000000000	-0.066e-03	-0.000e-03	-0.000e-03
K31	B.G.1	0.000000000	0.000805707	0.000000000	-0.068e-03	-0.000e-03	-0.000e-03
K32	B.G.1	0.000000000	0.000942978	0.000000000	-0.069e-03	-0.000e-03	-0.000e-03
K33	B.G.1	0.000000000	0.001081483	0.000000000	-0.069e-03	-0.000e-03	0.000e-03
K34	B.G.1	0.000000000	0.001220334	0.000000000	-0.069e-03	-0.000e-03	0.000e-03
K35	B.G.1	0.000000000	0.000541388	0.000000000	-0.063e-03	-0.000e-03	0.000e-03
K36	B.G.1	0.000000000	0.000671152	0.000000000	-0.066e-03	-0.000e-03	0.000e-03
K37	B.G.1	0.000000000	0.000805707	0.000000000	-0.068e-03	-0.000e-03	0.000e-03
K38	B.G.1	0.000000000	0.000942978	0.000000000	-0.069e-03	-0.000e-03	0.000e-03
K39	B.G.1	0.000000000	0.001081483	0.000000000	-0.069e-03	-0.000e-03	0.000e-03
K40	B.G.1	0.000000000	0.001220334	0.000000000	-0.069e-03	0.000e-03	0.000e-03
-	-	m	m	m	rad	rad	rad

PIC. B.G.1: PERMANENT ACTIONS DWARSKRACHT (VY)

Load Cases

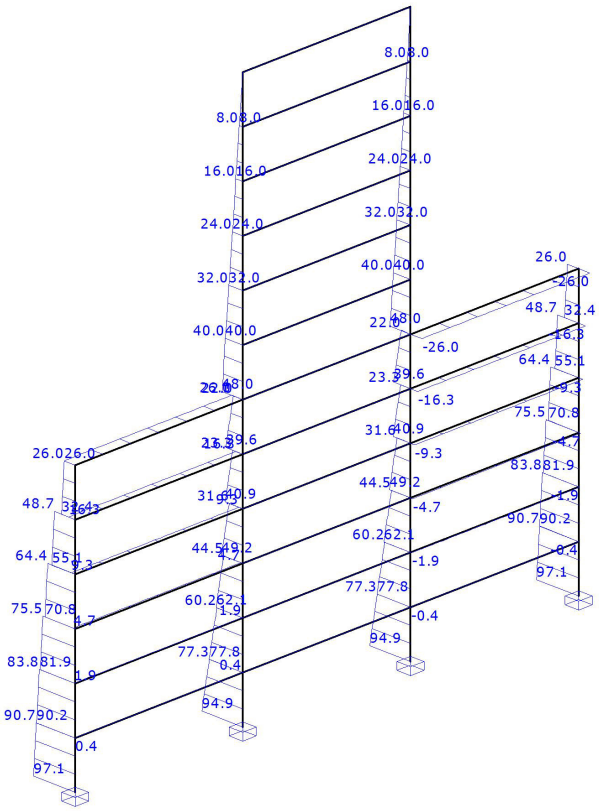

PIC. B.G.1: PERMANENT ACTIONS MOMENT (MZ) Load Cases

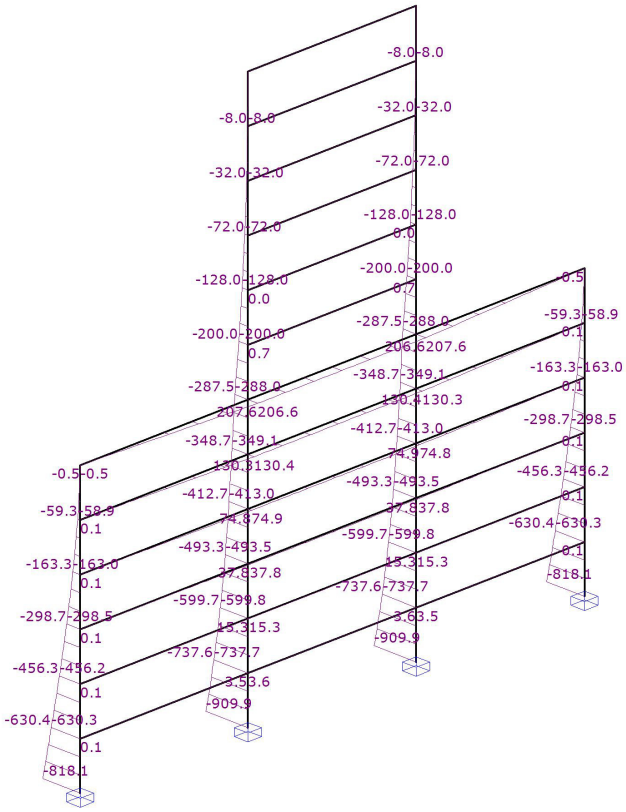

L.C. EXTREME MEMBER FORCES

Member	L.C.	Value	Mb	Mmax	xMmax	Me	x-M0	x-M0	TC	Nmax	Value	Vb	Vmax	Ve	Mxb	Mxe
S1	B.G.1	My	0.000	0.000	.00000000	0.000	00000000	00000000	-	0.000	Vz	0.000	0.000	0.000	**-0.024**	**-0.024**
		Mz	**-818.088**	0.000	.00000000	**-630.360**	00000000	00000000			Vy	**97.064**	**97.064**	**90.664**		
S2	B.G.1	My	0.000	0.000	.00000000	0.000	00000000	00000000	-	0.000	Vz	0.000	0.000	0.000	**-0.080**	**-0.080**
		Mz	**-630.319**	0.000	.00000000	**-456.262**	00000000	00000000			Vy	**90.228**	**90.228**	**83.828**		
S3	B.G.1	My	0.000	0.000	.00000000	0.000	00000000	00000000	-	0.000	Vz	0.000	0.000	0.000	**-0.154**	**-0.154**
		Mz	**-456.167**	0.000	.00000000	**-298.708**	00000000	00000000			Vy	**81.930**	**81.930**	**75.530**		
S4	B.G.1	My	0.000	0.000	.00000000	0.000	00000000	00000000	-	0.000	Vz	0.000	0.000	0.000	**-0.253**	**-0.253**
		Mz	**-298.542**	0.000	.00000000	**-163.307**	00000000	00000000			Vy	**70.817**	**70.817**	**64.417**		
S5	B.G.1	My	0.000	0.000	.00000000	0.000	00000000	00000000	-	0.000	Vz	0.000	0.000	0.000	**-0.379**	**-0.379**
		Mz	**-163.047**	0.000	.00000000	**-59.291**	00000000	00000000			Vy	**55.078**	**55.078**	**48.678**		
S6	B.G.1	My	0.000	0.000	.00000000	0.000	00000000	00000000	-	0.000	Vz	0.000	0.000	0.000	**-0.523**	**-0.523**
		Mz	**-58.917**	0.000	.00000000	**-0.497**	00000000	00000000			Vy	**32.410**	**32.410**	**26.010**		
S7	B.G.1	My	0.000	0.000	.00000000	0.000	00000000	00000000	-	0.000	Vz	0.000	0.000	0.000	**-0.012**	**-0.012**
		Mz	**-909.912**	0.000	.00000000	**-737.640**	00000000	00000000			Vy	**94.936**	**94.936**	**77.336**		
S8	B.G.1	My	0.000	0.000	.00000000	0.000	00000000	00000000	-	0.000	Vz	0.000	0.000	0.000	**-0.040**	**-0.040**
		Mz	**-737.681**	0.000	.00000000	**-599.738**	00000000	00000000			Vy	**77.772**	**77.772**	**60.172**		
S9	B.G.1	My	0.000	0.000	.00000000	0.000	00000000	00000000	-	0.000	Vz	0.000	0.000	0.000	**-0.077**	**-0.077**
		Mz	**-599.833**	0.000	.00000000	**-493.292**	00000000	00000000			Vy	**62.070**	**62.070**	**44.470**		
S10	B.G.1	My	0.000	0.000	.00000000	0.000	00000000	00000000	-	0.000	Vz	0.000	0.000	0.000	**-0.127**	**-0.127**
		Mz	**-493.458**	0.000	.00000000	**-412.693**	00000000	00000000			Vy	**49.183**	**49.183**	**31.583**		
S11	B.G.1	My	0.000	0.000	.00000000	0.000	00000000	00000000	-	0.000	Vz	0.000	0.000	0.000	**-0.190**	**-0.190**

Member	L.C.	Value	Mb	Mmax	xMmax	Me	x-M0	x-M0	TC	Nmax	Value	Vb	Vmax	Ve	Mxb	Mxe
		Mz	**-412.953**	0.000	.00000000	**-348.708**	00000000	00000000			Vy	**40.922**	**40.922**	**23.322**		
S12	B.G.1	My	0.000	0.000	.00000000	0.000	00000000	00000000	-	0.000	Vz	0.000	0.000	0.000	**-0.261**	**-0.261**
		Mz	**-349.083**	0.000	.00000000	**-287.503**	00000000	00000000			Vy	**39.590**	**39.590**	**21.990**		
S13	B.G.1	My	0.000	0.000	.00000000	0.000	00000000	00000000	-	0.000	Vz	0.000	0.000	0.000	**0.012**	**0.012**
		Mz	**-909.912**	0.000	.00000000	**-737.640**	00000000	00000000			Vy	**94.936**	**94.936**	**77.336**		
S14	B.G.1	My	0.000	0.000	.00000000	0.000	00000000	00000000	-	0.000	Vz	0.000	0.000	0.000	**0.040**	**0.040**
		Mz	**-737.681**	0.000	.00000000	**-599.738**	00000000	00000000			Vy	**77.772**	**77.772**	**60.172**		
S15	B.G.1	My	0.000	0.000	.00000000	0.000	00000000	00000000	-	0.000	Vz	0.000	0.000	0.000	**0.077**	**0.077**
		Mz	**-599.833**	0.000	.00000000	**-493.292**	00000000	00000000			Vy	**62.070**	**62.070**	**44.470**		
S16	B.G.1	My	0.000	0.000	.00000000	0.000	00000000	00000000	-	0.000	Vz	0.000	0.000	0.000	**0.127**	**0.127**
		Mz	**-493.458**	0.000	.00000000	**-412.693**	00000000	00000000			Vy	**49.183**	**49.183**	**31.583**		
S17	B.G.1	My	0.000	0.000	.00000000	0.000	00000000	00000000	-	0.000	Vz	0.000	0.000	0.000	**0.190**	**0.190**
		Mz	**-412.953**	0.000	.00000000	**-348.708**	00000000	00000000			Vy	**40.922**	**40.922**	**23.322**		
S18	B.G.1	My	0.000	0.000	.00000000	0.000	00000000	00000000	-	0.000	Vz	0.000	0.000	0.000	**0.261**	**0.261**
		Mz	**-349.083**	0.000	.00000000	**-287.503**	00000000	00000000			Vy	**39.590**	**39.590**	**21.990**		
S19	B.G.1	My	0.000	0.000	.00000000	0.000	00000000	00000000	-	0.000	Vz	0.000	0.000	0.000	**0.024**	**0.024**
		Mz	**-818.088**	0.000	.00000000	**-630.360**	00000000	00000000			Vy	**97.064**	**97.064**	**90.664**		
S20	B.G.1	My	0.000	0.000	.00000000	0.000	00000000	00000000	-	0.000	Vz	0.000	0.000	0.000	**0.080**	**0.080**
		Mz	**-630.319**	0.000	.00000000	**-456.262**	00000000	00000000			Vy	**90.228**	**90.228**	**83.828**		
S21	B.G.1	My	0.000	0.000	.00000000	0.000	00000000	00000000	-	0.000	Vz	0.000	0.000	0.000	**0.154**	**0.154**
		Mz	**-456.167**	0.000	.00000000	**-298.708**	00000000	00000000			Vy	**81.930**	**81.930**	**75.530**		
S22	B.G.1	My	0.000	0.000	.00000000	0.000	00000000	00000000	-	0.000	Vz	0.000	0.000	0.000	**0.253**	**0.253**
		Mz	**-298.542**	0.000	.00000000	**-163.307**	00000000	00000000			Vy	**70.817**	**70.817**	**64.417**		
S23	B.G.1	My	0.000	0.000	.00000000	0.000	00000000	00000000	-	0.000	Vz	0.000	0.000	0.000	**0.379**	**0.379**
		Mz	**-163.047**	0.000	.00000000	**-59.291**	00000000	00000000			Vy	**55.078**	**55.078**	**48.678**		
S24	B.G.1	My	0.000	0.000	.00000000	0.000	00000000	00000000	-	0.000	Vz	0.000	0.000	0.000	**0.523**	**0.523**
		Mz	**-58.917**	0.000	.00000000	**-0.497**	00000000	00000000			Vy	**32.410**	**32.410**	**26.010**		
S25	B.G.1	My	0.000	0.000	.00000000	0.000	00000000	00000000	-	0.000	Vz	0.000	0.000	0.000	**0.042**	**0.042**
		Mz	**0.056**	0.000	.00000000	**3.539**	00000000	00000000			Vy	**0.435**	**0.435**	**0.435**		
S26	B.G.1	My	0.000	0.000	.00000000	0.000	00000000	00000000	-	0.000	Vz	0.000	0.000	0.000	0.000	0.000
		Mz	**3.567**	0.000	.00000000	**3.567**	00000000	00000000			Vy	0.000	0.000	0.000		
S27	B.G.1	My	0.000	0.000	.00000000	0.000	00000000	00000000	-	0.000	Vz	0.000	0.000	0.000	**-0.042**	**-0.042**
		Mz	**3.539**	0.000	.00000000	**0.056**	00000000	00000000			Vy	**-0.435**	**-0.435**	**-0.435**		
S28	B.G.1	My	0.000	0.000	.00000000	0.000	00000000	00000000	-	0.000	Vz	0.000	0.000	0.000	**0.095**	**0.095**
		Mz	**0.074**	0.000	.00000000	**15.264**	00000000	00000000			Vy	**1.899**	**1.899**	**1.899**		
S29	B.G.1	My	0.000	0.000	.00000000	0.000	00000000	00000000	-	0.000	Vz	0.000	0.000	0.000	0.000	0.000
		Mz	**15.300**	0.000	.00000000	**15.300**	00000000	00000000			Vy	0.000	0.000	0.000		
S30	B.G.1	My	0.000	0.000	.00000000	0.000	00000000	00000000	-	0.000	Vz	0.000	0.000	0.000	**-0.095**	**-0.095**
		Mz	**15.264**	0.000	.00000000	**0.074**	00000000	00000000			Vy	**-1.899**	**-1.899**	**-1.899**		
S31	B.G.1	My	0.000	0.000	.00000000	0.000	00000000	00000000	-	0.000	Vz	0.000	0.000	0.000	**0.166**	**0.166**
		Mz	**0.099**	0.000	.00000000	**37.798**	00000000	00000000			Vy	**4.712**	**4.712**	**4.712**		
S32	B.G.1	My	0.000	0.000	.00000000	0.000	00000000	00000000	-	0.000	Vz	0.000	0.000	0.000	0.000	0.000
		Mz	**37.847**	0.000	.00000000	**37.847**	00000000	00000000			Vy	0.000	0.000	0.000		
S33	B.G.1	My	0.000	0.000	.00000000	0.000	00000000	00000000	-	0.000	Vz	0.000	0.000	0.000	**-0.166**	**-0.166**
		Mz	**37.798**	0.000	.00000000	**0.099**	00000000	00000000			Vy	**-4.712**	**-4.712**	**-4.712**		
S34	B.G.1	My	0.000	0.000	.00000000	0.000	00000000	00000000	-	0.000	Vz	0.000	0.000	0.000	**0.260**	**0.260**
		Mz	**0.126**	0.000	.00000000	**74.842**	00000000	00000000			Vy	**9.339**	**9.339**	**9.339**		
S35	B.G.1	My	0.000	0.000	.00000000	0.000	00000000	00000000	-	0.000	Vz	0.000	0.000	0.000	0.000	0.000
		Mz	**74.905**	0.000	.00000000	**74.905**	00000000	00000000			Vy	0.000	0.000	0.000		
S36	B.G.1	My	0.000	0.000	.00000000	0.000	00000000	00000000	-	0.000	Vz	0.000	0.000	0.000	**-0.260**	**-0.260**
		Mz	**74.842**	0.000	.00000000	**0.126**	00000000	00000000			Vy	**-9.339**	**-9.339**	**-9.339**		
S37	B.G.1	My	0.000	0.000	.00000000	0.000	00000000	00000000	-	0.000	Vz	0.000	0.000	0.000	**0.375**	**0.375**
		Mz	**0.143**	0.000	.00000000	**130.287**	00000000	00000000			Vy	**16.268**	**16.268**	**16.268**		
S38	B.G.1	My	0.000	0.000	.00000000	0.000	00000000	00000000	-	0.000	Vz	0.000	0.000	0.000	0.000	0.000
		Mz	**130.358**	0.000	.00000000	**130.358**	00000000	00000000			Vy	0.000	0.000	0.000		
S39	B.G.1	My	0.000	0.000	.00000000	0.000	00000000	00000000	-	0.000	Vz	0.000	0.000	0.000	**-0.375**	**-0.375**
		Mz	**130.287**	0.000	.00000000	**0.143**	00000000	00000000			Vy	**-16.268**	**-16.268**	**-16.268**		
S40	B.G.1	My	0.000	0.000	.00000000	0.000	00000000	00000000	-	0.000	Vz	0.000	0.000	0.000	**0.497**	**0.497**

Member	L.C.	Value	Mb	Mmax	xMmax	Me	x-M0	x-M0	TC	Nmax	Value	Vb	Vmax	Ve	Mxb	Mxe
		Mz	**-0.523**	0.000	.00000000	**207.556**	02008930	00000000			Vy	**26.010**	**26.010**	**26.010**		
S41	B.G.1	My	0.000	0.000	.00000000	0.000	00000000	00000000	-	0.000	Vz	0.000	0.000	0.000	0.000	0.000
		Mz	**206.592**	0.000	.00000000	**206.592**	00000000	00000000			Vy	0.000	0.000	0.000		
S42	B.G.1	My	0.000	0.000	.00000000	0.000	00000000	00000000	-	0.000	Vz	0.000	0.000	0.000	**-0.497**	**-0.497**
		Mz	**207.556**	0.000	.00000000	**-0.523**	97991027	00000000			Vy	**-26.010**	**-26.010**	**-26.010**		
S43	B.G.1	My	0.000	0.000	.00000000	0.000	00000000	00000000	-	0.000	Vz	0.000	0.000	0.000	**0.704**	**0.704**
		Mz	**-288.000**	0.000	.00000000	**-200.000**	00000000	00000000			Vy	**48.000**	**48.000**	**40.000**		
S44	B.G.1	My	0.000	0.000	.00000000	0.000	00000000	00000000	-	0.000	Vz	0.000	0.000	0.000	**0.002**	**0.002**
		Mz	**-200.000**	0.000	.00000000	**-128.000**	00000000	00000000			Vy	**40.000**	**40.000**	**32.000**		
S45	B.G.1	My	0.000	0.000	.00000000	0.000	00000000	00000000	-	0.000	Vz	0.000	0.000	0.000	**0.000**	**0.000**
		Mz	**-128.000**	0.000	.00000000	**-72.000**	00000000	00000000			Vy	**32.000**	**32.000**	**24.000**		
S46	B.G.1	My	0.000	0.000	.00000000	0.000	00000000	00000000	-	0.000	Vz	0.000	0.000	0.000	**0.000**	**0.000**
		Mz	**-72.000**	0.000	.00000000	**-32.000**	00000000	00000000			Vy	**24.000**	**24.000**	**16.000**		
S47	B.G.1	My	0.000	0.000	.00000000	0.000	00000000	00000000	-	0.000	Vz	0.000	0.000	0.000	0.000	0.000
		Mz	**-32.000**	0.000	.00000000	**-8.000**	00000000	00000000			Vy	**16.000**	**16.000**	**8.000**		
S48	B.G.1	My	0.000	0.000	.00000000	0.000	00000000	00000000	-	0.000	Vz	0.000	0.000	0.000	0.000	0.000
		Mz	**-8.000**	0.000	.00000000	0.000	00000000	00000000			Vy	**8.000**	**8.000**	**0.000**		
S49	B.G.1	My	0.000	0.000	.00000000	0.000	00000000	00000000	-	0.000	Vz	0.000	0.000	0.000	**-0.704**	**-0.704**
		Mz	**-288.000**	0.000	.00000000	**-200.000**	00000000	00000000			Vy	**48.000**	**48.000**	**40.000**		
S50	B.G.1	My	0.000	0.000	.00000000	0.000	00000000	00000000	-	0.000	Vz	0.000	0.000	0.000	**-0.002**	**-0.002**
		Mz	**-200.000**	0.000	.00000000	**-128.000**	00000000	00000000			Vy	**40.000**	**40.000**	**32.000**		
S51	B.G.1	My	0.000	0.000	.00000000	0.000	00000000	00000000	-	0.000	Vz	0.000	0.000	0.000	**0.000**	**0.000**
		Mz	**-128.000**	0.000	.00000000	**-72.000**	00000000	00000000			Vy	**32.000**	**32.000**	**24.000**		
S52	B.G.1	My	0.000	0.000	.00000000	0.000	00000000	00000000	-	0.000	Vz	0.000	0.000	0.000	**0.000**	**0.000**
		Mz	**-72.000**	0.000	.00000000	**-32.000**	00000000	00000000			Vy	**24.000**	**24.000**	**16.000**		
S53	B.G.1	My	0.000	0.000	.00000000	0.000	00000000	00000000	-	0.000	Vz	0.000	0.000	0.000	0.000	0.000
		Mz	**-32.000**	0.000	.00000000	**-8.000**	00000000	00000000			Vy	**16.000**	**16.000**	**8.000**		
S54	B.G.1	My	0.000	0.000	.00000000	0.000	00000000	00000000	-	0.000	Vz	0.000	0.000	0.000	0.000	0.000
		Mz	**-8.000**	0.000	.00000000	0.000	00000000	00000000			Vy	**8.000**	**8.000**	**0.000**		
S55	B.G.1	My	0.000	0.000	.00000000	0.000	00000000	00000000	-	0.000	Vz	0.000	0.000	0.000	0.000	0.000
		Mz	**0.702**	0.000	.00000000	**0.702**	00000000	00000000			Vy	0.000	0.000	0.000		
S56	B.G.1	My	0.000	0.000	.00000000	0.000	00000000	00000000	-	0.000	Vz	0.000	0.000	0.000	0.000	0.000
		Mz	**0.002**	0.000	.00000000	**0.002**	00000000	00000000			Vy	0.000	0.000	0.000		
S57	B.G.1	My	0.000	0.000	.00000000	0.000	00000000	00000000	-	0.000	Vz	0.000	0.000	0.000	0.000	0.000
		Mz	**0.000**	0.000	.00000000	**0.000**	00000000	00000000			Vy	0.000	0.000	0.000		
S58	B.G.1	My	0.000	0.000	.00000000	0.000	00000000	00000000	-	0.000	Vz	0.000	0.000	0.000	0.000	0.000
		Mz	**0.000**	0.000	.00000000	**0.000**	00000000	00000000			Vy	0.000	0.000	0.000		
-	**-**	**-**	**kNm**	**kNm**	**m**	**kNm**	**m**	**m**	**-**	**kN**	**-**	**kN**	**kN**	**kN**	**kNm**	**kNm**

C.4 Super Element 3 MatrixFrame Report

Here the MatrixFrame report for super element 3 (one core and one wall) is included.

C.4.1 Matrix Frame report with dimensions when $D < 0$

Project name	core wall validation	Project number	
Part description		Structural engineer	
Client		Units	m, kN, kNm
File	D:\My Documents\Documents\Babette\Matrix Frame Models\validation_se3_corewall_25_01.mxe		

PIC. GEOMETRIE RAAMWERK

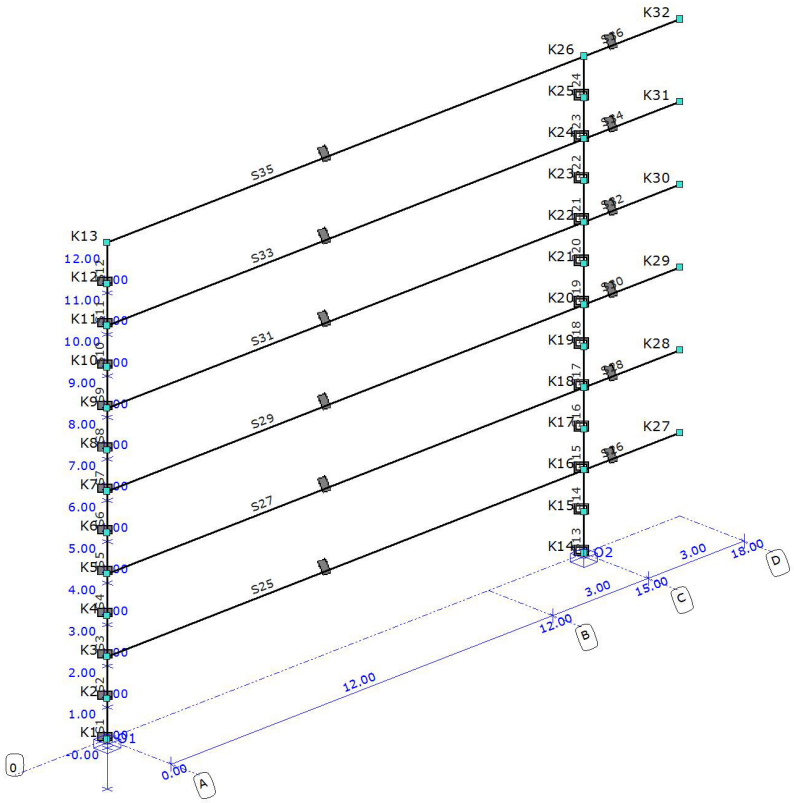

PIC. GEOMETRIE 1 STAVEN EN KNOPEN

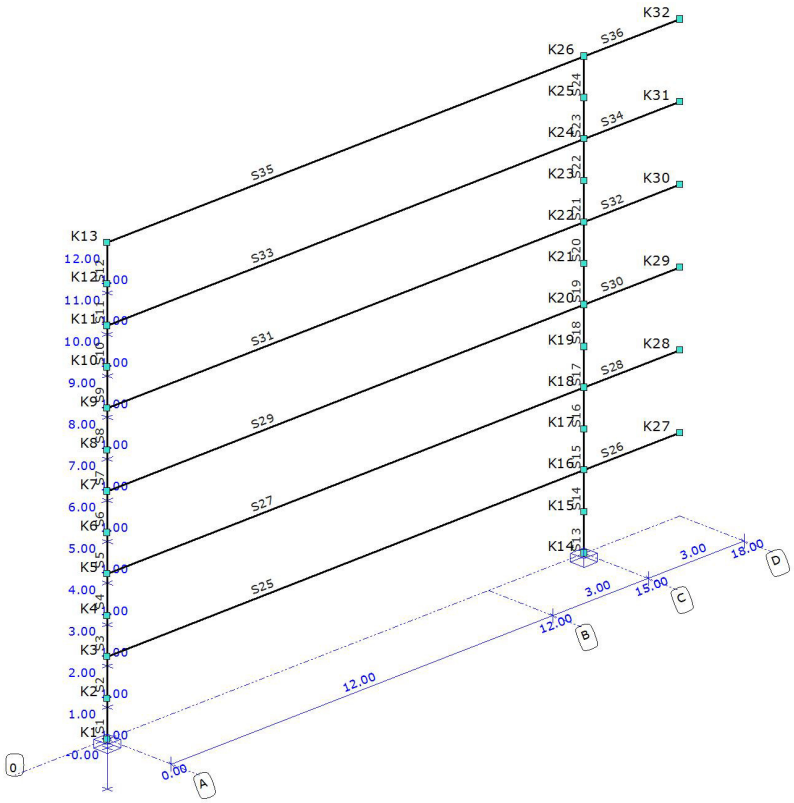

PIC. GEOMETRIE 2 STAVEN EN KNOPEN

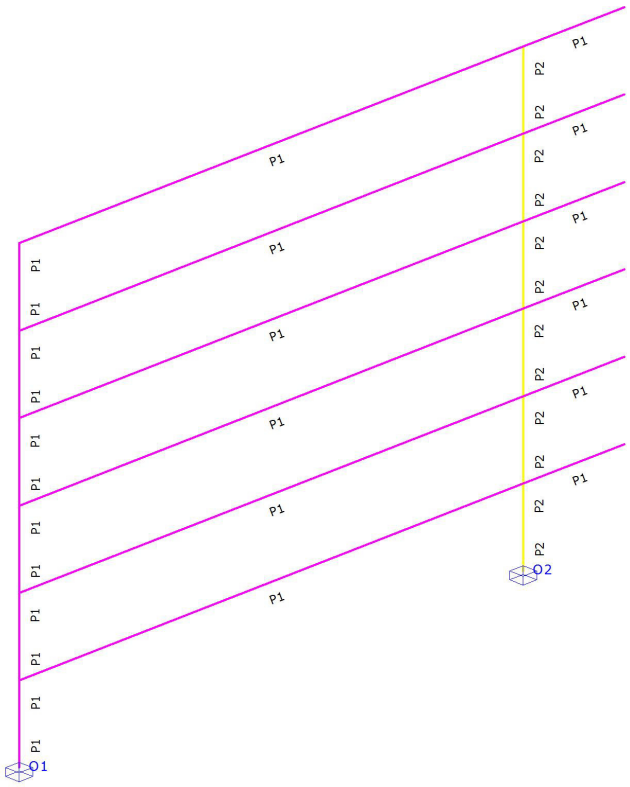

SECTIONS

Section	Section Name	Area	It	Iy	Iz	Material	Angle
P1	R6000x200	1.2000e+00	1.6000e-02	4.0000e-03	3.6000e+00	C30/37	0.0
P2	K6000x6000x200x200	4.6400e+00	3.9022e+01	2.6046e+01	2.6046e+01	C30/37	0.0
-	-	m2	m4	m4	m4	-	°

SECTION SHAPES

Section	Tapered	hB	hE	tf	tw	tf2	B	b1	b2	Castellate	Height
P1	No	0.20000000	0.20000000	0.00000000	0.00000000	0.00000000	6.00000000	0.00000000	0.00000000	No	0.00000000
P2	No	6.00000000	6.00000000	0.20000000	0.20000000	0.00000000	6.00000000	0.00000000	0.00000000	No	0.00000000
-	-	m	m	m	m	m	m	m	m	-	m

MATERIALS

Material Name	Poison	Density	Youngs mod.	Lin. Exp.
C30/37	0.30	25.000	3.0000e+07	10.0000e-06
-	-	kN/m3	kN/m2	C°m

SUPPORTS

Support	Nodes	X	Y	Z	Xr	Yr	Zr	AngleXr	AngleYr	AngleZr
O1	K1	fixed	fixed	fixed	fixed	fixed	fixed	0	0	0
O2	K14	fixed	fixed	fixed	fixed	fixed	fixed	0	0	0
-	-	kN/m	kN/m	kN/m	kNm/rad	kNm/rad	kNm/rad	°	°	°

B.G.1: PERMANENT ACTIONS

Type	Value Begin	Value End	Dist. Begin	Dist. End	Direction	Member/Node
B.G.1: Permanent actions						
q	5.625	5.625	0.00000000	1.00000000(L)	Y"	S1-S12
q	12.375	12.375	0.00000000	1.00000000(L)	Y"	S13-S24
q	-6.000	-6.000	0.00000000	1.00000000(L)	X"	S13-S24
N	-23.675				Zr	K15-K26
Sum of loads	**X: -72.000**	**kN**	**Y: 216.000**	**kN**	**Z: 0.000**	**kN**
-	**-**	**-**	**-**	**m**	**m**	**- -**

B.G.1: PERMANENT ACTIONS

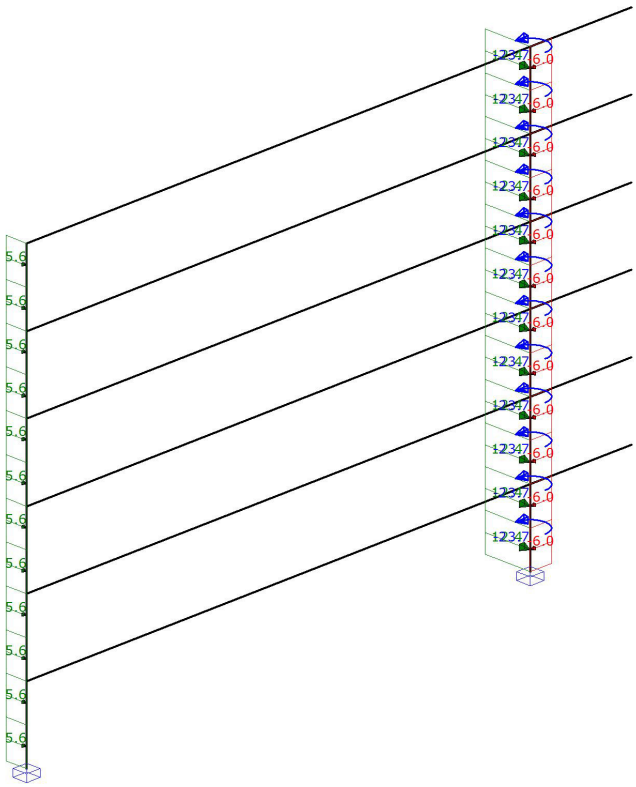

PIC. B.G.1: PERMANENT ACTIONS VERPLAATSINGEN

Load Cases

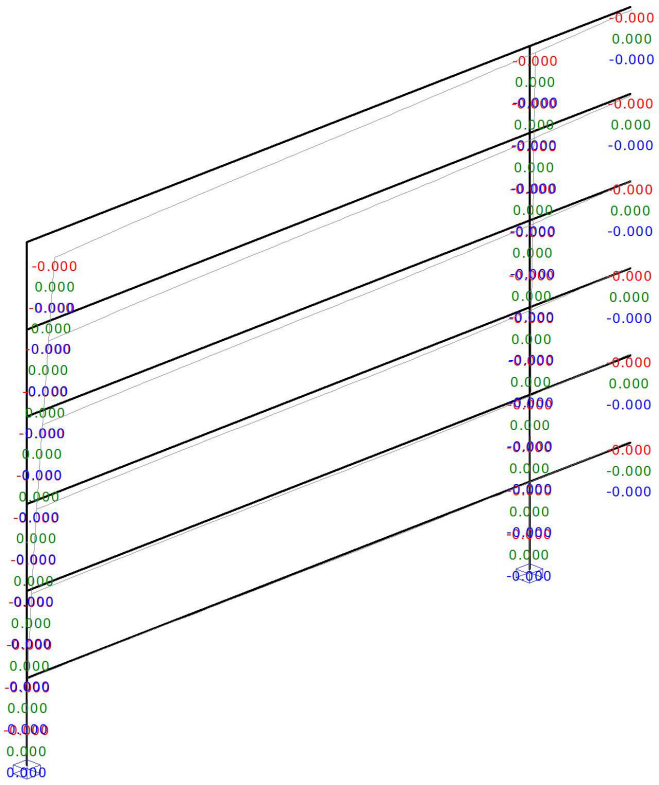

L.C. NODAL DISPLACEMENTS

Node	L.C.	X	Y	Z	Xr	Yr	Zr
K1	B.G.1	0.000000000	0.000000000	0.000000000	-0.000e-03	0.000e-03	-0.000e-03
K2	B.G.1	-0.000000279	0.000001728	0.000000002	-0.003e-03	0.001e-03	-0.000e-03
K3	B.G.1	-0.000000992	0.000006509	0.000000004	-0.006e-03	0.001e-03	-0.000e-03
K4	B.G.1	-0.000002108	0.000013781	0.000000005	-0.008e-03	0.001e-03	0.000e-03
K5	B.G.1	-0.000003515	0.000023041	0.000000007	-0.010e-03	0.001e-03	0.001e-03
K6	B.G.1	-0.000005183	0.000033844	0.000000009	-0.011e-03	0.002e-03	0.001e-03
K7	B.G.1	-0.000007028	0.000045801	0.000000010	-0.012e-03	0.002e-03	0.002e-03
K8	B.G.1	-0.000009020	0.000058585	0.000000011	-0.013e-03	0.002e-03	0.002e-03
K9	B.G.1	-0.000011099	0.000071925	0.000000012	-0.014e-03	0.002e-03	0.003e-03
K10	B.G.1	-0.000013239	0.000085605	0.000000013	-0.014e-03	0.002e-03	0.004e-03
K11	B.G.1	-0.000015440	0.000099465	0.000000014	-0.014e-03	0.002e-03	0.005e-03
K12	B.G.1	-0.000017684	0.000113395	0.000000014	-0.014e-03	0.002e-03	0.005e-03
K13	B.G.1	-0.000019794	0.000127338	0.000000014	-0.014e-03	0.002e-03	0.006e-03
K14	B.G.1	0.000000000	0.000000000	0.000000000	-0.000e-03	0.000e-03	0.000e-03
K15	B.G.1	-0.000000261	0.000000545	0.000000000	-0.001e-03	0.001e-03	0.001e-03
K16	B.G.1	-0.000000985	0.000002064	-0.000000001	-0.002e-03	0.001e-03	0.001e-03
K17	B.G.1	-0.000002093	0.000004393	-0.000000001	-0.003e-03	0.001e-03	0.002e-03
K18	B.G.1	-0.000003511	0.000007381	-0.000000002	-0.003e-03	0.002e-03	0.002e-03
K19	B.G.1	-0.000005175	0.000010896	-0.000000002	-0.004e-03	0.002e-03	0.002e-03
K20	B.G.1	-0.000007026	0.000014817	-0.000000003	-0.004e-03	0.002e-03	0.003e-03
K21	B.G.1	-0.000009015	0.000019040	-0.000000003	-0.004e-03	0.002e-03	0.003e-03

Node	L.C.	X	Y	Z	Xr	Yr	Zr
K22	B.G.1	-0.000011100	0.000023477	-0.000000003	-0.005e-03	0.002e-03	0.004e-03
K23	B.G.1	-0.000013247	0.000028052	-0.000000003	-0.005e-03	0.002e-03	0.004e-03
K24	B.G.1	-0.000015428	0.000032709	-0.000000004	-0.005e-03	0.002e-03	0.004e-03
K25	B.G.1	-0.000017625	0.000037403	-0.000000004	-0.005e-03	0.002e-03	0.004e-03
K26	B.G.1	-0.000019826	0.000042110	-0.000000004	-0.005e-03	0.002e-03	0.004e-03
K27	B.G.1	-0.000000985	-0.000001192	-0.000002788	-0.002e-03	0.001e-03	0.001e-03
K28	B.G.1	-0.000003511	0.000001271	-0.000004655	-0.003e-03	0.002e-03	0.002e-03
K29	B.G.1	-0.000007026	0.000006198	-0.000005786	-0.004e-03	0.002e-03	0.003e-03
K30	B.G.1	-0.000011100	0.000012748	-0.000006366	-0.005e-03	0.002e-03	0.004e-03
K31	B.G.1	-0.000015428	0.000020402	-0.000006578	-0.005e-03	0.002e-03	0.004e-03
K32	B.G.1	-0.000019826	0.000028955	-0.000006607	-0.005e-03	0.002e-03	0.004e-03
-	-	m	m	m	rad	rad	rad

PIC. B.G.1: PERMANENT ACTIONS MOMENT (MX)

Load Cases

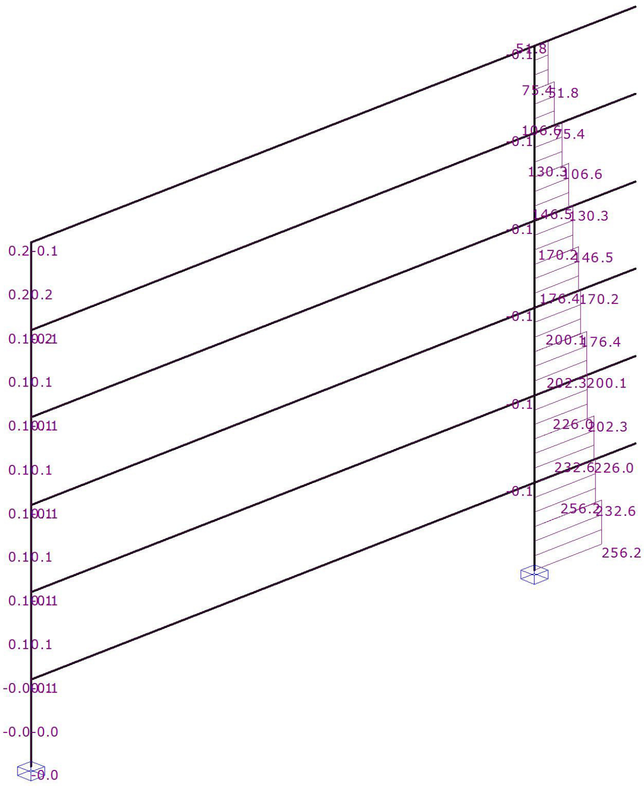

PIC. B.G.1: PERMANENT ACTIONS MOMENT (MY)

Load Cases

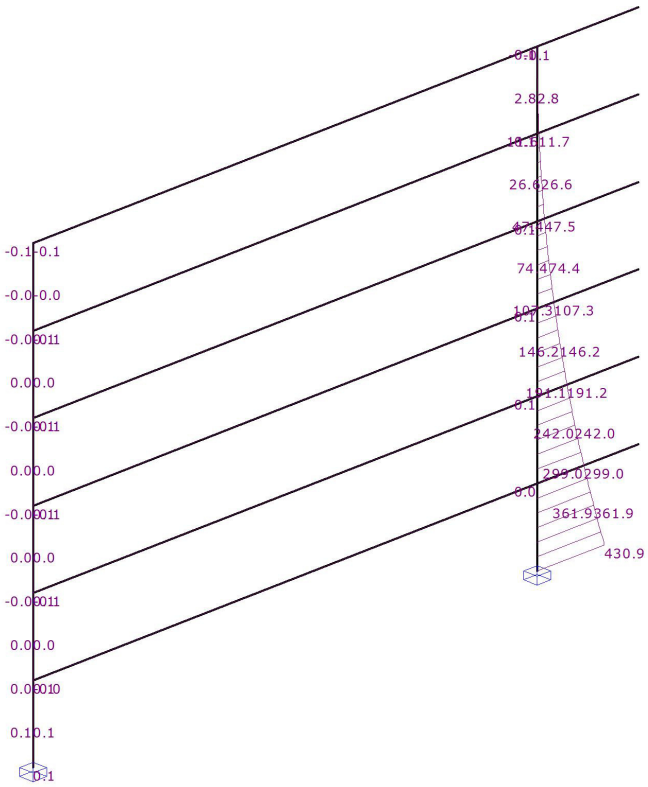

PIC. B.G.1: PERMANENT ACTIONS MOMENT (MZ) Load Cases

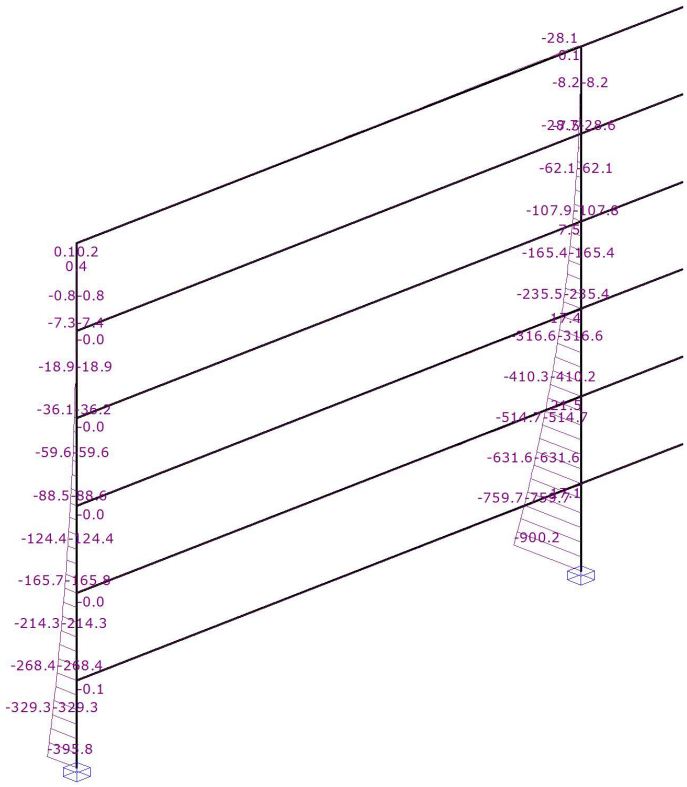

PIC. B.G.1: PERMANENT ACTIONS DWARSKRACHT (VY) Load Cases

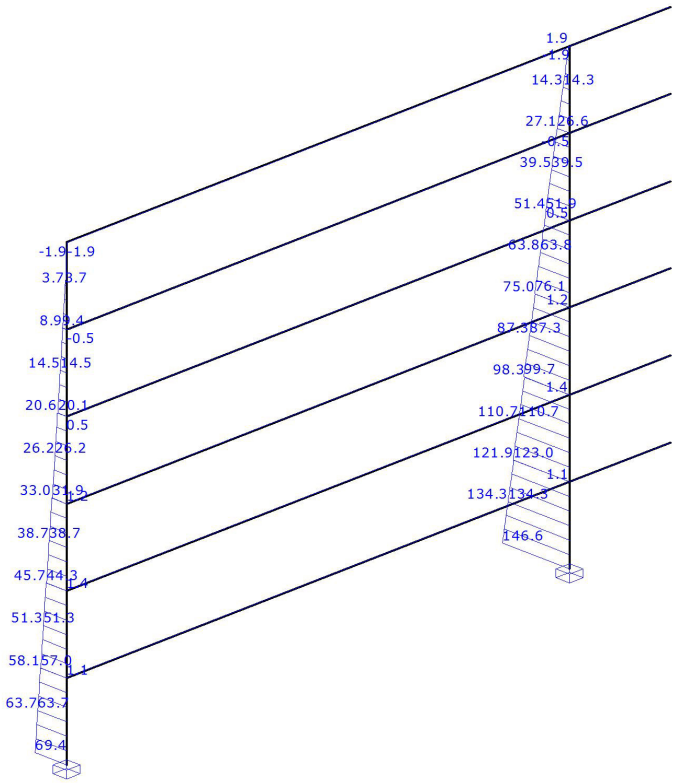

PIC. B.G.1: PERMANENT ACTIONS DWARSKRACHT (VZ) Load Cases

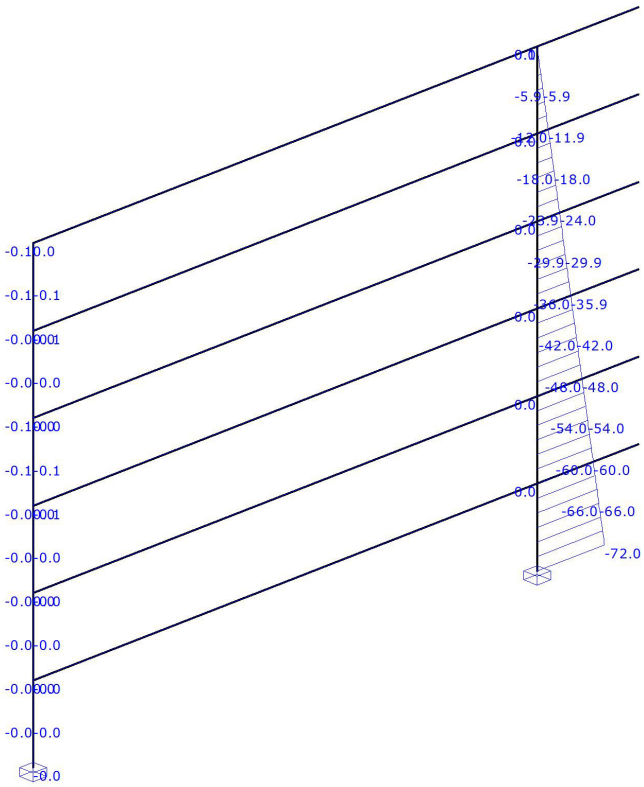

L.C. EXTREME MEMBER FORCES

Member	L.C.	Value	Mb	Mmax	xMmax	Me	x-M0	x-M0	TC	Nmax	Value	Vb	Vmax	Ve	Mxb	Mxe
S1	B.G.1	My	**0.074**	0.000	.00000000	**0.052**	00000000	00000000	C	**-0.067**	Vz	**-0.022**	**-0.022**	**-0.022**	**-0.009**	**-0.009**
		Mz	**-395.835**	0.000	.00000000	**-329.289**	00000000	00000000			Vy	**69.359**	**69.359**	**63.734**		
S2	B.G.1	My	**0.052**	0.000	.00000000	**0.030**	00000000	00000000	C	**-0.067**	Vz	**-0.022**	**-0.022**	**-0.022**	**-0.009**	**-0.009**
		Mz	**-329.289**	0.000	.00000000	**-268.367**	00000000	00000000			Vy	**63.734**	**63.734**	**58.109**		
S3	B.G.1	My	**0.072**	0.000	.00000000	**0.035**	00000000	00000000	C	**-0.061**	Vz	**-0.038**	**-0.038**	**-0.038**	**0.060**	**0.060**
		Mz	**-268.419**	0.000	.00000000	**-214.266**	00000000	00000000			Vy	**56.965**	**56.965**	**51.340**		
S4	B.G.1	My	**0.035**	0.000	.00000000	**-0.003**	92854231	00000000	C	**-0.061**	Vz	**-0.038**	**-0.038**	**-0.038**	**0.060**	**0.060**
		Mz	**-214.266**	0.000	.00000000	**-165.738**	00000000	00000000			Vy	**51.340**	**51.340**	**45.715**		
S5	B.G.1	My	**0.068**	0.000	.00000000	**0.021**	00000000	00000000	C	**-0.052**	Vz	**-0.047**	**-0.047**	**-0.047**	**0.103**	**0.103**
		Mz	**-165.822**	0.000	.00000000	**-124.353**	00000000	00000000			Vy	**44.282**	**44.282**	**38.657**		
S6	B.G.1	My	**0.021**	0.000	.00000000	**-0.026**	45215389	00000000	C	**-0.052**	Vz	**-0.047**	**-0.047**	**-0.047**	**0.103**	**0.103**
		Mz	**-124.353**	0.000	.00000000	**-88.509**	00000000	00000000			Vy	**38.657**	**38.657**	**33.032**		
S7	B.G.1	My	**0.063**	0.000	.00000000	**0.010**	00000000	00000000	C	**-0.040**	Vz	**-0.052**	**-0.052**	**-0.052**	**0.129**	**0.129**
		Mz	**-88.611**	0.000	.00000000	**-59.557**	00000000	00000000			Vy	**31.867**	**31.867**	**26.242**		
S8	B.G.1	My	**0.010**	0.000	.00000000	**-0.042**	19978646	00000000	C	**-0.040**	Vz	**-0.052**	**-0.052**	**-0.052**	**0.129**	**0.129**
		Mz	**-59.557**	0.000	.00000000	**-36.128**	00000000	00000000			Vy	**26.242**	**26.242**	**20.617**		
S9	B.G.1	My	**0.055**	0.000	.00000000	**0.007**	00000000	00000000	C	**-0.027**	Vz	**-0.048**	**-0.048**	**-0.048**	**0.145**	**0.145**
		Mz	**-36.239**	0.000	.00000000	**-18.935**	00000000	00000000			Vy	**20.117**	**20.117**	**14.492**		
S10	B.G.1	My	**0.007**	0.000	.00000000	**-0.041**	14939733	00000000	C	**-0.027**	Vz	**-0.048**	**-0.048**	**-0.048**	**0.145**	**0.145**
		Mz	**-18.935**	0.000	.00000000	**-7.256**	00000000	00000000			Vy	**14.492**	**14.492**	**8.867**		
S11	B.G.1	My	**0.061**	0.000	.00000000	**-0.016**	79029606	00000000	C	**-0.013**	Vz	**-0.077**	**-0.077**	**-0.077**	**0.157**	**0.157**

Member	L.C.	Value	Mb	Mmax	xMmax	Me	x-M0	x-M0	TC	Nmax	Value	Vb	Vmax	Ve	Mxb	Mxe
		Mz	**-7.369**	0.000	.00000000	**-0.815**	00000000	00000000			Vy	**9.367**	**9.367**	**3.742**		
S12	B.G.1	My	**-0.016**	0.000	.00000000	**-0.094**	00000000	00000000	C	**-0.013**	Vz	**-0.077**	**-0.077**	**-0.077**	**0.157**	**0.157**
		Mz	**-0.815**	**0.429**	.66516697	**0.114**	27462669	00000000			Vy	**3.742**	**3.742**	**-1.883**		
S13	B.G.1	My	**430.921**	0.000	.00000000	**361.943**	00000000	00000000	T	**0.067**	Vz	**-71.978**	**-71.978**	**-65.978**	**256.228**	**56.228**
		Mz	**-900.165**	0.000	.00000000	**-759.711**	00000000	00000000			Vy	**146.641**	**146.641**	**134.266**		
S14	B.G.1	My	**361.943**	0.000	.00000000	**298.966**	00000000	00000000	T	**0.067**	Vz	**-65.978**	**-65.978**	**-59.978**	**232.553**	**32.553**
		Mz	**-759.711**	0.000	.00000000	**-631.633**	00000000	00000000			Vy	**134.266**	**134.266**	**121.891**		
S15	B.G.1	My	**299.009**	0.000	.00000000	**242.047**	00000000	00000000	T	**0.061**	Vz	**-59.962**	**-59.962**	**-53.962**	**225.961**	**25.961**
		Mz	**-631.581**	0.000	.00000000	**-514.734**	00000000	00000000			Vy	**123.035**	**123.035**	**110.660**		
S16	B.G.1	My	**242.047**	0.000	.00000000	**191.084**	00000000	00000000	T	**0.061**	Vz	**-53.962**	**-53.962**	**-47.962**	**202.286**	**02.286**
		Mz	**-514.734**	0.000	.00000000	**-410.262**	00000000	00000000			Vy	**110.660**	**110.660**	**98.285**		
S17	B.G.1	My	**191.157**	0.000	.00000000	**146.204**	00000000	00000000	T	**0.052**	Vz	**-47.953**	**-47.953**	**-41.953**	**200.073**	**00.073**
		Mz	**-410.178**	0.000	.00000000	**-316.647**	00000000	00000000			Vy	**99.718**	**99.718**	**87.343**		
S18	B.G.1	My	**146.204**	0.000	.00000000	**107.251**	00000000	00000000	T	**0.052**	Vz	**-41.953**	**-41.953**	**-35.953**	**176.398**	**76.398**
		Mz	**-316.647**	0.000	.00000000	**-235.491**	00000000	00000000			Vy	**87.343**	**87.343**	**74.968**		
S19	B.G.1	My	**107.342**	0.000	.00000000	**74.394**	00000000	00000000	T	**0.040**	Vz	**-35.948**	**-35.948**	**-29.948**	**170.171**	**70.171**
		Mz	**-235.389**	0.000	.00000000	**-165.443**	00000000	00000000			Vy	**76.133**	**76.133**	**63.758**		
S20	B.G.1	My	**74.394**	0.000	.00000000	**47.446**	00000000	00000000	T	**0.040**	Vz	**-29.948**	**-29.948**	**-23.948**	**146.496**	**46.496**
		Mz	**-165.443**	0.000	.00000000	**-107.872**	00000000	00000000			Vy	**63.758**	**63.758**	**51.383**		
S21	B.G.1	My	**47.546**	0.000	.00000000	**26.594**	00000000	00000000	T	**0.027**	Vz	**-23.952**	**-23.952**	**-17.952**	**130.307**	**30.307**
		Mz	**-107.761**	0.000	.00000000	**-62.065**	00000000	00000000			Vy	**51.883**	**51.883**	**39.508**		
S22	B.G.1	My	**26.594**	0.000	.00000000	**11.642**	00000000	00000000	T	**0.027**	Vz	**-17.952**	**-17.952**	**-11.952**	**106.632**	**06.632**
		Mz	**-62.065**	0.000	.00000000	**-28.744**	00000000	00000000			Vy	**39.508**	**39.508**	**27.133**		
S23	B.G.1	My	**11.746**	0.000	.00000000	**2.823**	00000000	00000000	T	**0.013**	Vz	**-11.923**	**-11.923**	**-5.923**	**75.445**	**75.445**
		Mz	**-28.631**	0.000	.00000000	**-8.185**	00000000	00000000			Vy	**26.633**	**26.633**	**14.258**		
S24	B.G.1	My	**2.823**	**-0.100**	.98710286	**-0.100**	80443266	00000000	T	**0.013**	Vz	**-5.923**	**-5.923**	**0.077**	**51.770**	**51.770**
		Mz	**-8.185**	0.000	.00000000	**-0.114**	00000000	00000000			Vy	**14.258**	**14.258**	**1.883**		
S25	B.G.1	My	**-0.043**	0.000	.00000000	**0.044**	41444229	00000000	T	**0.015**	Vz	**0.006**	**0.006**	**0.006**	**-0.051**	**-0.051**
		Mz	**-0.068**	0.000	.00000000	**17.082**	05983279	00000000			Vy	**1.143**	**1.143**	**1.143**		
S27	B.G.1	My	**-0.071**	0.000	.00000000	**0.073**	41396865	00000000	T	**0.010**	Vz	**0.010**	**0.010**	**0.010**	**-0.084**	**-0.084**
		Mz	**-0.043**	0.000	.00000000	**21.463**	03017033	00000000			Vy	**1.434**	**1.434**	**1.434**		
S29	B.G.1	My	**-0.089**	0.000	.00000000	**0.091**	41636095	00000000	T	**0.005**	Vz	**0.012**	**0.012**	**0.012**	**-0.103**	**-0.103**
		Mz	**-0.026**	0.000	.00000000	**17.447**	02223633	00000000			Vy	**1.165**	**1.165**	**1.165**		
S31	B.G.1	My	**-0.097**	0.000	.00000000	**0.099**	41224322	00000000	C	**-0.004**	Vz	**0.013**	**0.013**	**0.013**	**-0.111**	**-0.111**
		Mz	**-0.016**	0.000	.00000000	**7.486**	03195039	00000000			Vy	**0.500**	**0.500**	**0.500**		
S33	B.G.1	My	**-0.102**	0.000	.00000000	**0.104**	44487150	00000000	T	**0.029**	Vz	**0.014**	**0.014**	**0.014**	**-0.114**	**-0.114**
		Mz	**-0.012**	0.000	.00000000	**-7.512**	00000000	00000000			Vy	**-0.500**	**-0.500**	**-0.500**		
S35	B.G.1	My	**-0.094**	0.000	.00000000	**0.100**	26725065	00000000	C	**-0.077**	Vz	**0.013**	**0.013**	**0.013**	**-0.114**	**-0.114**
		Mz	**0.157**	0.000	.00000000	**-28.095**	08332357	00000000			Vy	**-1.883**	**-1.883**	**-1.883**		
-	**-**	**-**	**kNm**	**kNm**	**m**	**kNm**	**m**	**m**	**-**	**kN**	**-**	**kN**	**kN**	**kN**	**kNm**	**kNm**

L.C. INTERNAL FORCES & DEFLECTIONS

L.C.	Member	Position	Uy	Uz	Uy'	Uz'	Nx	Vy	Vz	Mx	My
B.G.1	S1	0.00000000	0.000000000	0.000000000	0.000000000	0.000000000	-0.067	69.359	-0.022	-0.009	0.074
B.G.1		0.10000000	0.000000018	-0.000000003	0.000000155	0.000000025	-0.067	68.796	-0.022	-0.009	0.072
B.G.1		0.20000000	0.000000072	-0.000000012	0.000000273	0.000000044	-0.067	68.234	-0.022	-0.009	0.070
B.G.1		0.30000000	0.000000162	-0.000000027	0.000000356	0.000000057	-0.067	67.671	-0.022	-0.009	0.068
B.G.1		0.40000000	0.000000286	-0.000000048	0.000000405	0.000000064	-0.067	67.109	-0.022	-0.009	0.065
B.G.1		0.50000000	0.000000445	-0.000000074	0.000000419	0.000000066	-0.067	66.546	-0.022	-0.009	0.063
B.G.1		0.60000000	0.000000637	-0.000000105	0.000000400	0.000000062	-0.067	65.984	-0.022	-0.009	0.061
B.G.1		0.70000000	0.000000862	-0.000000141	0.000000348	0.000000054	-0.067	65.421	-0.022	-0.009	0.059
B.G.1		0.80000000	0.000001119	-0.000000182	0.000000263	0.000000041	-0.067	64.859	-0.022	-0.009	0.057
B.G.1		0.90000000	0.000001408	-0.000000228	0.000000147	0.000000023	-0.067	64.296	-0.022	-0.009	0.054
B.G.1		L(1.00000000)	0.000001728	-0.000000279	0.000000000	0.000000000	-0.067	63.734	-0.022	-0.009	0.052
B.G.1	S2	0.00000000	0.000001728	-0.000000279	0.000000000	0.000000000	-0.067	63.734	-0.022	-0.009	0.052
B.G.1		0.10000000	0.000002078	-0.000000334	0.000000128	0.000000016	-0.067	63.171	-0.022	-0.009	0.050
B.G.1		0.20000000	0.000002458	-0.000000393	0.000000225	0.000000029	-0.067	62.609	-0.022	-0.009	0.048

C.4.2 Matrix Frame report with dimensions when $D > 0$

Project name	core wall validation	Project number	
Part description		Structural engineer	
Client		Units	m, kN, kNm
File	D:\My Documents\Documents\Babette\Matrix Frame Models\validation_se3_Dgreater0.mxe		

PIC. GEOMETRIE RAAMWERK

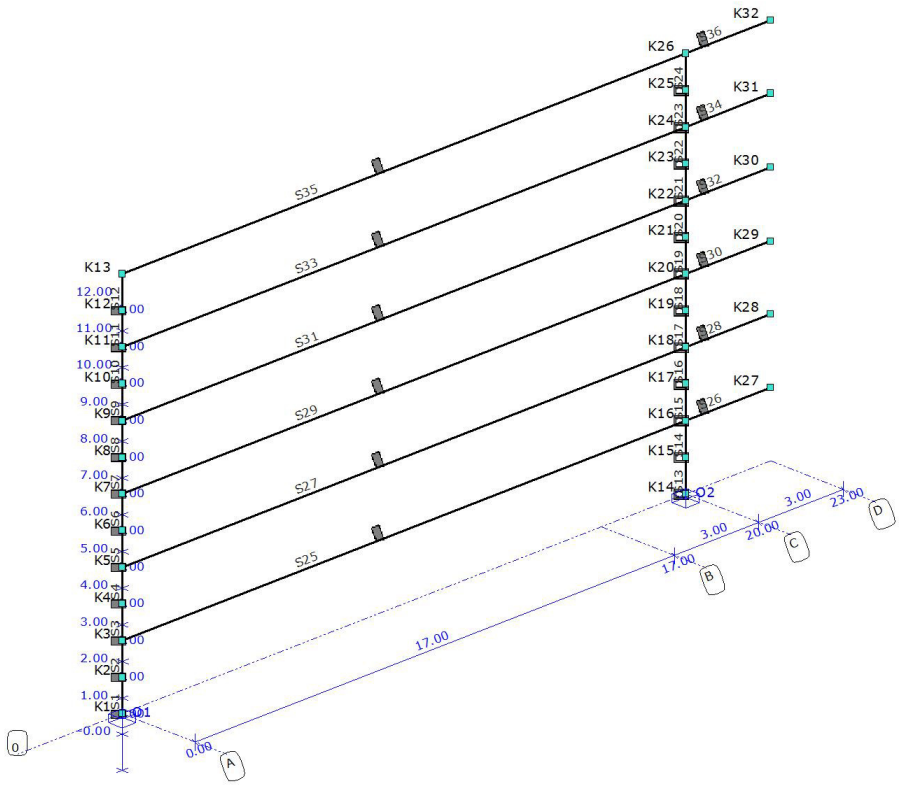

PIC. GEOMETRIE 1 STAVEN EN KNOPEN

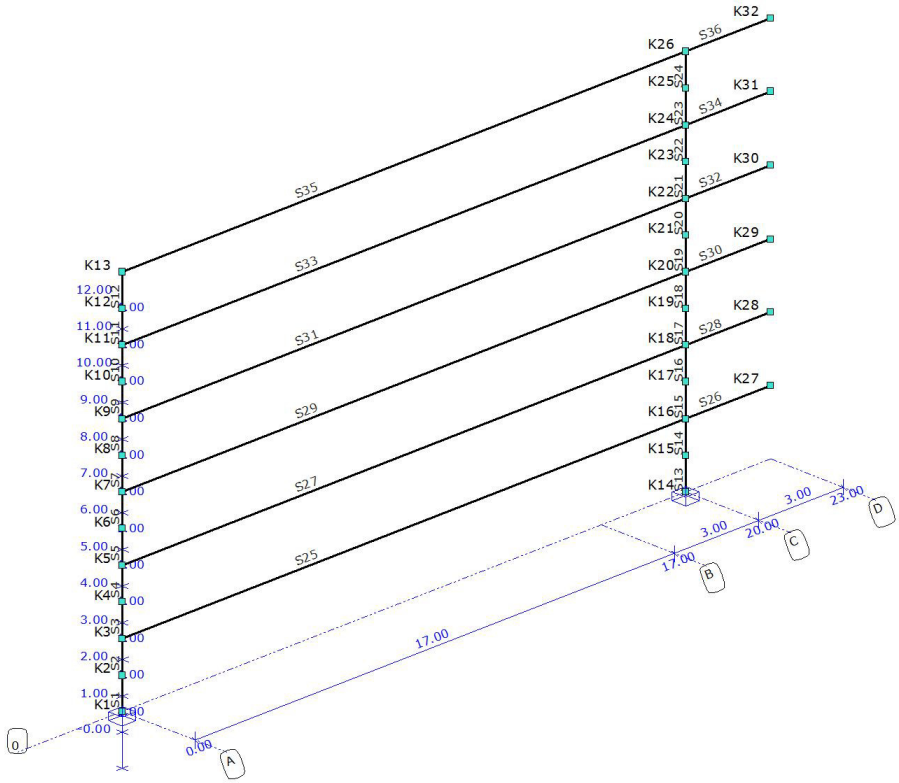

PIC. GEOMETRIE 2 STAVEN EN KNOPEN

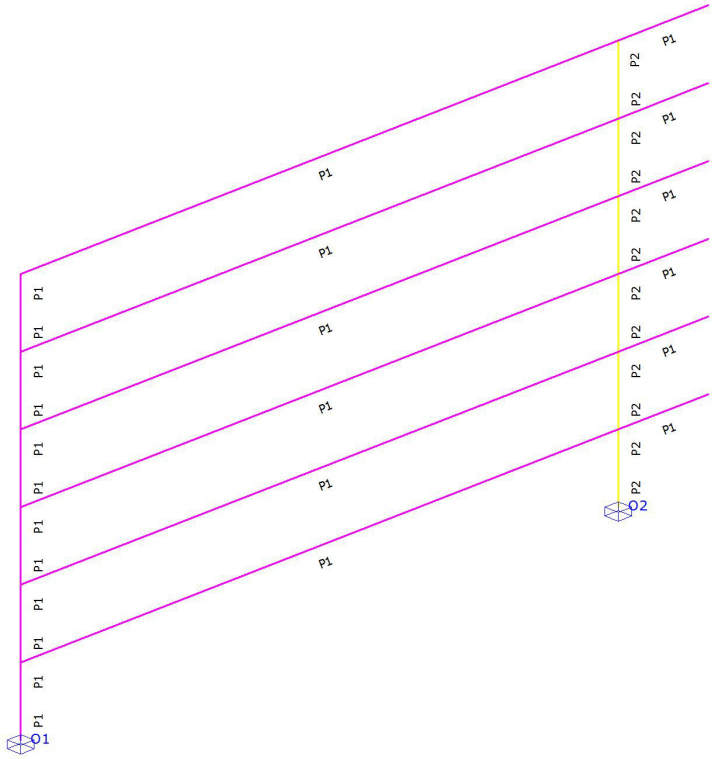

SECTIONS

Section	Section Name	Area	It	Iy	Iz	Material	Angle
P1	R8000x200	1.6000e+00	2.1333e-02	5.3333e-03	8.5333e+00	C30/37	0.0
P2	K6000x6000x200x200	4.6400e+00	3.9022e+01	2.6046e+01	2.6046e+01	C30/37	0.0
-	-	m2	m4	m4	m4	-	°

SECTION SHAPES

Section	Tapered	hB	hE	tf	tw	tf2	B	b1	b2	Castellate	Height
P1	No	0.20000000	0.20000000	0.00000000	0.00000000	0.00000000	8.00000000	0.00000000	0.00000000	No	0.00000000
P2	No	6.00000048	6.00000048	0.20000000	0.20000000	0.00000000	6.00000048	0.00000000	0.00000000	No	0.00000000
-	-	m	m	m	m	m	m	m	m	-	m

MATERIALS

Material Name	Poison	Density	Youngs mod.	Lin. Exp.
C30/37	0.30	25.000	3.0000e+07	10.0000e-06
-	-	kN/m3	kN/m2	C°m

SUPPORTS

Support	Nodes	X	Y	Z	Xr	Yr	Zr	AngleXr	AngleYr	AngleZr
O1	K1	fixed	fixed	fixed	fixed	fixed	fixed	0	0	0
O2	K14	fixed	fixed	fixed	fixed	fixed	fixed	0	0	0
-	-	kN/m	kN/m	kN/m	kNm/rad	kNm/rad	kNm/rad	°	°	°

B.G.1: PERMANENT ACTIONS

Type	Value Begin	Value End	Dist. Begin	Dist. End	Direction	Member/Node
B.G.1: Permanent actions						
q	7.500	7.500	0.00000000	1.00000000(L)	Y"	S1-S12
q	15.500	15.500	0.00000000	1.00000000(L)	Y"	S13-S24
q	-8.000	-8.000	0.00000000	1.00000000(L)	X"	S13-S24
N	-45.500				Zr	K15-K26
Sum of loads	**X: -96.000**	**kN**	**Y: 276.000**	**kN**	**Z: 0.000**	**kN**
-	**-**	**-**	**-**	**m**	**m**	**- -**

B.G.1: PERMANENT ACTIONS

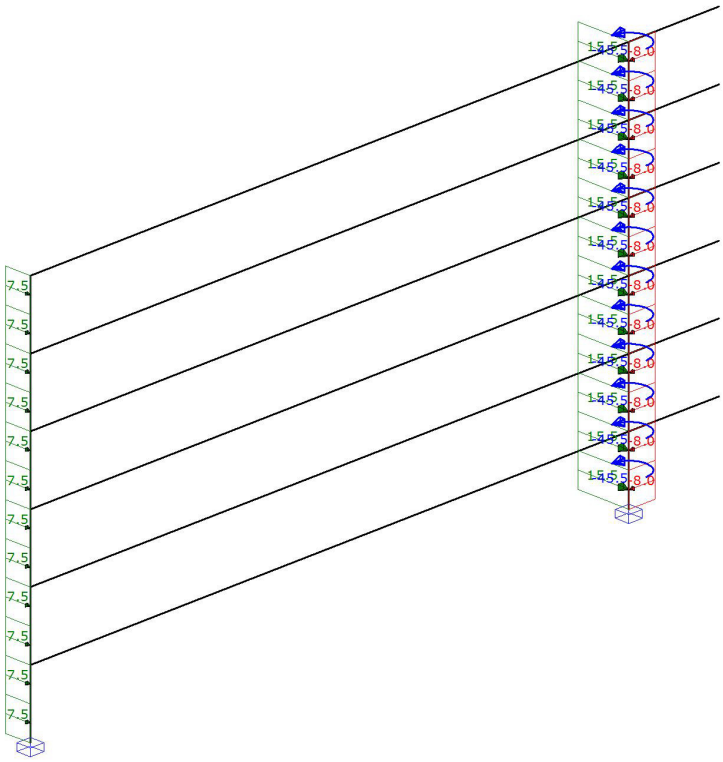

PIC. B.G.1: PERMANENT ACTIONS VERPLAATSINGEN

Load Cases

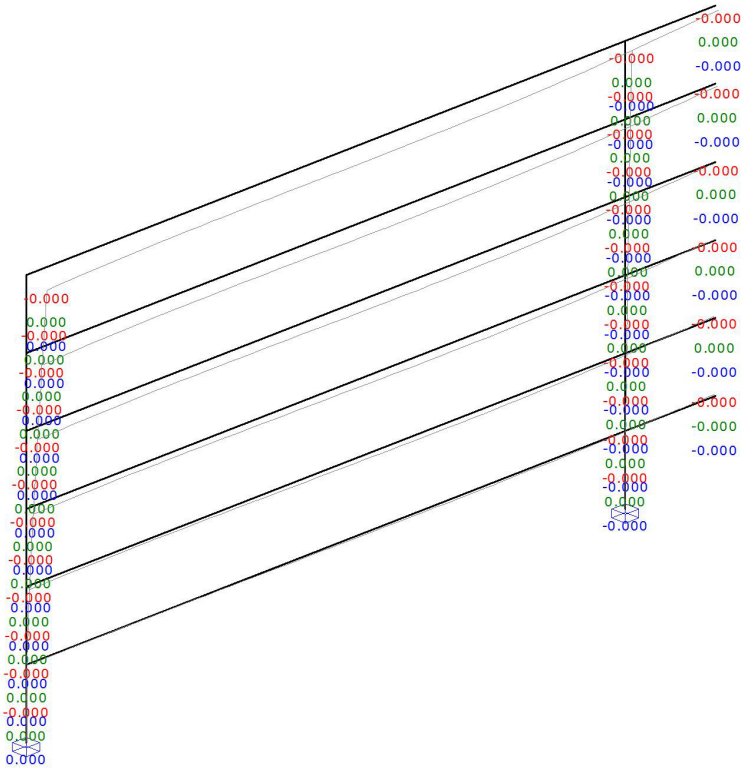

L.C. NODAL DISPLACEMENTS

Node	L.C.	X	Y	Z	Xr	Yr	Zr
K1	B.G.1	0.000000000	0.000000000	0.000000000	-0.000e-03	0.000e-03	-0.000e-03
K2	B.G.1	-0.000000367	0.000001191	0.000000001	-0.002e-03	0.001e-03	-0.000e-03
K3	B.G.1	-0.000001322	0.000004508	0.000000003	-0.004e-03	0.001e-03	-0.000e-03
K4	B.G.1	-0.000002808	0.000009584	0.000000004	-0.006e-03	0.002e-03	-0.000e-03
K5	B.G.1	-0.000004687	0.000016090	0.000000005	-0.007e-03	0.002e-03	-0.000e-03
K6	B.G.1	-0.000006908	0.000023727	0.000000006	-0.008e-03	0.002e-03	-0.000e-03
K7	B.G.1	-0.000009370	0.000032232	0.000000008	-0.009e-03	0.002e-03	0.000e-03
K8	B.G.1	-0.000012023	0.000041378	0.000000008	-0.009e-03	0.003e-03	0.000e-03
K9	B.G.1	-0.000014797	0.000050971	0.000000009	-0.010e-03	0.003e-03	0.000e-03
K10	B.G.1	-0.000017655	0.000060852	0.000000010	-0.010e-03	0.003e-03	0.001e-03
K11	B.G.1	-0.000020585	0.000070899	0.000000010	-0.010e-03	0.003e-03	0.001e-03
K12	B.G.1	-0.000023559	0.000081024	0.000000011	-0.010e-03	0.003e-03	0.001e-03
K13	B.G.1	-0.000026388	0.000091173	0.000000011	-0.010e-03	0.003e-03	0.002e-03
K14	B.G.1	0.000000000	0.000000000	0.000000000	-0.000e-03	0.000e-03	0.000e-03
K15	B.G.1	-0.000000348	0.000000612	0.000000000	-0.001e-03	0.001e-03	0.001e-03
K16	B.G.1	-0.000001314	0.000002311	-0.000000001	-0.002e-03	0.001e-03	0.001e-03
K17	B.G.1	-0.000002791	0.000004907	-0.000000001	-0.003e-03	0.002e-03	0.001e-03
K18	B.G.1	-0.000004681	0.000008230	-0.000000002	-0.004e-03	0.002e-03	0.002e-03
K19	B.G.1	-0.000006899	0.000012126	-0.000000002	-0.004e-03	0.002e-03	0.002e-03
K20	B.G.1	-0.000009367	0.000016461	-0.000000003	-0.005e-03	0.003e-03	0.002e-03
K21	B.G.1	-0.000012019	0.000021119	-0.000000003	-0.005e-03	0.003e-03	0.003e-03

Node	L.C.	X	Y	Z	Xr	Yr	Zr
K22	B.G.1	-0.000014799	0.000026001	-0.000000003	-0.005e-03	0.003e-03	0.003e-03
K23	B.G.1	-0.000017661	0.000031027	-0.000000003	-0.005e-03	0.003e-03	0.003e-03
K24	B.G.1	-0.000020569	0.000036133	-0.000000004	-0.005e-03	0.003e-03	0.003e-03
K25	B.G.1	-0.000023498	0.000041274	-0.000000004	-0.005e-03	0.003e-03	0.003e-03
K26	B.G.1	-0.000026432	0.000046425	-0.000000004	-0.005e-03	0.003e-03	0.003e-03
K27	B.G.1	-0.000001314	-0.000000709	-0.000003717	-0.002e-03	0.001e-03	0.001e-03
K28	B.G.1	-0.000004681	0.000002944	-0.000006206	-0.004e-03	0.002e-03	0.002e-03
K29	B.G.1	-0.000009367	0.000009421	-0.000007713	-0.005e-03	0.003e-03	0.002e-03
K30	B.G.1	-0.000014799	0.000017622	-0.000008486	-0.005e-03	0.003e-03	0.003e-03
K31	B.G.1	-0.000020569	0.000026836	-0.000008769	-0.005e-03	0.003e-03	0.003e-03
K32	B.G.1	-0.000026432	0.000036728	-0.000008808	-0.005e-03	0.003e-03	0.003e-03
-	-	m	m	m	rad	rad	rad

PIC. B.G.1: PERMANENT ACTIONS MOMENT (MX) Load Cases

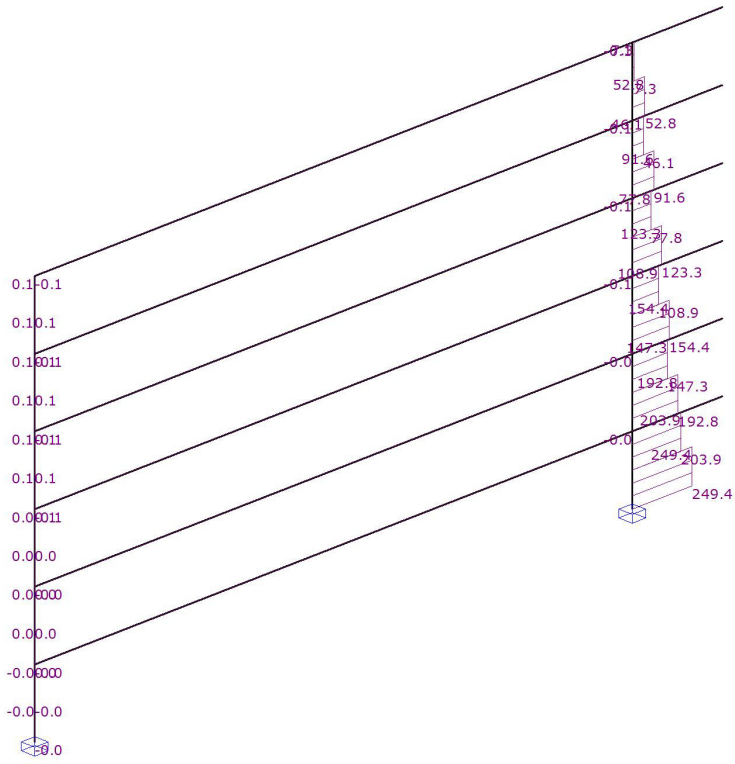

PIC. B.G.1: PERMANENT ACTIONS MOMENT (MY)

Load Cases

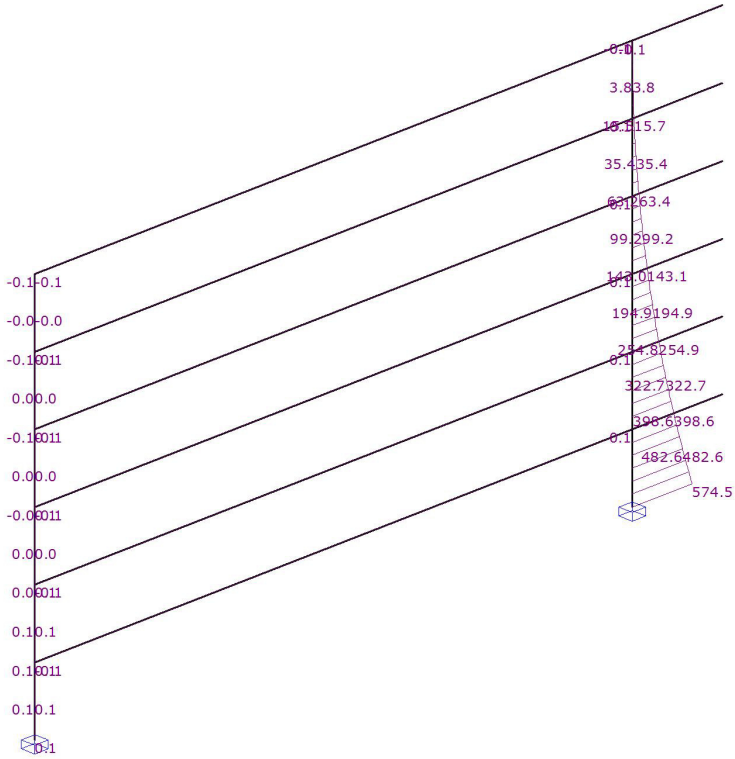

PIC. B.G.1: PERMANENT ACTIONS MOMENT (MZ) Load Cases

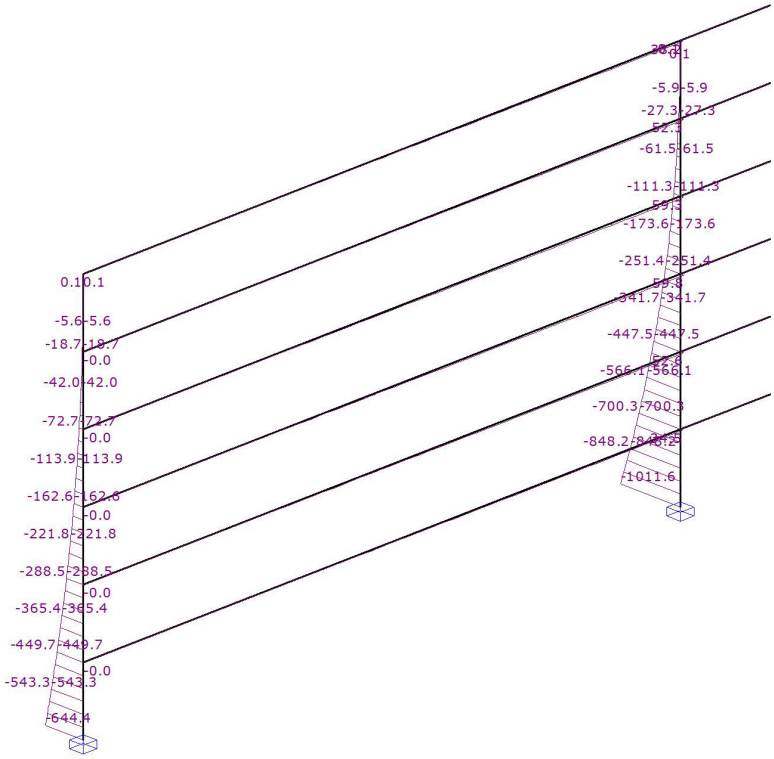

PIC. B.G.1: PERMANENT ACTIONS DWARSKRACHT (VY) Load Cases

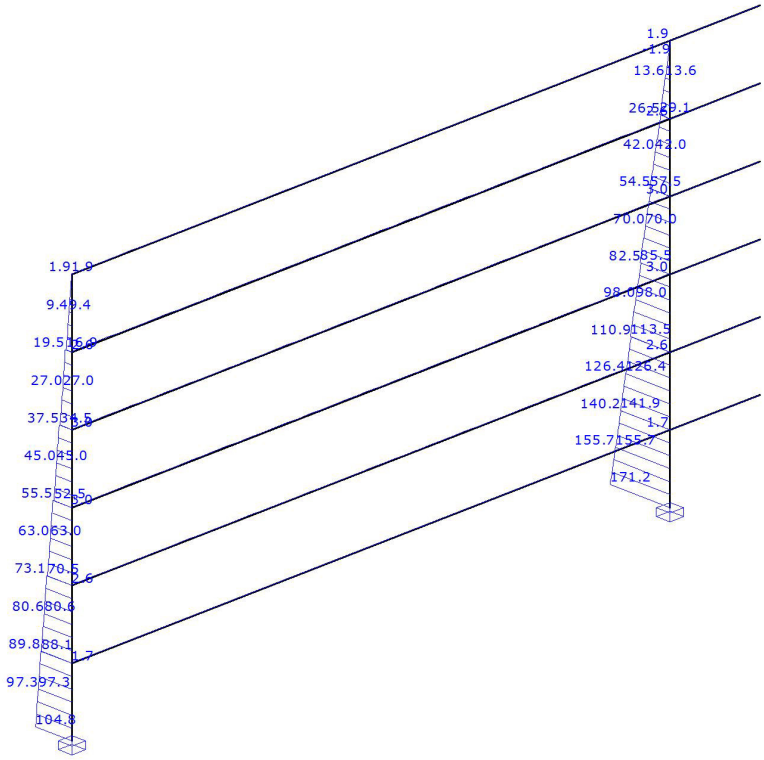

PIC. B.G.1: PERMANENT ACTIONS DWARSKRACHT (VZ) Load Cases

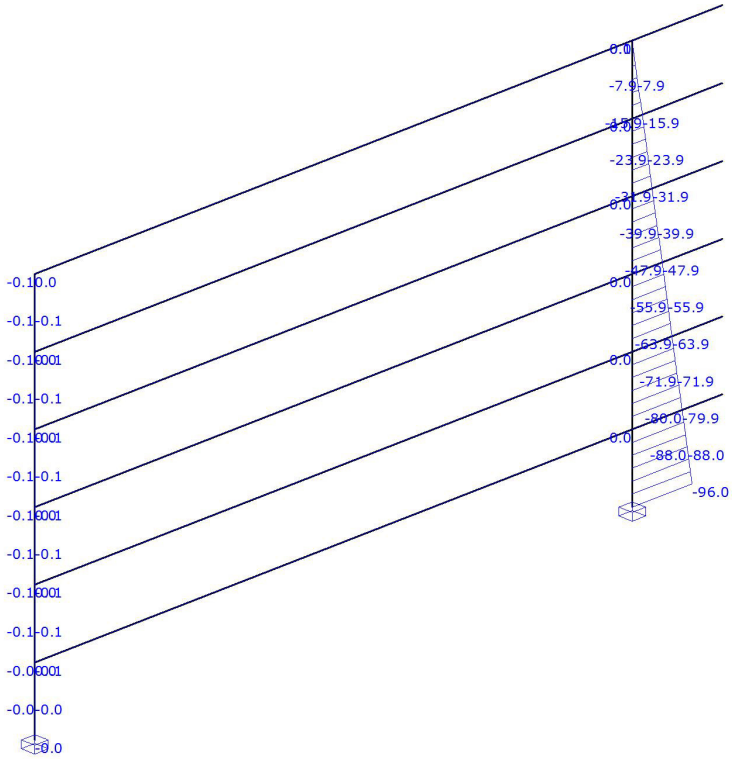

L.C. EXTREME MEMBER FORCES

Member	L.C.	Value	Mb	Mmax	xMmax	Me	x-M0	x-M0	TC	Nmax	Value	Vb	Vmax	Ve	Mxb	Mxe
S1	B.G.1	My	**0.129**	0.000	.00000000	**0.094**	00000000	00000000	C	**-0.068**	Vz	**-0.035**	**-0.035**	**-0.035**	**-0.042**	**-0.042**
		Mz	**-644.352**	0.000	.00000000	**-543.267**	00000000	00000000			Vy	**104.834**	**104.834**	**97.334**		
S2	B.G.1	My	**0.094**	0.000	.00000000	**0.059**	00000000	00000000	C	**-0.068**	Vz	**-0.035**	**-0.035**	**-0.035**	**-0.042**	**-0.042**
		Mz	**-543.267**	0.000	.00000000	**-449.683**	00000000	00000000			Vy	**97.334**	**97.334**	**89.834**		
S3	B.G.1	My	**0.117**	0.000	.00000000	**0.063**	00000000	00000000	C	**-0.062**	Vz	**-0.054**	**-0.054**	**-0.054**	**0.006**	**0.006**
		Mz	**-449.709**	0.000	.00000000	**-365.350**	00000000	00000000			Vy	**88.109**	**88.109**	**80.609**		
S4	B.G.1	My	**0.063**	0.000	.00000000	**0.009**	00000000	00000000	C	**-0.062**	Vz	**-0.054**	**-0.054**	**-0.054**	**0.006**	**0.006**
		Mz	**-365.350**	0.000	.00000000	**-288.491**	00000000	00000000			Vy	**80.609**	**80.609**	**73.109**		
S5	B.G.1	My	**0.105**	0.000	.00000000	**0.038**	00000000	00000000	C	**-0.052**	Vz	**-0.066**	**-0.066**	**-0.066**	**0.037**	**0.037**
		Mz	**-288.534**	0.000	.00000000	**-221.806**	00000000	00000000			Vy	**70.478**	**70.478**	**62.978**		
S6	B.G.1	My	**0.038**	0.000	.00000000	**-0.028**	57868877	00000000	C	**-0.052**	Vz	**-0.066**	**-0.066**	**-0.066**	**0.037**	**0.037**
		Mz	**-221.806**	0.000	.00000000	**-162.578**	00000000	00000000			Vy	**62.978**	**62.978**	**55.478**		
S7	B.G.1	My	**0.091**	0.000	.00000000	**0.019**	00000000	00000000	C	**-0.040**	Vz	**-0.072**	**-0.072**	**-0.072**	**0.057**	**0.057**
		Mz	**-162.632**	0.000	.00000000	**-113.897**	00000000	00000000			Vy	**52.485**	**52.485**	**44.985**		
S8	B.G.1	My	**0.019**	0.000	.00000000	**-0.053**	26609914	00000000	C	**-0.040**	Vz	**-0.072**	**-0.072**	**-0.072**	**0.057**	**0.057**
		Mz	**-113.897**	0.000	.00000000	**-72.662**	00000000	00000000			Vy	**44.985**	**44.985**	**37.485**		
S9	B.G.1	My	**0.078**	0.000	.00000000	**0.011**	00000000	00000000	C	**-0.027**	Vz	**-0.067**	**-0.067**	**-0.067**	**0.072**	**0.072**
		Mz	**-72.721**	0.000	.00000000	**-41.954**	00000000	00000000			Vy	**34.518**	**34.518**	**27.018**		
S10	B.G.1	My	**0.011**	0.000	.00000000	**-0.055**	17240868	00000000	C	**-0.027**	Vz	**-0.067**	**-0.067**	**-0.067**	**0.072**	**0.072**
		Mz	**-41.954**	0.000	.00000000	**-18.686**	00000000	00000000			Vy	**27.018**	**27.018**	**19.518**		
S11	B.G.1	My	**0.082**	0.000	.00000000	**-0.023**	78046691	00000000	C	**-0.013**	Vz	**-0.105**	**-0.105**	**-0.105**	**0.084**	**0.084**

Member	L.C.	Value	Mb	Mmax	xMmax	Me	x-M0	x-M0	TC	Nmax	Value	Vb	Vmax	Ve	Mxb	Mxe
		Mz	**-18.747**	0.000	.00000000	**-5.593**	00000000	00000000			Vy	**16.904**	**16.904**	**9.404**		
S12	B.G.1	My	**-0.023**	0.000	.00000000	**-0.128**	00000000	00000000	C	**-0.013**	Vz	**-0.105**	**-0.105**	**-0.105**	**0.084**	**0.084**
		Mz	**-5.593**	0.000	.00000000	**0.062**	96951741	00000000			Vy	**9.404**	**9.404**	**1.904**		
S13	B.G.1	My	**574.518**	0.000	.00000000	**482.553**	00000000	00000000	T	**0.068**	Vz	**-95.965**	**-95.965**	**-87.965**	**249.360**	**49.360**
		Mz	**1011.649**	0.000	.00000000	**-848.233**	00000000	00000000			Vy	**171.166**	**171.166**	**155.666**		
S14	B.G.1	My	**482.553**	0.000	.00000000	**398.588**	00000000	00000000	T	**0.068**	Vz	**-87.965**	**-87.965**	**-79.965**	**203.860**	**03.860**
		Mz	**-848.233**	0.000	.00000000	**-700.317**	00000000	00000000			Vy	**155.666**	**155.666**	**140.166**		
S15	B.G.1	My	**398.646**	0.000	.00000000	**322.700**	00000000	00000000	T	**0.062**	Vz	**-79.946**	**-79.946**	**-71.946**	**192.818**	**92.818**
		Mz	**-700.291**	0.000	.00000000	**-566.150**	00000000	00000000			Vy	**141.891**	**141.891**	**126.391**		
S16	B.G.1	My	**322.700**	0.000	.00000000	**254.754**	00000000	00000000	T	**0.062**	Vz	**-71.946**	**-71.946**	**-63.946**	**147.318**	**47.318**
		Mz	**-566.150**	0.000	.00000000	**-447.509**	00000000	00000000			Vy	**126.391**	**126.391**	**110.891**		
S17	B.G.1	My	**254.852**	0.000	.00000000	**194.918**	00000000	00000000	T	**0.052**	Vz	**-63.934**	**-63.934**	**-55.934**	**154.404**	**54.404**
		Mz	**-447.466**	0.000	.00000000	**-341.694**	00000000	00000000			Vy	**113.522**	**113.522**	**98.022**		
S18	B.G.1	My	**194.918**	0.000	.00000000	**142.984**	00000000	00000000	T	**0.052**	Vz	**-55.934**	**-55.934**	**-47.934**	**108.904**	**08.904**
		Mz	**-341.694**	0.000	.00000000	**-251.422**	00000000	00000000			Vy	**98.022**	**98.022**	**82.522**		
S19	B.G.1	My	**143.106**	0.000	.00000000	**99.178**	00000000	00000000	T	**0.040**	Vz	**-47.928**	**-47.928**	**-39.928**	**123.250**	**23.250**
		Mz	**-251.368**	0.000	.00000000	**-173.603**	00000000	00000000			Vy	**85.515**	**85.515**	**70.015**		
S20	B.G.1	My	**99.178**	0.000	.00000000	**63.250**	00000000	00000000	T	**0.040**	Vz	**-39.928**	**-39.928**	**-31.928**	**77.750**	**77.750**
		Mz	**-173.603**	0.000	.00000000	**-111.338**	00000000	00000000			Vy	**70.015**	**70.015**	**54.515**		
S21	B.G.1	My	**63.383**	0.000	.00000000	**35.450**	00000000	00000000	T	**0.027**	Vz	**-31.933**	**-31.933**	**-23.933**	**91.575**	**91.575**
		Mz	**-111.279**	0.000	.00000000	**-61.546**	00000000	00000000			Vy	**57.482**	**57.482**	**41.982**		
S22	B.G.1	My	**35.450**	0.000	.00000000	**15.517**	00000000	00000000	T	**0.027**	Vz	**-23.933**	**-23.933**	**-15.933**	**46.075**	**46.075**
		Mz	**-61.546**	0.000	.00000000	**-27.314**	00000000	00000000			Vy	**41.982**	**41.982**	**26.482**		
S23	B.G.1	My	**15.655**	0.000	.00000000	**3.760**	00000000	00000000	T	**0.013**	Vz	**-15.895**	**-15.895**	**-7.895**	**52.828**	**52.828**
		Mz	**-27.253**	0.000	.00000000	**-5.907**	00000000	00000000			Vy	**29.096**	**29.096**	**13.596**		
S24	B.G.1	My	**3.760**	**-0.135**	.98686444	**-0.134**	80302834	00000000	T	**0.013**	Vz	**-7.895**	**-7.895**	**0.105**	**7.328**	**7.328**
		Mz	**-5.907**	**0.055**	.87713414	**-0.062**	79254173	96172654			Vy	**13.596**	**13.596**	**-1.904**		
S25	B.G.1	My	**-0.057**	0.000	.00000000	**0.058**	91491729	00000000	T	**0.019**	Vz	**0.006**	**0.006**	**0.006**	**-0.026**	**-0.026**
		Mz	**-0.047**	0.000	.00000000	**34.458**	02741477	00000000			Vy	**1.725**	**1.725**	**1.725**		
S27	B.G.1	My	**-0.096**	0.000	.00000000	**0.098**	91334346	00000000	T	**0.012**	Vz	**0.010**	**0.010**	**0.010**	**-0.043**	**-0.043**
		Mz	**-0.031**	0.000	.00000000	**52.585**	01188380	00000000			Vy	**2.631**	**2.631**	**2.631**		
S29	B.G.1	My	**-0.119**	0.000	.00000000	**0.121**	91562209	00000000	T	**0.006**	Vz	**0.012**	**0.012**	**0.012**	**-0.053**	**-0.053**
		Mz	**-0.020**	0.000	.00000000	**59.847**	00681765	00000000			Vy	**2.993**	**2.993**	**2.993**		
S31	B.G.1	My	**-0.131**	0.000	.00000000	**0.133**	91273072	00000000	C	**-0.005**	Vz	**0.013**	**0.013**	**0.013**	**-0.059**	**-0.059**
		Mz	**-0.014**	0.000	.00000000	**59.325**	00478553	00000000			Vy	**2.967**	**2.967**	**2.967**		
S33	B.G.1	My	**-0.137**	0.000	.00000000	**0.139**	94504406	00000000	T	**0.038**	Vz	**0.014**	**0.014**	**0.014**	**-0.061**	**-0.061**
		Mz	**-0.012**	0.000	.00000000	**52.253**	00461496	00000000			Vy	**2.613**	**2.613**	**2.613**		
S35	B.G.1	My	**-0.128**	0.000	.00000000	**0.134**	75866527	00000000	C	**-0.105**	Vz	**0.013**	**0.013**	**0.013**	**-0.062**	**-0.062**
		Mz	**0.084**	0.000	.00000000	**38.172**	00000000	00000000			Vy	**1.904**	**1.904**	**1.904**		
-	**-**	**-**	**kNm**	**kNm**	**m**	**kNm**	**m**	**m**	**-**	**kN**	**-**	**kN**	**kN**	**kN**	**kNm**	**kNm**

L.C. INTERNAL FORCES & DEFLECTIONS

L.C.	Member	Position	Uy	Uz	Uy'	Uz'	Nx	Vy	Vz	Mx	My
B.G.1	S1	0.00000000	0.000000000	0.000000000	0.000000000	0.000000000	-0.068	104.834	-0.035	-0.042	0.129
B.G.1		0.10000000	0.000000013	-0.000000004	0.000000107	0.000000033	-0.068	104.084	-0.035	-0.042	0.125
B.G.1		0.20000000	0.000000050	-0.000000016	0.000000188	0.000000057	-0.068	103.334	-0.035	-0.042	0.122
B.G.1		0.30000000	0.000000111	-0.000000035	0.000000246	0.000000075	-0.068	102.584	-0.035	-0.042	0.118
B.G.1		0.40000000	0.000000197	-0.000000062	0.000000280	0.000000085	-0.068	101.834	-0.035	-0.042	0.115
B.G.1		0.50000000	0.000000306	-0.000000096	0.000000290	0.000000087	-0.068	101.084	-0.035	-0.042	0.112
B.G.1		0.60000000	0.000000438	-0.000000137	0.000000276	0.000000083	-0.068	100.334	-0.035	-0.042	0.108
B.G.1		0.70000000	0.000000594	-0.000000185	0.000000240	0.000000072	-0.068	99.584	-0.035	-0.042	0.105
B.G.1		0.80000000	0.000000771	-0.000000239	0.000000182	0.000000054	-0.068	98.834	-0.035	-0.042	0.101
B.G.1		0.90000000	0.000000970	-0.000000300	0.000000102	0.000000030	-0.068	98.084	-0.035	-0.042	0.098
B.G.1		L(1.00000000)	0.000001191	-0.000000367	0.000000000	0.000000000	-0.068	97.334	-0.035	-0.042	0.094
B.G.1	S2	0.00000000	0.000001191	-0.000000367	0.000000000	0.000000000	-0.068	97.334	-0.035	-0.042	0.094
B.G.1		0.10000000	0.000001434	-0.000000439	0.000000089	0.000000023	-0.068	96.584	-0.035	-0.042	0.091
B.G.1		0.20000000	0.000001697	-0.000000517	0.000000158	0.000000040	-0.068	95.834	-0.035	-0.042	0.087